PhD Thesis

November 2013

CityZoom UP (Urban Pollution): A computational tool for the fast generation and setup of urban scenarios for CFD and dispersion modelling simulation

By

Pablo Colossi Grazziotin, MSc

PhD Candidate
Alβan Code E06D104001BR

Supervisors
Dr. Herve Morvan
Dr. David Hargreaves

School of Civil Engineering

University of Nottingham

Abstract

This research presents the development of CityZoom UP, the first attempt to extend existing urban planning software in order to assist in modelling urban scenarios and setting up simulation parameters for Gaussian dispersion and CFD models. Based on the previous capabilities and graphic user interfaces of CityZoom to model and validate urban scenarios based on Master Plan regulations, new graphic user interfaces, automatic mesh generation and data conversion algorithms have been created to seamlessly generate input data for dispersion model AERMOD and CFD packages CFX and OpenFOAM.

A key feature of CityZoom UP is the introduction of vehicular pollution source parameters in dispersion and CFD models, allowing the urban designer to assess the local impact of adding or modifying a building or group of buildings on the street air quality. Traffic emissions are modelled as sequence of point sources.

CityZoom UP uses Atmospheric Dispersion model AERMOD to assess the dispersion of pollutants in large scale urban environments for strategic planning, quickly providing results for different alternatives of urban scenarios, meteorological and traffic profiles. Sensitivity and validation tests are performed and the results are compared to wind tunnel and real world tracer experiments from the DAPPLE campaign. For the first time in the available literature AERMOD is used to perform dispersion simulation using tracer emission data from mobile vehicular sources in a complex urban scenario, considering building wake effects.

CityZoom UP also provides automated 3D meshing, including mesh refinement, identification of physical boundaries in the mesh, and automatic setup of CFD simulations of urban scenarios, for the detailed calculation of air flow and dispersion of pollutants in specific areas inserted in urban environments. These capabilities can greatly reduces the time necessary for the setup CFD cases, even if it does not affect the computational time needed to run the CFD simulations. Tests show how CityZoom UP can be used to model alternative scenarios for a given location, e.g. present situation and future scenario including a new tall building, and to easily automate the generation of different meshes for each scenario, based on boundary layer and size function refinement parameters.

The present and possible future situations of a real world scenario in Porto Alegre are modelled as a show case for CityZoom UP. The capabilities to assist in modelling alternative urban scenarios and setting up AERMOD and CFD simulations based on those scenarios is demonstrated.

Acknowledgments

This research is supported by the Programme Alβan, the European Union Programme of High Level Scholarships for Latin America, scholarship no. E06D104001BR.

I would like to thank my family for their help, support and encouragement throughout my PhD, especially in the most stressful times.

Table of Contents

List of Figures

List of Tables

Notation

C	concentration of air pollutant (g/m^3)
C/Q	normalized concentration
C^*	non-dimensional concentration
D	dosage (gs/m^3)
D/M	normalised dosage
H_a	average building height (m)
H_m	height of the tallest building in the domain (m)
H	street canyon height (m)
H_e	effective height of the centerline of the plume (m)
H/W	street canyon height to width aspect ratio
K	von Karman's constant
L	Monin-Obhukov length scale (m)
M	total mass of material released (g)
Q	emission rate (gs^{-1})
Q_S	emission rate for source S (gs^{-1})
Q_T	total emission rate for all sources combined (gs^{-1})
Q_H	sensible heat flux (W/m^2)
RH	relative humidity
T_0	surface temperature (K)
U	surface wind speed (ms^{-1})
W	street canyon width (m)
W/H	street canyon width to height aspect ratio
Z	boundary layer depth (m)
d	zero plane displacement (m)
u	wind speed (ms^{-1})
u_r	wind speed at reference height z_r (ms^{-1})
u_*	friction velocity (ms^{-1})
z	reference height (m)
z_0	surface roughness (m)
z_r	reference height for wind speed u_r (m)
α	atmospheric stability coefficient
ε	dissipation rate
ζ	building density
θ	wind direction (degrees)
κ	turbulent kinetic energy
μ_t	turbulent viscosity
ρ	air density (g/m^3)
τ	surface shearing stress (Pa)

1. Introduction

To evaluate a city new development is not an easy or fast task. During the design of a new building, it would be ideal to quickly assess its impact over the neighbourhood where it is to be built. There are many environmental factors to be considered and they are more often than not in conflict and quite difficult to ponder in their relative importance. The use of a computational tool to make preliminary assessments and to help establish positive relationships between these different factors would prove advantageous.

Planning regulations are supposed to guide the urban occupation, leading to better quality of the built environment. However, in most cases, these regulations have been limited to the establishment of very general volumetric rules (lot coverage, floor area ratio, height limits) usually relating the building shape and size to its lot shape and size. Some regulations, especially in growing countries, such as Brazil, are based in frozen pre-figurations of a very dynamic urban configuration. This leads planners and city planning authorities to constantly modify these rules, resulting, very often, in chaotic images of the urban space.

Examples of such environmental factors are insolation and daylight parameters, which should be considered during the planning process in order to establishing the benefits to be obtained from the sun in and around buildings (thermal and visual comfort and energy conservation). The process requires understanding and making allowances for the urban and site attributes that affect how and where the solar radiation and daylight can be used (Pereira et al. 2001). Theoretically, the ideal is to exclude from the urban environment the undesirable radiation and accept all of the desirable part. Pereira proposes that some initial criteria are used to define the property line angle to be respected for each possible building orientation, but a complete optimisation is impossible as the occupation takes place from the ground level upwards.

Oke (1988) tried to show by example how to apply urban climatology findings into urban planning and design. His paper posed the simple but very fundamental question "Does urban climate research have quantitative guidelines to offer regarding street geometry?" Obviously there is no single solution, i.e., there is no universally optimum geometry. The goal is to find general guidelines, flexible enough to cater to special needs and situations, avoiding a rigid "solution" whose blind application leads to further problems. Planning choices are not obvious, even considering only the physical results. For example, for a mid or high-latitude city, the goals may be: to maximize shelter; to maximize dispersion of pollutants; to maximize urban warmth; and to maximize solar access.

These objectives and the structures they impose are in conflict. Shelter and warmth are best provided by narrow streets and compactness, while dispersion and solar access demand separation, openness and low building density. Assuming most cities want to meet each of these goals at least minimally, Oke investigates the existence of a "zone of compatibility", i.e., a range of canyon geometries and building densities which avoid the worse aspects of not providing shelter, dispersion, warmth or access.

A computational tool capable of simultaneously representing the correlation and effects of planning regulations together with physical and environmental comfort parameters in urban scenarios could not be found in the available literature.

CityZoom (Grazziotin et al. 2004; Turkienicz et al. 2007; CityZoom 2008; Turkienicz et al. 2008) is a software developed by the SimmLab – UFRGS (Laboratory for the Simulation and Modelling in Architecture and Urbanism – Federal University of Rio Grande do Sul – Brazil), with prominent participation of the author of the present research, which attempts to provide a computational environment where different design and planning attributes can be considered simultaneously, aiming to optimize the urban planning process. CityZoom can help users to evaluate and to modify the city model according to different constraints such as solar radiation, luminance, planning regulations, terrain's permeable conditions, etc.

CityZoom originated from a challenge raised by the Mayor of Porto Alegre (Brazil), Tarso Genro, in 1994. Genro wanted to implement a bonus policy allowing the exchange of plot ratios between urban plots. The plot ratio is the relationship between the building's built area and the plot area. Urban regulations dictate a maximum plot ratio, based on parameters such as available infrastructure and desired urban configurations. If a plot or region does not reach the maximum allowed ratio, part of it can, potentially, be used on another plot. In order to assess how much could be transferred, and how beneficial those transfers would actually be, an issue needed to be answered, i.e. how much could be built in a particular urban plot.

To answer this question, the City Hall asked UFRGS through SimmLab to elaborate a study to show the possible impact of the existing and alternative Master Plan Rules over five different neighbourhoods of Porto Alegre to provide guidelines for the city's development (Turkienicz 1994). The building volumes for this report were manually edited, in a time-consuming and labour-intensive process.

This experience led SimmLab to invest in the creation of software capable of automatically generating buildings according to planning regulations. In 1996, CityZoom's research project started, incubated at UFRGS' Institute of Informatics, where the author joined as an undergraduate research student and programmer. All of CityZoom's modules, functions and libraries were created from scratch, in order to provide a 3D computational environment where different building performance models could operate interactively, aiming to optimize the urban planning process.

The first performance model developed was BlockMagic (Grazziotin and Turkienicz 1999; Turkienicz et al. 1999), a model for simulating the application of urban regulations to sets of urban plots. It can swiftly generate sets of buildings in the most different urban scenarios, according to the regulations and user-input parameters that determine which of the building attributes are to be assessed or optimized, such as number of floors, front or size width, slab area, plot occupation and plot ratio. BlockMagic can also be used to validate designed or existing buildings.

The work of the author on the development of BlockMagic was acknowledged with the award of best paper of the section and the indication for the "Young Researcher Award" in the 1999 Salão de Iniciação Cientifica – UFRGS (Undergraduate Science Fair, Grazziotin and Turkienicz 1999). In that same year, BlockMagic was used by other undergraduate students in a study to evaluate the impact of different sets of urban regulations (Modena et al. 1999).

After his graduation in the beginning of 2000, the author undertook the role of programming team leader at the SimmLab, guiding and assisting undergraduate students to develop new tools for CityZoom. An OpenGL based 3D visualization tool and the analytical tool Mosaic (Scheidegger et al. 2001) were developed, as well as an interface to import and export Geographic Information Systems (GIS) files.

Over many years of development, different tools and solutions were devised to solve questions raised by several different cities and research partners in Brazil and abroad. Ely et al. (1999), Cruz et al. (2001) and Bigolin and Kowarick (2006) are some of the research works that have used CityZoom. CityZoom has been used by the SimmLab team in the elaboration of complete Master Plan regulations for the cities of Aracajú, Eldorado do Sul, Farroupilha, Horizontina, Santa Clara do Sul and São Gabriel, elaboration of Local Plan for Social Housing for the cities Canela, Guaíba, Nova Santa Rita, Parobé, Portão, Taquara and Taquari, Master Plan revision for the cities of Caxias do Sul and Taquara, and for environmental impact studies in Porto Alegre (SimmLab 2012).

As part of the author's MSc research (Grazziotin et al. 2002), BlockMagic was extended to addresses environmental comfort issues, through the use of the Solar Envelope technique (Pereira et al. 2001). The Solar Envelope is a construct of space and time: the site location (latitude and longitude), the physical boundaries of surrounding properties and the period of their assured access to sunshine. The introduction of such parameters in the design process can substantially affect the land use, building density and urban land value.

Likewise, the introduction of physical parameters in the CityZoom environment, such as the effects of air flow and pollution, along with the planning regulations, can also improve the urban design. The desire to better understand the intricacies of the fluid dynamics and to develop a module for CityZoom capable of handing such physical parameters has led the author to join the Faculty of Engineering CFD (Computational Fluid Dynamics) Group at the University of Nottingham, led by Morvan and Hargreaves.

CFD modelling and solving are accurate but also time-consuming processes, for which existing solutions, of various resolution levels, have already been developed. However, when dealing with urban planning and design, especially during the beginning of a design evaluation process, quick responses to the extensive amount of factors and design alternatives are desirable and more strategic than exceedingly precise ones. This is the philosophy behind CityZoom, and the first goal to be achieved by the current research: to provide simplified means to obtain fast, approximate, and yet good quality results for the dispersion of pollutants in urban environments. The second component to the research is to offer the possibility to carry out more detailed CFD calculations in regions of interest and as part of the design process, e.g. to look at the impact of a particular building or to assess the impact of one particular rule at a given location. For both goals, CityZoom would be used as a tool to assist in the modelling and setup of the problem, feeding data to simulation software and reading back the obtained results.

A good understanding of the existing dispersion modelling, CFD techniques and approaches capable of meeting the above needs is necessary in order to create a new version of CityZoom that is indeed capable of modelling the necessary parameters and assisting in the setup of the simulation to be performed by such specialized software. By implementing such modifications in the CityZoom environment and allowing interface with dispersion and CFD tools, the author expects to obtain a tool capable of simultaneously representing the correlation and effects of planning regulations along with physical and environmental comfort parameters for urban scenarios. Such tool is desired not only by planners, but also by architects, engineers, government authorities and laymen.

1.1. Aims and Objectives

The aims of this PhD research are to understand the dispersion of pollutants in urban environments and to create a computational tool that can assist in modelling urban scenarios and setting up simulation parameters for:

- the fast calculation of the dispersion of pollutants in such urban environments, through atmospheric dispersion models, and
- the detailed calculation of air flow and dispersion of pollutants in specific areas inserted in urban environments, through Computational Fluid Dynamics (CFD) tools and algorithms.

This new and extended version of CityZoom – CityZoom UP (Urban Pollution) – will be capable of considering different urban aspects, such as the city's geometry and Master Plan regulations, insolation data, as well as wind and pollution parameters, all in an integrated environment. Also, by assisting in the modelling and setting up of urban scenarios for the simulation of dispersion of pollutants, the tool will allow for a broader variety of options to be analyzed and discussed, both before and after simulation. Not only the impact of changes to emission parameters can be evaluated, but also how different building alternatives can affect the dispersion of pollutants.

A tool capable of simulating possible future developments based on these parameters is not only craved, but needed by architects, engineers, urban planners and even laymen in order to better understand the relationships between the parameters and improve the urban design.

This will be achieved through the attainment of the following objectives:

- Study of the physics and equations governing wind flow, dispersion and transport of pollutants in urban environments;
- Study of the existing numerical techniques and computational tools for dispersion and CFD calculations;
- Choice of models, techniques or computational tools appropriate for using in conjunction with CityZoom;

- Implementation of a new version of CityZoom, capable of handling the parameters necessary for modelling and setting up urban scenarios to be used by dispersion of pollutants and CFD simulation tools;
- Modelling of urban scenarios and simulation using the chosen dispersion model, comparing the results with available data, such as that from the DAPPLE campaign;
- Modelling of typical urban canyon scenarios and simulation using the chosen CFD tool;
- Demonstration of the application of the tool to model existing and hypothetical scenarios and then to predict and compare the dispersion of pollutants in these scenarios; and
- Assessment of what can be gained from the use of this kind of tool.

1.2. Thesis Structure

This thesis details the efforts of the author during his stay at the University of Nottingham to understand the problem and to create a computational tool capable of assisting in the modelling and setting up of urban scenarios to be used in the simulation of air flow and transport of pollutants.

Chapter 1 introduces the background and context of the research. The aims, objectives and outline of the research are presented.

Chapter 2 reviews the literature on the dispersion of pollutants in urban environments. Computational models for the dispersion simulation are reviewed. Environmental characteristics that affect the dispersion and available tools to model these characteristics are discussed. Finally, existing datasets of urban flow and dispersion are presented.

Chapter 3 describes the implementation of CityZoom UP, an extension of CityZoom to assist in the modelling and setting up of urban scenarios for dispersion and CFD simulation.

Chapter 4 details the tests performed. CityZoom UP features to assist in the modelling and setup of urban scenarios for dispersion and CFD simulation are tested. AERMOD results for the simulation of the dispersion of pollutants in urban environments are compared to measurement data from the DAPPLE project.

Chapter 5 demonstrates the capabilities of CityZoom UP applied to a real world scenario.

Chapter 6 presents the conclusions drawn from the present research and indicates further work to be developed.

2. Literature Review

2.1. Introduction

The aim of this chapter is to provide the reader with an overview of the challenges encountered in the modelling and simulation of how pollutants disperse in urban environments. The two widely accepted and used computational approaches to simulate the dispersion of pollutants in the ambient atmosphere are reviewed: Atmospheric Dispersion Modelling and Computational Fluid Dynamics (CFD).

Atmospheric dispersion models use mathematical equations to simulate how pollutants disperse and are capable of properly predicting the relationships between emissions and the concentration levels in the street (Berkowicz et al. 2006). Several models exist, with different degrees of sophistication, and are able to quickly describe the dispersion conditions. Hanna et al. (2001) and Vardoulakis et al. (2003; 2007) review some of the existing models and their suitability for street canyon applications. A typical dispersion simulation can run on a standard desktop computer in minutes rather than hours or days.

Computational Fluid Dynamics or CFD is the analysis of systems involving fluid flow, heat transfer and associated phenomena such as chemical reactions by means of computer-based simulation (Versteeg and Malalasekera 1995). With the rapid development in computer hardware and numerical algorithms, CFD techniques are becoming widely used to study the wind field and pollutant transport in urban scenarios. Li et al. (2006) reviewed the recent advancements and achievements in street-canyon pollution research using mathematical modelling approaches.

The dispersion of pollutants in urban environments is affected by several characteristics of the environment, such as street canyons aspect ratio, configuration of buildings in urban intersections, ambient wind direction, position and emission rate of the sources, vehicle-induced turbulence, etc. The effects of such characteristics are also reviewed in this chapter, as well as the tools and techniques available to model them as parameters to be used by dispersion and CFD models.

Finally, existing datasets of urban flow and dispersion are presented. Measurement data is available from different projects, such as Dispersion of Air Pollution and its Penetration into the Local Environment (DAPPLE) project (Arnold et al. 2004; Wood et al. 2009; Robins 2011), Joint Urban 2003 (Allwine et al. 2004; Clawson et al. 2005), Instrumented City (Chen and Bell 2002), and Mock Urban Setting Test (Biltoft 2001), which can be used to validate the results of the present work.

2.2. Atmospheric Boundary Layer

The lowest portion of the Atmosphere is vital to human life, as it is where the human being dwells and breathes, and also where anthropogenic gaseous emissions are discharged. The Earth's surface interacts with the lowest 10 km of the Atmosphere in a layer called the troposphere (Oke 1987). Over time periods of about one day this influence is restricted to a much shallower zone known as the Atmospheric Boundary Layer (ABL), characterized by well developed turbulence generated by frictional drag as the atmosphere moves across the rough and rigid surface of the Earth, and by the "bubbling-up" of air parcels from the heated surface. The ABL is the most important layer with respect to the emission, transport and dispersion of airborne pollutants. The height of the ABL is not constant with time, it depends upon the strength of the surface-generated mixing.

The wind field in the boundary layer is largely controlled by the frictional drag imposed on the flow by the underlying rigid surface. The drag retards motion close to the ground and gives rise to a sharp decrease of mean horizontal wind speed ($\bar{u}$) as the surface is approached. In the absence of strong thermal effects the depth of this frictional influence depends on the roughness of the surface. The depth of this layer increases with increasing roughness. The top of the layer is at the gradient height, z_g, where the surface drag is negligible and above which $\bar{u}$ becomes approximately constant with height, receiving the name of gradient wind speed.

The actual form of the wind variation with height under neutral stability has been found to be accurately described by a logarithmic decay curve. The log wind profile estimates the wind speed (u, in meters per second) at height (z, in meters) above the ground using the following equation:

$$u = \frac{u_*}{K} \ln\left(\frac{z-d}{z_0}\right) \tag{1}$$

where u_* is the friction velocity (in meters per second), K is the von Karman's constant (≈ 0.40), d is the zero plane displacement, and z_0 is the surface roughness (in meters).

The zero plane displacement is the height in meters above the ground at which zero wind speed is achieved as a result of flow obstacles such as trees or buildings. It is sometimes approximated as $^2/_3$ of the average height of the obstacles (Oke 1987). The surface roughness is a measure of the aerodynamic roughness of the surface and is related, but not equal to, the height of the roughness elements. It is also a function of the shape and density distribution of elements. Usual values are between $^1/_{10}$th and $^1/_{30}$th of the average height of the roughness elements on the ground.

The force exerted on the surface by the air being dragged over it is called the surface shearing stress (τ). It has been found that the shearing stress is proportional to the square of the wind velocity at some arbitrary reference height. Thus u_* is introduced for which this square law holds exactly so that:

$$u_*^2 = \frac{\tau}{\rho} \tag{2}$$

where ρ is the air density.

When surface roughness or stability information is not available, the log wind profile is often substituted by the power law relationship:

$$\frac{u}{u_r} = \left(\frac{z}{z_r} \right)^{\alpha} \tag{3}$$

where u is the wind speed at height z, u_r is the known wind speed at reference height z_r, and α is the atmospheric stability coefficient.

The value of α depends on the atmospheric stability and surface roughness. Typical values range from 0.15 to 0.60 for urban (rough) terrain and 60% of that for rural (smooth) terrain (Cooper and Alley 1990).

2.3. Computational Simulation of the Dispersion of Pollutants in Urban Environments

Wind field models together with dispersion models can be used to simulate the pollutant transport phenomena. There are several dispersion models developed for the simulation of urban environments with different complexities for various applications. Two main categories can be identified: dispersion models and CFD models. The dispersion models usually need some empirical or semi-empirical parameters from observation and make several crude simplifications. CFD models solve the three-dimensional Reynolds averaged equations for flow, pressure, turbulence parameters and concentration distribution.

Dispersion models are a relatively simple and fast way to assess concentrations in urban scenarios, but have a coarse resolution. On the other hand, CFD tools, although more computationally expensive, can reproduce the entire flow and concentration fields for the same scenarios in a much higher resolution. A combination of both techniques could provide important results to both the urban planning and air quality management areas.

2.3.1. Dispersion Modelling

Atmospheric dispersion modelling uses mathematical formulations to characterize the atmospheric processes that disperse a pollutant emitted by a source (SCRAM 2008). It is usually performed with computer programs that solve the mathematical equations and algorithms which simulate the pollutant dispersion (e.g., by assuming a Gaussian distribution of pollution within the plume). Based on the emissions from sources (e.g., industrial stacks and traffic), meteorological inputs (e.g., wind speed and direction, atmospheric stability class, ambient air temperature), terrain elevations, and obstruction data, dispersion models can be used to predict concentrations at downwind receptor locations.

Dispersion models are typically used to determine whether existing or proposed new industrial facilities are or will be in compliance with the National Ambient Air Quality Standards (NAAQS) in the United States and other nations (Hanna et al.

2001; Soulhac et al. 2003; Vardoulakis et al. 2003). The models have also been used to assist in the design of effective control strategies to reduce emissions of harmful air pollutants (Kaur et al. 2007; Murena et al. 2008) and to predict the dispersion of contaminants in large cities (Pullen et al. 2005).

The EPA's Guidelines on Air Quality Models (USEPA 1986) provides a list of preferred/recommended models, such as AERMOD (Cimorelli et al. 1998), as well as alternative models, e.g., ADMS-3 (Carruthers et al. 1994) and ISC3 (EPA 1995). There are also several semi-empiric parametric models, specially designed to produce pollutant concentrations within or around near-regular canyons, such as the Danish OSPM (Berkowicz 2000a; Gokhale et al. 2005; Solazzo et al. 2007) and TEMMS (Namdeo et al. 2002) and PUFFER (Hargreaves and Baker 1997) from the UK.

ADMS (Atmospheric Dispersion Modelling System) was developed by the Cambridge Environmental Research Consultants (CERC), in collaboration with the UK Meteorological Office, National Power plc and the University of Surrey. The current version, ADMS 4, is limited to 300 point sources and 25 buildings, which is a number too small for the aspirations of this research, and requires a license to be used.

In 1991, the American Meteorological Society (AMS) and the U.S. Environmental Protection Agency (EPA) created the AMS/EPA Regulatory Model Improvement Committee (AERMIC) working group, with the goal of introducing current Planetary Boundary Layer (PBL) concepts into regulatory dispersion models. The AERMIC Model – AERMOD (Cimorelli et al. 1998) – was developed as a complete replacement for the EPA Industrial Source Complex Model – ISC3 (EPA 1995).

AERMOD is an open source steady-state plume model. It assumes that concentrations at all distances during a modelled hour are governed by the temporally averaged meteorology of the hour. In the stable boundary layer (SBL), the concentration distribution is assumed to be Gaussian (Figure 2-1) in both the vertical and horizontal.

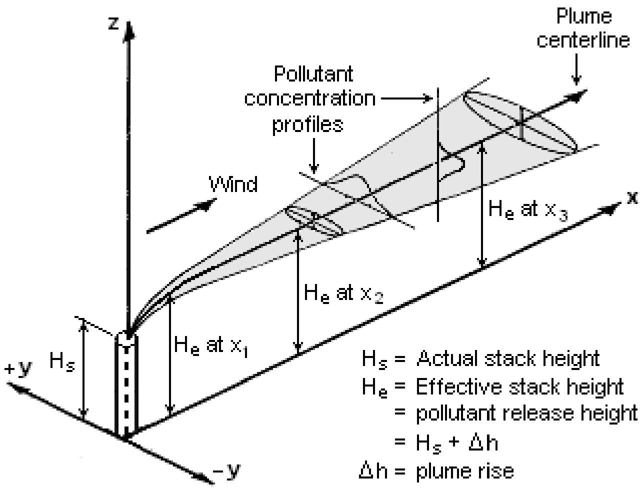

Figure 2-1: Visualization of a buoyant Gaussian air pollutant dispersion plume (GNU image. Author: Milton Beychok).

In the convective boundary layer (CBL), the horizontal distribution is assumed to be Gaussian, but the vertical distribution is described with a bi-Gaussian probability density function (Figure 2-2), since AERMOD approximates the skewed distribution by superimposing the updraft and downdraft Gaussian distributions.

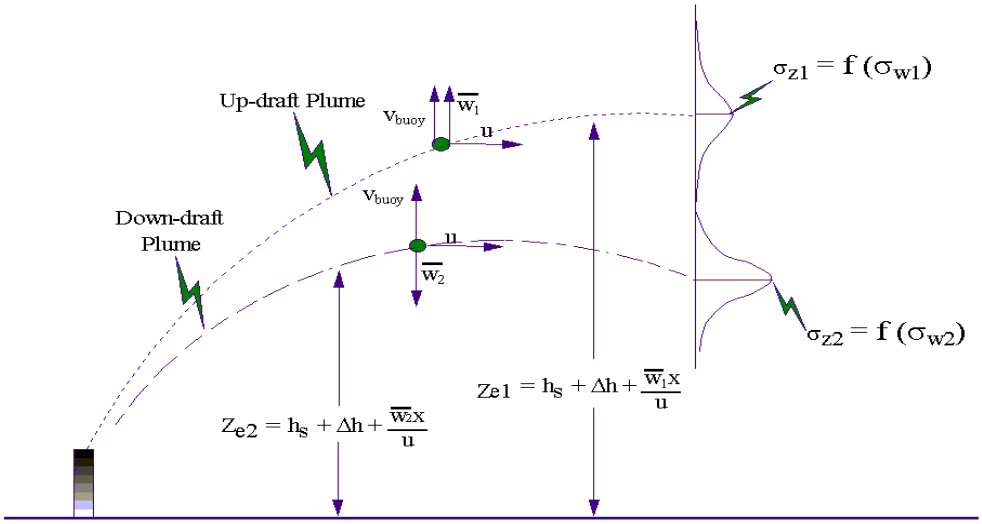

Figure 2-2: AERMOD's pdf approach for plume dispersion in the CBL (source: AERMOD MFD).

The general Gaussian Dispersion Equation, used by many steady-state plume models, is:

$$C(x, y, z; H_e) = \frac{Q}{2\pi\sigma_y\sigma_z u} \cdot \exp\left[-\frac{y^2}{2\sigma_y^2}\right] \cdot \left\{\exp\left[-\frac{(H_e - z)^2}{2\sigma_z^2}\right] + \exp\left[-\frac{(H_e + z)^2}{2\sigma_z^2}\right]\right\} \tag{4}$$

where C is the air pollutant concentration (kg/m^3) at position (x, y, z), Q is the pollutant emission rate (kgs^{-1}), u is the wind speed at the point of release (ms^{-1}), σ_y is the standard deviation of the crosswind concentration distribution at a distance x downstream (m), σ_z is the standard deviation of the vertical concentration distribution at a distance x downstream (m), and H_e is the effective height of the centreline of the plume (m).

The standard deviations σ_y and σ_z are also known as the dispersion coefficients or the dispersion parameters. These coefficients are function of the distance downwind (the plume becomes more spread out downstream), the stability class and the surface roughness. The most widely used dispersion coefficients are the Pasquill-Gilford dispersion coefficients (Turner 1970).

The stability classes are categories of atmospheric turbulence. For many years, the most commonly used method for categorizing the atmospheric turbulence was the method developed by Pasquill (1961). He categorized the atmospheric turbulence into six stability classes named A, B, C, D, E and F with class A being the most unstable or most turbulent class, class D representing a neutral atmosphere, and class F being the most stable or least turbulent class.

AERMOD and many of the more advanced air pollution dispersion models no longer use the simple Pasquill stability classes. Instead, some form of the Monin-Obukhov similarity theory (Venkatram 1980) is used. This theory establishes a relationship describing the vertical behaviour of nondimensionalized mean flow and turbulence properties within the surface boundary layer (the lowest 10% or so of the atmospheric boundary layer, where mechanical generation of turbulence exceed buoyant generation and the friction velocity is nearly constant with height) as a function of the Monin-Obukhov key parameters. These key parameters are the height above the surface, the buoyancy parameter ratio of inertia and buoyancy forces, the kinematic surface stress, and the surface virtual temperature flux.

AERMOD atmospheric dispersion modelling system consists of two pre-processors and the dispersion model. The meteorological pre-processor AERMET provides AERMOD with the meteorological information it needs to characterize the ABL. The terrain pre-processor AERMAP both characterizes the terrain and generates receptor grids for the dispersion model. The steady-state dispersion model AERMOD was designed for short-range dispersion of air pollutant emissions from stationary industrial point, area, and volume sources. It has undergone evaluation utilizing many different datasets (Paine et al. 1998; Perry et al. 2004). Results confirmed that the model performed well in the tested scenarios, which was consistent with the expectations.

AERMOD incorporates the Plume Rise Model Enhancements (PRIME) algorithms (Schulman et al. 2000) for estimating enhanced plume growth and restricted plume rise for plumes affected by building wakes. This algorithm requires additional input to be prepared and included in order to run the models. The Building Profile Input Program (BPIP) was designed to calculate the necessary direction-specific information for all building downwash cases. It is important to note that the buildings are not explicitly modelled in AERMOD (i.e., they do not act like blockages), but only their influence over each source is considered.

There are many studies comparing the accuracy and uncertainty of the results from AERMOD with those from other dispersion models (Caputo et al. 2003; Perry et al. 2004; Hanna et al. 2007; Silverman et al. 2007; Harsham and Bennet 2008; Melo et al. 2012), as well as evaluating the performance of AERMOD for different scenarios (Venkatram et al. 2004; Perry et al. 2004; Orloff et al. 2006; Stein et al. 2007; Zhang et al. 2008; Zou et al. 2010; Seangkiatiyuth et al. 2011). These studies indicate that AERMOD has good performance for a variety of scenarios and suitable for environmental impact assessment.

Perry et al. (2004) presented a test of AERMOD in an urban area, for a single stack near the downtown business district. The results were good and the authors expected the formulation to translate well to other urban areas. Venkatram et al. (2004)

evaluated the performance of AERMOD for estimating ground-level concentrations in the vicinity of small sources located in urban areas. Results showed that pollutant concentrations were overestimated near the sources, since the PRIME algorithm neglects wind meandering. Another possible explanation for this overestimation is that PRIME was designed for buoyant releases, but small sources in urban areas are likely to be non-buoyant. Model improvements are suggested to improve the quality of the results for this type of sources.

Zhang et al. (2008) used AERMOD to estimate annual average concentrations from stationary and mobile sources in the urban area of Hangzhou, China. Simulated concentrations agreed reasonably with observations from several monitoring stations. Concentration was underestimated in two of these stations because the simulations did not consider terrain effects.

Zou et al. (2010) studied the performance of AERMOD in estimating urban concentrations at different time scales. The pollution sources considered were point and mobile emissions along major roads, and the emission rate was obtained by dividing the annual total emissions by the emission time period. Results showed that AERMOD performed well at the annual, monthly, daily and 8h time scales. It is suggested that the results could be further improved if more detailed input data was available, e.g. off-road emissions were not available for the simulation, and the annual emission rate cannot reflect the short-time variations of the emission rates. Building wake effects were not taken into account in the simulations because it would be very time consuming to produce the building data.

AERMOD uses simple text files, called "runstream setup files", to define the simulation options, source locations and parameters, receptor locations, and output options (EPA 2004). Likewise, the results are output in simple text format. The lack of a graphic tool to model the inputs and visualize the outputs makes it quite difficult to model, understand modify and verify the data. Graphic User Interfaces for AERMOD do exist, such as ISC-AERMOD View (Lakes 2008), by Lakes Environmental, and BREEZE AERMOD (Trinity 2008), by Trinity Consultants, but are all under commercial licenses and not openly available for academic use.

The long list of features and validation studies indicate AERMOD as the ideal dispersion modelling software to be studied and used in this research. AERMOD is a well accepted and documented open source tool which can deal with building downwash and uses input and output files that are simple to read and generate. Another important feature, this one common to all dispersion models, is the relatively small amount of input information and computational resources needed to perform dispersion simulations when compared to computational fluid dynamics models. However, more elaborate computational techniques, such as CFD, are required in order to obtain more accurate predictions of plume dispersion and the resulting concentration patterns closer to the sources, where the interaction between the plume and complex structures dominates the plume path and dispersion (Melo et al. 2012).

2.3.2. CFD

Computational Fluid Dynamics or CFD is the analysis of systems involving fluid flow, heat transfer and associated phenomena such as chemical reactions by means of computer-based simulation (Ferzigeer and Peric 1995; Versteeg and Malalasekera 1995). The study of such flows is of prime importance in many sectors of modern engineering, and has great value to practising engineers and researchers of different areas, such as aerospace, architecture, automotive industry, civil engineering, movies and computer graphics, steel industry, turbomachinery, etc. CFD models solve the equations of flow motion, known as the Navier-Stokes equations, within a given geometry and physical context.

CFD techniques are often used to study the wind field and transport of pollutants within urban environments. The standard κ-ε (Sini et al. 1996; Baik and Kim 1999; Chan et al. 2001; Kim and Baik 2001; Jeong and Andrews 2002; Chan et al. 2003; Kim and Baik 2003), renormalization group (RNG) κ-ε (Tsai and Chen 2004; Li et al. 2005) and realizable κ-ε (Jicha et al. 2000) turbulence closure schemes are the most commonly used Reynolds-averaged Navier-Stokes (RANS) models in urban research.

Large Eddy Simulation (LES) is another often used approach to turbulence simulation (Liu and Barth 2002; Baker et al. 2004; Liu et al. 2004; Liu et al. 2005), which is capable of handling the turbulent motions in a transient manner. While many of the CFD results help to elucidate the physical processes within urban areas, the current status of CFD modelling is still far from meeting the needs of assessing and monitoring air quality. A brief overview of the basic theory behind CFD techniques and existing CFD software are presented next.

2.3.2.1. Structure of a CFD Code

CFD codes are structured around the numerical algorithms to solve the fluid flow problem. Commercial packages include user interfaces to input problem parameters and to examine the results. Most CFD codes are composed of three elements: a pre-processor, a solver and a post-processor.

2.3.2.1.1. Pre-Processor

Pre-processing is the input of the flow problem to the CFD program and subsequent transformation of this input into a form suitable for use by the solver. Usually this requires the user to perform the following steps:

- Define the geometry of the region of interest (the computational domain);
- Generate the grid, i.e., sub-divide the domain into a number of smaller, non-overlapping sub-domains (a grid, or mesh, of cells, or control volumes, or elements). The fineness of the grid will determine both the accuracy of a solution and its cost in terms of necessary computer hardware and calculation time;
- Select the physical and chemical phenomena that need to be modelled;

- Define the fluid properties; and
- Specify appropriate boundary conditions at cells which coincide with or touch the domain boundary.

2.3.2.1.2. Solver

There are three different streams of numerical solution techniques: finite difference, finite element and spectral methods. The most used method in commercial environments is the Finite Volume Method (FVM), a special formulation of the Finite Difference Method (FDM) (Versteeg and Malalasekera 1995). The basic steps of a CFD numerical algorithm are:

- Integration of the governing equations of fluid flow over the control volumes of the domain;
- Discretisation, i.e., conversion of the resulting integral equations into a system of algebraic equations. CFD codes contain discretisation techniques suitable for the treatment of the key transport phenomena, convection and diffusion, as well as the source terms and the rate of change with respect to time; and
- Solution of the algebraic equations by an iterative method.

The solver is the core of any CFD software. More details on how it operates will be given in section 2.3.2.3.

2.3.2.1.3. Post-Processor

Post-Processing is the stage of visualization and analysis of the results. CFD packages data visualization tools include:

- Domain geometry and grid display;
- Vector plots;
- Line and shaded contour plots;
- 2D and 3D surface plots;
- Particle tracking;
- View manipulation (translation, rotation, scaling, etc.); and
- Dynamic (animated) result display.

As in many other areas, these graphic output capabilities help the communication of ideas to the non-specialists.

2.3.2.2. Governing Equations

The governing equations of fluid flows represent mathematical statements of the conservation laws of physics:

- The mass of fluid is conserved;
- The rate of change of momentum equals the sum of the forces on a fluid particle (Newton's second law); and
- The rate of change of energy is equal to the sum of the rate of heat addition to the rate of work done on a fluid particle (first law of thermodynamics)

2.3.2.2.1. Navier-Stokes Equations

It is possible to re-write the momentum equations, assuming constant volumetric mass, constant molecular viscosity and using the continuity equation, resulting in the Navier-Stokes equations:

$$\frac{\partial U_i}{\partial t} + U_j \frac{\partial U_i}{\partial x_j} + \frac{1}{\rho} \cdot \frac{\partial P}{\partial x_i} = \nu \cdot \frac{\partial^2 U_i}{\partial x_j^2} + g_i \tag{5}$$

This equation can be viewed as the general transport equation for U_i. Similar principles can be applied to derive extra transport equations, such as the energy equation, or an equation for pollutant transport concentration.

2.3.2.3. CFD Solving

CFD codes solve the Navier-Stokes equations of flow motion within a given geometry and physical context. Numerical solutions are computed over discrete grids representing the domain of interest using different numerical methods. In order to solve the mathematical problem using computers, it first needs to be formulated as a numerical problem amenable to a computer. Boundary and initial conditions must be set to define the variables and close the numerical problem at its boundaries. Many, if not most, flows of engineering significance are turbulent, so the turbulence needs to be represented in some way. Finally, iterative techniques are needed to actually solve the systems of algebraic equations.

2.3.2.3.1. Numerical Discretization Methods

For most cases, an analytical solution cannot be found for the Navier-Stokes equations. Computers must then be used to find a numerical solution to a discretized form of the equations. Discretization is the process of representing the fluid flow at a finite number of points, known as grid points or mesh points, to store an approximate solution on the computer. Any computational solution is only an approximation to the true solution, so it is important to try to estimate the size of the errors in the approximation.

There are different categories of methods for discretization, each one with its own advantages and applications for which it is best suited. These include the finite difference method (FDM), probably the simplest to apply; the finite element method (FEM); the finite volume method (FVM), the natural choice when there is a conservation law; spectral methods, very accurate provided the problem is smooth and the geometry is simple; boundary element methods; and meshless methods. The Finite Volume Method is the most used in commercial CFD implementations. All the CFD simulations performed during the present research used this discretization method.

The Finite Volume Method is one discretization method based around the fact that the governing equations of fluid mechanics can be written in the form of a conservation law. A conservation law states that a particular measurable property of an isolated system does not change as the system evolves, i.e., the rate of change of the amount of that property in a given volume is the rate at which that property flows through the surfaces of the volume. Conservation laws can be written in integral or differential form. In the FDM, the differential forms of the governing and Navier-Stokes equations are discretized, while in the FVM the integral forms are used.

The first step in the FVM is to divide the space into control volumes, where the variable of interest is located at the centroid of the control volume. The governing equations are then integrated over each control volume. Some interpolation is required, since the values are stored in the centre of each volume, but what need to be found are the fluxes at the edges. The resulting discretized equations express the conservation principles for the variables inside the control volume.

2.3.2.3.2. Turbulence Models

Most flows of practical interest are turbulent for at least some of the time. Turbulence both takes energy out of the flow and mixes it, so it is an important parameter to consider when modelling fluid flow or when trying to understand thermal effects or pollutant transport.

There are several classes of turbulence models, from simple low-cost ones to exact and computationally expensive ones. Only the most relevant and well-known models will be briefly discussed here. A more complete list can be found in Versteeg and Malalasekera (1995) or CFD-Online (2008).

2.3.2.3.2.1. Direct Numerical Simulation

A Direct Numerical Simulation (DNS) is a CFD simulation in which the Navier-Stokes equations are numerically solved without any explicit turbulence model. A very fine grid and a very small timestep are needed in order to resolve the smallest length and time scales of turbulence. Even though some work has been done using DNS, it is still impractical for most problems, and will definitely not be used in the present research. DNS was impossible 30 years ago, so other methods were devised.

2.3.2.3.2.2. RANS

The Reynolds Averaged Navier-Stokes (RANS) equations provide a time average leading to a statistically steady description of the turbulent flow. For comparison with wind tunnel experiments, this is considered an adequate representation of wind tunnel's reality as the time averaged flow conditions of the tunnel do not change.

The κ-ε model is one of the most used RANS turbulence models. It is a two equation model, i.e., it includes two extra transport equations to represent the turbulence properties of the flow. The first transported variable is the turbulent kinetic energy, κ, which determines the energy in the turbulence. The second transported variable is the turbulent dissipation, ε, which determines the scale of the turbulence.

This model gives a realistic representation for many relevant flows without being too expensive (two extra partial differential equations), but it can have poor performance in a variety of important cases. There are a few variations of this model, such as the standard κ-ε (Tennekes and Lumley 1972), the RNG (Renormalization Group) κ-ε (Yakhot et al. 1992), and the realisable κ-ε. Recent research expanded the capability of simple two equations RANS models to predict mean concentrations, concentration variances and peak concentrations necessary to estimate short time exposures from near ground point releases in complex terrains (Efthimiou et al. 2011). These results further strengthen the evidence that the RANS approaches are capable of dealing properly with dispersion phenomena in complex urban scenarios.

2.3.2.3.2.3. Large Eddy Simulation

Large Eddy Simulation (LES) is becoming a popular technique for the simulation of turbulent flows. An implication of Kolmogorov's theory of self similarity is that the large eddies of the flows are dependent on the geometry while the smaller scales are more universal (Smagorinsky 1963). This lead to the idea of directly resolving the large scale eddies present in turbulent flows and modelling the smaller scale ones using a subgrid-scale model (SGS model).

Instead of time-averaging, LES uses a spatial average. In LES, direct calculations are used to resolve the eddies that are larger than the size of the finite volume cell, while a simple model is used to model the eddies that are smaller than the mesh size. This results in an extra term in the Navier-Stokes equations, in a similar way to RANS models. LES have several restrictions, which end up resulting in computational times at least an order of magnitude greater than the ones required for RANS simulations. For this reason, this turbulence model, although being increasingly used in urban scenario simulations, is also unlikely to be used in the development of the present work. There are also hybrid RANS-LES approaches, such as the Detached Eddy Simulation (DES), but the computational cost makes their use prohibitive for the intended scenarios.

2.3.2.4. CFD Models for the Transport of Pollutants

CFD dispersion models generally adopt either Lagrangian or Eulerian approaches. The difference between the two lies in the way in which the position in the field is identified.

2.3.2.4.1. Lagrangian Models

Particle tracking methods are extremely popular for modeling the Lagrangian dispersion characteristics of pollutants in a variety of fluid flow fields due to their flexibility and ease of use (Li et al. 2006). In the Lagrangian Particle Dispersion (LPD) approach, the turbulent transport is modelled by tracing the trajectories of a large number of particles as they are advected with the air flow, which is generated in prior by a wind field model and represented by mean flow and turbulent fluctuations. The release of particles may be either sequential (as a plume) or simultaneous (as a puff). Concentration fields are determined from the spatial distribution of particles. The LPD models are convenient tools to describe the pollutant transport phenomena especially when the time dependent wind field data are obtained.

2.3.2.4.2. Eulerian Models

Eulerian models for pollutant dispersion involve the solving of an advection-diffusion equation of conserved scalars (e.g. mean concentration or mass fraction) for a set of receptors in 2D or 3D computational domains. Eulerian models can manage the production and loss terms, which may include exchanges with the surrounding grid elements, emissions, chemical transformations, and dry and wet deposition. Eulerian models are appropriate for describing long-range transport with chemical reactions and transformations.

With the ever-increasing computer power, most of the advanced CFD models currently can simultaneously solve the advection-diffusion equation of conservative scalars coupled with the Navier-Stokes equations describing the wind field, with either RANS models (Jeong and Andrews 2002; Chan and Stevens 2004; Santiago and Martín 2005) or LES models (Chan and Stevens 2004; Liu et al. 2005).

2.3.2.4.3. Hybrid Models

To fully utilize the advantages of both Eulerian and Lagrangian models, hybrid models were developed by combining a Lagrangian particle model with an Eulerian model. It seems that these hybrid models can provide a new and unique approach for the next generation of chemistry-transport coupled models (Li et al. 2006).

Hybrid models have two main applications. One is to adopt the Lagrangian approach to deal with the subgrid-scale aspects of pollutant release while using the Eulerian approach to take over when the pollutant is dispersed to a degree that it is adequately resolved on the applied computational grid. The other application is to model the dispersion of pollutants released from moving sources, such as vehicles (Jicha et al. 2000).

2.3.2.5. CFD Modelling of the Atmospheric Boundary Layer

It has been said that the Atmospheric Boundary Layer extends for a considerable distance above the Earth's surface relative to the average building height. For many wind engineering applications only the lower 200m or less of this layer is of interest. Moreover, CFD models can only represent a small, finite distance because of hardware limitations and the complexity of including a meteorological model, so the ABL needs to be modelled in some way (Hargreaves and Wright 2007). Similarly, smaller scale features such as vegetation and small buildings cannot be included in the computational grid and therefore are represented by a roughness model. For most RANS (Reynolds-Averaged Navier-Stokes) closure models, such as the κ-ε turbulence model, the surface roughness is incorporated through a wall function approach that is based on boundary-layer theory for the computational cell immediately adjacent to the wall. Turbulence models are introduced to model all the turbulent motions.

RANS approaches have been the most widely used models in general CFD applications and also in wind engineering and near-field dispersion problems in the last decade. Because of their computational robustness and efficiency, the mainly used turbulence models are the standard κ-ε turbulence model (Sini et al. 1996; Chan et al. 2001; Jeong and Andrews 2002; Chan et al. 2003; Solazzo et al. 2009) and its variants, RNG κ-ε model (Kim and Baik 2004; Li et al. 2005; Santiago and Martín 2005; Xie et al. 2007), and the realizable κ-ε model (Jicha et al. 2000; Chan et al. 2002). According to Li et al. (2006), other RANS models, e.g., Reynolds Stress Models (Gromke et al. 2008) and Spalart-Almaras, have been used in some studies, to compare with κ-ε. These RANS models, however, are not widely used in street-canyon pollution research.

The advances in computer power are allowing the use of other approaches, such as Large Eddy Simulation (LES), to be increasingly being applied to wind engineering problems (Chan and Stevens 2004; Liu et al. 2005; So et al. 2005; Letzel et al. 2008). LES techniques require less computational effort than Direct Numerical Simulation (DNS) methods, but more than RANS methods. However, LES might prove too time-consuming for the scale proposed in the current research, i.e. whole cities or neighbourhoods, and the desired fast simulation times. Even though RANS can only determine mean fields, it is the natural choice when a quick and reasonable solution is desired.

Much of the mentioned modelling, whether using RANS or LES models, has been conducted with the buildings embedded in a neutral ABL because buoyancy-induced turbulence need not be modelled. However, there has always been an underlying problem in that the ABL has often not been modelled in a standard or reproducible manner.

Richards and Hoxey (1993) have addressed the modelling of the ABL using CFD. Their approach is based on a set of assumptions about the ABL, which they use to derive formulae for the velocity and turbulence quantities, producing a set of boundary conditions to ensure an homogeneous boundary layer. From Ludwig and Sundaram (1969), Richards and Hoxey get their basic conditions for simulating the atmospheric boundary layer: *"… regardless of the manner of its generation, any flow that is fully aerodynamically rough, horizontally homogeneous, and relatively free from any pressure gradients, constitute a suitable model for the atmospheric surface layer."*

They assume that in steady incompressible 2D flow modelling of the ABL using the κ-ε turbulence model, the existence of homogeneous flow has the following implications:

i- The vertical velocity is zero
ii- The pressure is constant in both the vertical and streamwise directions
iii- The shear stress is constant

i.e. $$\mu_t \frac{\partial u}{\partial z} = \tau_0 = \rho u_*^2 \tag{6}$$

where μ_t is the turbulent viscosity, u is the streamwise component of the wind speed, ρ is the air density, and u_* is the friction velocity.

iv- The turbulent kinetic energy κ and the dissipation rate ε satisfy their respective conservation equations, which reduce to (reformulated by Hargreaves and Wright 2007):

$$\frac{\partial}{\partial z}\left(\frac{\mu_t}{\sigma_k}\frac{\partial \kappa}{\partial z}\right) + G_\kappa \frac{\varepsilon}{\kappa} - \rho\varepsilon = 0 \tag{7}$$

and $$\frac{\partial}{\partial z}\left(\frac{\mu_t}{\sigma_\varepsilon}\frac{\partial \varepsilon}{\partial z}\right) + C_{\varepsilon 1} G_\kappa \frac{\varepsilon}{\kappa} - C_{\varepsilon 2}\rho\frac{\varepsilon^2}{\kappa} = 0 \tag{8}$$

where the production of turbulent kinetic energy is given by

$$G_\kappa = \mu_t \left(\frac{\partial u}{\partial z}\right)^2 \tag{9}$$

and the turbulent viscosity is given by

$$\mu_t = \rho C_\mu \frac{\kappa^2}{\varepsilon} \tag{10}$$

and σ_κ, σ_ε, $C_{\varepsilon 1}$, $C_{\varepsilon 2}$ and C_μ are model constants, usually assigned the values 1.0, 1.3, 1.44, 1.92 and 0.09.

Richards and Hoxey then suggest that these may be satisfied by using

$$u = \frac{u_*}{K} \ln\left(\frac{z + z_0}{z_0}\right) \tag{11}$$

$$\kappa = \frac{u_*^2}{\sqrt{C_\mu}} \tag{12}$$

$$\varepsilon = \frac{u_*^3}{K(z + z_0)} \tag{13}$$

where K is the von Karman's constant and z_0 is the surface roughness length.

Eq. (11) is a standard representation of the log wind profile in the ABL. Richards and Hoxey found that Equations (11)-(13) automatically satisfy Eq. (7), but they only satisfy Eq. (8) when

$$\sigma_\varepsilon = \frac{K^2}{(C_{\varepsilon 2} - C_{\varepsilon 1})\sqrt{C_\mu}} \tag{14}$$

which gives a value of $\sigma_\varepsilon = 1.11$ when $K = 0.4$.

However, Hargreaves and Wright (2007) use the contrived situation of a completely empty fetch to demonstrate that Richards and Hoxey's inlet boundary conditions by themselves are not sufficient to produce a sustainable ABL when using the κ-ε turbulence model. This empty fetch is justifiable on the grounds that most CFD modelling of the ABL have a domain in which there is a sizeable upstream fetch. In such situations, invariably the inlet velocity and turbulence profiles will have changed before the building is reached, which might explain some of the discrepancies between the results from CFD modelling and experimental measurements.

The difference between the results obtained by commercial software and Richards and Hoxey is in the treatment of the turbulence kinetic energy and dissipation rate in the cell next to the ground. Modifications to wall boundary condition and the boundary at the top of the domain are required to produce the sustainable ABL of Richards and Hoxey. Similarly, the laws of the wall that appear in commercial CFD software require complex modifications before they can be successfully used to sustain an ABL along an empty fetch.

Many wind engineers adopt only a subset of the Richards and Hoxey boundary conditions (i.e., those at the inlet) and assume that the boundary layer will be maintained up to the point at which the building is encountered. If an unmodified commercial code is being used, then as short a fetch as possible is in fact more desirable (Blocken et al. 2007; Hargreaves and Wright 2007), reducing any changes in the profile introduced by using a longer fetch.

Hargreaves and Wright (2007) also show that it is not sufficient to rely on a law of the wall originally intended for smooth or sand grain-type roughness walls to model a portion of the much larger ABL. Ideally, two types of wall functions should be provided: one for smooth walls, such as buildings, and one for the ground. Further into wall function problems, Blocken et al. (2007) show how the accuracy of CFD simulations for atmospheric studies can be compromised when wall-function roughness modifications based on experimental data for sand-grain roughened pipes and channels are used. The explicit modelling of the roughness elements as rectangular blocks, using wall functions to model the small-scale roughness of the surface of these blocks, and the use of variable height of wall-adjacent cells are possible measures to rectify the problems. However, no measure was found to be totally satisfactory. Yang et al. (2009) introduces a new set of inflow turbulence conditions theoretically derived for the standard κ-ε model and verifies its capability to model an equilibrium ABL.

2.3.2.6. CFD Software

There are several well-established software for meshing, CFD solving and visualization of results. This section describes briefly the computational tools studied and used in this research.

2.3.2.6.1. Commercial CFD

ANSYS CFX (2008) software is a powerful and flexible general-purpose computational fluid dynamics (CFD) package used for engineering simulations of all levels of complexity. It offers a comprehensive range of physical models that can be applied to a broad range of industries and applications. It has been applied to the simulation of water flowing past ship hulls, gas turbine engines (including the compressors, combustion chamber, turbines and afterburners), aircraft aerodynamics, pumps, fans, heating, ventilation and air conditioning (HVAC) systems, mixing vessels, hydrocyclones, vacuum cleaners, and more.

ANSYS CFX takes advantage of data and information common to many simulations. This begins with common geometry: Users can link to existing native computer-aided design (CAD) packages as well as create and/or modify CAD models in an intuitive solid modelling environment. Complementing the common geometry model is a suite of meshing tools, designed to ensure easy generation of the most appropriate mesh for the given application. ANSYS CFX tools then guide the user through the setup of operating conditions, selection of materials and definition of models.

The ANSYS CFX solver uses the most modern solution technology with a coupled algebraic multi-grid solver and extremely efficient parallelization to help ensure that solutions are ready for analysis quickly and reliably. Solution analysis with the ANSYS CFX post-processor then gives users the power to extract any desired quantitative data from the solution; it also provides a comprehensive set of flow visualization options. Animations of flow simulations are easily generated, and 3-D images can be directly created and shared with any colleagues or clients using the freely-distributable 3-D viewer from ANSYS CFX.

Similar to CFX, Fluent (2008) is a general-purpose CFD code based on the finite volume method on a collocated grid. Fluent technology offers a wide array of physical models that can be applied to a wide array of industries. Fluent can treat turbulence, dynamic and moving meshes, acoustics, reacting flows, heat transfer, phase change, radiation, multispecies flows. Users can post-process their data in Fluent software, creating contours, pathlines, and vectors to display the data.

CFX and Fluent are well-established commercial CFD software. Most of the experiments conducted during this work were done using CFX. The main reasons were the training in CFX the author received during the module H24CFD – Applied Computational Fluid Dynamics, and the reliability and documentation provided for the software.

2.3.2.6.2. Open Source CFD

The OpenFOAM (Open Field Operation and Manipulation) CFD Toolbox (OpenCFD 2007) is a general purpose open source CFD code. It can simulate anything from complex fluid flows involving chemical reactions, turbulence and heat transfer, to solid dynamics, electromagnetics and the pricing of financial options. OpenFOAM is produced by OpenCFD Ltd and is freely available, licensed under the GNU General Public Licence.

The core technology of OpenFOAM is a flexible set of C++ modules. A wide range of solvers, to simulate specific problems in engineering mechanics, is implemented. OpenFOAM relies on the user's choice of third party pre- and post-processing utilities, but provides utilities to perform tasks such as mesh conversion, import and export to a number of leading commercial packages for the visualization of solution data and meshes.

OpenFOAM is supplied with numerous pre-configured solvers, utilities and libraries and so can be used like any typical simulation package. However, it is open, not only in terms of source code, but also in its structure and hierarchical design, so that its solvers, utilities and libraries are fully extensible.

2.3.2.6.3. Meshing

GAMBIT (2007) is a single, integrated pre-processor for Computational Fluid Dynamics analysis. The acronym stands for Geometry And Mesh Building Intelligent Toolkit. GAMBIT is Fluent's geometry and mesh generation software. GAMBIT's single interface for geometry creation and meshing brings together most of Fluent's pre-processing technologies in one environment.

Most models can be built directly within GAMBIT's solid geometry modeller, or imported from any major CAD/CAE system. Using a virtual geometry overlay and advanced cleanup tools, imported geometries can quickly be converted into suitable flow domains for Fluent, CFX or any other CFD software. GAMBIT also has a boundary layer mesher for growing optimum grid cells off walls, and tools for mesh quality examination and boundary zone assignment.

The mesh generation utility *blockMesh*, supplied with OpenFOAM, creates parametric meshes with grading and curved edges. The principle behind *blockMesh* is to decompose the domain geometry into a set of three dimensional hexahedral blocks. Each block of the geometry is defined by 8 vertices, which are written in lists contained in dictionary files. The utility reads this dictionary file, generates the mesh and writes out the data to points, faces, cells and boundary files.

A dictionary file is a simple text file used by OpenFOAM to define geometries or to setup simulation parameters. While the idea is easy to understand, it is very difficult to create dictionaries for complex mesh generation without a graphical user interface.

Another OpenFOAM mesh generation utility is *snappyHexMesh*, which can generate three dimensional meshes containing hexahedra and split-hexahedra automatically from triangulated surface geometries in Stereolithography (STL) format. The mesh approximately conforms to the surface by iteratively refining a starting mesh (generated by the *blockMesh* utility) and morphing the resulting split-hex mesh to the surface. The meshing process is controlled by switches defined in the appropriate dictionary file.

2.3.2.6.4. Data Visualization

ParaView (Kitware 2008) is an open-source, multi-platform data analysis and visualization application. Users can quickly build visualizations to analyze their data using qualitative and quantitative techniques. The data exploration can be done interactively in 3D or programmatically using ParaView's batch processing capabilities.

ParaView is built on top of the Visualization Tool Kit (VTK) libraries (Martin et al. 2008), which provide visualization services for data, task, and pipeline parallelism. It provides many tools for scientific visualization, but the most commonly used are: isocontouring, clipping, cutting, volume rendering, thresholding, subsetting, and picking.

VisIt (LLNL 2008) is another free interactive parallel visualization and graphical analysis tool, very similar to ParaView. It can be used for viewing scientific data on UNIX and PC platforms. Users can quickly generate visualizations from their data, animate them through time, manipulate them, and save the resulting images for presentations. VisIt contains a rich set of visualization features so that the user can view data in a variety of ways. It can be used to visualize scalar and vector fields defined on two- and three-dimensional (2D and 3D) structured and unstructured meshes.

Either tool could be used just as easily to visualize both CityZoom UP and OpenFOAM generated data, using VTK format files, as described on Chapter 3.

2.4. Modelling Concerns

Many environmental characteristics can affect the dispersion of pollutants in urban scenarios. Building configuration, street canyon aspect ratio, ambient wind direction, and source positions and emission rates play major roles in the resulting concentration of pollutants within urban areas. These characteristics and their effects are discussed in this section.

2.4.1. City Geometry

The building configuration of a city affects the ambient wind direction and speed, leading to changes in the way pollutants are dispersed in the urban environment. Two main structures are identified: street canyons and street intersections.

2.4.1.1. Street Canyons

A street canyon generally refers to a relatively narrow street in-between buildings that line up continuously along both sides (Figure 2-3). It constitutes one of the basic geometric units of urban areas. This unit is also bounded by the ground surface at the bottom and the roof level at the top.

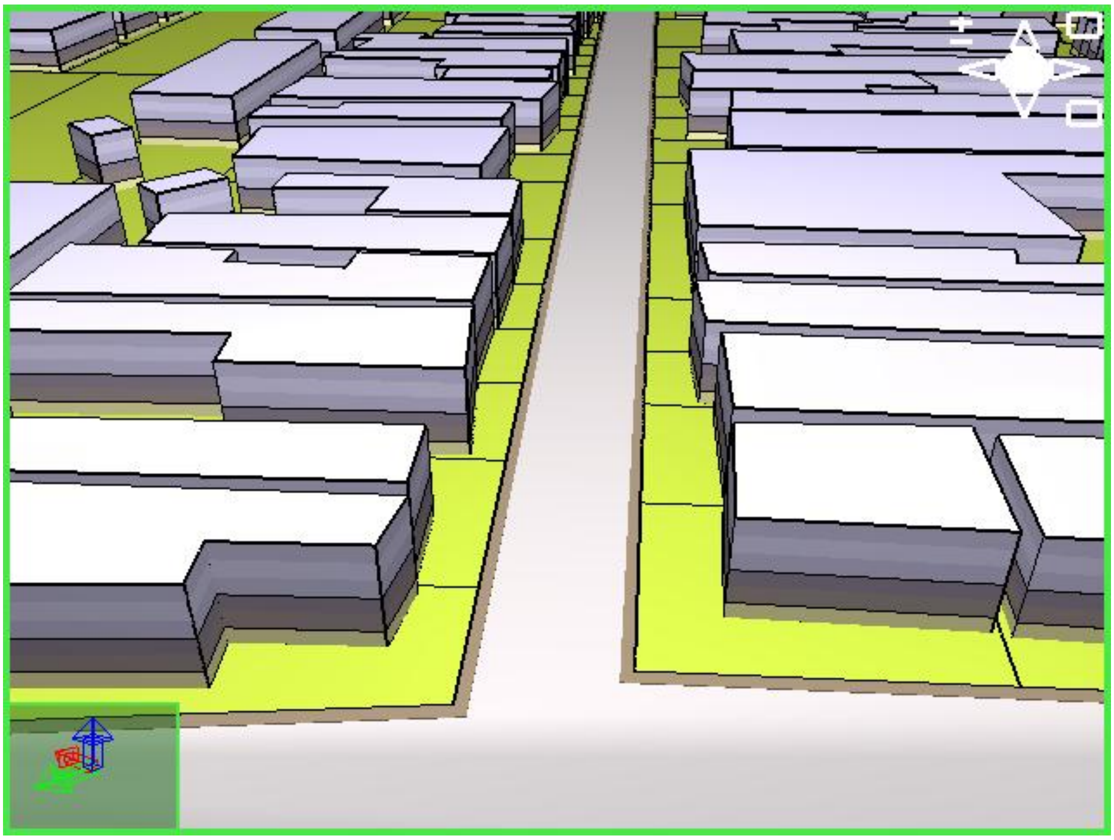

Figure 2-3: Representation of a typical street canyon (generated by CityZoom UP).

Depending on the angle the wind makes with the canyon, complex vortex patterns may exist inside the canyon with obvious consequences for the mixing of the pollutant released from vehicles on the road. From the point of view of pedestrian health (if not comfort), it would be preferable if the noxious gases could be flushed from the canyon by the resident airflow (Hargreaves 1995).

There are several known works on street canyons. In one of the most cited papers in the urban wind engineering literature, Oke (1988) introduces the idea of aspect ratio and the resulting flow regimes for different aspect ratios. He considered that:

- the street canyon is the basic geometric unit. It can be approximated by a two-dimensional cross-section, i.e., neglect street junctions and assume the buildings flanking the canyon are semi-infinite in length;
- the urban cross-section is approximated by a simple repetition of these street canyon units; and
- the predominant airflow direction is approximately normal (±30°) to the long axis of the street canyon.

According to Oke, the city geometry can be described by the aspect ratio *H/W* (where *H* is the average height of the canyon walls and *W* is the canyon width) and the building density $\zeta = A_r/A_l$ (where A_r is the plan or roof area of the average building and A_l is the plot area or unit ground area occupied by each building).

The wind flow pattern inside street canyons depends on their geometry, in particular, the aspect ratio. Oke identified three flow regimes for wind direction perpendicular to the street axis. If the buildings are well apart ($H/W < 0.05$) their flow fields do not interact. At a bit closer spacings ($0.05 < H/W < 0.3$), such as Figure 2-4(a), the wakes are disturbed, but the buildings do not interact and the flow is called “isolated roughness flow” (IRF).

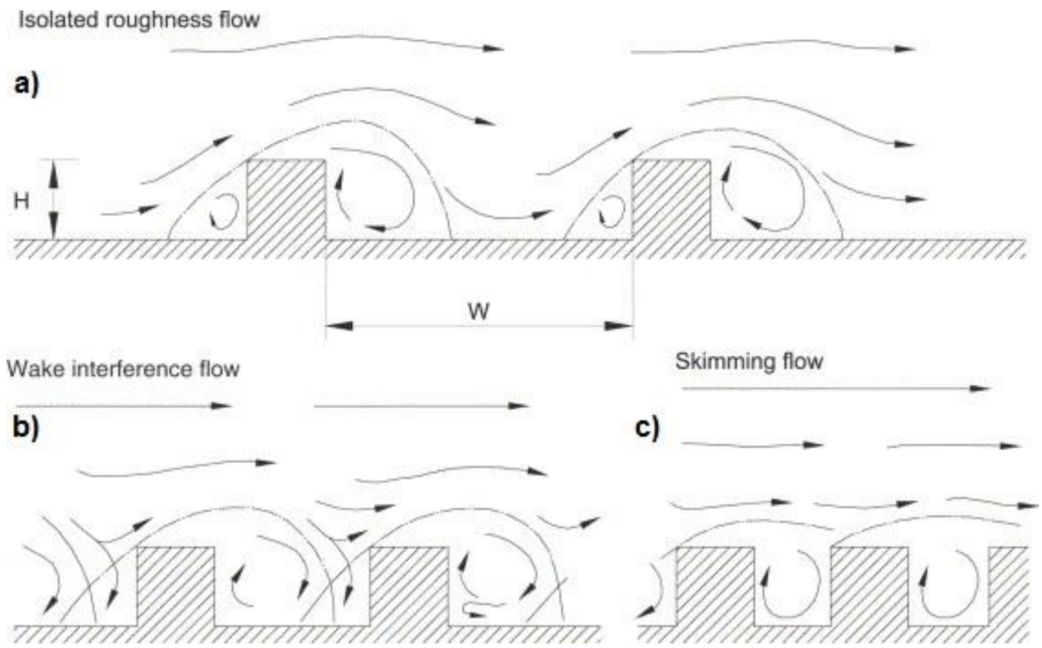

Figure 2-4: Three flow regimes associated with air flow over different building aspect ratios H/W (after Oke, 1988).

When the height, spacing and density of the array combine to disturb the bolster and cavity eddies ($0.3 < H/W < 0.7$), the regime changes to one referred to as "wake interference flow" (WIF, Figure 2-4(b)). At even greater aspect ratios ($H/W > 0.7$) and density, a stable circulatory vortex is established in the canyon and transition to a "skimming flow" (SF) regime occurs where the bulk of the flow does not enter the canyon (Figure 2-4(c)). Under this circumstance the vehicular pollutants at the street level could not be easily ventilated resulting in high pollutant concentration and poor air quality.

Most of the pollutant transport studies focus on the skimming flow regime because it provides minimal ventilation and is relatively ineffective in removing pollutants (Li et al. 2006). Many metropolises, like New York and Hong Kong, suffer from this flow situation which leads to poor air quality within street canyons.

The street canyon aspect ratio not only influences the flow regimes (SF, WIF, IRF) but also characterizes, together with the *L/H* aspect ratio (street length to building height), different flow patterns within the same flow regime. Several studies with the flow patterns as a function of the *H/W* and *L/H* ratios aimed at identifying optimum urban canyon geometries for efficient dispersion of pollutants. Some of these studies are presented next.

DePaul and Sheih (1986) used photographic observations of small tracer balloons to determine the velocity flow field in an urban street canyon. Lee and Park (1994) studied twenty seven cases of different aspect ratio street canyons and found out that for very high aspect ratios ($H/W > 2.7$) a secondary vortex is formed in the lower part of the street canyon.

The studies of Sini et al. (1996) showed that in very narrow streets the main vortex is offset to the upper part of the canyon and gives place to one ($W/H = 0.51$, Sini used the width to height ratio) or even two ($W/H = 0.33$) additional stretched and weak vortices in the lower part. This multi-vortex version of the skimming flow regime results in a high reduction factor of the horizontal wind speed and produces excellent sheltering effect at pedestrian level. The rather weak turbulence intensity and very slow advective transport that characterize the lower vortex region also act to protect efficiently the pedestrian level from pollutant penetration from the roof level. However, the main source of urban pollution comes from the street level, hence the pedestrians can get caught in a region of high pollution which is not very well ventilated.

Jeong and Andrews (2002) described the critical canyon aspect ratios that distinguish a cascade of vortex patterns that form in an urban street canyon. They investigated the mean flow, turbulent kinetic energy, turbulent eddy viscosity, turbulent length scale, and Reynolds stress for the aspect ratios $W/H = 1.0$, 0.5 and 0.3, using a κ-ε turbulence model. The schematic diagram of the computational domain modelled is shown in Figure 2-5.

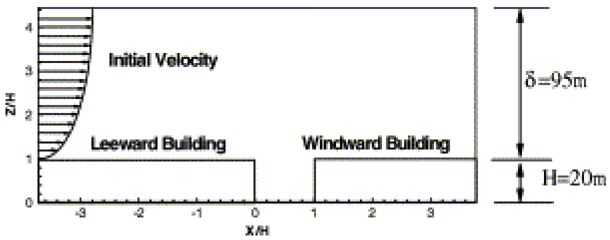

Figure 2-5: Schematic diagram of computational domain of (Jeong and Andrews 2002).

They found the critical *W/H* of the two and three vortex regimes to be in the range from 0.325 to 0.35 (mean 0.33) and one and two vortex regimes in the range from 0.625 to 0.65 (mean 0.63). In a one vortex regimes for *W/H* > 0.63, at the critical point of 0.63, a weak vortex appears in the leeward and windward lower corner of the street canyon. In the two and three vortex regimes, the lower part of the street canyon has weak counter-rotating vortices. These weak vortices, and the transition region between vortices, inhibit local pollutant exchange creating a mean flow stagnant zone. The very weak third vortex produced by some RANS models (Kim and Baik 2001; Jeong and Andrews 2002) has not yet been confirmed by water channel (Baik et al. 2000) or wind tunnel (Kovar-Panskus et al. 2002) studies. Selected computational results for streamlines that occur near vortex transition regions are shown in Figure 2-6.

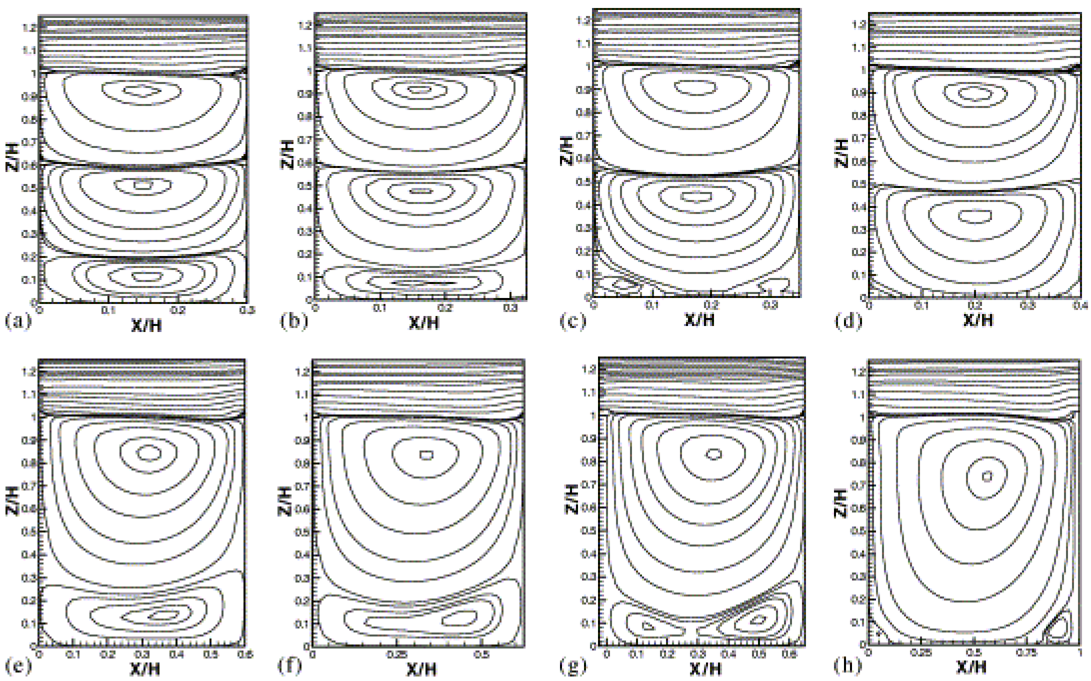

Figure 2-6: Selected streamlines of the near transition flow regions of (Jeong and Andrews 2002). (a) *W/H*=0.3, (b) *W/H*=0.325, (c) *W/H*=0.35, (d) *W/H*=0.4, (e) *W/H*=0.60, (f) *W/H*=0.625, (g) *W/H*=0.65 (h) *W/H*=1.0.

The urban street canyon is, in fact, the most common structure in urban areas and, even today, the most studied one (Nunez and Oke 1977; DePaul and Sheih 1986; Baik and Kim 1999; Santiago and Martín 2005; Xie et al. 2005; Gromke et al. 2008; Taseiko 2009). The understanding of the flow patterns within these canyons is of great importance to develop algorithms to assess such flows and their effects. The relationship between the parameters described, such as aspect ratio, and their resulting flow regimes (Lee and Park 1994; Kim and Baik 2004) can be used to create a database (Liu and Barth 2002; Liu et al. 2004; Liu et al. 2005) or as a guide for heuristic approaches. These can then be used to speed up CFD calculations for already known or similar scenarios.

Most studies of street canyons (Kim and Baik 2001; Xie et al. 2007; Oliveira Panão et al. 2009) use 2D or quasi-2D approaches, driven by perpendicular flow, characterizing the worst case scenario. However, both the turbulence and the flow in urban scenarios are fully 3D (Gromke et al. 2008; Letzel et al. 2008), so the dispersive fluxes along canyon direction are not negligible, and 3D models should be used for turbulence simulations.

2.4.1.2. Street Intersections

Street intersections are common geometries in realistic city scenarios. In fact, the street canyon intersection is considered the focus of the DAPPLE project (Arnold et al. 2004) as it provides the basic urban topography to demonstrate most of the factors that will apply in a different urban situations. Street intersections can introduce lateral eddies into street canyons and create low-pressure zones, which will suck the nearby flow and greatly modify the air flow inside the canyon and affect pollutant distribution (Li et al. 2006). Belcher (2005) also analysed the mixing and transport at street intersections, and acknowledged the importance of such urban geometry in the lateral dispersion.

Soulhac et al. (2001) showed that at the intersection part of the flow separated and was diverted into one of the side streets, while an equal flow entered the intersection on the opposite side, coming from the other side street. This complicated flow pattern had an important influence on the dispersion and mixing within the intersection, making the pollutant concentrations vary significantly around the intersection.

Chan et al. (2003) observed that the introduction of a crossroad between buildings produces a very distinct wind profile within the street canyon. The regimes described by Oke (1988) are no longer valid for commenting the flow inside the canyon. Crossroads introduce a horizontal path for the pollutants to disperse away, resulting in an overall reduction in retention values as compared to continuous canyons.

The inherent 3D and intermittent nature of the flow in urban scenarios, coupled to the lateral dispersion provided by street intersections, only reinforce the affirmative that 3D models need to be used to simulate such scenarios. Letzel et al. (2008) identified potential weaknesses in his study, using the commonly accepted methodologies, and suggested *"further research with realistic boundary layer depths, inflow-outflow boundary conditions with turbulent inflow, an ensemble of different approaching wind directions, and different roof geometries"*, ideas similar to the ones sought in the present work.

2.4.2. Sources of Pollutants

Air pollution arises from a series of human activities. To a large extent the various sources emit the same compounds, only in different proportions (Fenger et al. 1998). Stationary sources, such as public power and heating plants, industrial plants and processes and waste incineration plants, contribute to urban pollution. However, being usually located in the outskirts of the cities and equipped with high stacks, their impact is much smaller at street level than that from mobile sources, such as automobiles and buses.

In fact, vehicular emission is one of the major sources of anthropogenic pollutants in urbanized cities. The large amount of vehicular pollutants emitted at the ground level considerably deteriorates the local air quality and imposes direct impacts on human health.

Unlike the free stream over the buildings, the wind flow and pollutant transport within street canyons are complicated by the surrounding high-rise buildings and narrow streets geometries (Liu et al. 2005). It is important to find out how these pollutants are transported and distributed in street canyons, so that design parameters and urban planning strategies can be modified to ease the air pollution problems at pedestrian level and along building walls.

Chan et al. (2001) showed that the source position *s/w* (distance *s* from the windward building relative to the canyon width *w*) has little effect on the canyon flow. However, it does affect substantially the dispersion process. The study reveals that no matter where the source position is located, concentrations are highest at the base of the leeward wall. While the source position may not have a direct relation in promotion of urban geometry planning, it is recommended that heavily polluting firms or sites are positioned at the leeward side of street canyons.

The quality of simulation results is proportional to the quality and level of detail of the available emission data (Zout et al. 2010), but it is not feasible to measure traffic emissions in real conditions for every road. As a rule, emissions are calculated based on traffic data and vehicle specific emission factors (Berkowicz et al. 2006). Different methods and models (Hickman et al. 1999; Coelho et al. 2005) exist to determine emission factors. A deeper study of such models would be needed in order for them to be used with the dispersion and CFD models proposed by the present research. The study of these models is not part of the objectives of this research, so measured and user-defined emission data are instead used for the tests.

2.4.3. Ambient Wind

The effect of ambient wind is an extensively studied problem in street-canyon research. Nunez and Oke (1977) discussed how the advection contributions were dependant on the wind direction and speed. The higher the wind speed, the more effectively the pollutants tend to be diluted.

Most studies focus on the wind perpendicular to the street axis, because this is the worst situation for air pollutants to dilute from street canyons. Kim and Baik (2004) used a model with RNG κ-ε turbulence scheme to investigate the effects of ambient wind direction on flow and dispersion in urban areas. They demonstrated that changes in the ambient wind direction could make large differences in the mean flow recirculation and hence the pollutant distributions.

Different wind speed and directions generate differences in the flow and are important for the CFD analysis of wind flow and dispersion in urban environments. The automation of CFD simulation for different wind directions reduces the modelling and simulation times (Morvan et al. 2007), making this a desirable feature for the present work.

2.4.4. Other Contributing Factors

While many studies have focused on the effects of the wind as the main process driving the dispersion of pollutants in street canyons, there are also other contributing factors, far less understood. The turbulence-inducing motion of traffic and temperature differences (due to insolation and vehicle heat) are two important factors that can modify the flow pattern in urban scenarios and, consequently, affect the pollutant dispersion.

Considering the nature of CityZoom (detailed in section 2.5.3), it would make sense to account for the thermal effects of solar radiation on building facades. However, due to the complexity of the problem, it is not possible to actually address such parameters during the development of the research. The importance of these factors is acknowledged and a brief review of the work done in the area is presented next.

2.4.4.1. Traffic-Induced Turbulence

Vehicular traffic plays a significant role in altering the flow patterns around traffic constructions, such as tunnels, street intersections and urban street canyons (Jicha et al. 2000). Traffic induced flow rate and turbulence have important influence in the mixing processes in the proximity of traffic paths within the canopy layer, namely in very low wind speed situations. Moving vehicles intensify both micro- and large-scale mixing processes by inducing turbulence and enhancing advection by entraining masses of air in the direction of vehicle motion.

Jicha et al. (2000) simulated different traffic situations and showed the effects of one- and two-way traffic and traffic rates per lane on the pollutant dispersion. Turbulence was modelled using a non-linear low-Reynolds κ-ε model. The traffic-induced turbulence was modelled as additional kinetic energy induced by the moving objects, and added as an additional source to the κ-equation. Considering that turbulence is induced mainly in the wake behind the vehicle, the additional sources were added only in the control volumes along the trajectories of the vehicles.

Xia et al. (2006) simulated the flow-field around moving objects in street canyons, based on characteristic parameters, such as vehicle speed, canyon width, and distance between objects. A parametric study was carried to investigate the influence of these parameters on the wake of the moving objects.

The study by Solazzo et al. (2008) presented a CFD modelling methodology for the simulation of the flow and turbulence induced by wind and vehicle motion within street canyons. First they account for the vehicle's motion without the ambient wind. The resulting boundary conditions of flow and turbulence are then used to model the combined effects of wind and vehicular traffic in the street canyon. The interaction of the two flow fields could be studied in detail. Their methodology allowed overcoming the simplifications adopted in previous studies by explicitly simulating the mechanical processes generating flow and turbulence in the street. The methodology is also computationally efficient when compared to more demanding approaches.

2.4.4.2. Thermal effects

Over the last decades, most of the studies conducted on flow and pollutant dispersion in street canyons were under isothermal conditions. There are, in fact, very few studies that include thermal effects. However, the thermal effects are an important factor affecting street canyon wind flow and pollutant transport. Direct solar radiation on building facades and ground surfaces heat up the air in the vicinity, influencing the air motion and wind structure in the canyons (Xie et al. 2007).

In 1977 Nunez and Oke (1977) investigated the energy exchanges occurring within an urban canyon, considering not only the energy balances of each of the canyon component surfaces (walls and floor), but also the balance of the canyon system and of the air volume contained therein.

There was, at the time, no comprehensive study concerning the surface energy balance of urban areas. The most common approach was to treat the city from a holistic point of view, i.e., ignore the exact nature of the surfaces and to treat the canyon as an integrated system. The energy and mass flows were assumed to relate to some datum height at about roof level, leaving the workings of the urban atmosphere below this datum as a "black box". However, the study of the energy exchanges *within* the canopy layer was needed to understand the energy loading of buildings and organisms, the importance of achieving a physical basis for the understanding of canopy layer microclimates, and the provision of realistic lower boundary conditions for urban boundary layer and urban air pollution dispersion modelling.

Nunez and Oke showed that the timing and magnitude of the surface energy balances of the canyon walls and floor were strongly conditioned by the influence of the canyon geometry and orientation on the radiation exchanges. Preliminary studies of the advective transports indicated that with airflow parallel to the canyon sides the advective contribution depended upon the wind speed, as well as the energy availability exterior to the canyon system. With airflow at an angle to the canyon axis it appeared as if the transport by the mean flow may be important, but this could not be evaluated in the study.

Sini et al. (1996) demonstrated that the differential heating of the canyon surfaces can largely influence the in-street flow's capability to transport and exchange pollutants. They used a street canyon of *H/W* ratio 1.12 with each one of its three surfaces overheated by 5° Celsius. In the cases of warm ground or leeward wall, the flow structure was similar to the isothermal case, except that the intensity of the recirculation was slightly increased, enhancing the vertical exchange of pollutants. In the case of a warm windward wall, the buoyancy generated tends to oppose the recirculation motion. The result is the splitting of the vortex and a change of the flow regime from the one-vortex SF to the multi-vortex SF, with the consequence of a large reduction of the vertical exchanges.

Kim and Baik (2001) investigated the recirculation structure and turbulence intensity within urban street canyons with bottom heating. They characterized the flow regimes according to various aspect ratios (from 0.6 to 3.6 with intervals of 0.2) and potential temperature difference ($\Delta\Theta$) between the street canyon bottom and the air ($\Delta\Theta$ from 0 to 16 K with intervals of 2 K). Five flow regimes were identified, indicating that thermal heating plays a significant role in determining the flow fields within street canyons.

In both Sini et al. (1996) and Kim and Baik (2001) a κ-ε turbulent closure scheme is used, including the thermodynamic energy equation to simulate thermal effects, and using a wall function to represent the heat transfer between the air and the building walls or street canyon bottom. This wall function is derived from the works of Abadie and Schiestel (1986) and Ciofalo and Collins (1989).

Xie et al. (2007) investigated the impact of both ground and building facades heating on the wind flow and transport of pollutants in street canyons. They ran tests on street canyons of aspect ratio *H/W* equal to 0.1, 0.5, 1, and 2, covering the basic flow regimes (SF, WIF, and IF).

They verified that the heating of building facades and ground surfaces lead to a strong buoyant force close to those solid boundaries receiving direct solar radiation. Turbulent motions and transport were modelled using the Renormalization Group (RNG) κ-ε turbulence scheme. Thermal effects and turbulence production due to buoyancy were included in the turbulent kinetic energy and dissipation equations.

The combined buoyancy and mechanically induced force substantially modifies the wind flow structure and pollutant transport characteristics in the street canyons. In contrast to single surface heating, the multi surface heating configuration has greater influence on the flow field and transport of pollutants.

2.5. Modelling Tools

The first step for an urban dispersion modelling or CFD simulation is to define the geometry of the urban scenario to be simulated. Whether it is an existing or proposed scenario, this includes drawing the buildings and positioning the sources which are relevant to the problem. Many tools exist that can aid the user in different ways. Computer-aided design (CAD) tools are the most commonly adopted solution, but specialized tools also exist for the parametric generation of urban scenarios.

2.5.1. CAD Tools

Computer-aided design (CAD) tools are computational systems to assist in the creation, modification, analysis or optimization of a design. These tools can provide capabilities as simple as drawing coloured points and lines or as complex as 3D parametric solid modelling. AutoCAD (1982) is perhaps the most used software in the world, being an everyday tool for many architects, engineers, project managers and others.

Despite being called "design tools", when it comes to the modelling of urban scenarios, these are often no more than "drawing tools", as they do not provide any intelligence to assist in such task. Existing Graphic User Interfaces for input of simulation data for AERMOD, such as the BREEZE AERMOD (Trinity 2008) suffer from this same weakness. Specialized tools do exist, which can assist urban planners in the generation of urban scenarios based on different parameters. Some of these tools are presented next.

2.5.2. Parametric Tools for Generation of Urban Scenarios

This new class of computational tool is becoming increasingly popular between architects, urbanists and urban planners. The idea behind "parametric" tools is that if something changes in a design, then all design-related information is automatically updated. These tools can help visualising ideas and concepts for urban situations, which is important to better understand each particular place. They are often based on the concept of Building Information Modelling (BIM), modelling both the physical and functional characteristics of the facilities.

CityCAD (2005), Modelur (2009), CityZoom (Grazziotin et al. 2004; Turkienicz et al. 2007; CityZoom 2008; Turkienicz et al. 2008), CityEngine (2008), CyberCity 3D (CyberCity 2009), PixelActive World Editor (PixelActive 2008) and Urban Pad (UrbanPAD 2009) are some examples of parametric tools. PixelActive and Urban Pad focus on the procedural generation of realistic-looking complex scenarios, sometimes even whole cities, to be used by the movie and gaming industry. Both projects have been recently acquired by big companies and then discontinued.

CityCAD is a 3D tool for the conceptual planning of sites. Based on road layouts and built density parameters, it can generate city blocks, parcels and buildings. It claims to have been created specifically for the needs of the city design and planning community, enabling integrated, holistic analysis in the early stages of urban design.

Modelur can generate buildings based on a combination of desired final parameters, such as built area, gross floor area and number of storeys. When one of the basic parameters is changed, the built area is immediately adjusted - all buildings get updated and urban control values recalculated. Modelur can also detect if a building is in conflict with urban parameters or given restrictions.

CityEngine offers tools to design and edit urban layouts with streets, blocks and plots. Street constructions and block subdivisions are controlled via parametric interfaces, giving immediate visual feedback. Whole cities and be generated from a combination of pre-defined templates and user-defined parameters.

CyberCity 3D generates 3D GIS information in the form for accurately-measured 3D buildings, streets, trees and urban objects, enhancing urban planning via accurate, data-rich models. It provides tools for data capture, automated modelling and semi-automated editing of urban scenarios.

CityZoom, developed by the SimmLab – UFRGS (Laboratory for the Simulation and Modelling in Architecture and Urbanism – Federal University of Rio Grande do Sul – Brazil), with prominent participation of the author of the present research, is detailed in the next section.

2.5.3. CityZoom

CityZoom (Grazziotin et al. 2004; Turkienicz et al. 2007; CityZoom 2008; Turkienicz et al. 2008) is a full Decision Support System (DSS) for urban planning. It provides a computational environment where different building performance models can operate interactively, aiming to optimize the urban planning process. A built-in object-oriented city model (Figure 2-7) represents the urban structure (city, blocks, roads, plots, buildings, etc.), associating geometry to information, which can be retrieved at any required level.

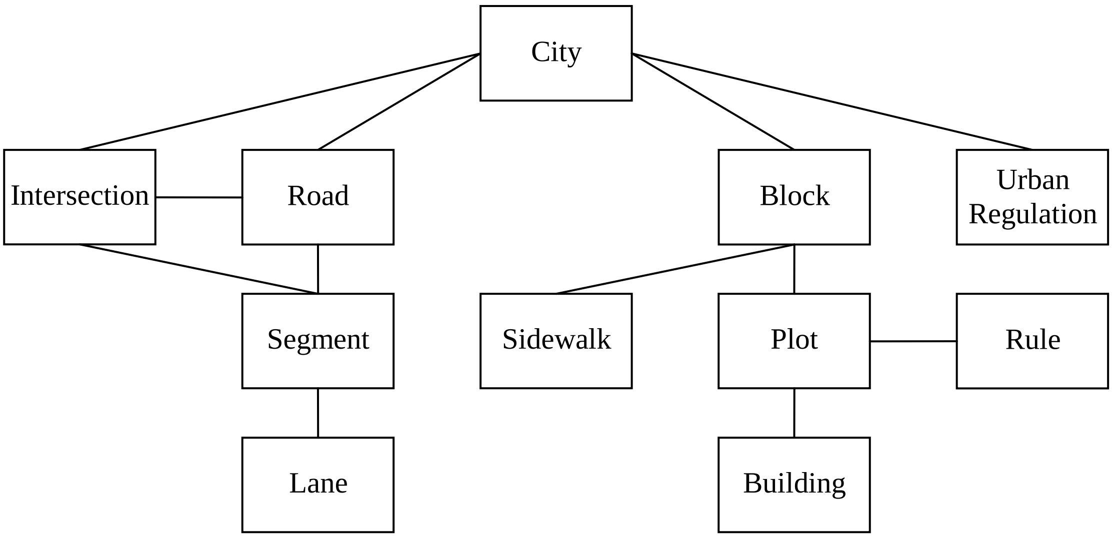

Figure 2-7: CityZoom city model.

CityZoom's main tool is a graphical editor of urban features, Figure 2-8. Data can be fed in different ways, such as: freehand drawing, using a background layer such as an aerial picture as reference, importing neutral file types (AutoCAD DXF, ArcView SHP, etc.), or by a direct connection to a spatial database. Once read in, data can then be used by CityZoom's models.

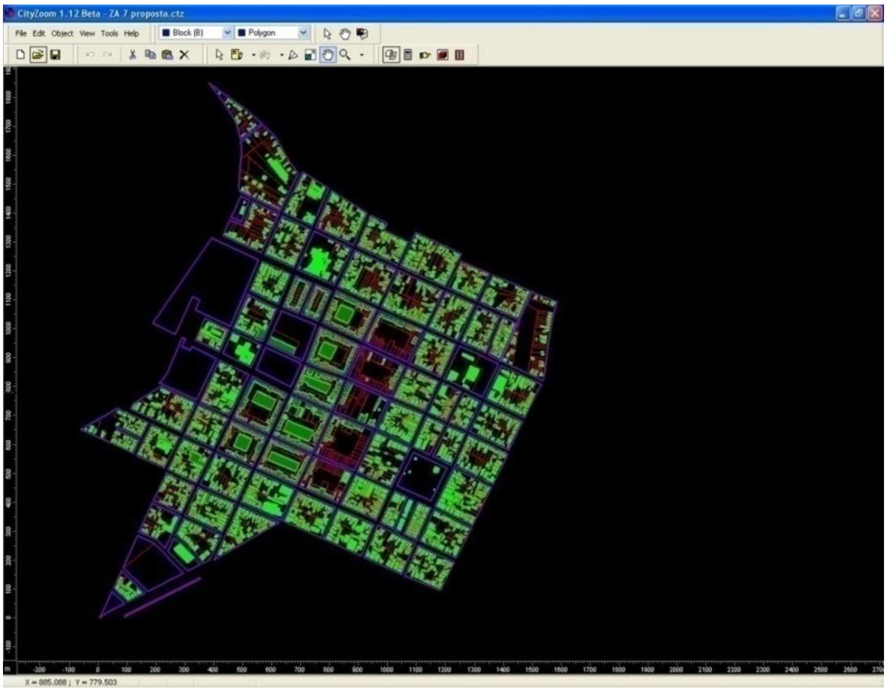

Figure 2-8: CityZoom user interface.

BlockMagic (Turkienicz et al. 1999) is CityZoom's model for simulating given urban regulations applied to a set of urban plots. It can swiftly generate large sets of buildings in the most different urban scenarios, or validate designed or already built buildings. The regulations can be inserted and edited with the Urban Regulations Editor, Figure 2-9, allowing the user to set the Master Plan parameters, such as maximum number of floors, maximum commercial and residential plot ratios, maximum slab area projection and minimum setbacks. Buildings are generated according to the regulations and using the user-input parameters which determine which of the building attributes are to be assessed or optimized, such as number of floors, front or size width, slab area, plot occupation and plot ratio.

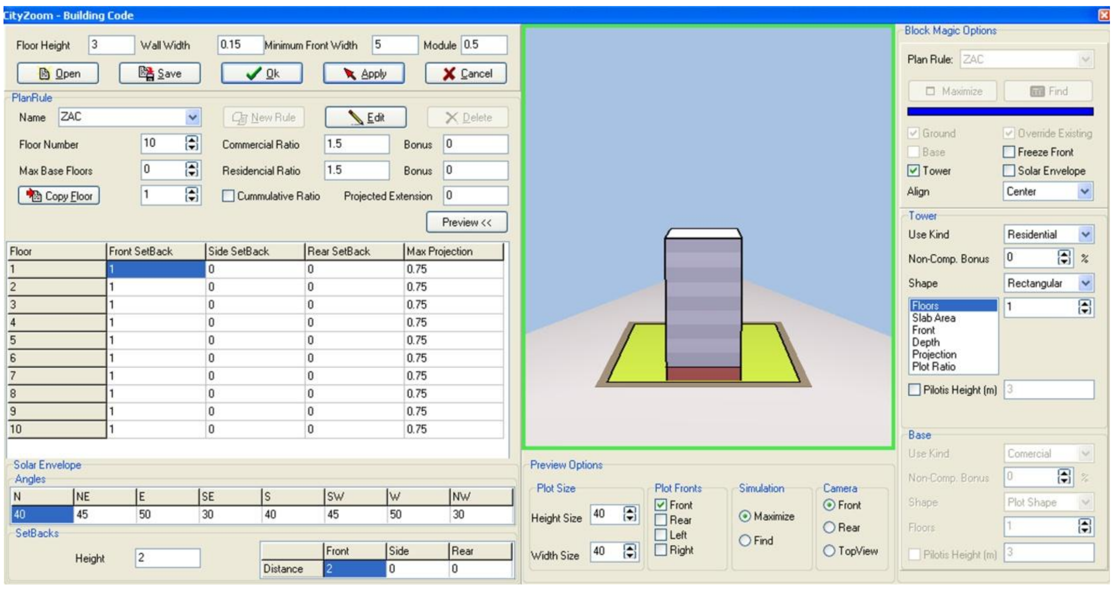

Figure 2-9: Urban Regulation Editor and BlockMagic simulation window.

BlockMagic also addresses environmental comfort issues, through the use of the Solar Envelope technique (Grazziotin et al. 2002). The Solar Envelope is a construct of space and time: the physical boundaries of surrounding properties and the period of their assured access to sunshine (Pereira et al. 2001). The way these measures are set determines the envelope’s final size and shape. Planning for insolation is essential in establishing the visual and thermal comfort, i.e., the benefits to be obtained from the sun in and around the buildings. The introduction of such parameters in the design process can substantially affect the land use, building density and urban land value.

Using the Urban Regulations Editor, the user can set the obstruction angles for every possible plot orientation. These angles are then applied to the plot’s edges, generating a set of geometric boundaries. Buildings restrained within this volume will not project undesirable shadows over the neighbouring buildings during critical periods of the year.

Any change in the Urban Regulations can impact the final shape of the simulated buildings. Hence, there is a preview window in the Urban Regulations Editor that allows the user to see the effects of the changes to the rules associated to a given plot in real time. Thus, the users can have both an idea of the final result due to the application of that rule or they can change the shape of the buildings (acquiring the correspondent rule) to obtain the desired result.

Results from the simulations can be visualized both in quantitative and qualitative ways, i.e., CityZoom can summarize numerical data generated by the performance models in tables and graphs as easily as it can show 3D graphical previews of the city, Figure 2-10. These allow the user to observe the desired results and navigate through hypothetical scenarios.

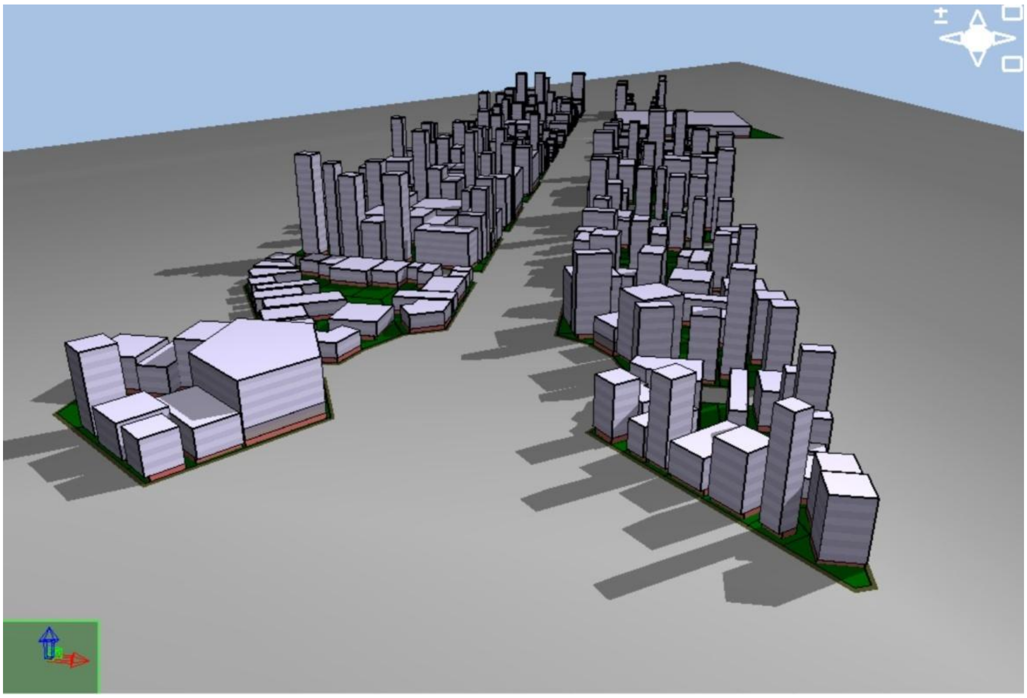

Figure 2-10: CityZoom 3D Visualization window.

Numerical data can be retrieved from the geometric objects in the city, such as the area of a block, or simply inferred as, for instance, the population inhabiting a building. Data can be extracted for the whole city, or its specific regions, and subsequently visualized with the Numerical Results Viewer module. Land area, built area, plot ratio, average building height, and other important attributes can be clearly displayed.

CityZoom's 3D visualization tool, implemented using the OpenGL library, makes it possible to interactively navigate through the three-dimensional scenario which represents the city being modelled, with the blocks, plots, buildings and reconstruction of the 3D terrain. It also supports the generation of realistic shadows in real time, based on the city's location, date, and time input by the user, and the display of the Solar Envelope superposed to the existing or simulated city objects. This allows the assessment of relations between buildings such as the overall impact of a building shadow over its neighbourhood.

CityZoom goes beyond simulation and visualization through its analytical tool, Mosaic (Scheidegger et al. 2002). Mosaic, Figure 2-11, is a model correlation tool, which allows visual access to the information generated by the performance models. By applying a regular orthogonal grid over the simulated area and dividing it in cells of the same size, attributes such as building footprints or building heights can be represented by assigning to each of these cells a numeric value. The grid will then work as a spatial representation, where each cell holds a value corresponding to the relative intensity of the attribute. In order to determine patterns or clusters of attribute's density, a colour scale is used in each grid.

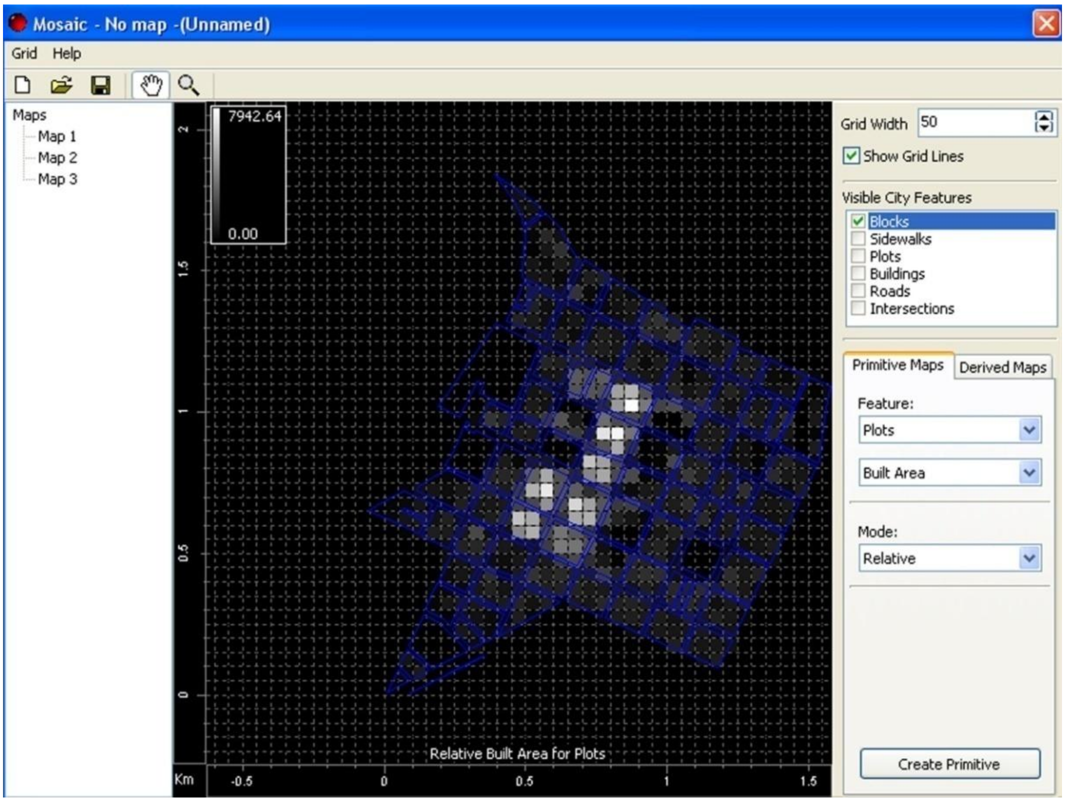

Figure 2-11: Mosaic window.

The information can be retrieved at any required scale (blocks, plots or buildings) or can be aggregated or disaggregated on a modular basis in different and progressive steps. This allows a modular grid to be disaggregated into a 10 x 10 meter grid (the actual size of a small building projection) and to be aggregated up to a 200 x 200 meter grid (the size of a group of blocks).

From an original grid (primitive map) it is possible to derive new ones, using map algebra (such as sum, multiplication, etc) and image-processing filters, similarly to map operations performed by raster GIS. Mosaic's potential to analyze and correlate different aspects of the city allows the unveiling of underlying structures and patterns which are normally blurred by complex sets of data.

Acknowledging the increasing demand for integrated CAD and GIS SimmLab has collaborated with regional Idrisi Developer (IDRISI 2007), LabGeo, in order to implement CityZoom's interface with shape files (.SHP), ESRI's geospatial vector data format (ESRI 2008). The achieved interface allows both the importing and exporting of neutral GIS files to and from CityZoom. With the interface, CityZoom can feed data to commercial GIS software, such as ArcMap, Figure 2-12, enabling a whole new set of analyses to be done over CityZoom-generated data. Similarly, GIS files can be edited in CityZoom, providing a very intuitive and longed user interface, not available in most GIS packages.

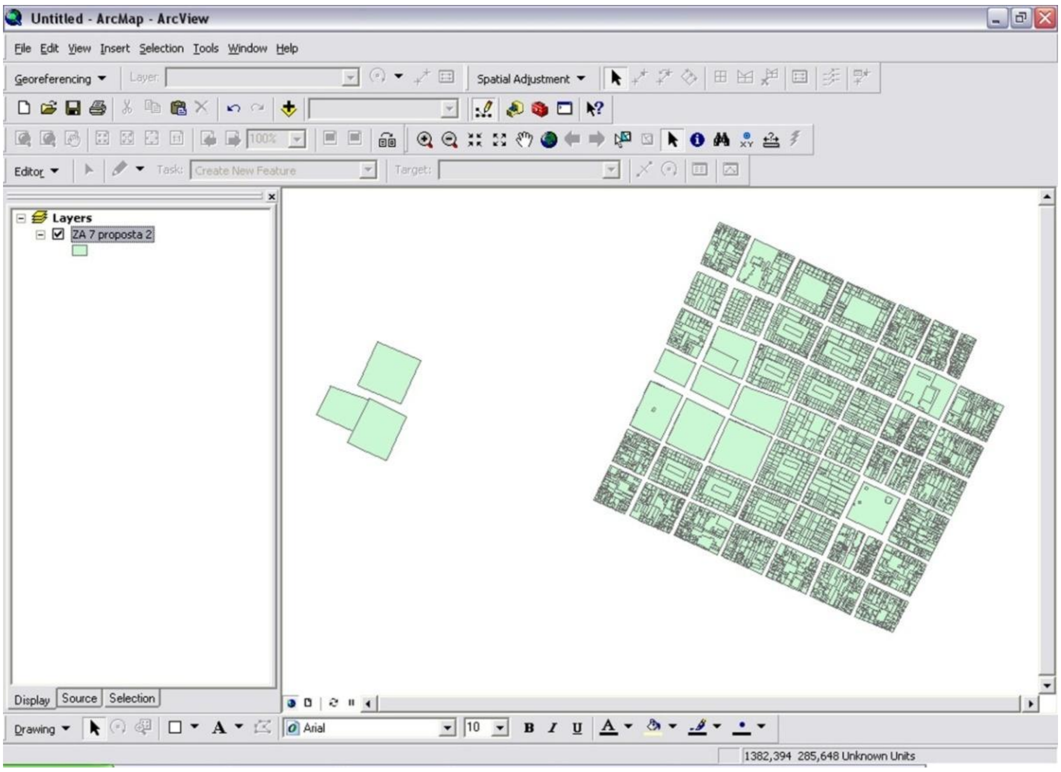

Figure 2-12: Visualization of CityZoom data using ArcMap.

CityZoom can also export data for different types of analyses using free tools and educational software packages, opening the path for a new branch of data analyses and editing. Interesting results have been obtained through the interface with Google Earth, Sketch Up or Apolux (Claro et al. 2005).

The visualization of results using Google Earth, Figure 2-13, allows users to visualize the simulation of a given plan rule as well as to see how the city actually is situated over the existing topography. Using Sketch Up as a final result-editing tool it is possible, for example, to insert 3D objects such as trees, benches, lamps, cars, etc into the simulated city. This results in a model that is very close to reality, thus making it even more intuitive in presentations for laymen.

Figure 2-13: Visualization using Google Earth (2009).

The interface with Apolux allows for the consideration of different daylighting parameters, based on the radiosity method. Apolux can calculate and generate graphics of form factors and illuminance levels. It can also generate luminance distributions of different points of the sky (Figure 2-14), solar obstruction masks, both inside and outside buildings, as well as semi realistic images.

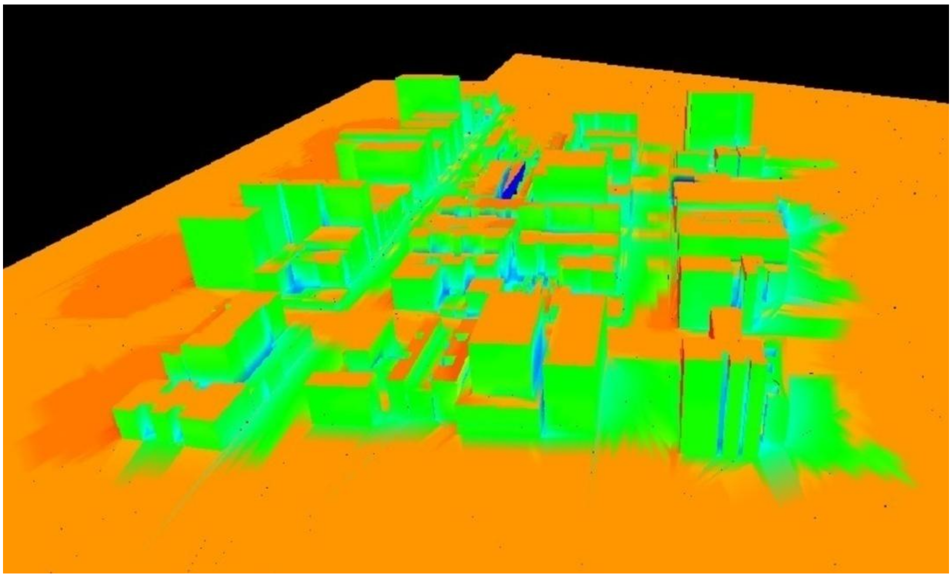

Figure 2-14: Visualization using Apolux

This section has presented CityZoom, a computational environment for urban planning purposes, where city objects can be designed or generated based on iterative user-designed parameters.

The use of CityZoom to assist in the modelling of urban scenarios and setting up of simulation parameters can massively reduce the time spent in such tasks, while improving the quality of the models to be used by the dispersion and CFD software. By allowing simulation results to be read back into CityZoom, the correlations between the built environment, planning regulations, physical and environmental comfort parameters can be analysed.

2.6. Urban Flow and Dispersion Datasets

Measurement data is available from different projects, such as Dispersion of Air Pollution and its Penetration into the Local Environment (DAPPLE) project (Arnold et al. 2004; Wood et al. 2009; Robins 2011), Joint Urban 2003 (Allwine et al. 2004; Clawson et al. 2005), Instrumented City (Chen and Bell 2002), and Mock Urban Setting Test (Biltoft 2001), which can be used to validate the results of the present work.

The Instrumented City (iC) database is a multi-purpose, transport-related database facility for use by the entire academic transport research community (Chen and Bell 2002). Since 1992 data from the UK Leicester City Council and Nottinghamshire County Council traffic management computers was logged and archived on a continuous base by the Leeds University's Institute for Transport Studies. This has been used for studies and applications such as network analysis and traffic, air quality and noise monitoring, modelling, management and control.

In April 2010 the author visited the city of Leeds to meet the research group responsible for the Instrumented City project, and to see the instruments and methodologies being used for the new monitor project in Leeds, the Instrumented Junction. Three traffic sensors and five air quality sensors provide high resolution measurements of traffic flow and speed, gaseous air pollution concentrations and background wind. Unfortunately, a few months later the project was terminated and measurement data could not be obtained. In fact, very little information can still be found online about the project.

The Mock Urban Setting Test (MUST) was a scaled urban dispersion experiment conducted at the U.S. Army Dugway Proving Ground Horizontal Grid test site, located in the Great Basin desert west of Utah, on 6-27 September 2001 (Biltoft 2001). The objective was to acquire meteorological and dispersion data sets at near full-scale for the development and validation of urban toxic hazard assessment models. MUST was designed using a 12 by 10 array of shipping containers spaced to produce a flow regime bordering between wake interference and isolated flow. Tracer gas was released from positions upwind of the MUST array, and dispersion was measured through the array. Sixty-eight usable trial events were completed during MUST.

The Joint Urban 2003 (JU2003) atmospheric dispersion study (Allwine et al. 2004; Clawson et al. 2005) was a major urban study funded by the U.S. Departments of Defense, Energy, and Homeland Security aimed at creating high-resolution urban dispersion data sets. The study was conducted from 28 June through 31 July 2003 in Oklahoma City, Oklahoma, with the participation of over 150 scientists and engineers from over 120 U.S. and foreign institutions, and has advanced knowledge about movement of contaminants in and around cities and into and within building interiors. Resulting data is still being used to improve, refine and verify computer models that simulate the atmospheric transport of contaminants in urban areas.

Hundreds of papers and presentations have been given on scientific findings and model evaluations based on the field study results. In fact, Volume 46 Issue 12 of the Journal of Applied Meteorology and Climatology was a special issue presenting 12 papers providing a cross section of the scientific investigations pursued using JU2003 Data (Allwine and Leach 2007).

The Dispersion of Air Pollution and its Penetration into the Local Environment (DAPPLE) project (Arnold et al. 2004; Wood et al. 2009; Robins 2011) consisted of a number of large urban meteorology and dispersion studies in the area around the Marylebone Road and Gloucester Place intersection in Central London.

The first stage of the project ran from to 2002 until 2006 and was funded by the UK Engineering and Physical Sciences Research Council. Experts from six universities undertook field measurements (meteorology, roadside pollution levels, traffic flow, personal exposure and inert tracer releases), wind tunnel modelling and computational simulations to better understand the physical processes affecting street and neighbourhood scale flow of air, traffic and people, and their corresponding interactions with the dispersion of pollutants at street canyon intersections.

The second stage was funded by the UK Home Office and ran between 2006 and 2010. The project concentrated on flow and dispersion in the urban canopy, aiming to produce substantial data sets for a range of source types and meteorological conditions, to characterise street level wind and dispersion conditions with respect to prevailing meteorological conditions, and to use the knowledge obtained to assess the performance of urban dispersion models.

A total of fifty-seven tracer release experiments from static sources were undertaken during different stages of the DAPPLE project (Wood et al. 2009). While these do provide interesting data for emergency planning and response, and for the development and evaluation of dispersion models, traffic-related emissions are mobile sources. For this reason, eight experiments were carried out with moving sources – a steady emission from a car moving along Marylebone Road.

Greater variability in the level of tracer detected at receptors was observed in comparison with fixed source experiments, due to narrow and concentrated plumes in the proximity of the release (Robins 2011). The modelling of such releases is not straightforward as the emission pattern from each drive-through is different, reflecting the times and locations when and where the vehicle was stationary. In fact, no two 'drive-throughs' were identical.

Emissions from a moving source are line-like when the vehicle is moving at steady speed and point-like when the vehicle is stationary (Tate 2010). However, overall dispersion does not follow either the point or line source pattern because the emission is a transient line source, and the emission rate per unit length of the line is variable, depending on the speed of the moving source.

Robins (2011) suggests that a model comprising a series of point sources is likely to be more appropriate than one based on a line source to represent moving sources. The overall plume from many instantaneous point sources released along a line quickly (within a few city blocks from the release road) becomes a homogenous plume and the tracer amounts observed are then mostly dependent on distance away from the source street and are less dependent on wind direction.

A list of DAPPLE project publications and conference presentations is available online at http://www.dapple.org.uk/pubs.html.

2.7. Conclusion

This chapter has presented an overview of the challenges behind the modelling and simulation of the dispersion of pollutants in urban environments. The two mostly used computational approaches were reviewed: Atmospheric Dispersion Modelling and Computational Fluid Dynamics (CFD). The basic theory, existing software and researches addressing different techniques were presented.

Dispersion models require a relatively small amount of input information and computational resources, which make them an attractive alternative to CFD, especially in the early stages of strategic urban planning. AERMOD presents itself as the ideal dispersion modelling software to be studied and used in this research, for several reasons: it is an open source system, it is well documented, validated and accepted, it can deal with building downwash through the PRIME algorithm, and the input and output files are simple to read and generate.

More elaborate computational techniques, such as CFD, are required in order to obtain more accurate predictions of plume dispersion and the resulting concentration patterns closer to the sources, where the interaction between the plume and complex structures dominates the plume path and dispersion. Commercial and Open-Source CFD models are available. CFX was the clear choice for commercial model to be used, as that was the preferred software used by the CFD research group and on the CFD modules taught at the University of Nottingham. Expensive licences are needed to use CFX outside of the academic environment, so Open Source CFD model OpenFOAM was also selected to be studied as an alternative.

Environmental characteristics affecting the dispersion of pollutants in urban scenarios were also presented, along with the existing tools and techniques that can be used to assist in the modelling of such characteristics to be used by dispersion and CFD models. CityZoom provides a computational environment where city objects can be designed or generated based on iterative user-designed parameters. The use of CityZoom to assist in the modelling of urban scenarios and setting up of simulation parameters can massively reduce the time spent in such tasks, while improving the quality of the models to be used by the dispersion and CFD software. By allowing simulation results to be read back into CityZoom, the correlations between the built environment, planning regulations, physical and environmental comfort parameters can be analysed.

In order to validate the use of CityZoom for the modelling of simulation scenarios, as well as the use of AERMOD for the simulation of dispersion in urban scenarios, comparison with existing data has to be established. The use of the DAPPLE data sets was a natural choice. Traffic-related emissions are the main source of pollutants in busy urban conglomerates (Berkowicz 2000b), and the DAPPLE project included moving source experiments which tried to reproduce traffic-related emission patterns. The project was conducted by a consortium of UK universities, so access to the data was easy to obtain, and the author even had the opportunity to attend a DAPPLE Workshop in March 2010 to learn more about the project directly from the masterminds behind it.

The concepts, techniques and tools presented in this Chapter are used in the implementation of a new version of CityZoom, detailed in Chapter 3. Some the presented data sets are used in the model tests performed in Chapter 4.

3. Implementation of CityZoom UP (Urban Pollution)

3.1. Introduction

This chapter describes the implementation of CityZoom UP, an extension of CityZoom to assist in the modelling and setting up of urban scenarios for dispersion and CFD simulation. CityZoom UP introduces the capacity of handling urban pollution related objects and data: source positions and emission rates, receptor positions, networks of receptors, meteorological data and simulation control parameters.

Topography can also affect the dispersion of pollutants in the environment. However, terrain elevation introduces a high level of complexity to the modelling of scenarios for dispersion and CFD simulations. While some researches, such as Zhang et al. (2008), do take topography into account, the present work will focus on the flat terrain cases.

Atmospheric dispersion modelling system AERMOD was chosen to be used for the fast calculation of the dispersion of pollutants in urban environments. CFD packages CFX and OpenFOAM were chosen as the commercial and open source solutions for the detailed calculation of air flow and dispersion of pollutants in specific areas inserted in urban environments. The mesh generators GAMBIT, *blockMesh* and *snappyHexMesh* were also studied for use with CityZoom UP.

3.2. Sources of Pollutants

When dealing with typical urban scenarios, such as street canyons with intense traffic, the main contribution to the pollution is attributed to direct emissions from the street traffic, with only a small portion coming from background contribution (Berkowicz 2000b). Motor vehicles on roads are usually modelled as continuously emitting line sources. However, for the case of a single vehicle driving through a street, emissions are line-like when the vehicle is moving at steady speed and point-like when the vehicle is stationary (Tate 2010). Overall dispersion does not follow either the point or line source pattern because the emission is a transient line source, and the emission rate per unit length of the line is variable, depending on the speed of the vehicle.

After discussions between the author and his supervisors, a model comprising a series of point sources distributed along the road axes was developed. Each point source should have a diameter approximately equal to the road width, and the sources should be distributed with a distance between centres approximately equal to this diameter, as represented in figure 3-1. This is based on the assumption that the traffic emissions should be mixed enough in the street level, and the source area should cover the entire street.

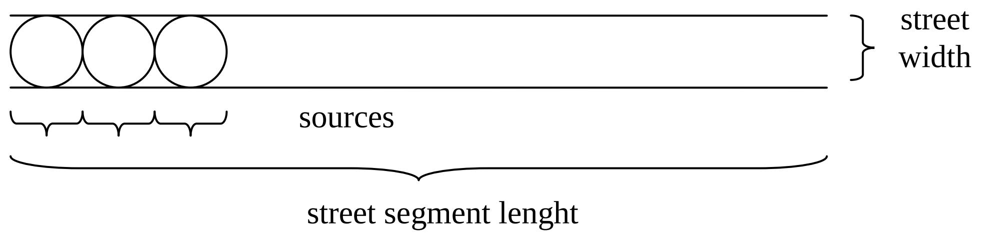

Figure 3-1: Line source as a sequence of point sources.

A similar approach had been used by Shallcross et al. (2009) and Tate (2010) to characterize the emission patterns from a single vehicle in the line-source experiments, undertaken in March 2008 in central London, during the DAPPLE campaign. Robins (2011) later suggested that this type of model is likely to be more appropriate than one based on a line source to represent moving sources, since the overall plume from many instantaneous point sources released along a line quickly becomes a homogenous plume.

The quality of the simulation results is heavily dependent on the quality and level of detail of the input data (Zou et al. 2010). The modelling, measuring, and estimation of pollutant emissions from transport is a problem itself, and has already been researched by numerous other studies, such as Hargreaves (1995), Frey et al. (2001), Ahn et al. (2002), Namdeo et al. (2002), Nejadkoorki et al. (2008), Ariotti et al. (2008), and Ariotti and Cybis (2010).

While a simple model could be created based on a fixed emission rate of 10 mgs^{-1} of CO, representative of on-board measurements in a typical gasoline powered vehicle in cruise speed (Coelho et al. 2005), it would be ideal to measure the emissions rates of all types of vehicles composing the site fleet, as well as the type and level of use of the site roads, and then estimate the total emissions (Hickman et al. 1999). The rates should also vary depending on the time of the day and traffic signal cycle times (Rakha and Ahn 2004). For all these reasons, the author has decided to not attempt to automatically generate traffic-related emission profiles. Emission data to be used as input for all the tests should either be measurement data or carefully calculated by hand data, based on known existing profiles.

CityZoom already had some simple road representation capabilities, but it was necessary to implement a routine to create the sources and to calculate and to position their centres along the road axis, based on the desired source diameter or road width. At present, each road is represented as a single traffic lane, and all sources have the same user-defined diameter.

3.3. Meteorological data

The atmospheric conditions, specially wind speed, wind direction and stability class, are the main factors driving the dispersion of pollutants in the environment. Similarly to the vehicle emission data, proper meteorological data are needed to ensure correct results.

AERMOD uses meteorological files as the input for meteorological data, generated by the AERMET pre-processor. The data needed to generate these files include surface boundary layer parameters, wind speed, wind direction, and turbulence parameters. These can be obtained from meteorological stations near the site of interest or purchased from internet websites (e.g., http://www.worldgeodata.com/ and http://www.webmet.com/), sometimes already in the format needed for AERMOD.

For CFD models, the Power Law and Log Law wind profiles are commonly used to represent wind speed and atmospheric stability at the inlet, based on the following equations:

$$\frac{u}{u_r} = \left(\frac{z}{z_r}\right)^{\alpha} \tag{1}$$

and

$$u = \frac{u_*}{K}\ln\left(\frac{z-d}{z_0}\right) \tag{2}$$

where u is the wind speed (in meters per second) at height z (in meters), u_r is the known wind speed at reference height z_r, α is the atmospheric stability coefficient, u_* is the friction velocity (in meters per second), K is the von Karman's constant, d is the zero plane displacement and z_0 is the surface roughness (in meters).

Using the CFX Expression Language (CEL), both the Power Law and Log Law wind profiles were modelled for the inlet conditions, resulting in the set of equations shown in Figure 3-2.

```
pwrspd = ur * ( y / yr ) ^ expon
logspd = ( ur / 0.41 ) * loge( ( max( y, yr ) - disp ) / y0 )
yr = 10 [m]
expon = 0.143
ur = 1 [m s^-1]
disp = 10 [m] * 2 / 3
y0 = 10 * 0.1 [m]
```

Figure 3-2: Power Law and Log Law equations in CEL.

The desired wind profiles are generated by applying these equations to the inlet. Examples of these profiles are plotted in the vertical cross section of a street canyon model in Figures 3-3 and 3-4. The vectors represent wind velocity.

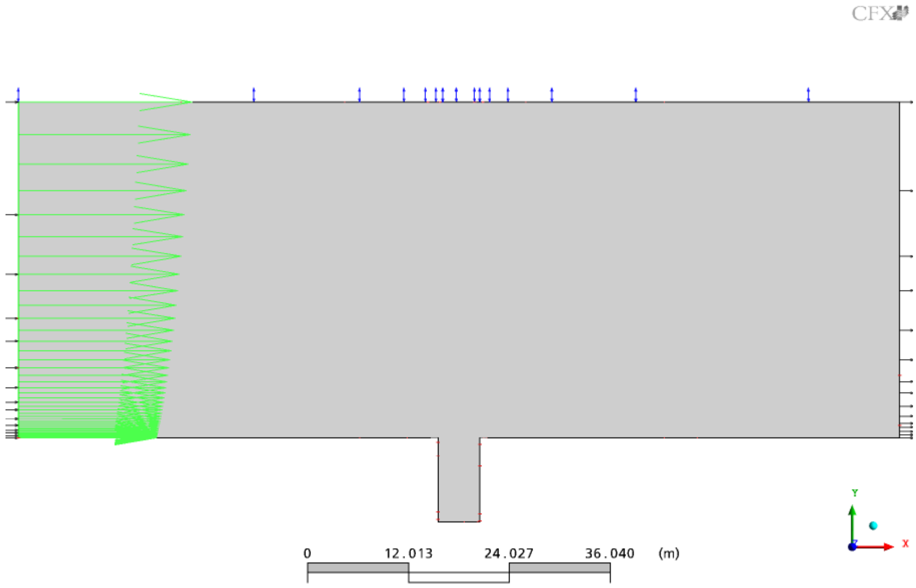

Figure 3-3: Power Law wind profile using CFX.

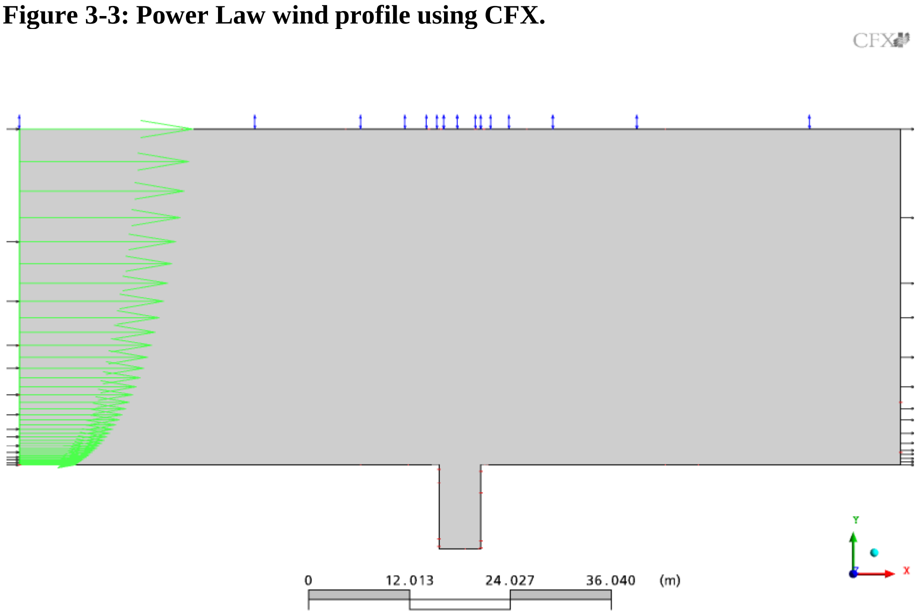

Figure 3-4: Log Law wind profile using CFX.

To represent the effect of wind direction in CFD models, the whole scenario must be rotated within the simulation domain so that the buildings are properly aligned with the required wind direction. One way of doing this would be to rotate the geometry before the meshing, and then reform the whole domain for each simulation. Another method is to use CFX General Grid Interface (GGI), which allows the use of multiple domains connected via non-conformal interfaces, as seen in Morvan et al. (2007). The city objects are placed on a virtual disc and meshed independently from the fetch. These meshes then only need to be constructed, tested, and validated once. The disc can automatically be positioned within the fetch and rotated to match different wind directions (Figure 3-5).

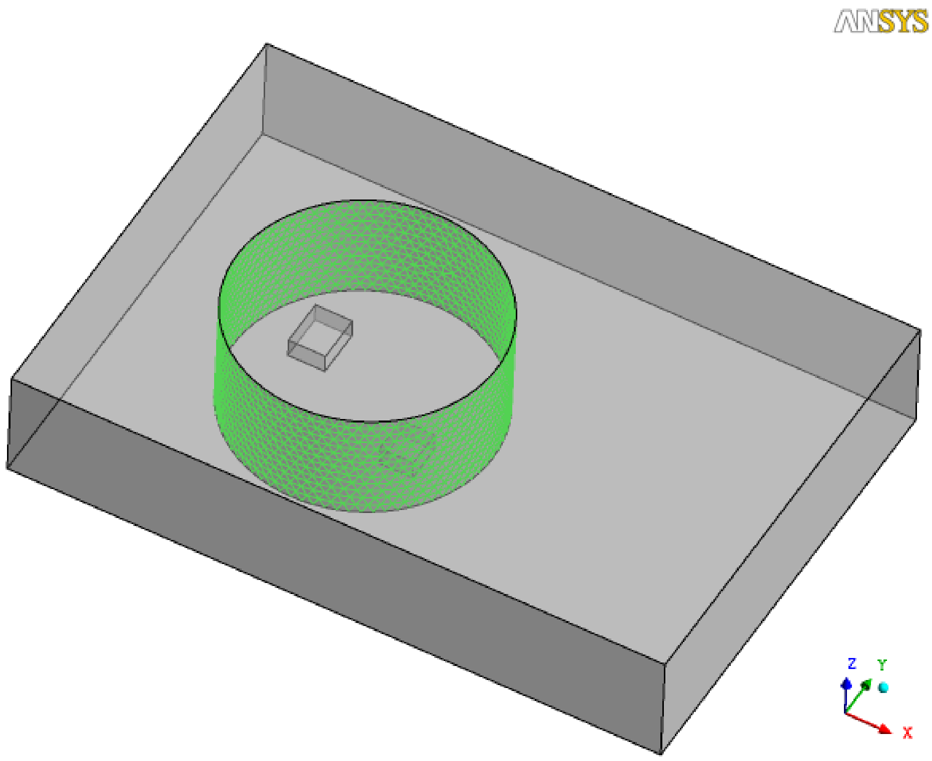

Figure 3-5: Domain and virtual disc.

Figures 3-6 and 3-7 show the local velocity for a simple CFD scenario using the virtual plate approach for different wind directions. The scenario represents a street intersection with buildings of different heights. A coarse mesh and simple simulation parameters are used, resulting in poor quality outputs.

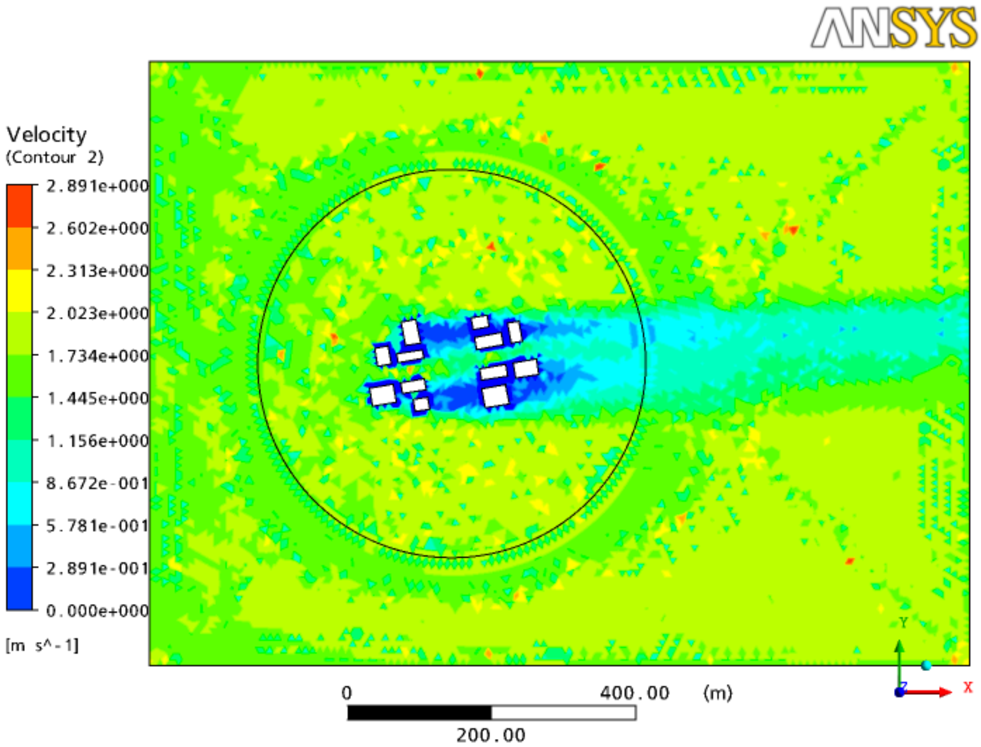

Figure 3-6: Local velocity contour plot on plane XY (z = 2) for wind direction 0 degrees.

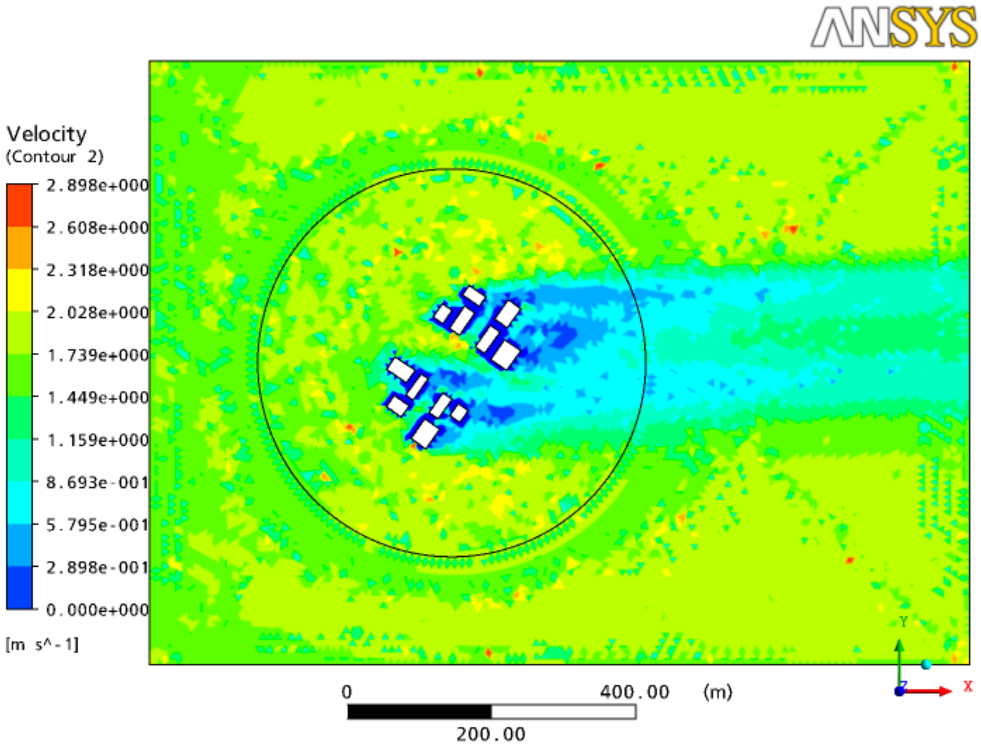

Figure 3-7: Local velocity contour plot on plane XY (z = 2) for wind direction 45 degrees.

The virtual plate approach was used for early tests, but was later discarded for a series of reasons: first, it requires the use General Grid Interface (GGI) which is not supported by the official releases of OpenFOAM, and there was the intention to use OpenFOAM with CityZoom UP; second, the round edges seemed to produce some artefacts in the simulations (Figures 3-6 and 3-7); finally, CityZoom UP should make it very easy to quickly generate from scratch complete meshes for each desired wind direction.

3.4. AERMOD requirements

In order to achieve the level of understanding necessary to create a software capable of assisting in modelling urban scenarios and setting up complete AERMOD simulations using these scenarios, the author studied the AERMOD manuals (user guide, implementation guide, and description of model formulation), the manuals for the various modules: AERMET (meteorological data pre-processor), AERMAP (terrain pre-processor), and BPIP (Building Profile Input Program), as well as several sample files. The main AERMOD program and these auxiliary modules all use text files for input, output, and error reporting.

The lack of a graphic tool to model the inputs and visualize the outputs makes it difficult to understand and verify the data. Graphic User Interfaces for AERMOD do exist, such as ISC-AERMOD View (Lakes 2008), by Lakes Environmental, and BREEZE AERMOD (Trinity 2008), by Trinity Consultants, but are all under commercial license. A 3-day trial license for BREEZE AERMOD was obtained, which was used to create a set of sample files similar to the urban scenarios desired for a CityZoom implementation.

A very simple test case scenario was conceived, consisting of two buildings, two sources positioned near the buildings, a default 21x21 Cartesian grid of receptors (distributed with 100 meters spacing between them) and sample meteorology files provided with the AERMOD examples. The sources were modelled to represent stationary vehicles. Source parameters were set as follows: elevation = 0 m (as it has been said, topography is not considered to avoid the extra complexity); constant emission rate = 0.01 gs^{-1} which was based on mean CO emission rates for different vehicles driving through different test corridors (Frey et al. 2001); source height = 0.2 m; inside diameter = 0.1 m (representative of a vehicle escape exhaust); exit temperature = 425 K; exit velocity = 0.001 ms^{-1} (to suppress the plume momentum and simulate a horizontal stack); urban source = true (incorporate the effects of increased surface heating from an urban area on pollutant dispersion under stable atmospheric conditions); and all the building downwash information generated by BPIP. This simple scenario proved itself very useful in helping understand the inner workings of the software, especially the downwash information specifications.

One of the basic inputs to AERMOD is the runstream setup file which contains the selected modelling options, as well as source location and parameter data, receptor locations, meteorological data file specifications, and output options (EPA 2004). This input files uses a keyword/parameter approach to specify the options and input data for running the model. The keywords specify the type of option or input data being entered on each line of the input file, and the parameters following the keyword define the specific options selected or the actual input data. The runsteam file is divided into functional “pathways”, identified by a two-character pathway ID at the beginning of each line. The pathways and the order in which they are input to the model are as follows: CO for specifying overall job COntrol options; SO for specifying SOurce information; RE for specifying REceptor information; ME for specifying MEteorology information; EV for specifying EVent processing; and OU for specifying OUtput options. An example of a runstream file is shown in Figure 3-8.

CityZoom UP must be able to generate these AERMOD runstream input files, trigger an AERMOD run, and read back the results from the generated output files. It has already been said that CityZoom is a tool for urban planning purposes, capable of dealing with city objects and their geometry. CityZoom UP needs to be able to also handle sources and receptors, as these data are needed for setting up pollution dispersion model simulations.

AERMOD is capable of handing multiple sources, including point, line, area, and volume sources. However, the PRIME algorithm for calculation of building downwash effects can only be used with point sources. The author and his supervisors agreed that building downwash should always be taken into account when calculating concentrations in urban environments, so the only type of source to be treated by CityZoom UP was the point source. This agrees with the previous decision to represent linear sources as sequences of point sources.

```
CO STARTING
CO TITLEONE Simple Example Problem for AERMOD-PRIME
CO MODELOPT CONC FLAT
CO AVERTIME 3 24 PERIOD
CO POLLUTID CO
CO RUNORNOT RUN
CO FINISHED

SO STARTING
SO LOCATION STACK01 POINT 218 306 0
SO SRCPARAM STACK01 0.01 0.2 425 0.001 10
SO BUILDHGT STACK01 0 18 18 18 0 0 0 0 0
SO BUILDHGT STACK01 0 0 0 18 18 18 18 18 18
SO BUILDHGT STACK01 18 18 18 0 0 0 0 0 0
SO BUILDHGT STACK01 0 0 0 0 18 18 18 18 18
SO BUILDWID STACK01 0 37.03 39.05 39.89 0 0
SO BUILDWID STACK01 0 0 0 0 0 0
SO BUILDWID STACK01 0 24.79 24.54 37.03 33.89 29.71
SO BUILDWID STACK01 33.89 37.03 39.05 39.89 0 0
SO BUILDWID STACK01 0 0 0 0 0 0
SO BUILDWID STACK01 0 24.79 24.54 23.55 21.84 19.47
SO BUILDLEN STACK01 0 35.2 37.93 39.51 0 0
SO BUILDLEN STACK01 0 0 0 0 0 0
SO BUILDLEN STACK01 0 24.29 23.04 35.2 31.39 26.64
SO BUILDLEN STACK01 31.39 35.2 37.93 39.51 0 0
SO BUILDLEN STACK01 0 0 0 0 0 0
SO BUILDLEN STACK01 0 24.29 23.04 21.1 18.52 15.37
SO XBADJ    STACK01 0 34.86 31.07 26.34 0 0 0 0 0
SO XBADJ    STACK01 0 0 0 0 31.64 34.51 -63.8 -65.81 -65.82
SO XBADJ    STACK01 -68.99 -70.06 -69 -65.85 0 0 0 0 0
SO XBADJ    STACK01 0 0 0 0 -55.93 -57.56 -57.43 -55.57 -52.01
SO YBADJ    STACK01 0 9.36 18.33 26.74 0 0 0 0 0
SO YBADJ    STACK01 0 0 0 0 -16.78 -8.92 26.55 18.13 9.15
SO YBADJ    STACK01 -0.11 -9.36 -18.33 -26.74 0 0 0 0 0
SO YBADJ    STACK01 0 0 0 0 16.78 8.92 0.79 -7.37 -15.3
SO SRCGROUP ALL
SO FINISHED

RE STARTING
RE GRIDCART GC1 STA
RE GRIDCART GC1 XYINC -1000 21 100 -1000 21 100
RE GRIDCART GC1 END
RE FINISHED

ME STARTING
ME SURFFILE AERMET2.SFC
ME PROFFILE AERMET2.PFL
ME SURFDATA 14735 1988 ALBANY,NY
ME UAIRDATA 14735 1988 ALBANY,NY
ME SITEDATA 99999 1988 HUDSON
ME PROFBASE 0.0 METERS
ME FINISHED

OU STARTING
OU RECTABLE ALLAVE FIRST SECOND
OU MAXTABLE ALLAVE 50
OU FINISHED
```

Figure 3-8: Example of runstream input file for AERMOD for sample problem.

AERMOD's PRIME algorithm requires the downwash information to be specified for each source with downwash, using direction-specific building dimensions. There are 36 building heights, widths, lengths, and along-flow and across flow distances from the stack center to the center of the upwind face of the projected buildings, which must be entered with appropriate keywords, one value for each 10 degree sector beginning with the 10 degree flow vector (direction toward which the wind is blowing), and continuing clockwise.

Given then desire to account for building downwash in the AERMOD simulations setup by CityZoom UP, it is first necessary to calculate the downwash data for each source. The Building Profile Input Program (BPIP) is a module designed to calculate the downwash information for input to the AERMOD model. From the source positions and nearby buildings geometries, BPIP generates the values for each 10 degree sector for each source.

CityZoom UP needs to be able to export building and source geometry data to the BPIP input file format, so that the downwash information can be generated and imported back to each source modelled on CityZoom UP, thus providing CityZoom UP with the data necessary to set the AERMOD runs properly to account for building downwash.

AERMOD calculates concentration at user-defined receptor locations. It is possible to specify single receptors, as well as Cartesian or polar grid receptor networks. CityZoom UP must be able to model single receptors as well as Cartesian grid of receptors, allowing for concentration to be calculated for the whole area of interest.

3.5. CFD requirements

Early CFD researches focused on what was considered the worst case scenario (Oke 1988): street canyons with airflow direction normal to the long axis of the canyon. Canyons were approximated by a two-dimensional cross section, neglecting street intersections and assuming the buildings flanking the canyon are semi-infinite in length.

This type of canyon can be modelled based on simple building height *H* and street canyon width *W* parameters, according to the schematic in Figure 3-9.

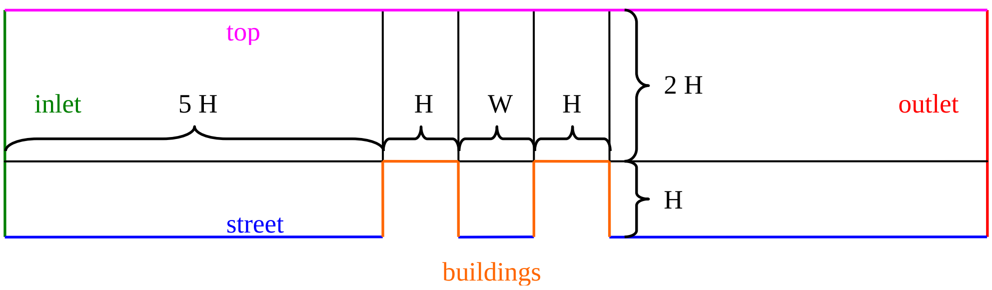

Figure 3-9: Schematic of a 2D canyon model.

The main area of interest is the W region between the buildings. The length of 5H from the inlet to the buildings allows for the flow to be established properly before the obstacles. The domain height of 3H allows the flow to go over these obstacles without being blocked by the domain. Finally, the 5H from the buildings to the outlet allow for the flow to re-develop behind the wake region.

However, these idealized street canyons do not exist in real urban scenarios. First, because street intersections are common geometries, which introduce lateral eddies into the canyons and create low-pressure zones, greatly modifying the air flow and affecting the distribution of pollutants (Li et al. 2006). Second, because the wind direction in urban environments is not always normal to the street canyons. And finally, because the flows in urban scenarios have an inherently 3D and intermittent nature.

Another reason for the use of simplified 2D models by early researches was the lack of computational power to perform simulation of more complex scenarios. Advancements in computer hardware now allow for the CFD simulation of complete 3D scenarios within fractions of the time once needed for the simulation of simplified 2D canyon models.

CityZoom UP must be able generate 3D geometries, use GAMBIT or snappyHexMesh to convert 3D geometries into 3D meshes, and then setup either CFX or OpenFOAM to run CFD simulations using the 3D domain meshes. The only relevant city objects are the ones that can block the air flow, i.e., the buildings, and the ones that release pollutants, i.e., the sources. Meteorological parameters must be input to the simulation by assigning a wind profile at the inlet and rotating the domain to match the wind direction.

The domain or fetch where the wind flow develops is a box around the area of interest, which must be generated automatically based on the dimensions of the city objects and the parameters suggested by “COST Action 732 – Best Practice Guideline for the CFD Simulation of Flows in the Urban Environment” (Franke et al. 2007) for the choice of the computational domain (Figure 3-10).

For urban areas with multiple buildings, with H_m as the height of the tallest building, the top and lateral boundaries of the domain should be at least $5H_m$ from the boundaries of the built area (e.g. buildings). This large distance from the top of the built area to the top of the domain is necessary to prevent artificial acceleration of the flow over the buildings, as most boundary conditions applied at the top of the computational domain do now allow fluid to leave the domain. The lateral distance between the built area and the boundaries of the domain is defined in order to reach a blockage smaller than 3%.

The same $5H_m$ distance is recommended between the inflow boundary and the built area, to allow for a realistic flow establishment. A distance of $15H_m$ between the built area and the outflow boundary should be used to allow for flow re-development behind the wake region.

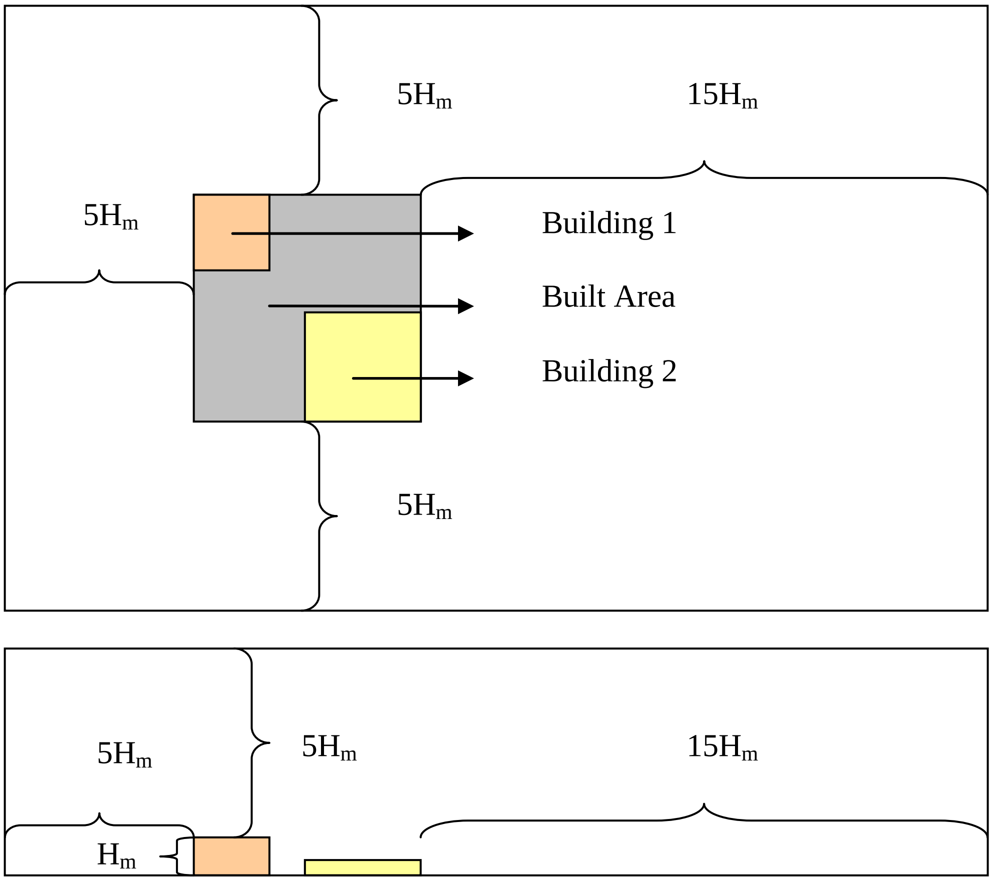

Figure 3-10: Schematic of computational domain for urban CFD simulations.

3.6. Data Model

The first coding step for the implementation of CityZoom UP was the creation of the data model. In order to allow CityZoom UP to manipulate both the data needed for dispersion models and CFD simulation inputs and the data generated by AERMOD outputs, three new objects were defined and modelled: sources, receptors and networks of receptors. These objects were modelled and implemented as the classes TSource (Figure 3-11), TReceptor (Figure 3-12), and TRecNetwork (Figure 3-13). Each class contains all the variables associated to the respective object, such as position, elevation, and emission rate, as well as methods for setting, saving and loading the values of these variables.

```
(*------- Source ------------------------------------------*)

  TSource = class( TCityVisual )
    private
      procedure CenterWrite( C : TVertex2DF );
      procedure DiameterWrite( D : double );
    public
      FCenter : TVertex2DF;
      FElevation, FEmissionRate, FHeight, FExitTemperature,
      FExitVelocity, FInsideDiameter : double;
      FBuildHgt, FBuildWid, FBuildLen, FXbadj,
      FYbadj : array[ 0..35 ] of double;
      FUrbanSrc : boolean;
      constructor Create;
      destructor Destroy; override;
      procedure Copy( Source : TSource );
      procedure UpdateCenter( P : TPolyDiv2D );
      property Center : TVertex2DF read FCenter write CenterWrite;
      property Diameter : double read FInsideDiameter
                                 write DiameterWrite;
      procedure FileSave( var F : TextFile ); override;
      procedure FileOpen( var F : TextFile ); override;
    end;
```

Figure 3-11: TSource Class definition.

```
(*------- TReceptor ------------------------------------------*)

  TReceptor = class( TCityVisual )
    private
      procedure CenterWrite( C : TVertex2DF );
    public
      FCenter : TVertex2DF;
      FElevation, FHill, FFlag, FConcentration : double;
      FAve, FGrp, FHiVal, FDate : String;
      constructor Create;
      constructor CreateVal( x, y, c, e, h, f : double;
                             ave, grp, hival, date : string );
      destructor Destroy; override;
      procedure Copy( Receptor : TReceptor );
      procedure UpdateCenter( P : TPolyDiv2D );
      property Center : TVertex2DF read FCenter write CenterWrite;
      procedure FileSave( var F : TextFile ); override;
      procedure FileOpen( var F : TextFile ); override;
    end;
```

Figure 3-12: TReceptor Class definition.

```
(*------- TRecNetwork -------------------------------------------*)

  TRecNetwork = class( TCityObject )
    private
      function GetReceptor( i : integer ) : TReceptor;
    public
      ReceptorList : TListFree;
      FXInit : double;
      FXNum : integer;
      FXDelta : double;
      FYInit : double;
      FYNum : integer;
      FYDelta : double;
      constructor Create;
      destructor Destroy; override;
      procedure Copy( RecNet : TRecNetwork );
      procedure CreateReceptors;
      property Receptors[ i : integer ] : TReceptor read GetReceptor;
      procedure FileSave( var F : TextFile ); override;
      procedure FileOpen( var F : TextFile ); override;
    end;
```

Figure 3-13: TRecNetwork Class definition.

The TCity class (Figure 3-14), which represents the top-level object in the city structure hierarchy, also had to be modified to include the newly modelled objects.

```
(*------- TCity --------------------------------------------------*)

  TCity = class( TCityVisual )
    private
      ...
      function GetRecNetwork( i : integer ) : TRecNetwork;
      function GetSource( i : integer ) : TSource;
    public
      ...
      RecNetworkList : TListFree;
      SourceList : TListFree;
      ...
      property RecNetworks[ i : integer ] : TRecNetwork
               read GetRecNetwork;
      property Sources[ i : integer ] : TSource read GetSource;
      ...
    end;
```

Figure 3-14: TCity Class definition modified for the new objects.

The modified CityZoom city model is shown schematically in Figure 3-15, with the new objects in the hierarchy being coloured grey.

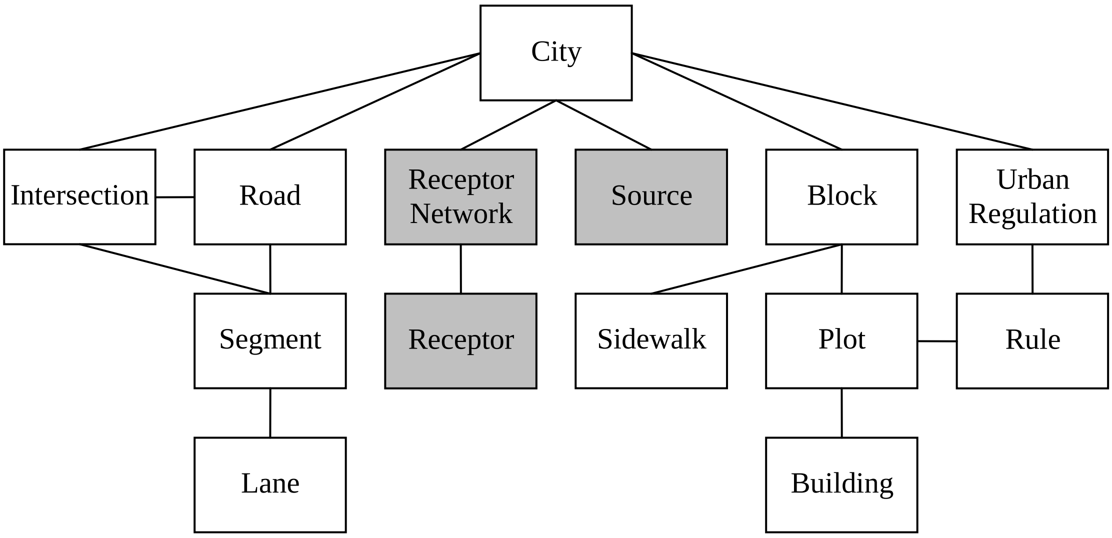

Figure 3-15: Modified CityZoom city model.

The implementation of the CityZoom UP was done using the Object Pascal language, same one used in most of CityZoom source code, in the Delphi 7 programming environment. Over many years of development, CityZoom source code has amounted to over 70,000 lines distributed in over 70 units (files containing source code with classes and functions definitions and implementations). In order to allow CityZoom UP to manipulate the data needed for the desired integration, several of these units had to be modified, and a few new ones had to be created, for example the ones for the new receptor and source objects.

First, the skeletons of the new objects (Source, Receptor, and Receptor Network) were coded into the LCity file, which contains the definitions and methods of all the city objects manipulated by CityZoom. The classes TSource, TReceptor, and TRecNetwork were created, with all the attributes necessary to set up a dispersion or CFD simulation, and with the methods needed to manipulate objects of that type during run time (Create, Destroy, Copy) and for disk storage (Save, Open). Modifications were also made to the TCity object in the same file, as mentioned above. Of special importance are the methods for saving these objects into files and reading object properties from files, since CityZoom UP had to be able to read and save files not only its own file format, but also in file formats used by BPIP, AERMOD, GAMBIT, CFX and OpenFOAM.

After creating the classes representing the data model, it was necessary to implement the methods to draw the objects on the screen and to allow the user interface with them (e.g., insertion and selection using the mouse). This represented modifications to the CEngine2D unit, the graphic engine of CityZoom, and to the FCityZoom unit, the main form, parent of every other form, method and object.

3.7. *Automated Setup of AERMOD Simulations*

In order to setup and start AERMOD simulations, two whole new units were created, LAermod, and FAermod. Following the CityZoom naming standard, the LAermod unit is a library containing the TAermod class. This class contains every "non-city" parameter needed to set an AERMOD run:

- the modeling options and the averaging periods to be calculated for a particular run,
- the methods to equally distribute the source points over the street axes,
- the methods to setup, start, and read back the downwash data from BPIP,
- the methods to create the AERMOD input files based on modeling parameters plus city objects,
- the capacity to start an AERMOD simulation,
- and the methods for reading the output files back to CityZoom.

The FAermod unit defines the form (and its component buttons, edit boxes, check boxes, etc.) shown to the user to set all the attributes for the TAermod object and start the AERMOD run (Figure 3-16).

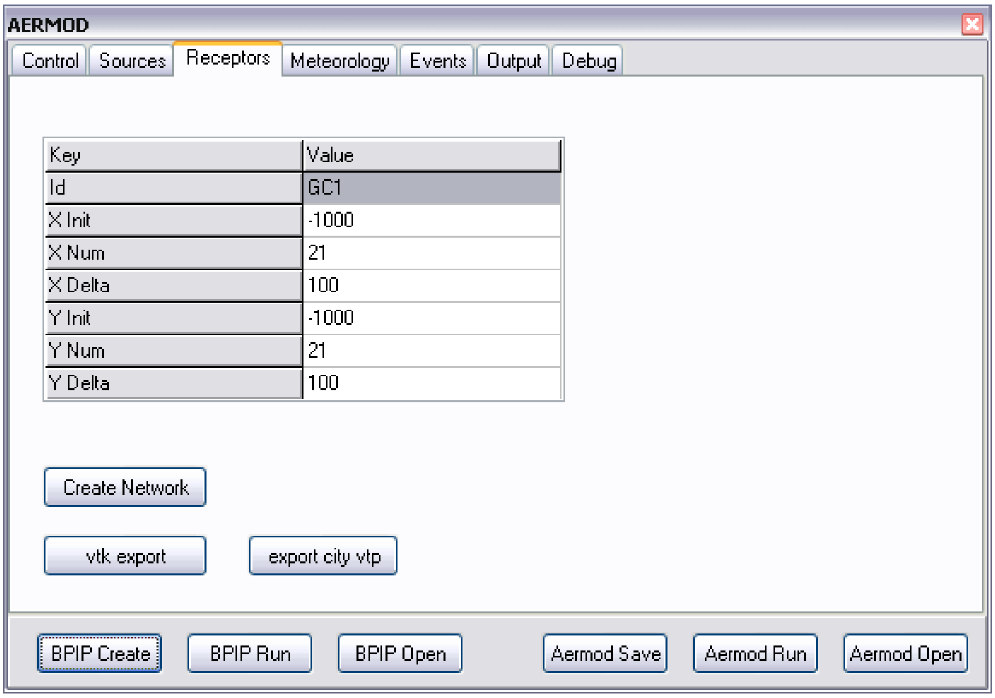

Figure 3-16: AERMOD setup form in CityZoom.

3.7.1. Visualization of results

While CityZoom UP can provide a nice GUI for users to input data to AERMOD, some way of visualizing the generated output files was also needed. The initial idea was to use Mosaic (presented in Section 2.5.3), however it would be ideal to provide a graphical visualization of the results using methods such as contour, surface and pseudocolor plots. There are several free scientific visualization tools available, such as Paraview (Kitware 2008) and VisIt (LLNL 2008), which already have these functionalities.

Scientific visualization tools can usually import several different popular file formats. The Visualization Toolkit (VTK) has its own file format, which seeks to offer a consistent data representation scheme for a variety of dataset types, and to provide a simple method to communicate data between software. This widely used and accepted VTK file format was chosen to export the AERMOD data from CityZoom UP to visualization tools.

There are two different styles of file formats available in VTK. The simplest are the legacy formats, serial formats that are easy to read and write either by hand or programmatically. The second type includes the XML based file formats, which are more flexible than the legacy ones (and consequently more complex), supporting random access, parallel I/O, and portable data compression.

A simple test scenario representing a street intersection was modelled using CityZoom UP (Figure 3-17), so that the resulting AERMOD output files could be used for the VTK export tests. Four blocks and two street segments were drawn, and the point sources automatically distributed over the street segments. A low random number was used for the emission rates from the sources far from the intersection, while a large number was used near the center of the intersection. Again a Cartesian grid of receptors distributed 100 meters from each other and the sample meteorology files provided with the AERMOD examples were used.

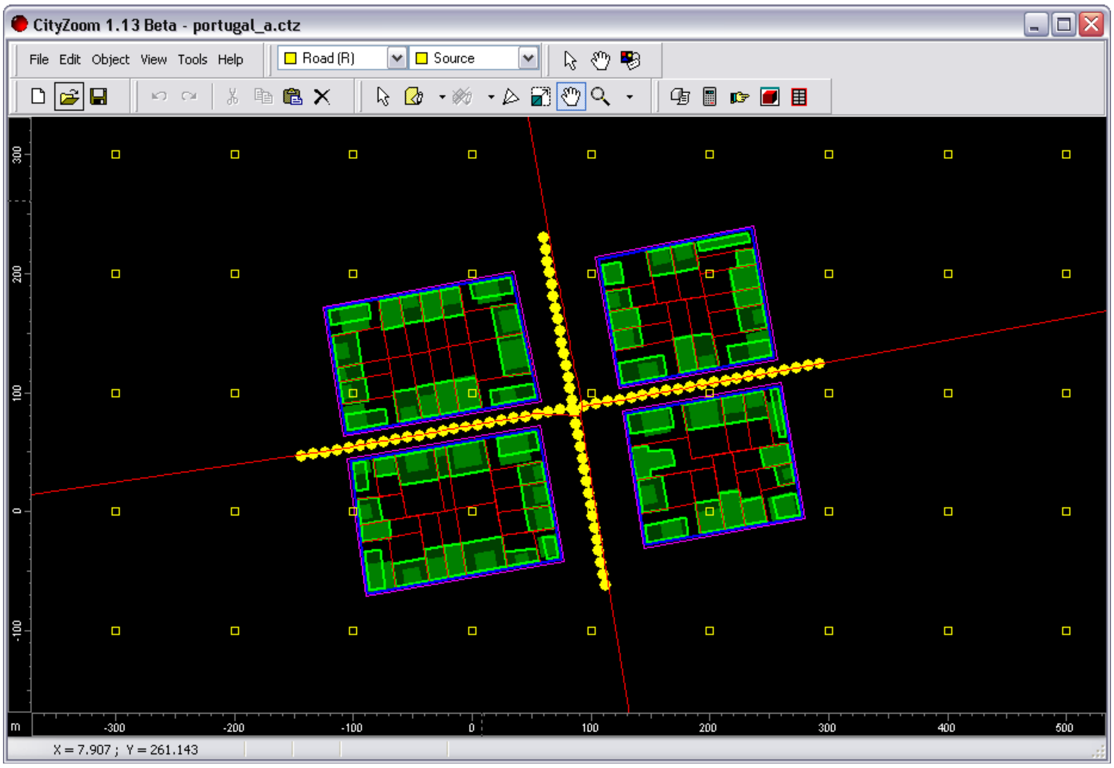

Figure 3-17: City geometry, sources and receptors in CityZoom UP.

The resulting concentration information contained in the receptor network grid is easy to serialize, so the simple VTK legacy format was used to export the location and concentration data from the receptors. A 3D structured grid dataset was used, with the x and y dimensions matching the receptor network grid dimensions and z equal to the flagpole height of the receptors. Each receptor was exported as x-y-z values for each point of the grid, and the concentrations were associated to the points as scalars. Part of an AERMOD results file (maximum concentration for 24 hours averaging period) is shown in Figure 3-18, followed by the VTK equivalent generated by CityZoom UP (Figure 3-19), and its graphic visualization in VisIt (Figure 3-20).

```
*  PLOT FILE OF  HIGH 1ST  HIGH 24-HR VALUES FOR SOURCE GROUP: ALL
*  FOR A TOTAL OF 441 RECEPTORS.
*  FORMAT: (3(1X,F13.5),3(1X,F8.2),3X,A5,2X,A8,2X,A4,6X,A8,2X,I8)
*   X        Y      AVG CONC  ZELEV ZHILL ZFLAG  AVE   GRP HIVAL NETID  DATE
* ______  ______  _________  ____  ____  ____  _____  ___  ___ ___  ________
    0.00    0.00   68.42622  0.00  0.00  1.00  24-HR  ALL  1ST GC1  88030324
  100.00    0.00  149.58302  0.00  0.00  1.00  24-HR  ALL  1ST GC1  88030424
  200.00    0.00   79.04977  0.00  0.00  1.00  24-HR  ALL  1ST GC1  88030124
  300.00    0.00   51.51380  0.00  0.00  1.00  24-HR  ALL  1ST GC1  88030124
  400.00    0.00   37.98667  0.00  0.00  1.00  24-HR  ALL  1ST GC1  88030224
  500.00    0.00   27.95574  0.00  0.00  1.00  24-HR  ALL  1ST GC1  88030224
  600.00    0.00   21.12033  0.00  0.00  1.00  24-HR  ALL  1ST GC1  88030224
  700.00    0.00   16.41482  0.00  0.00  1.00  24-HR  ALL  1ST GC1  88030224
  800.00    0.00   12.92936  0.00  0.00  1.00  24-HR  ALL  1ST GC1  88030224
  900.00    0.00   10.25483  0.00  0.00  1.00  24-HR  ALL  1ST GC1  88030224
 1000.00    0.00    8.34986  0.00  0.00  1.00  24-HR  ALL  1ST GC1  88030224
-1000.00  100.00    2.53846  0.00  0.00  1.00  24-HR  ALL  1ST GC1  88030324
 -900.00  100.00    3.05196  0.00  0.00  1.00  24-HR  ALL  1ST GC1  88030324
 -800.00  100.00    3.73190  0.00  0.00  1.00  24-HR  ALL  1ST GC1  88030324
 -700.00  100.00    4.66486  0.00  0.00  1.00  24-HR  ALL  1ST GC1  88030324
 -600.00  100.00    5.95808  0.00  0.00  1.00  24-HR  ALL  1ST GC1  88030324
 -500.00  100.00    7.79599  0.00  0.00  1.00  24-HR  ALL  1ST GC1  88030324
 -400.00  100.00   10.63349  0.00  0.00  1.00  24-HR  ALL  1ST GC1  88030324
 -300.00  100.00   15.80611  0.00  0.00  1.00  24-HR  ALL  1ST GC1  88030324
 -200.00  100.00   28.03732  0.00  0.00  1.00  24-HR  ALL  1ST GC1  88030324
 -100.00  100.00   54.01528  0.00  0.00  1.00  24-HR  ALL  1ST GC1  88030324
```

Figure 3-18: AERMOD output file.

```
# vtk DataFile Version 2.0
CityZoom generated file
ASCII
DATASET STRUCTURED_GRID
DIMENSIONS 21 21 1
POINTS 441 float
...
0 0 1
100 0 1
200 0 1
300 0 1
400 0 1
500 0 1
600 0 1
700 0 1
800 0 1
900 0 1
1000 0 1
-1000 100 1
-900 100 1
-800 100 1
-700 100 1
-600 100 1
-500 100 1
-400 100 1
-300 100 1
-200 100 1
-100 100 1
...
POINT_DATA 441
SCALARS conc float 1
LOOKUP_TABLE default
...
68.42622
149.58302
79.04977
51.5138
37.98667
27.95574
21.12033
16.41482
12.92936
10.25483
8.34986
2.53846
3.05196
3.7319
4.66486
5.95808
7.79599
10.63349
15.80611
28.03732
54.01528
...
```

Figure 3-19: Concentration file generated by CityZoom UP in VTK format.

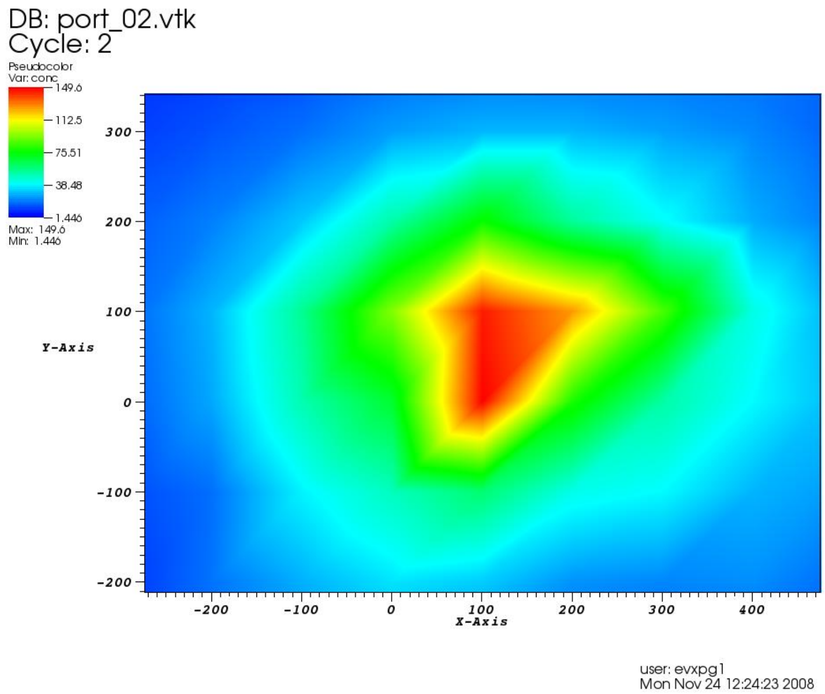

Figure 3-20: Visualization of concentration file generated by CityZoom UP in VTK format.

The more complex VTK XML format was used to export the city geometry, as unstructured PolyData. Each piece (subset of data) describes the polygon of a block, plot, building, or source, independent from the other pieces. VTK allows an arbitrary number of data arrays to be associated with the points and cells of a dataset. Initially, the only data exported with the geometry were the building heights and a scalar indexing the object color, but other information could easily be added, such as the land use type. Part of a VTK XML example file and its graphic equivalent are shown in Figures 3-21 and 3-22.

```
<?xml version="1.0"?>
<VTKFile type="PolyData" version="0.1" byte_order="LittleEndian">
 <PolyData>
  <Piece  NumberOfPoints="4"  NumberOfVerts="0"  NumberOfLines="0"  NumberOfStrips="0"
NumberOfPolys="1">
   <Points>
    <DataArray type="Float32" NumberOfComponents="3" format="ascii">-106.457 65.732 0
55.4200000000001 94.553 0 33.3240000000001 199.269 0 -123.269 170.448 0 </DataArray>
   </Points>
   <CellData Scalars="cell_scalars">
    <DataArray type="Int32" Name="cell_scalars" format="ascii">0</DataArray>
   </CellData>
   <Polys>
    <DataArray type="Int32" Name="connectivity" format="ascii">0 1 2 3 </DataArray>
    <DataArray type="Int32" Name="offsets" format="ascii">4</DataArray>
   </Polys>
  </Piece>
  <Piece  NumberOfPoints="4"  NumberOfVerts="0"  NumberOfLines="0"  NumberOfStrips="0"
NumberOfPolys="1">
   ...
  </Piece>
  ...
 </PolyData>
</VTKFile>
```

Figure 3-21: City geometry file generated by CityZoom UP in VTK format.

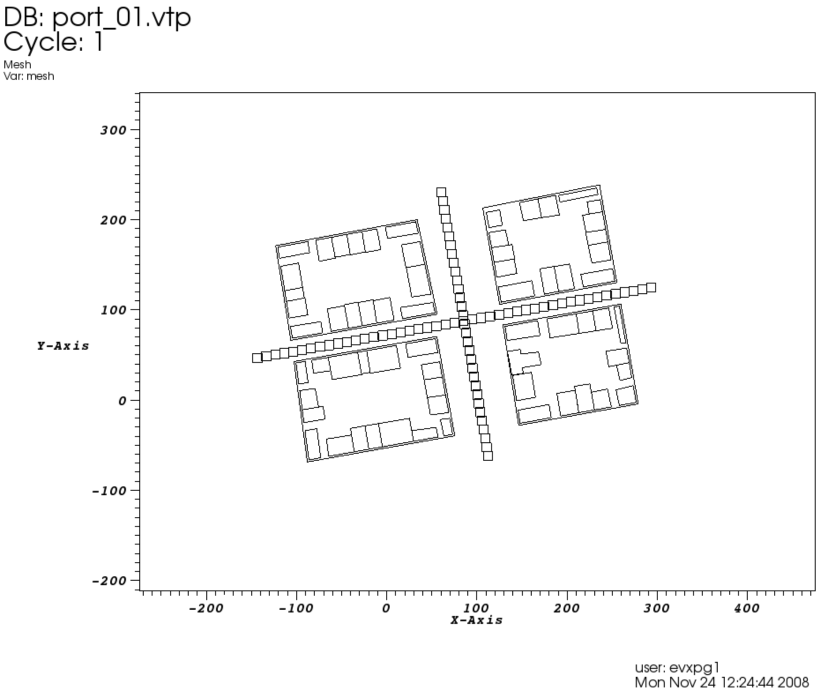

Figure 3-22: Visualization of city geometry file generated by CityZoom UP in VTK format.

Combined, these two files allow for the visualization of the concentrations calculated by AERMOD for CityZoom UP generated scenarios, overlaid with the city objects. The combined final result for the simple simulation scenario is shown in Figures 3-23, overlaying the modelled blocks, buildings and sources with a pseudocolor plot of the resulting average concentration.

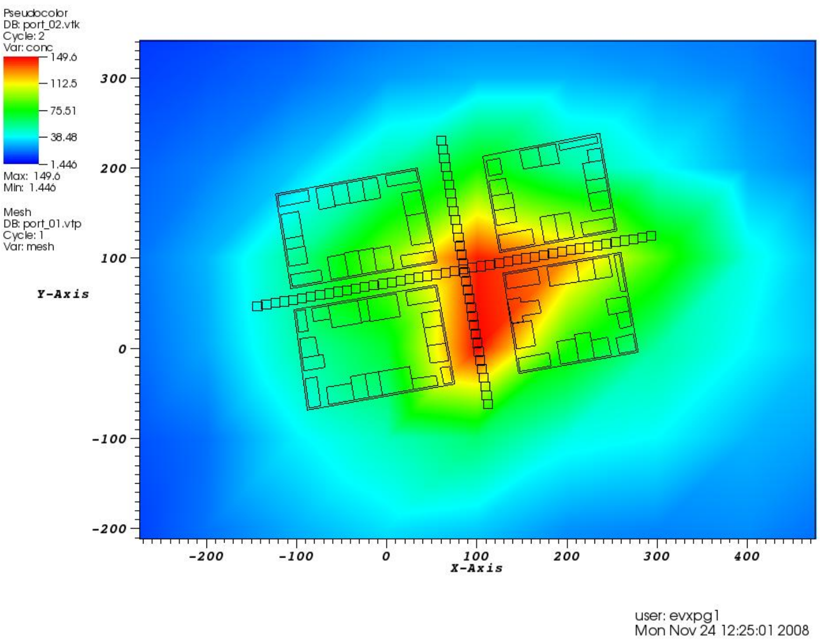

Figure 3-23: Visualization of both concentration and city geometry files.

3.8. Automated Meshing and CFD Analysis

This section details the work done to provide CityZoom UP with the capacity to export data as input to meshing and CFD tools, as a proof of concept of the automation of the process. GAMBIT and CFX, well established commercial tools, were chosen for the first prototype, for being much more stable, reliable, and better documented than the existing free package OpenFOAM. For flexibility and economic reasons, CityZoom UP should also be usable with OpenFOAM, since its open source code would allow it to be used by researches and urban planners anywhere and without costs.

A refined mesh and the proper setup of a CFD simulation are crucial to obtain valid results. The first step in a CFD simulation is to generate the meshes to be used. Journal files can be used to run GAMBIT in batch mode, providing the coordinates and operations needed to generate a 3D mesh. This mesh can then be imported into the CFD package and used in the simulations. An initial attempt to use a virtual plate approach was made, to avoid having to re-mesh the scenarios for each different wind direction, but was discarded in the final version of the prototype, as CityZoom UP should allow for the quickly generation of better quality meshes for each desired wind direction.

.

The LCity unit was modified to allow the buildings to be saved in the Journal format. Another two need units were created, LCfd, and FCfd. Following CityZoom naming standard, the LCfd unit is a library containing the TCfd class. This class has every "non-city" parameter needed to set a GAMBIT run, such as the type of elements to be used and mesh interval size, and the methods to actually create the GAMBIT Journal files based on these parameters plus the city objects (calling the LCity save methods), and to start the GAMBIT run. The FCfd unit defines the form (and its component buttons, edit boxes, check boxes, etc.) shown to the user to set all the attributes for the TCfd object and start the GAMBIT run (Figure 3-24). Some minor changes were needed in the FCityZoom unit, the application main form, to link everything together.

In order to obtain refined meshes, which would allow better quality of simulation results, CityZoom UP was designed to generate journal files with advanced meshing parameters.

The left side panel is used to setup basic meshing parameters:

- The type of volume elements to be used in the generation of the mesh: Hex (Map) specifies that the mesh includes only hexahedral elements and creates a regular, structured grid of such elements; Hex (Submap) also specifies that the mesh includes only hexahedral elements, but divides an unmappable volume into mappable regions and then creates a structured grid of hexahedral mesh elements in each region; Tet/Hybrid specifies that the mesh is composed primarily of tetrahedral elements but may include hexahedral, pyramidal, and wedge elements where appropriate;
- Base file/folder allows the user to set the path where the journal files will be saved;
- GAMBIT path specifies the path for the GAMBIT executable file, allowing it to be started by CityZoom UP in batch mode; and

- Generate mesh indicates if the mesh should be generated or not. Leaving the box unchecked would result in a journal file containing only the commands to create the geometry of the city objects in the scenario.

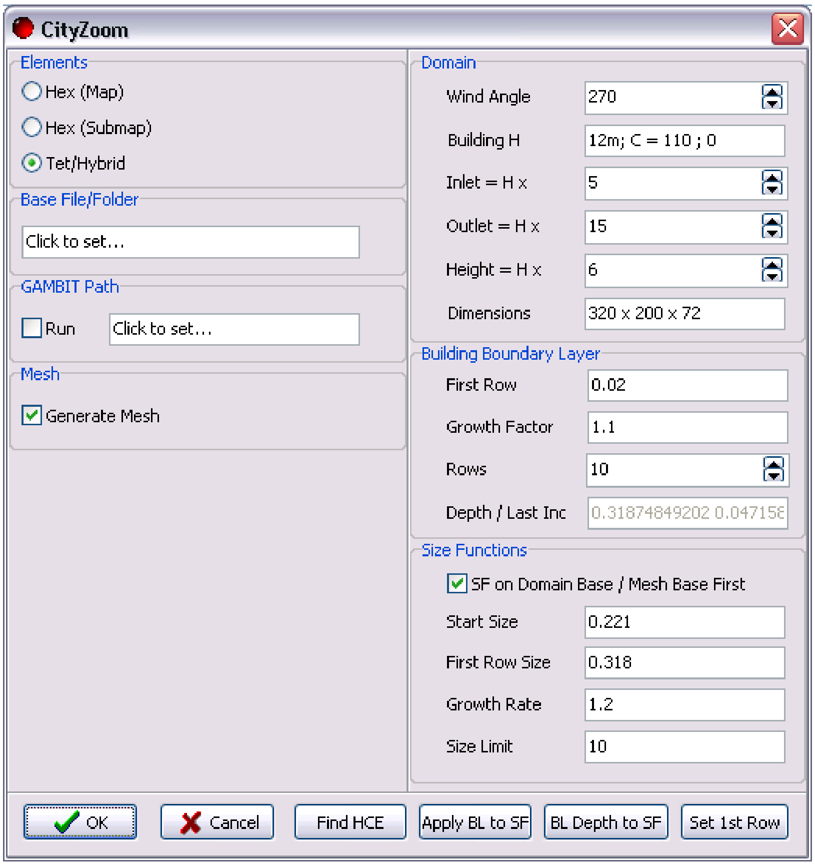

Figure 3-24: CityZoom advanced meshing parameters interface.

The advanced meshing parameters included in the journal files via the right side panel in CityZoom UP user interface are:

- The wind direction, given as an angle from North. Default value is 270°, which represents the wind "from the left to the right" in the floor plan view, along the x axis;
- Distance between the built region and the inlet, outlet and top (height) of the domain. These define the size of the domain box as a function of H_m, the height of the tallest building in the scenario, automatically given by CityZoom UP. Default values for the domain size are 5 x H_m from the inlet and side walls to the nearest building, 15 x H_m from the outlet to the nearest building, and 6 x H_m from the ground to the top of the domain (5 x H_m from the top of the domain to the top of the tallest building);
- Boundary layers around all buildings, based on the size of the first row, the growth rate and the number of rows. "Depth / Last Inc" represents the size of the last cell in the boundary layer, which is automatically estimated and ouput by CityZoom UP; and
- Size functions to increase the cell size as the distance of cells from the buildings increase. A starting size, growth rate and size limit must be informed.

The starting size is considered to be the size of the cells that would be touching the buildings, but since there is the boundary layer around the buildings, the first row of cells generated by the size function is further away and their real size is larger. In order to guarantee a continuity of the growth rate on the boundary layer to size function transition, some functions were implemented in CityZoom UP.

The button "*Apply BL to SF*" calculates the size of the cells in the last row of the boundary layer and then estimates which starting size the size function should have in order to have a cell size in the first row of the function that is proportional to the cell size in the last row of the boundary layer. As an example, setting the boundary layer parameters to first row = 0.02, growth rate = 1.2 and rows = 10. When this button is pressed the values 0.519 and 0.10 are shown for the BL "*Depth / Last Inc*" (meaning the resulting boundary layer will have a depth of 0.519 m and the last cell will be approximately 0.1 m x 0.1 m x 0.1 m) and the size function start size and first row size are set to 0.02 and 0.124 (meaning the first cell generated by the size function would have 0.02 m x 0.02 m x 0.02 m if it was touching the building, but since there are 10 rows of cells from the boundary layer, the real size of the first cell will be 0.124 m x 0.124 m x 0.124 m).

The button "*BL Depth to SF*" functions in a similar way, but estimates the starting size of the size function in order to have the cell size in the first row of the function proportional to the depth of the whole boundary layer around the building. Using the same example as above, when this button is pressed the size function start size and first row size are set to 0.361 and 0.52 (the depth of the boundary layer was calculated to be 0.519 m, so the start size 0.361 m should generate a first cell in the size function with size 0.52 m x 0.52 m x 0.52 m).

The button "*Set 1st Row*" calculates the start size of the size function in order for the first row of generated cells to have the size given by the user. The button "*Find HCE*" recalculates the domain height, centre and extensions after a change to the wind angle, inlet, outlet or height, and displays the updated domain dimensions on the appropriate field.

An example of the application of a boundary layer around a building followed by a size function growing the mesh as the distance from the building increases is shown in Figure 3-25. Parameters used are: BL first row = 0.05 m, BL growth rate = 1.2, number of BL rows = 10, SF start size = 0.5 m, SF growth rate = 1.2, SF size limit = 15 m.

The Journal files generated by CityZoom UP define not only the geometry and meshing parameters, but also set the boundaries and continuum zones of the domain, using a "natural" nomenclature, which makes it easier to understand and check the objects and boundaries in CFX: the inflow boundary is named "w_inflow", the outflow boundary is named "w_outflow", and so on for the top, bottom, sides, sources and building walls. GAMBIT processes the journal file and generates another two files, a .dbs file containing the geometry and mesh in the GAMBIT proprietary format, and a .cdb file containing the mesh in the ANSYS format used by CFX.

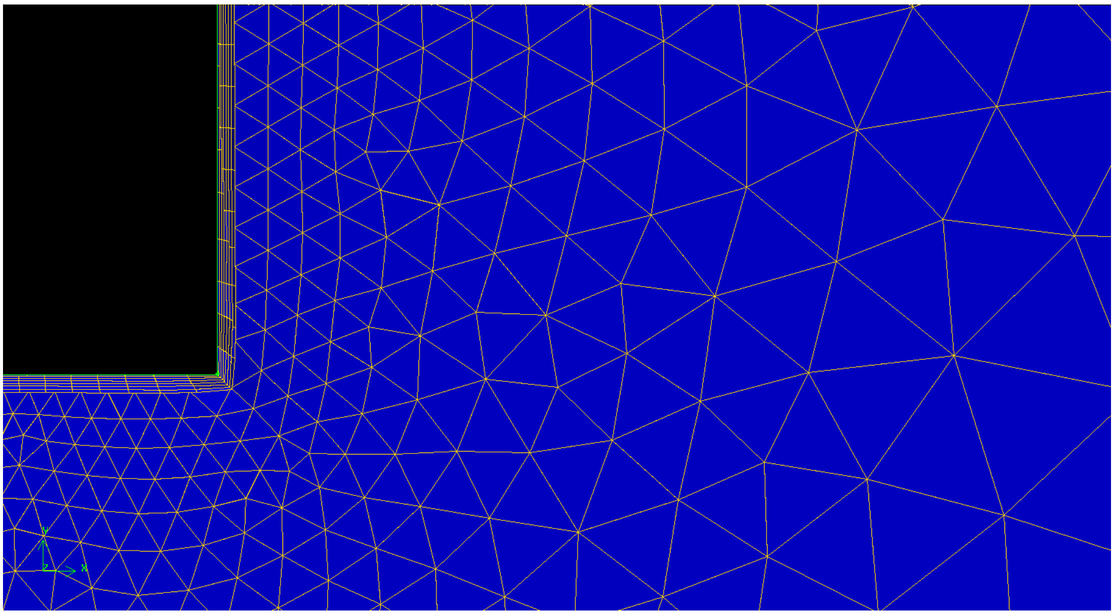

Figure 3-25: Boundary Layer around building and Size Function in the base of the domain box.

The ANSYS .cdb file representing the domain and city geometry can then be imported into CFX, where the simulation parameters, and boundary and initial conditions can be set. As mentioned, the boundaries were already defined and named in the Journal files, so the user only needs to set them properly: INFLOW on the “w_inflow” boundary, OUTFLOW on the “w_outflow” boundary, etc. The automation of this part of the process can be done using script files, as in Morvan (2005).

3.8.1. Automation for OpenFOAM

The OpenFOAM (Open Field Operation and Manipulation) CFD Toolbox (OpenCFD 2007) is a general purpose open source CFD code. The possibility to use CityZoom UP to setup CFD simulations using OpenFOAM increases the viability for use outside of the academic environment, by avoiding the expenses with commercial CFD software.

A CFD run in OpenFOAM is defined using several text files of .dict extension, called “Dictionaries”. Each of these files can be used to set different parameters, such as boundary conditions, initial conditions, or turbulence model variables. CityZoom UP was programmed to generate the whole directory structure and set of files necessary to run a simple one phase flow CFD simulation in OpenFOAM 1.6 (Figure 3-26). These files contain the full description of the case mesh, the physical properties for the application, the parameters associated with the solution itself, and the initial values and boundary conditions. Since CityZoom UP runs on Windows and OpenFOAM runs on Linux, these files need to be manually copied between the different systems in order to run the simulations and then analyse the results.

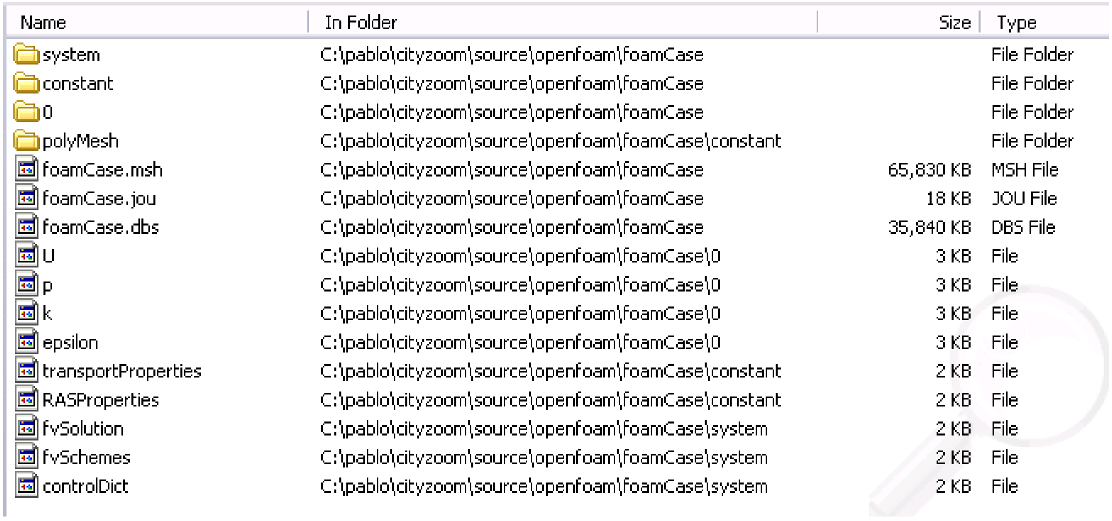

Name	In Folder	Size	Type
system	C:\pablo\cityzoom\source\openfoam\foamCase		File Folder
constant	C:\pablo\cityzoom\source\openfoam\foamCase		File Folder
0	C:\pablo\cityzoom\source\openfoam\foamCase		File Folder
polyMesh	C:\pablo\cityzoom\source\openfoam\foamCase\constant		File Folder
foamCase.msh	C:\pablo\cityzoom\source\openfoam\foamCase	65,830 KB	MSH File
foamCase.jou	C:\pablo\cityzoom\source\openfoam\foamCase	18 KB	JOU File
foamCase.dbs	C:\pablo\cityzoom\source\openfoam\foamCase	35,840 KB	DBS File
U	C:\pablo\cityzoom\source\openfoam\foamCase\0	3 KB	File
p	C:\pablo\cityzoom\source\openfoam\foamCase\0	3 KB	File
k	C:\pablo\cityzoom\source\openfoam\foamCase\0	3 KB	File
epsilon	C:\pablo\cityzoom\source\openfoam\foamCase\0	3 KB	File
transportProperties	C:\pablo\cityzoom\source\openfoam\foamCase\constant	2 KB	File
RASProperties	C:\pablo\cityzoom\source\openfoam\foamCase\constant	2 KB	File
fvSolution	C:\pablo\cityzoom\source\openfoam\foamCase\system	2 KB	File
fvSchemes	C:\pablo\cityzoom\source\openfoam\foamCase\system	2 KB	File
controlDict	C:\pablo\cityzoom\source\openfoam\foamCase\system	2 KB	File

Figure 3-26: OpenFOAM file structure generated by CityZoom UP.

Three options are available for the generation of the meshes to be used by OpenFOAM. The first option is to use GAMBIT and then copy the mesh file to the OpenFOAM folder. The second option is to use the OpenFOAM's simple meshing utility *blockMesh*. Finally, the third option is the advanced meshing generation utility *snappyHexMesh*.

The simple tool *blockMesh* requires the geometries to be defines as vertexes and ordered blocks, and then meshes each block based on user-defined parameters. As OpenFOAM does not provide a graphical modelling tool, Windows Notepad was used to define the geometry of a simple street canyon case test. This geometry was based on the block schematic shown in Figure 3-27, and resulted in the text (ASCII) file shown in Figure 3-28.

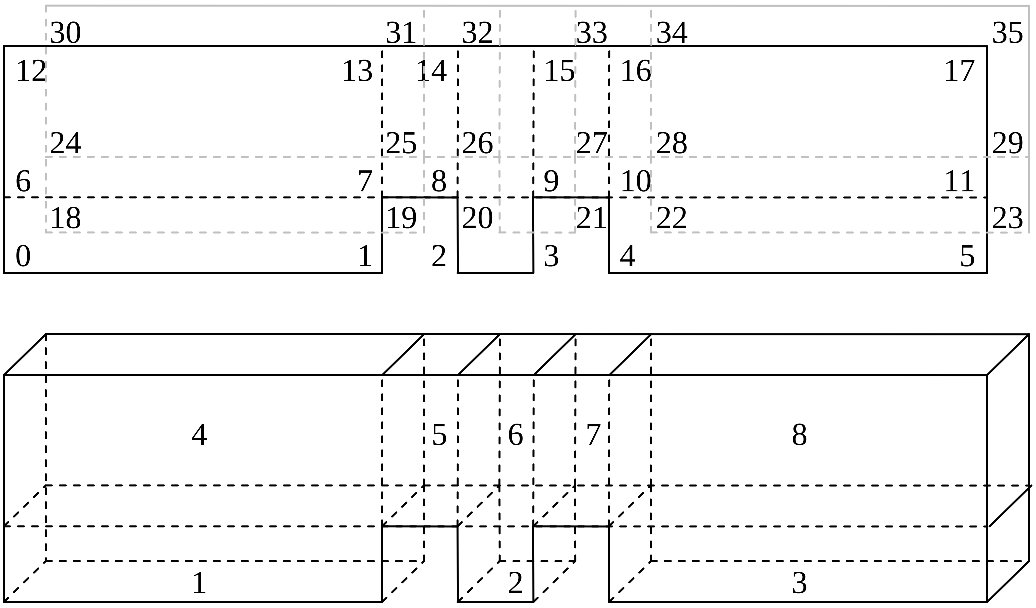

Figure 3-27: Simple street canyon schematic – vertices and blocks.

```
vertices
(
    (0 0 -0.05)
    (5 0 -0.05)
    (6 0 -0.05)
    (7 0 -0.05)
    (8 0 -0.05)
    (13 0 -0.05)
    (0 1 -0.05)
    (5 1 -0.05)
    (6 1 -0.05)
    (7 1 -0.05)
    (8 1 -0.05)
    (13 1 -0.05)
    (0 3 -0.05)
    (5 3 -0.05)
    (6 3 -0.05)
    (7 3 -0.05)
    (8 3 -0.05)
    (13 3 -0.05)
    (0 0 0.05)
    (5 0 0.05)
    (6 0 0.05)
    (7 0 0.05)
    (8 0 0.05)
    (13 0 0.05)
    (0 1 0.05)
    (5 1 0.05)
    (6 1 0.05)
    (7 1 0.05)
    (8 1 0.05)
    (13 1 0.05)
    (0 3 0.05)
    (5 3 0.05)
    (6 3 0.05)
    (7 3 0.05)
    (8 3 0.05)
    (13 3 0.05)
);

blocks
(
    hex (0 1 7 6 18 19 25 24) (50 10 1) simpleGrading (1 1 1)
    hex (2 3 9 8 20 21 27 26) (20 20 1) simpleGrading (1 1 1)
    hex (4 5 11 10 22 23 29 28) (50 10 1) simpleGrading (1 1 1)
    hex (6 7 13 12 24 25 31 30) (50 20 1) simpleGrading (1 1 1)
    hex (7 8 14 13 25 26 32 31) (10 20 1) simpleGrading (1 1 1)
    hex (8 9 15 14 26 27 33 32) (10 20 1) simpleGrading (1 1 1)
    hex (9 10 16 15 27 28 34 33) (10 20 1) simpleGrading (1 1 1)
    hex (10 11 17 16 28 29 35 34) (50 20 1) simpleGrading (1 1 1)
);
```

Figure 3-28: ASCII file defining the street canyon geometry (partial).

This file was meshed using the *blockMesh* utility provided by OpenFOAM. The resulting mesh is shown in Figure 3-29.

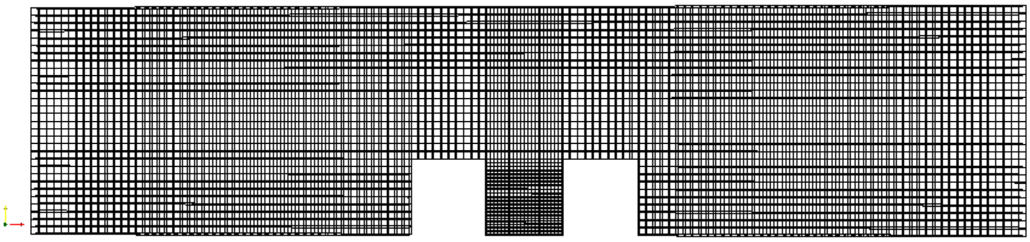

Figure 3-29: ParaView visualization of canyon mesh generated by blockMesh.

This street canyon mesh was used to run a simple *icoFoam* simulation (OpenFOAM solver for laminar, isothermal, incompressible flow). The results for each time step are calculated and stored in separate text files, which can then be converted for visualization in ParaView. Results for this simple simulation are shown in Figure 3-30. The colours represent wind speed, cooler colours (towards blue) are lower wind speeds and warmer colours (towards red) are higher wind speeds.

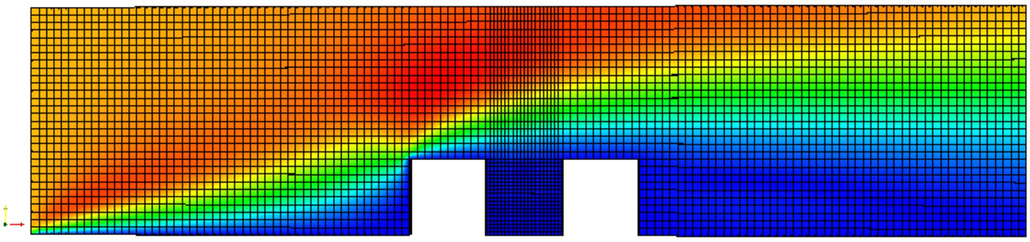

Figure 3-30: Simple canyon simulation results from OpenFOAM.

The advanced mesh generation utility *snappyHexMesh* can generate three dimensional meshes containing hexahedra and split-hexahedra automatically from triangulated surface geometries in Stereolithography (STL) format. The mesh approximately conforms to the surface by iteratively refining a starting mesh (generated by the *blockMesh* utility) and morphing the resulting split-hex mesh to the surface. The meshing process is controlled by switches defined in the appropriate dictionary file.

CityZoom UP can export the simulation domain and each building as a separate STL file, along with the control dictionary. These files need to be manually copied to the Linux system, where *snappyHexMesh* can then be used to generate the mesh and OpenFOAM can be used to run the simulation.

The School of Engineering Linux cluster Stokes was used for the OpenFOAM simulations. The CFD group led by Dr. David Hargreaves uses this machine regularly for similar cases and have created customized boundary conditions to replicate the atmospheric boundary layer for urban simulations in OpenFOAM.

CityZoom UP was used to create a simple scenario for simulation using OpenFOAM. The STL file for a single building was generated and the mesh was created using *snappyHexMesh*. A few simple simulations were run but there are no significant results to show at present. Some simple results of this OpenFOAM simulation generated and set by CityZoom UP are illustrated in Figure 3-31. Once again the colours represent wind speed (cooler colours towards blue are lower wind speeds and warmer colours towards red are higher wind speeds), but now in a 3D scenario. Further development is needed to modify the setup files to set OpenFOAM for the simulation of multispecies flows.

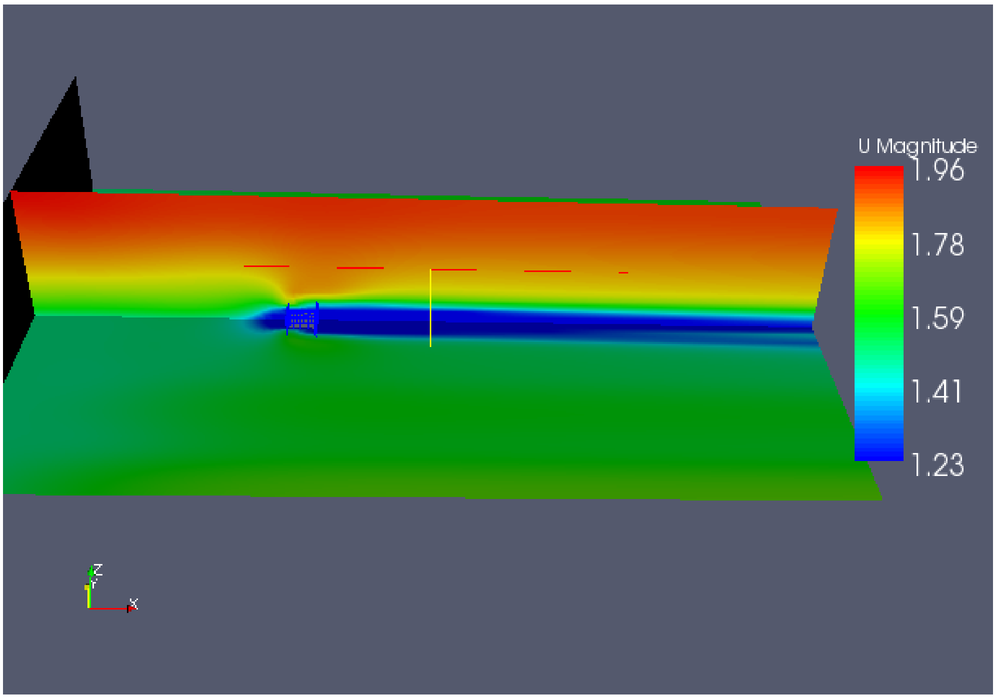

Figure 3-31: Single building test using OpenFOAM. Wind speed profile at the xy and xz planes.

3.9. Conclusions

CityZoom UP, an extension of CityZoom to assist in the modelling and setting up of urban scenarios for dispersion and CFD simulation, has been successfully implemented. CityZoom data model and user interfaces were modified, introducing the capacity of handling urban pollution related objects and data: source positions and emission rates, receptor positions, networks of receptors, meteorological data and simulation control parameters.

Given the city geometry, traffic emission rates and meteorology data, the developed software can be used to automatically setup and launch AERMOD simulations. Resulting highest or hourly concentrations can be read back into CityZoom UP and then exported for visualization using VTK files. The city geometry and the spatially distributed sources and associated emission rates can also be exported on these VTK files.

The approach to model traffic emissions as sequences of point sources was well accepted by the traffic specialists at LASTRAN – UFRGS (Ariotti et al. 2008; Ariotti and Cybis 2010) as a more natural and intuitive way to represent the emission profiles (as opposed to the traditional line source approach), and even led to the collaborative paper “Validation and sensitivity testing of CityZoom-AERMOD model” (Grazziotin et al. 2010). Robins (2011) later suggested that this type of model is likely to be more appropriate to represent moving sources than the usual line source approach.

Modelling and setup of urban scenarios for the simulation using CFD tools was achieved with some limitations. For the commercial tools, automated meshing was developed with good flexibility in the refinement parameters via GAMBIT journals. The boundaries are also automatically generated and identified using names related to their physics properties to be used in the simulation (domain base, top, inlet, outlet, buildings, and symmetries), which facilitates the setup of the cases using CFX.

The capability to automate the mesh generation based on user-defined refinement parameters and to automatically set the domain boundaries can greatly reduces the time necessary for the setup CFD cases, even if it does not affect the computational time needed to run the CFD simulations.

For the open source tools, both the mesh generation and case setup for single phase flows are automated via dictionary files, however further study and development are needed in order to automate the setup for multispecies flows.

To test and validate the developed tool and proposed methodology, scenarios must be modelled in order to compare the simulated results with measured airflow and pollution data. Measurement data is available from different projects, such as DAPPLE and the Instrumented City. The following chapter presents the tests performed using CityZoom UP.

4. Testing CityZoom UP

This chapter describes the tests performed to validate CityZoom UP as a tool to assist in the modelling and setup of urban scenarios for dispersion and CFD simulation, as well as the use of AERMOD for the simulation of the dispersion of pollutants in urban environments. Comparison with existing data must be established.

Meteorological and dispersion measurement data is available from different projects described on Chapter 2, such as DAPPLE (Arnold et al. 2004; Wood et al. 2009; Robins 2011), Joint Urban 2003 (Allwine et al. 2004; Clawson et al. 2005), Instrumented City (Chen and Bell 2002), and Mock Urban Setting Test (Biltoft 2001). The initial plan was to use the Instrumented City data, since the proximity to Leeds, where the Institute of Transport Studies hosted the project, could facilitate the discussion and understanding of the data. The author visited the city of Leeds and met the ITS group, but, the project was terminated a few months later and the data was never obtained. The DAPPLE data sets were then chosen for the tests, since the project included moving source experiments which tried to reproduce traffic-related emission patterns.

All the tests used CityZoom UP as the tool to model the urban scenario. The tests performed included: sensitivity tests of AERMOD, validation of AERMOD against wind tunnel experimental data, validation of AERMOD against tracer release experiments in central London, mesh generation and refinement tests, mesh independence tests, and semi-automated setup of multispecies flow simulation tests.

4.1. Sensitivity Tests

To verify that the CityZoom UP coupled to AERMOD model behaved consistently to variations of the different urban parameters, a set of tests was designed with the assistance of LASTRAN (Laboratory for Transport Systems, UFRGS, Brazil) researchers Helena Cybis and Paula Ariotti, experts in modeling traffic emissions (Ariotti et al. 2008; Ariotti and Cybis 2010). A set of urban scenarios was modelled, consisting of an array of 4 x 4 blocks of side 300 m, with either spread out 2-storey buildings (Figure 4-1a) or clustered 10-storey buildings (Figure 4-1b).

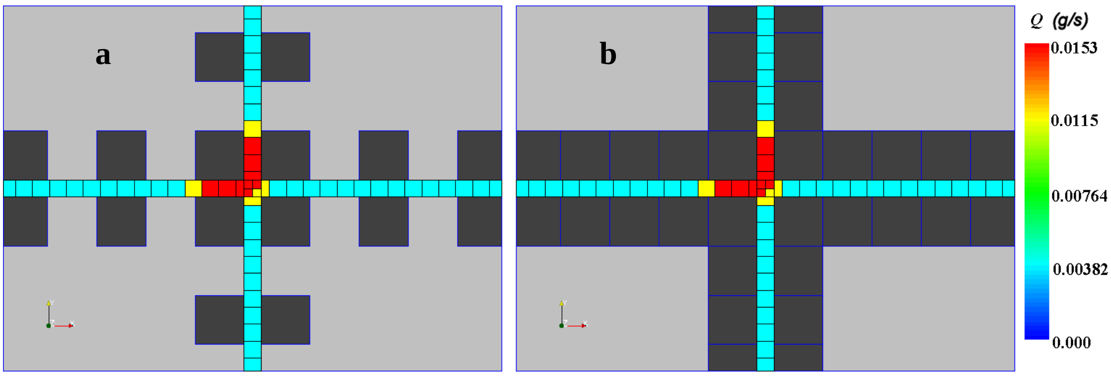

Figure 4-1: Emission rates at an intersection for traffic Profile 2 with (a) 2-storey and (b) 10-storey buildings. The dark-grey areas are buildings and the light-gray are open spaces.

Sources were distributed in 10 m intervals along the streets axes. The sources had the following properties: exit temperature = environment temperature + 50°C; exit velocity = 0.001 ms^{-1} and height = 0.03 m.

Emission rates were set based on 2 traffic profiles with equal total emissions: one corresponding to uniform emissions along the street axis (Profile 1 in Figure 4-2) and one representative of heavy traffic with traffic lights at every intersection (Profile 2 in Figure 4-2).

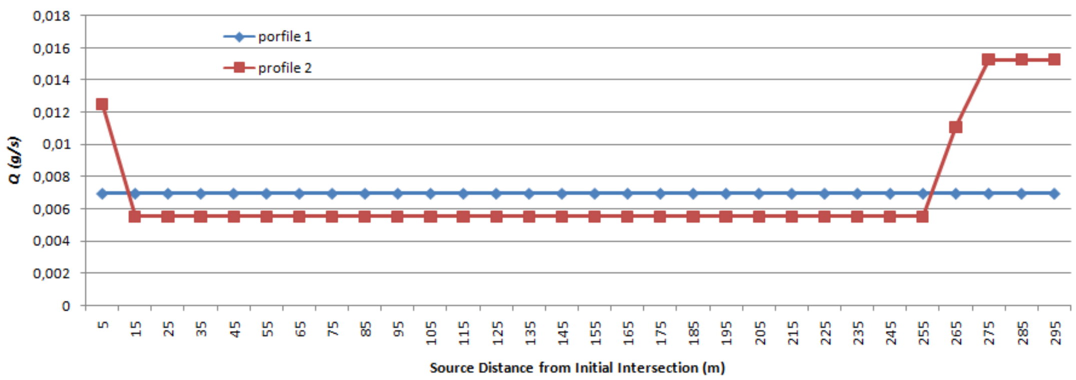

Figure 4-2: Emission profiles for each 300 m street segment, considering the initial intersection at 0 m and the final intersection at 300 m.

A set of neutral atmospheres was created for the tests, using AERMET (the AERMOD meteorological pre-processor) to generate combinations of the following parameters: surface wind speeds of 4 and 8 ms^{-1}, surface wind directions of 270° and 315° from the north and roughness lengths of 1 m and 3 m ($^1/_{10}$ of the average building heights), to be used with the 2- and 10-storey scenarios respectively. The simulations were run for a single hour. Concentrations were measured at the default AERMOD above ground-level height of 0.0 m. Initial tests showed that a domain size of at least 1000 m was necessary to capture all the highest concentrations for the proposed data set.

The sensitivity to surface wind speed was studied, and the simulations showed unexpected results. Contrary to common experience, the maximum final concentrations were higher for the 8 ms^{-1} tests than for the 4 ms^{-1}. This happened near the end of the domain, where the emissions from several sources overlapped, since the higher wind speeds carry the pollutants further, hence the receptors are influenced by a larger number of sources.

The same approach was used to verify the sensitivity to surface roughness. The 10-storey scenario was simulated for roughness lengths of 1m and 3m. Roughness acts by reducing the surface wind speed, so the higher roughness resulted in lower concentrations.

The resulting concentrations from the sensitivity tests are shown for the combination of parameters: surface wind speed of 4 ms^{-1}, wind directions of 270° and 315° from the north, urban scenarios with 2- and 10-storey buildings (z_0 of 1 m and 3 m respectively) and traffic profiles Profile 1 and Profile 2. Figure 4-3 shows the highest concentration for each case.

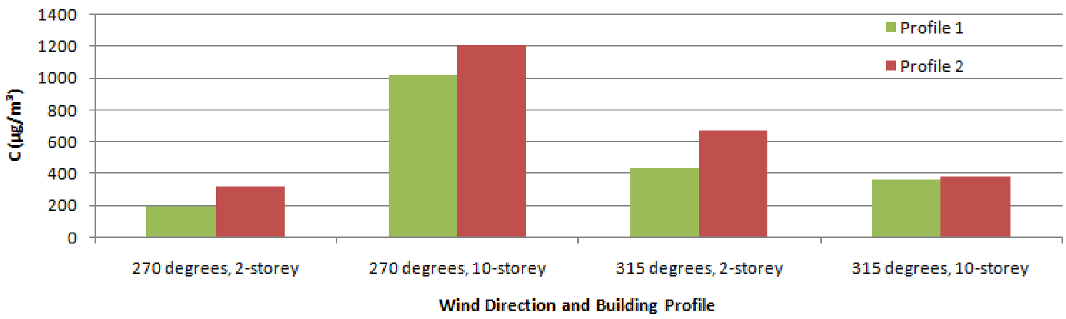

Figure 4-3: Highest concentrations for the combination of parameters.

Figure 4-4 shows a pseudocolor plot of the simulated concentrations for the wind direction of 270°. A cold to warm colour scale is used, where blue represents lower concentrations and red represents higher concentrations. It is important to highlight that the buildings are not solid objects, so concentrations can be calculated in points that would be inside the buildings.

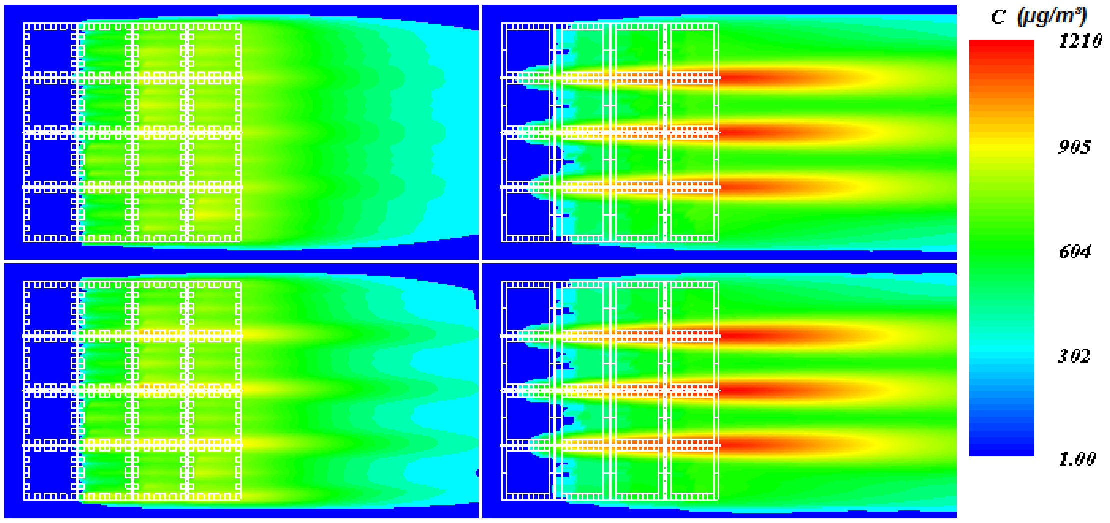

Figure 4-4: Pseudocolor plot of simulated concentrations at ground level for wind direction 270° from the north. Top: Profile 1. Bottom: Profile 2. Left: 2-storey buildings. Right: 10-storey buildings.

The left side of Figure 4-4 shows the combination of 2-storey buildings and uniform emission Profile 1 (top) and emission Profile 2 (bottom). It is noticeable how the pollutants can disperse uniformly over the domain. Small hot spots can be seen along the streets, where the sources are located.

The right side of Figure 4-4 shows how the tall 10-storey buildings act by funnelling the pollutants into the street and causing the emissions from the sources to overlap, resulting in very high concentrations for both Profile 1 (top) and Profile 2 (bottom). This is a result of the downwash effect introduced by the PRIME algorithm, since the buildings are not actually present as solid objects in the simulation.

A pseudocolor plot of the simulated concentrations for wind direction 315° from the North is presented on Figure 4-5. Once again, a cold to warm scale is used.

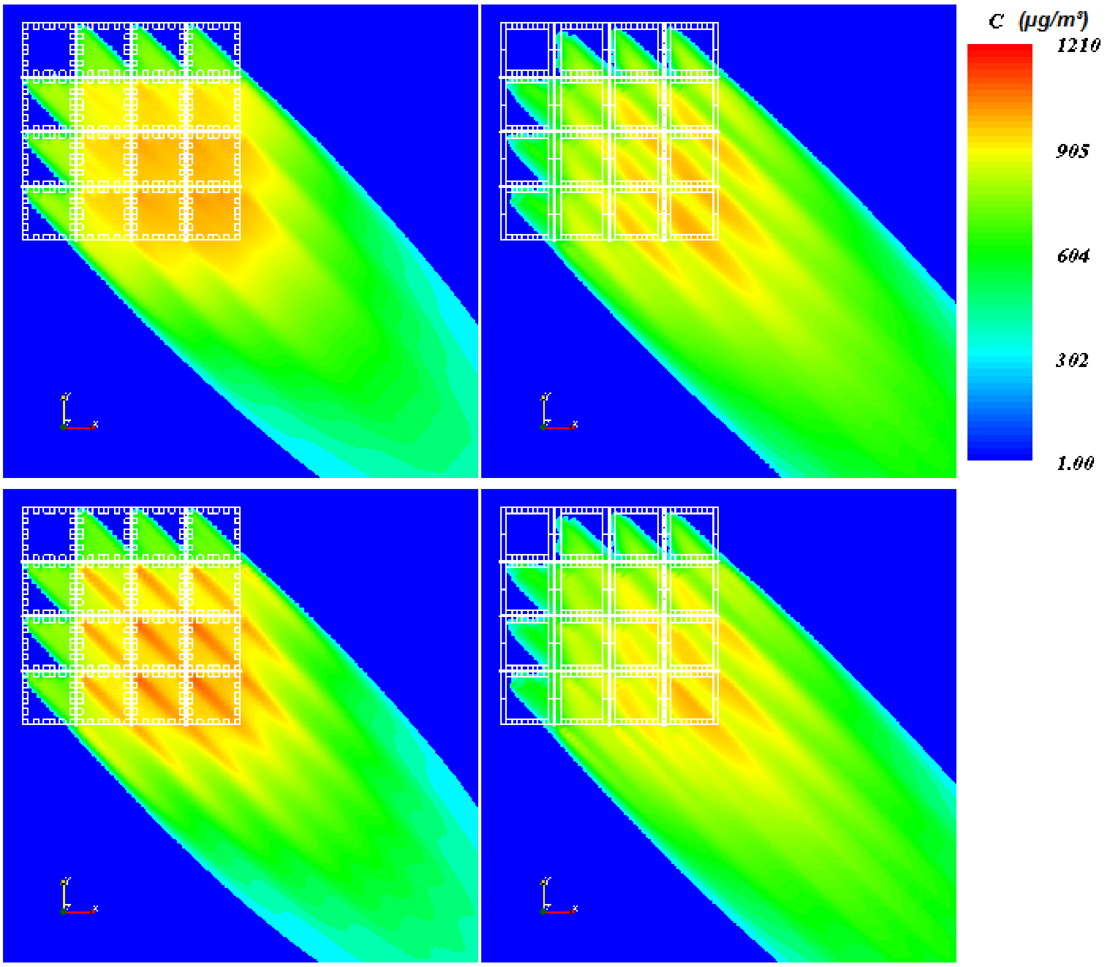

Figure 4-5: Pseudocolor plot of simulated concentrations at ground level for wind direction 315° from the north. Top: Profile 1. Bottom: Profile 2. Left: 2-storey buildings. Right: 10-storey buildings.

As in the previous image, Figure 4-5 shows the 2-story buildings on the left side and 10-story buildings on the right side, combined with emission Profile 1 on the top and Profile 2 on the bottom. The uniform emission Profile 1 (top) generates nearly uniform distributions of concentrations. Emission Profile 2 combined with 2-storey buildings (bottom left) results in hot spots along the wind direction, since the short buildings do not provide much protection from the high emission rates at the intersections. These hot spots are reduced for the combination of Profile 2 and 10-storey buildings (bottom right), since the wall of tall buildings blocks the pollutants from going too far downwind.

Sensitivity to emission profiles and to the built environment were successfully verified, although some results are questionable. Since the Gaussian equations do not account for recirculation, a building directly downwind from a source causes the concentrations to be lower further downwind, but does not cause the concentrations to be higher upwind. This is noticeable for the case where the wind direction is diagonal to the street axes and the tall buildings act by reducing the wind speed and result in a reduction of the dispersion of pollutants.

Overall, Profile 2 always results in higher concentrations, because the emissions are much higher near the intersections. The effect of the different emission profiles is more noticeable on the 2-storey building cases, as the short and spread buildings do not have great impact in the dispersion of pollutants.

Tall buildings, in the other hand, cause great impact in the dispersion. In conjunction with winds parallel to the street axes, they result in very high concentrations, since the buildings act by funnelling the wind and the pollutants, which cause receptors to be influenced by more distant sources as well as near ones. With wind direction diagonal to the street axes, the tall buildings act by reducing the wind speed and blocking the dispersion of pollutants.

This series of tests also served to demonstrate that the CityZoom UP was successful in working with AERMOD in terms of the data handling. AERMOD is not often used in such high density urban environments, but rather it is used for isolated sources with a small number of buildings causing downwash and wake interference. To be used in this manner creates a number of challenges. Most noticeably from Figures 4-4 and 4-5 is that the concentrations inside buildings are non-zero, since AERMOD does not model building as solid objects.

4.2. Validation Tests Using Wind Tunnel Experimental Data

Initial validation of the CityZoom UP coupled to AERMOD model consisted of a comparison with the wind tunnel experimental campaign from the DAPPLE project. The site geometry used at the wind tunnel experiments was scaled to full scale (0.1 m in the wind tunnel model is equivalent to 20 m at full scale) and imported into CityZoom UP, because AERMOD cannot handle the small scales seen in the wind tunnel. A case was then modelled, with a single source positioned at x = -6.4 m, y = -177.6 m, z = 2 m to use with wind direction from the south. The left side of Figure 4-6 shows the model in CityZoom UP and highlights the source position in red and receptor positions in orange. The right side of Figure 4-6 shows a 3D render of the modelled scenario in CityZoom UP. Additional source parameters were also scaled to: Q = 0.000583 gs^{-1} (equivalent to 2.005 litre/m at 17400 ppm), diameter = 1 m, exit velocity = 0.001 ms^{-1} and exit temperature = 0.0 (interpreted by AERMOD as equal to ambient temperature). The atmospheric conditions were modelled to try to replicate the wind tunnel conditions.

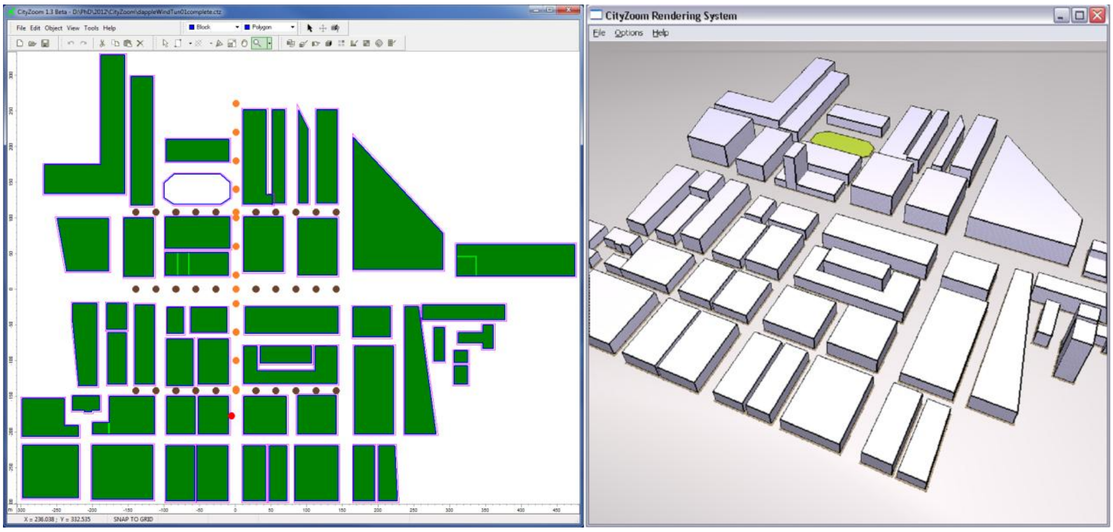

Figure 4-6: The DAPPLE site geometry in CityZoom UP. Left: 2D view, where the red dot represents the source and the orange and brown dots are the receptors. Right: 3D view.

In order to be able to compare full-scale measurements with results from the scaled wind tunnel model, the DAPPLE results are given as non-dimensional concentration, $C*$, defined by:

$$C* = CUA/Q \tag{1}$$

where C is the measured concentration, U is the surface wind speed, A is the square of the average building height H_a (H_a = 0.11 m for the wind tunnel model and H_a = 22 m for the CityZoom UP model) and Q is the emission rate. The same equation is used to establish a comparison between the DAPPLE wind tunnel data and the AERMOD simulation results.

Figure 4-7 shows a log plot of the non-dimensional concentration $C*$ by non-dimensional straight-line distance R/H_a to the source for the receptors along the x = 0 axis.

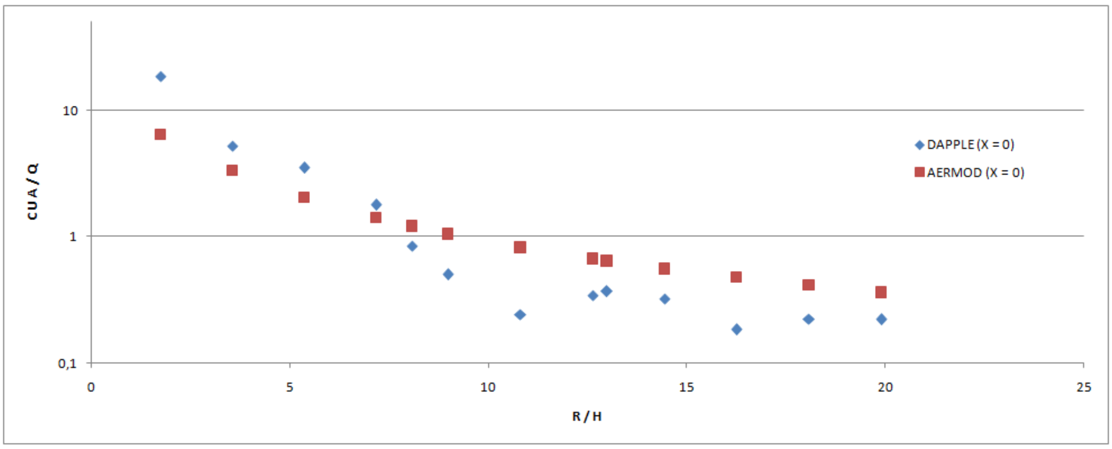

Figure 4-7: Non-dimensional concentration *CUA/Q* by non-dimensional distance R/H_a to the source over the *x = 0* axis.

The *x* axis of the plot represents the non-dimensional distance between the red source and the orange receptors in Figure 4-6. The *y* axis represents the non-dimensional concentration on each of these receptors. Concentration is higher near the source and diminishes faster as the distance to the source increases in the DAPPLE wind tunnel experiments in comparison with the AERMOD simulation results. Both lines follow a similar trend.

Figure 4-8 shows the log plot of non-dimensional concentrations *C** for the 3 horizontal receptor lines (brown receptors plus the 3 orange receptors that belong to each of those line of receptors) shown in Figure 4-6. The top line of receptors in Figure 4-6 is at y = 108, the middle one at y = 0 and the bottom one at y = -142.

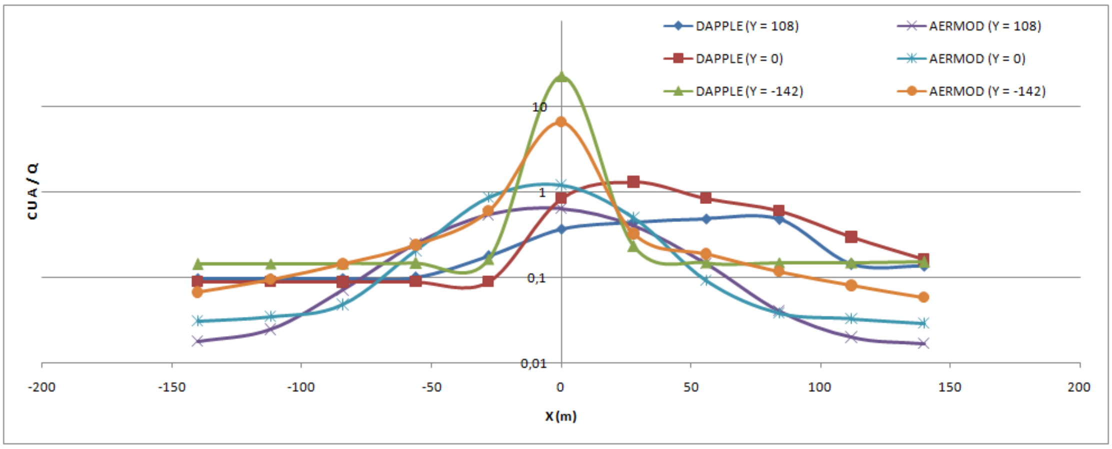

Figure 4-8: Non-dimensional concentration *CUA/Q* by *x* position of the receptor over *y* axes.

It can be noticed that the simulated concentration results follow the same distribution trend of the measured wind tunnel concentrations. The wind tunnel results show higher concentration than the simulated results for receptor sites near and downwind from the source, while the concentrations are lower for receptor sites far or crosswind from the source. One of the reasons for the differences is the fact that the buildings are not explicitly modelled in AERMOD (i.e., they do not act like blockages), but only their influence over each source is considered.

The results obtained are considered good for the purposes of a strategic urban decision tool, especially considering the computational time needed to achieve them is in the order of seconds. For more precise results, a detailed approach such as CFD is recommended, which is explored in the CFD-related part of the research.

4.3. Validation Tests using Data from Tracer Release Experiments in Central London

There are a number of urban tracer release experiments as well as mathematical and computational models for static sources (e.g., the whole DAPPLE Project and its extensions: Arnold et al. (2004); Wood et al. (2009); Shallcross et al. (2010)). However, traffic-related emissions are a mobile source, and with that in mind, novel mobile release experiments were conducted during the DAPPLE campaign in central London, presented in Chapter 2.

After a feasibility study in November 2004 (Shallcross et al. 2009), eight line-source experiments (30 minute duration each) were successfully undertaken in March 2008 (Tate 2010). Perfluoromethylcyclohexane (PMCH) 'tracer' gas was released at a constant rate (of order $2x10^{-4}$ mgs^{-1}), from a point close to the exhaust tail-pipe of the ITS Instrumented Car (Tate 2005) as it was driven through the Marylebone Road test area. A fixed source emission was included in each of the experiments.

Figure 4-9 shows the study site at the intersection between Marylebone Road and Gloucester Place. The receptor sites used in the experiments are marked as blue dots and fixed source site (Source X) is marked as a red dot. The line-source along Marylebone Road is indicated by a red line. Full tabulation of the experimental conditions and results are available in the report by Tate (2010), including the emission per 10 m segment of the line-source and the dosage measurements at each receptor site for the 8 experiments.

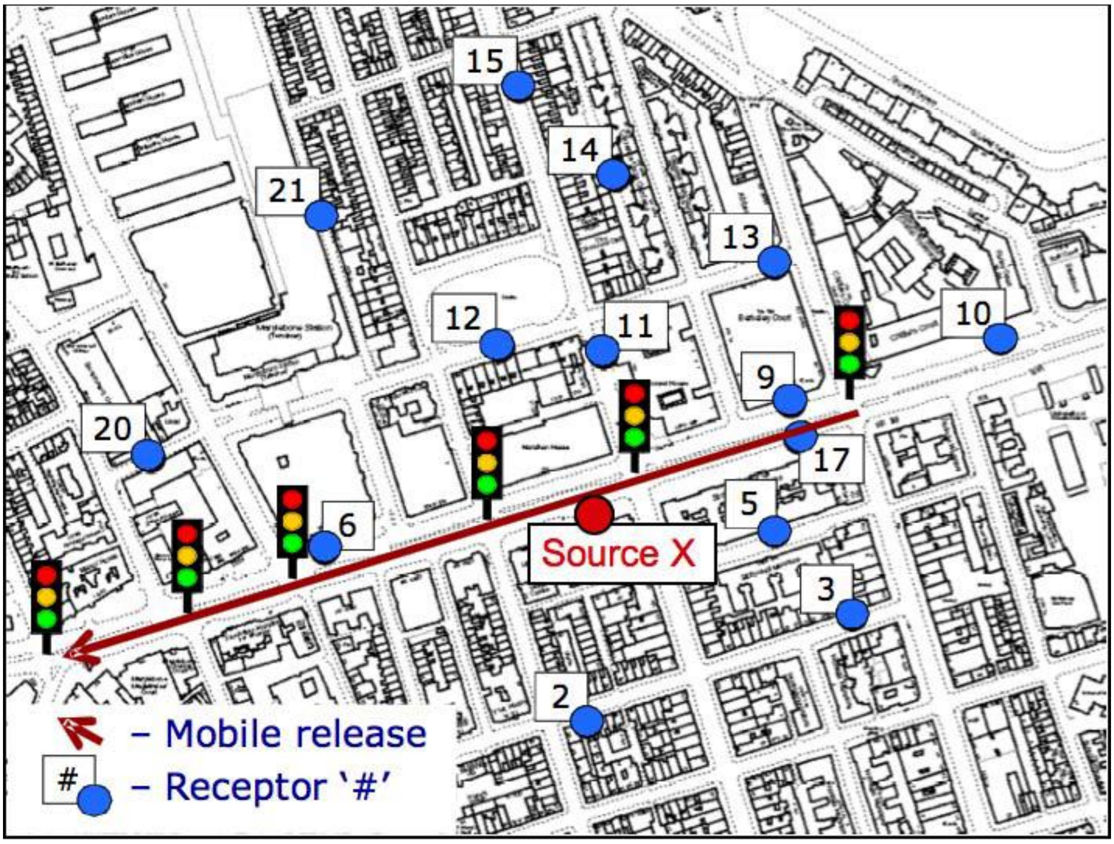

Figure 4-9: The study area, showing the fixed (X) and line-source (in red), and the tracer receptor sites (source: Tate 2010).

Studies such Paine et al. (1988), Perry et al. (2004), Venkatram et al. (2004), Silverman et al. (2007) and Melo et al. (2012) have used AERMOD for rural or urban scenarios where building wake effects had to be considered, but only with a limited number of static sources. In the other hand, Hanna et al. (2007), Stein et al. (2007), Zhang et al. (2008) and Zou et al. (2010) have tested AERMOD in urban scenarios including emission data from mobile sources, but not considering the building wake effects. No paper could be found in the available literature about the use of AERMOD to perform simulations of complex urban scenarios considering both the building wake effects and emission data from mobile vehicular sources.

In order to model the DAPPLE experiments in CityZoom UP and to establish a valid comparison between the results of real world tracer experiments and those of AERMOD, some assumptions had to be made.

First, the site geometry was rotated 17° clockwise in order to match the model that had already been generated for the previous tests. This is equivalent to the "street-aligned system" or "site co-ordinate system" used in the experiments.

Second, the meteorological data files (.SFC surface file and .PFL profile file) were generated based on the available data. For the whole period, sensible heat flux, Q_H = 40 Wm^{-2}; Monin-Obhukov length scale estimate, L = -380 m (Tate 2010); boundary layer depth, Z = 580 m (Barlow et al. 2010); relative humidity, RH = 80% (WeatherOnline 2012); and surface temperature, T_0 = 6° C (Met Office 2012). Average roof top wind speed and direction (at reference height = 18.4 m) during each of the 30 minute experimental periods are listed in Table 4-1. Wind directions, θ, indicate a "direction to" with angles positive anticlockwise with respect to Marylebone Road (Dobre et al. 2005).

Experiment	1	2	3	4	5	6	7	8
Wind Direction θ (degrees)	24	19	23	26	28	32	55	69
Wind Speed (ms^{-1})	2.3	2.7	2.5	2.3	2.3	2.3	2.0	1.7

Table 4-1: Roof top wind conditions during the 30 minute experimental periods (Tate 2010).

Some of the resulting parameters present in the meteorological files used for the simulations are listed in Table 4-2. Wind directions indicate the standard AERMOD "direction from" with angles positive clockwise from the North.

Experiment	1	2	3	4	5	6	7	8
W. Direction (degrees)	246	251	247	244	242	238	215	201
W. Speed (ms^{-1})	2.36	2.77	2.56	2.36	2.36	2.36	2.05	1.74
Friction Velocity (ms^{-1})	0.341	0.401	0.371	0.341	0.341	0.341	0.297	0.252

Table 4-2: Wind direction, wind speed (at reference height = 20 m) and friction velocity for each CityZoom-AERMOD simulation.

The emission profiles in the tracer experiments were generated by measuring the PMCH tracer emissions per 10 m segment for each experiment. The instrumented car was driven through the test area only once for each experiment, so there were different emission amounts at each segment for each moment of the experiment.

In order to translate these transient profiles into steady-state profiles that could be used in AERMOD simulations, it was assumed that the emissions generated by the whole fleet of vehicles driving through Marylebone Road at each 10 m segment and at every second would be equivalent to the emission generated by the one car at each 10 m segment, ignoring the moment it passed by and the time it spent in each segment.

AERMOD cannot handle the transient nature of a single moving car, so the emission rate from the single car is translated in a constant emission rate for a fleet of vehicles that follows the behaviour of the single car. Following this logic, if the single car arrived in the 20th 10 m segment 26.7 s after the experiment started and spent 1 s to go through that segment, releasing a total of 0.227 µg of tracer gas, then a constant emission rate of 2.27×10^{-7} gs^{-1} should be used to represent the constant emission rate for the source at that position.

Based on this assumption, each 10 m segment is considered to be 1 point source laid over the emission line (as described in section 3.2). The emission profiles for each modelled experiment are plotted in Figure 4-10 (the runs are presented in two separate plots for clarity, so that the results from each experiment do not overlap) and listed in Table 4-3:

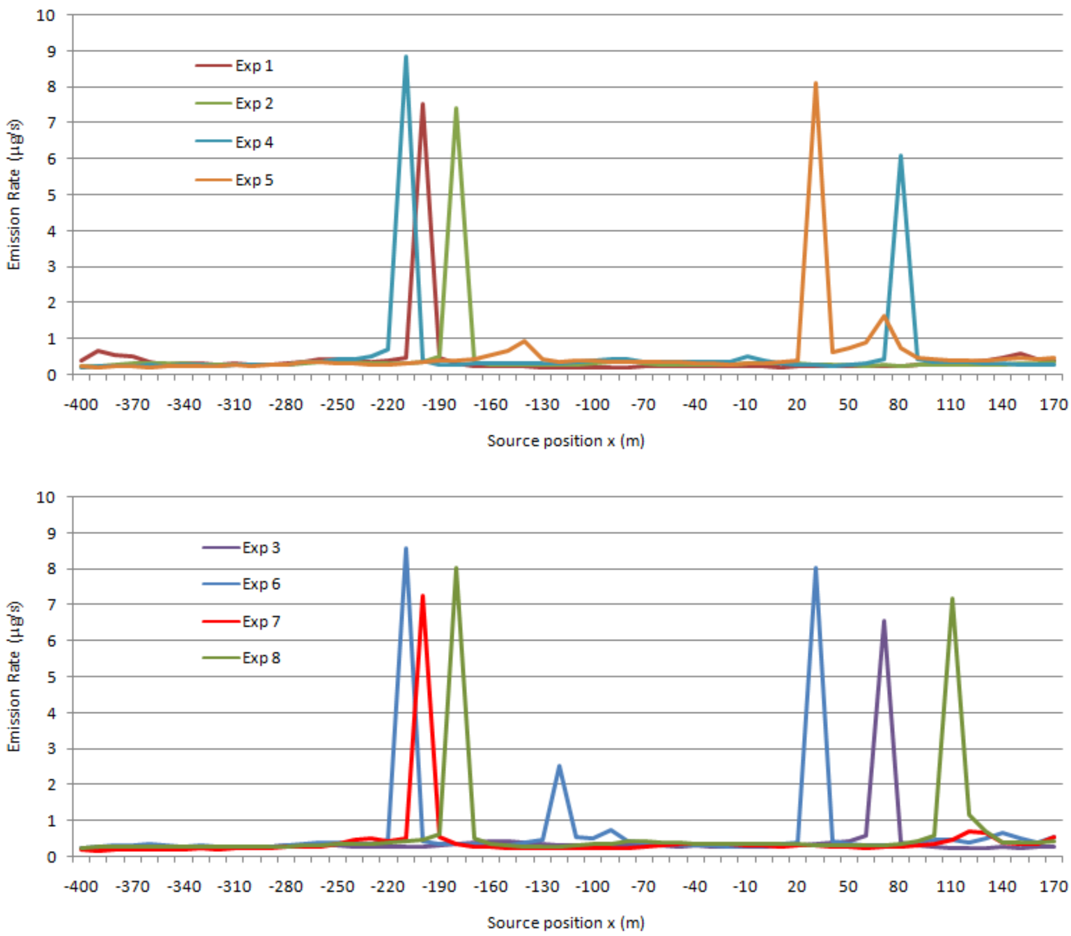

Figure 4-10: Emission rates by source position x for experiments 1 to 8. The runs are presented in two separate plots for clarity.

Segment start	Emission Rate per 10 m segment ($\mu g s^{-1}$)							
(m)	Exp 1	Exp 2	Exp 3	Exp 4	Exp 5	Exp 6	Exp 7	Exp 8
0	0.409	0.349	0.234	0.272	0.455	0.574	0.549	0.416
10	0.454	0.283	0.234	0.272	0.414	0.390	0.380	0.374
20	0.590	0.283	0.213	0.272	0.476	0.513	0.359	0.395
30	0.477	0.262	0.234	0.293	0.414	0.677	0.401	0.395
40	0.386	0.262	0.213	0.314	0.373	0.533	0.654	0.707
50	0.341	0.262	0.213	0.355	0.393	0.410	0.717	1.165
60	0.295	0.240	0.213	0.355	0.393	0.492	0.464	7.197
70	0.318	0.240	0.234	0.334	0.414	0.472	0.359	0.562
80	0.272	0.240	0.277	0.439	0.455	0.410	0.338	0.437
90	0.250	0.218	0.383	6.082	0.725	0.328	0.274	0.333
100	0.250	0.240	6.560	0.418	1.620	0.328	0.274	0.312
110	0.250	0.218	0.554	0.314	0.890	0.308	0.232	0.312
120	0.227	0.240	0.426	0.251	0.745	0.349	0.274	0.291
130	0.227	0.262	0.383	0.230	0.600	0.451	0.295	0.291
140	0.227	0.262	0.341	0.251	8.114	8.057	0.338	0.291
150	0.227	0.283	0.277	0.251	0.373	0.410	0.317	0.333
160	0.204	0.283	0.277	0.293	0.331	0.349	0.295	0.333
170	0.227	0.283	0.256	0.376	0.311	0.308	0.317	0.354
180	0.227	0.283	0.256	0.481	0.290	0.308	0.338	0.333
190	0.227	0.262	0.256	0.355	0.269	0.287	0.380	0.333
200	0.227	0.262	0.256	0.355	0.311	0.308	0.380	0.354
210	0.250	0.262	0.277	0.355	0.311	0.308	0.380	0.354
220	0.227	0.262	0.256	0.355	0.331	0.349	0.359	0.374
230	0.227	0.262	0.277	0.355	0.331	0.369	0.317	0.374
240	0.227	0.305	0.298	0.355	0.352	0.390	0.295	0.416
250	0.204	0.371	0.298	0.439	0.352	0.451	0.253	0.416
260	0.204	0.349	0.277	0.418	0.352	0.759	0.253	0.333
270	0.204	0.283	0.298	0.376	0.373	0.513	0.232	0.333
280	0.204	0.240	0.277	0.334	0.373	0.554	0.253	0.291
290	0.204	0.240	0.298	0.314	0.352	2.522	0.232	0.250
300	0.204	0.240	0.320	0.293	0.414	0.492	0.232	0.250
310	0.227	0.240	0.383	0.314	0.932	0.390	0.253	0.270
320	0.227	0.262	0.426	0.314	0.642	0.308	0.253	0.291
330	0.227	0.262	0.426	0.293	0.518	0.308	0.295	0.333
340	0.250	0.349	0.362	0.293	0.435	0.349	0.295	0.499
350	0.318	7.412	0.320	0.272	0.373	0.369	0.359	8.050
360	0.477	0.501	0.277	0.272	0.373	0.349	0.549	0.624
370	7.514	0.349	0.256	0.376	0.331	0.431	7.258	0.478
380	0.477	0.305	0.234	8.841	0.311	8.590	0.506	0.437
390	0.386	0.305	0.234	0.711	0.269	0.472	0.443	0.395
400	0.363	0.283	0.256	0.502	0.248	0.369	0.506	0.354
410	0.409	0.327	0.256	0.439	0.290	0.349	0.464	0.333
420	0.454	0.371	0.277	0.418	0.290	0.390	0.359	0.333
430	0.454	0.349	0.277	0.334	0.331	0.390	0.295	0.312
440	0.363	0.305	0.277	0.334	0.331	0.349	0.295	0.291
450	0.318	0.262	0.277	0.272	0.269	0.328	0.274	0.270
460	0.295	0.262	0.234	0.272	0.248	0.287	0.253	0.270
470	0.295	0.262	0.256	0.251	0.228	0.267	0.232	0.250
480	0.318	0.262	0.234	0.251	0.248	0.287	0.253	0.270
490	0.295	0.262	0.213	0.230	0.228	0.287	0.211	0.250
500	0.318	0.262	0.213	0.251	0.228	0.308	0.232	0.270
510	0.318	0.305	0.234	0.272	0.207	0.287	0.211	0.270
520	0.295	0.305	0.213	0.230	0.207	0.328	0.211	0.250
530	0.341	0.305	0.213	0.251	0.186	0.369	0.211	0.270
540	0.522	0.283	0.234	0.209	0.207	0.308	0.190	0.250
550	0.568	0.262	0.213	0.209	0.207	0.308	0.190	0.250
560	0.658	0.218	0.213	0.230	0.186	0.287	0.169	0.250
570	0.409	0.218	0.213	0.188	0.207	0.246	0.190	0.229

Table 4-3: Emission rate per 10 m segment from the experiment starting position (Tate 2010).

For a better understanding of the modelled experiments, emission rates by source for simulation experiments 1 and 6 are plotted as pseudocolor in Figures 4-11 and 4-12. The gray blocks represent the buildings and the white area represents open space. Pseudocolor plots of the emission rates for all the simulated cases are available in Appendix I.

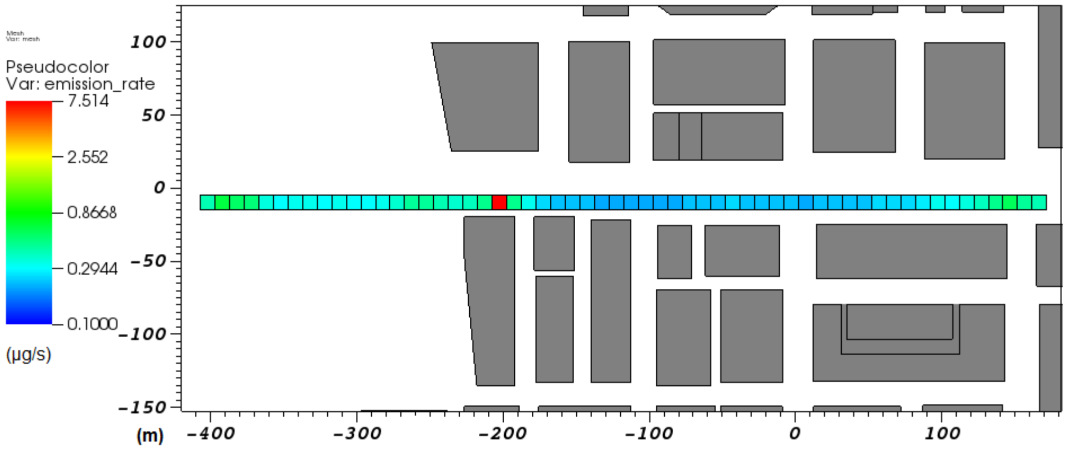

Figure 4-11: Pseudocolor plot of emission rates by source position for experiment 1.

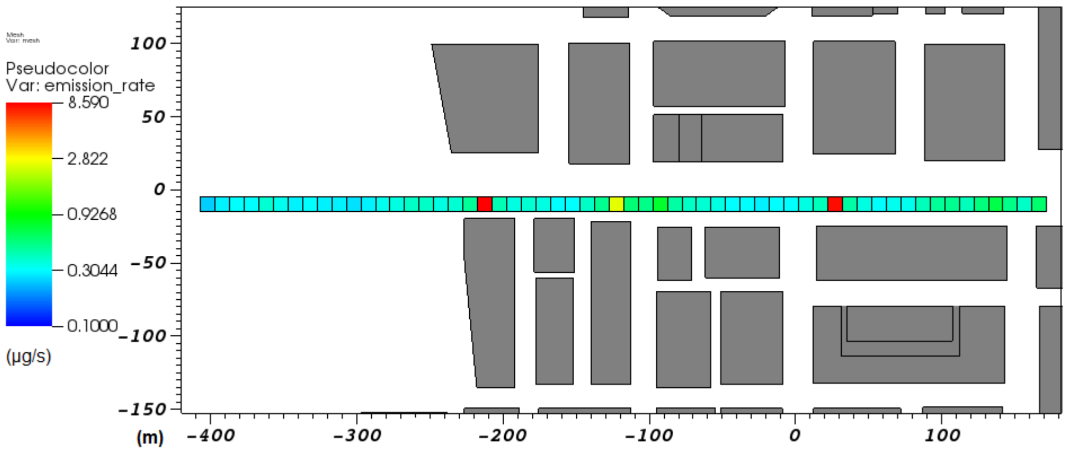

Figure 4-12: Pseudocolor plot of emission rates by source position for experiment 6.

The complete CityZoom UP modelled scenario for the simulations is shown in Figure 4-13. The sources distributed over the emission line are represented as red dots, the receptor sites are represented as number-identified orange dots, built areas are represented by the green blocks, and open spaces are represented as white areas. The intersection between Marylebone Road and Gloucester Place is considered to be the domain origin (x=0, y=0).

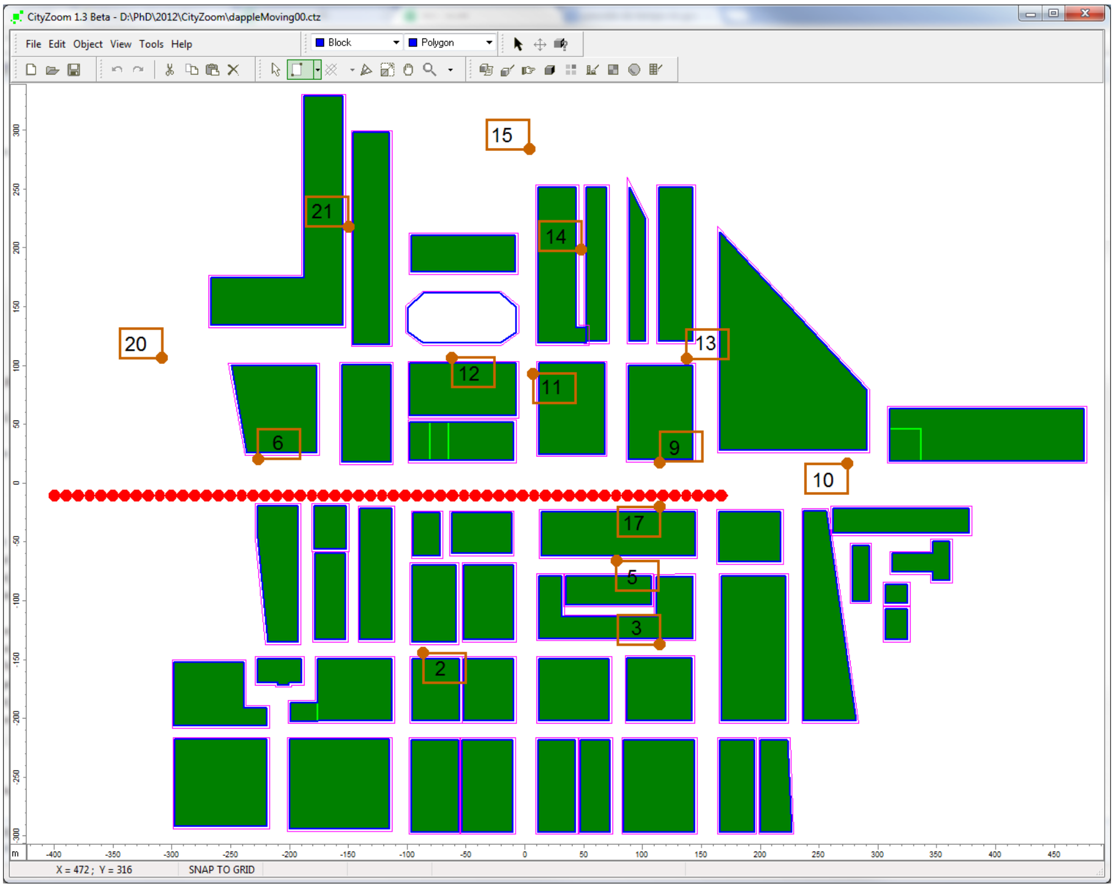

Figure 4-13: The simulation area modelled using CityZoom UP, showing the sources distributed over the emission line (red dots) and the receptor sites (orange dots).

The DAPPLE experiments results are given as normalised dosages, D/M, where D is the dosage (equal to the concentration integrated over the sample period) and M is the total mass of material released (equal to the release rate integrated over the release duration). The dosage D represents the total exposure to the emitted tracer, and was measured in 14 sample sites, using 1 sampling bag at each site for each 30 minute experimental period. More details about the sampling methodology are available from Wood et al. (2009).

AERMOD uses Gaussian formulation to simulate hourly average concentration values C, considering constant emission rates Q_s for each source for the whole period. This is equivalent to the instantaneous concentration calculation downwind from the sources in a steady-state scenario. The normalised concentrations, C/Q_t, are used in the comparison with the experimental results, where Q_t is the total release rate for all sources combined. Simulation results are listed side by side with the experimental results for each experiment in Tables 4-4 to 4-7.

The use of normalised dosages and concentrations removes some of the dependence on emission rates. Nonetheless, the DAPPLE measurements took place over 30 minute periods, while the emissions happened only during 2 to 3 minutes for each experiment, and the emissions actually happened in only one point source at a time and for only a few seconds.

Exact direct comparison between these dosages and concentrations cannot be established, since the primary data are very different. The transient nature of the DAPPLE tracer experiments makes those results time-dependent, the dosage could be different if there was a variation in the wind direction or if the sampling time was different. On the other hand, the steady-state AERMOD simulations are time-independent, i.e., the emission rates, meteorological conditions and concentration at each receptor site are constant for the whole simulation period. While it is very unlikely that any 2 tracer runs would have the same results, AERMOD simulations always generate the exact same results.

For this reason, the results are compared by trend, based on the average of the results obtained. Results up to half the average value are considered small; results over half the average and up to twice the average are considered medium; and results over twice the average are considered high. Results from receptor site 17 were not used for calculating the average, since the site is too close to the sources and presented results much higher than the other sites.

The average normalised dosage for the DAPPLE experiments is 6.25, hence results of value up to 3.1 are considered small, 3.1 to 12.5 are considered medium, and above 12.5 are considered high. The average normalised AERMOD simulated concentrations is 18.7, so results of value up to 9.3 are considered small, 9.3 to 37.4 are considered medium, and above 37.4 are considered high. The notation ExpX-RecY is used to indicate the receptor Y in experiment X.

It is also important to remind that the buildings are not present in AERMOD simulations. Their downwash effect over all the sources is pre-calculated, but only the nearest building in each direction is considered.

Tables 4-4 to 4-7 show the results of the DAPPLE moving source experiments compared to the AERMOD simulations for each scenario. Numerical results are listed along with the corresponding trend, the average distance from each receptor site to the sources and the position of the receptor site relative to the sources. When a receptor site is directly downwind from a high emission rate source, its position is listed as "straight downwind". A failed DAPPLE sample is indicated by the character "f".

On the upwind/crosswind receptors 2, 3 and 20, concentration is very small for all experiments (blue cells in Tables 4-4 to 4-7). Receptor 5 is also upwind/crosswind in all experiments, noticeable by the lower than background dosage registered for the tracer experiments, but since it is so close to the sources and the buildings do not impose real blockages in AERMOD, the simulated concentrations show medium values (orange cells).

Receptor 10 is unique for being the only receptor in these experiments that is positioned at an average distance downwind from the sources (except in experiments 7 and 8 where it is crosswind) and in the same street where the sources are (not blocked by any buildings). AERMOD does not simulate the complex mixing and transport processes that happen inside the street canyons, and for this reason the measured results can be very different than the simulated results (purple cells in Tables 4-4 and 4-6), especially in the crosswind cases (dark purple cells).

Site		Exp 1		Exp 2		Exp 3		Exp 4	
		DAPPLE	AERMOD	DAPPLE	AERMOD	DAPPLE	AERMOD	DAPPLE	AERMOD
2	Result	-0.16	1.82	-0.24	2.16	-0.14	1.94	-0.10	2.12
	Trend	small	small	small	small	small	small	small	small
	Distance	medium		medium		medium		medium	
	Position	upwind/crosswind		upwind/crosswind		upwind/crosswind		upwind/crosswind	
3	Result	-0.05	1.24	0.00	0.90	-0.21	3.15	-0.01	2.32
	Trend	small	small	small	small	small	small	small	small
	Distance	medium		medium		medium		medium	
	Position	upwind/crosswind		upwind/crosswind		upwind/crosswind		upwind/crosswind	
5	Result	-0.14	8.66	-0.20	7.39	-0.20	30.20	-0.02	21.30
	Trend	small	small	small	small	small	medium	small	medium
	Distance	near		near		near		near	
	Position	upwind/crosswind		upwind/crosswind		upwind/crosswind		upwind/crosswind	
6	Result	9.34	20.43	18.40	47.28	126.00	15.77	14.80	11.79
	Trend	medium	medium	high	high	high	medium	high	medium
	Distance	very near		very near		very near		very near	
	Position	downwind		downwind		downwind		downwind	
9	Result	2.29	31.45	18.50	32.97	8.00	31.21	8.83	27.85
	Trend	small	medium	high	medium	medium	medium	medium	medium
	Distance	very near		very near		very near		very near	
	Position	downwind		downwind		downwind		downwind	
10	Result	0.19	5.87	13.10	8.90	34.70	17.39	15.60	10.38
	Trend	small	small	high	small	high	medium	high	medium
	Distance	average		average		average		average	
	Position	downwind		downwind		downwind		downwind	
11	Result	5.89	47.03	10.80	56.04	5.34	32.52	13.90	44.57
	Trend	medium	high	medium	high	medium	medium	high	high
	Distance	medium		medium		medium		medium	
	Position	downwind		downwind		downwind		downwind	

Table 4-4: Results for experiments 1 to 4 at receptor sites 2 to 11. (f = failed sample).

Receptors 14, 15 and 21 are far downwind and blocked by several buildings, so they show small concentrations for most experiments (green cells in Tables 4-5 and 4-7). However, when they are straight downwind from the strongest emission sources, simulated concentration reach medium levels, such as in experiments 7 and 8 and the pairs Exp1-Rec14, Exp4-Rec14, Exp6-Rec14 (dark green cells).

Receptors 6, 9 and 17 are very close to the sources, so the results show medium to very high concentration for all experiments (red cells in Tables 4-4 to 4-7), depending on the strength of the nearby sources. However, the complex mixing processes inside the streets can cause some inconsistencies, such as the very elevated dosages measured in Exp3-Rec6 and Exp4-Rec17 (dark red cells) and the small dosages measured in Exp5-Rec9 and Exp3-Rec9 (light red cells).

Site		Exp 1		Exp 2		Exp 3		Exp 4	
		DAPPLE	AERMOD	DAPPLE	AERMOD	DAPPLE	AERMOD	DAPPLE	AERMOD
12	Result	9.24	55.83	6.65	58.73	6.81	26.73	5.46	46.54
	Trend	medium	high	medium	high	medium	medium	medium	high
	Distance	medium		medium		medium		medium	
	Position	downwind		downwind		downwind		downwind	
13	Result	2.45	33.39	6.63	49.42	2.56	61.90	4.15	49.21
	Trend	small	medium	medium	high	small	high	medium	high
	Distance	medium		medium		medium		medium	
	Position	downwind		downwind		downwind		downwind	
14	Result	f	15.77	2.61	3.98	2.00	6.46	2.99	17.01
	Trend	f	medium	small	small	small	small	small	medium
	Distance	far		far		far		far	
	Position	straight downwind		downwind		downwind		straight downwind	
15	Result	3.52	0.00	1.72	-0.51	1.23	-0.16	2.25	0.04
	Trend	medium	small	small	small	small	small	small	small
	Distance	far		far		far		far	
	Position	downwind		downwind		downwind		downwind	
17	Result	87.90	171.32	64.00	136.07	223.00	165.43	741.00	148.43
	Trend	high	high	high	high	high	high	high	high
	Distance	very near		very near		very near		very near	
	Position	upwind/crosswind		upwind/crosswind		upwind/crosswind		upwind/crosswind	
20	Result	f	4.04	0.67	2.62	0.58	1.76	3.11	2.77
	Trend	f	small	small	small	small	small	small	small
	Distance	medium		medium		medium		medium	
	Position	upwind/crosswind		upwind/crosswind		upwind/crosswind		upwind/crosswind	
21	Result	1.74	-0.15	1.90	-0.12	2.13	-0.13	1.35	-0.18
	Trend	small	small	small	small	small	small	small	small
	Distance	far		far		far		far	
	Position	downwind		downwind		downwind		downwind	

Table 4-5: Results for experiments 1 to 4 at receptor sites 12 to 21. (f = failed sample).

Receptors 11, 12 and 13 are downwind from the sources and show medium to high values for dosage and concentration (yellow cells in Tables 4-4 to 4-7). Since these sites are protected by buildings and at a medium distance from the sources, they show smaller dosage values than receptors 6 and 9 for most of the tracer experiments. When the receptor is straight downwind from the strongest emissions sources, the simulated concentration at receptors 11, 12 and 13 can get quite elevated, often higher than the value simulated for receptors 6 and 9, which are closer to the sources and are not blocked by any buildings (as it happens with receptors 14, 15 and 21, noticing again that the buildings do not exist as blockages in AERMOD).

Site		Exp 5		Exp 6		Exp 7		Exp 8	
		DAPPLE	AERMOD	DAPPLE	AERMOD	DAPPLE	AERMOD	DAPPLE	AERMOD
2	Result	-0.09	1.89	-0.15	2.01	-0.11	1.21	-0.17	1.50
	Trend	small	small	small	small	small	small	small	small
	Distance	medium		medium		medium		medium	
	Position	upwind/crosswind		upwind/crosswind		upwind		upwind	
3	Result	-0.02	2.74	-0.07	1.57	f	0.51	0.06	2.54
	Trend	small	small	small	small	f	small	small	small
	Distance	medium		medium		medium		medium	
	Position	upwind/crosswind		upwind/crosswind		upwind		upwind	
5	Result	-0.14	19.75	-0.15	10.97	-0.18	11.38	-0.11	23.69
	Trend	small	medium	small	medium	small	medium	small	medium
	Distance	near		near		near		near	
	Position	upwind/crosswind		upwind/crosswind		upwind		upwind	
6	Result	9.96	12.53	21.00	11.08	31.20	98.79	6.79	68.93
	Trend	medium	medium	high	medium	high	high	medium	high
	Distance	very near		very near		very near		very near	
	Position	downwind		downwind		downwind		downwind	
9	Result	4.81	67.69	5.88	48.02	3.45	45.06	4.37	179.32
	Trend	medium	high	medium	high	medium	high	medium	high
	Distance	very near		very near		very near		very near	
	Position	downwind		downwind		downwind		downwind	
10	Result	16.40	9.75	f	3.44	7.16	-0.45	23.80	-0.38
	Trend	high	medium	f	small	medium	small	high	small
	Distance	average		average		average		average	
	Position	downwind		downwind		crosswind		crosswind	
11	Result	5.12	36.85	7.89	48.19	4.60	15.27	2.92	10.14
	Trend	medium	medium	medium	high	medium	medium	small	medium
	Distance	medium		medium		medium		medium	
	Position	downwind		downwind		downwind		downwind	

Table 4-6: Results for experiments 5 to 8 at receptor sites 1 to 11. (f = failed sample).

Site		Exp 5		Exp 6		Exp 7		Exp 8	
		DAPPLE	AERMOD	DAPPLE	AERMOD	DAPPLE	AERMOD	DAPPLE	AERMOD
12		5.55	25.46	7.21	40.16	7.62	28.35	3.83	25.89
	Trend	medium	medium	medium	high	medium	medium	medium	medium
	Distance	medium		medium		medium		medium	
	Position	downwind		downwind		downwind		downwind	
13		4.47	71.55	6.28	44.06	3.25	23.15	3.27	6.53
	Trend	medium	high	medium	high	medium	medium	medium	small
	Distance	medium		medium		medium		medium	
	Position	downwind		downwind		downwind		downwind	
14	Result	2.63	7.30	5.35	17.94	3.00	14.51	1.52	9.16
	Trend	small	small	medium	medium	small	medium	small	small
	Distance	far		far		far		far	
	Position	downwind		straight downwind		straight downwind		straight downwind	
15	Result	1.50	-0.23	3.67	4.05	4.71	20.90	2.37	9.39
	Trend	small	small	medium	small	medium	medium	small	medium
	Distance	far		far		far		far	
	Position	downwind		downwind		straight downwind		straight downwind	
17	Result	172.00	170.64	297.00	131.93	201.00	383.65	f	1025.62
	Trend	high	high	high	high	high	high	f	high
	Distance	very near		very near		very near		very near	
	Position	upwind/crosswind		upwind/crosswind		upwind		upwind	
20	Result	0.88	1.10	2.70	2.30	2.32	3.44	6.81	4.73
	Trend	small	small	small	small	small	small	medium	small
	Distance	medium		medium		medium		medium	
	Position	upwind/crosswind		upwind/crosswind		cross/downwind		cross/downwind	
21	Result	0.67	-0.39	1.88	-0.21	7.11	18.81	6.70	22.74
	Trend	small	small	small	small	medium	medium	medium	medium
	Distance	far		far		far		far	
	Position	downwind		downwind		straight downwind		straight downwind	

Table 4-7: Results for experiments 5 to 8 at receptor sites 12 to 21. (f = failed sample).

Figure 4-14 shows a pseudocolor plot of the concentration for simulated experiment number 6, to help understand the AERMOD simulations. Concentration was calculated at a total of 8181 points, 10 meters from each other, receiving emissions from 58 sources. The simulation was run for a single hour of meteorological data and took ≈3 seconds to complete on a standard home PC.

The building wireframe is superimposed over the colour plot as an aid, but the buildings are not really present in the simulation model. For this reason, concentration can be calculated for points that are apparently inside buildings and would have C = 0 if the buildings were solid objects. Plots for all the simulated experiments are available in Appendix I.

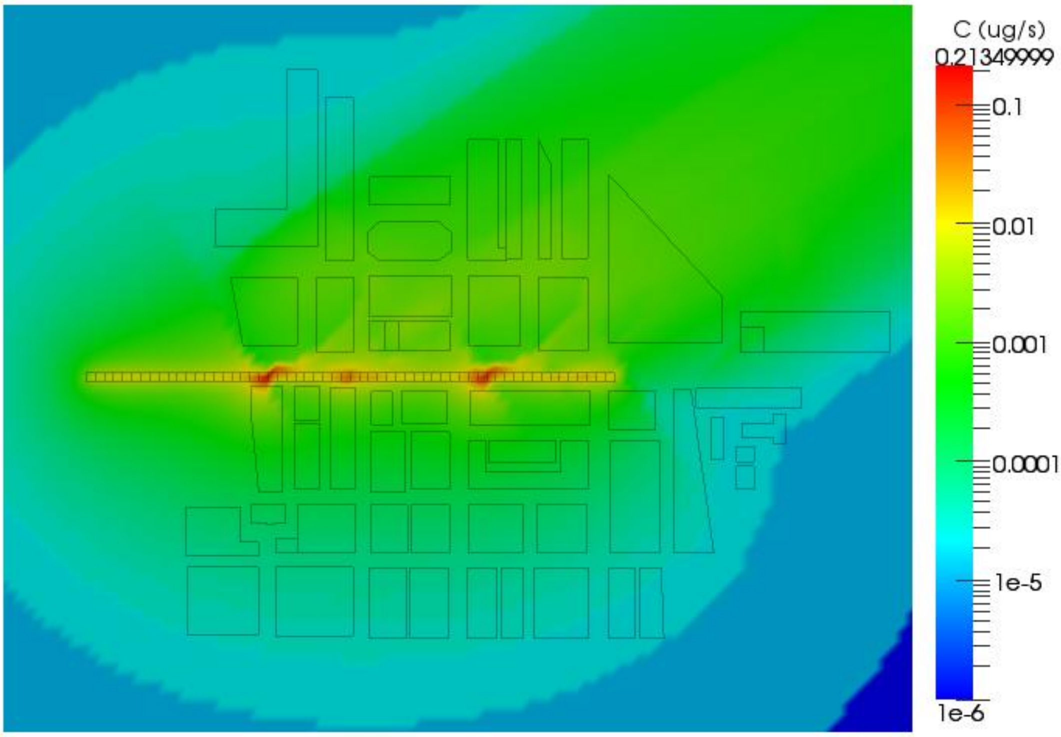

Figure 4-14: Pseudocolor plot of the entire domain for simulated experiment number 6.

Nonetheless, the effects of the buildings over the sources are noticeable, especially downwind from the stronger emission sources. Instead of smooth red to yellow to green transitions, building shaped sudden drops from red to green can be seen near the strong (red) sources in Figure 4-15 (detailed zoom from Figure 4-14). Without the use of the PRIME algorithm, the buildings would be completely ignored in the simulations and the concentration at receptors sites protected by buildings (such as sites 12, 13 and 14) would be greatly overestimated.

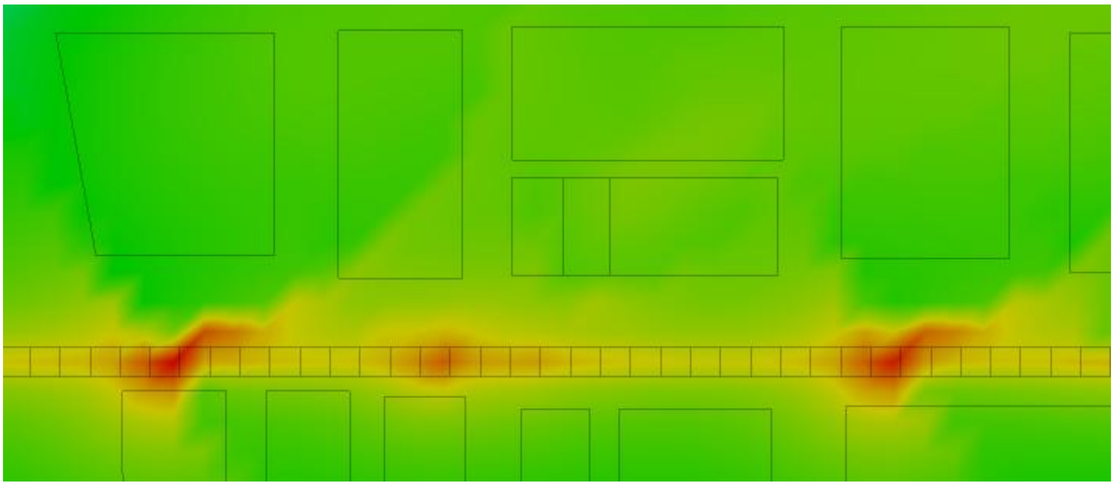

Figure 4-15: Zoomed-in detail of the building effects over the sources for simulated experiment number 6.

Based on observations and test results, the recommended step-by-step procedure to use the coupled CityZoom UP and AERMOD tools for urban planning consists of:

1) Model the existing scenario – urban geometry and emission profiles;
2) Model one or more alternative scenarios – proposed new urban geometry and estimated emission profiles;
3) Define a set of interest points for measurement of results – receptor sites;
4) Simulate the scenarios for all the available hourly meteorological conditions – considering a scenario with 50 sources (the equivalent to an emission line of 500 meters), the simulation times seen during several experiments, and assuming an average of 8760 hours in a year, the maximum average concentration for a whole year could be simulated in less than 5 seconds per point of interest.
5) Compare the maximum average concentrations between present and alternative scenarios, in order to identify locations that could be jeopardized should these alternative scenarios become reality.

The trend agreement seen in the results allow users to identify potential problems (namely exceedingly high concentrations of pollutants) at specific areas in different scenarios. These are valuable data for strategic urban planning purposes. Fast results can be obtained for different urban scenarios and using large sets of emission profiles and meteorological conditions.

4.4. Automated Mesh Generation Tests

To test the automated meshing, a scenario of dimensions X = 312 m, Y = 195 m and Z = 72 m and with 8 buildings was modelled. Using different refinement parameters (Table 4-8), a set of journal files was automatically generated by CityZoom UP, based on user-defined refinement parameters: size of the first boundary layer cell (BL 1st), growth rate of the boundary layer (BL rate), number of rows in the boundary layer (BL rows), starting size of the cells generated by the size function (SF start), growth rate of the size function (SF rate), and maximum size of the cells generated by the size function (SF limit). The column *"journal"* indicates the name of the journal file generated for that test case, the column "*basefaces*" represents the resulting number of faces in the base (ground) of the domain box, the column "*vol cells*" represents the resulting number of cells in the domain and the column "*RAM*" indicates an estimate of the amount of RAM memory needed to generate the mesh.

journal	BL 1st	BL rate	BL rows	SF start	SF rate	SF limit	base faces	vol cells	RAM
110m4f02	0,1	1,2	5	0,5	1,2	15	19508	1334185	NA
110m4f03	0,05	1,2	10	0,9	1,2	15	10846	695092	NA
110m4f04	0,05	1,2	5	0,25	1,2	15	34268	3292270	1.3 gb
110m4f05	0,02	1,2	10	0,5	1,2	15	19508	1756425	800 mb
110m4f06	0,05	1,2	10	0,5	1,2	15	19508	1565798	658 mb
110m4f07	0,05	1,2	7	0,5	1,2	15	19508	1506613	NA
110m4f08	0,2	1,2	5	1	1,2	15	9666	444778	NA
110m4f09	0,02	1,2	10	1	1,2	15	9666	625247	NA
110m4f10	0,05	1,2	10	1	1,2	15	9666	584762	NA

Table 4-8: Refinement parameters used during automated meshing.

The journal file 110m4f06.jou generated by CityZoom UP is partially shown in Figures 4-16 and 4-17. Comments were inserted in this example to explain the steps performed by the script (lines starting with “/”) and “…” are used to indicate part of the script was suppressed at that point.

```
/ Journal File for GAMBIT, generated by CityZoom
/ Pablo Grazziotin
/ Domain dimensions: 312 x 195 x 72
/ Built region: 72 x 75 x 12 C = 110 ; 0
/ BL: first 0.05 rate 1.2 rows 10
/ SF: start 0.5 rate 1.2 limit 15
solver select "FLUENT 5/6"
/ create domain box vertices
vertex create "v000" coordinates 14 -97.5 0
vertex create "v001" coordinates 14 -97.5 72
vertex create "v010" coordinates 14 97.5 0
vertex create "v011" coordinates 14 97.5 72
vertex create "v100" coordinates 326 -97.5 0
vertex create "v101" coordinates 326 -97.5 72
vertex create "v110" coordinates 326 97.5 0
vertex create "v111" coordinates 326 97.5 72
/ create domain box edges
edge create "e000to001" straight "v000" "v001"
...
edge create "e101to111" straight "v101" "v111"
/ create domain box faces
face create "fBase" wireframe "e000to010" "e000to100" "e010to110"
"e100to110" real
face create "fTop" wireframe "e001to011" "e001to101" "e011to111"
"e101to111" real
face create "fInlet" wireframe "e000to010" "e001to011" "e000to001"
"e010to011" real
face create "fSymmS" wireframe "e000to100" "e001to101" "e000to001"
"e100to101" real
face create "fSymmN" wireframe "e010to110" "e011to111" "e010to011"
"e110to111" real
face create "fOutlet" wireframe "e100to110" "e101to111" "e100to101"
"e110to111" real
/ create domain box volume
volume create "vDomain" stitch "fInlet" "fSymmS" "fSymmN" "fOutlet"
"fBase" "fTop"
/ create building vertices
vertex create "b0_14_0_0" coordinates 74 7.5 0
vertex create "b0_14_0_4" coordinates 74 7.5 12
/ create building edges
edge create "b0_14_0_ev_0" straight "b0_14_0_0" "b0_14_0_4"
...
/ create building faces
face create "b0_14_0_fv0" wireframe "b0_14_0_ev_0" "b0_14_0_ev_1"
"b0_14_0_eh_4" "b0_14_0_eh_0" real
...
/ create building volumes
volume create "b" stitch "b0_14_0_fv0" "b0_14_0_fv1" "b0_14_0_fv2"
"b0_14_0_fv3" "b0_14_0_top" "b0_14_0_base" real
volume subtract "vDomain" volumes "b"
/ repeat for all buildings
...
```

Figure 4-16: Journal file 110m4f06.jou generated by CityZoom UP (part 1).

```
/ create boundary layer around buildings
blayer create "b0_14_0_BL" first 0.05 growth 1.2 total 1.2979341056
rows 10 transition 1 trows 0 continuous
blayer attach "b0_14_0_BL" volume "vDomain" "vDomain" "vDomain"
"vDomain" "vDomain" face "b0_14_0_fv0" "b0_14_0_fv1" "b0_14_0_fv2"
"b0_14_0_fv3" "b0_14_0_top" add
/ create size function growing from building faces to domain volume
sfunction create "b0_14_0_sfv" sourcefaces "b0_14_0_fv0"
"b0_14_0_fv1" "b0_14_0_fv2" "b0_14_0_fv3" "b0_14_0_top" startsize 0.5
growthrate 1.2 sizelimit 15 attachvolumes "vDomain"  fixed
sfunction create "b0_14_0_sf" sourceedges "edge.25" "edge.26"
"edge.27" "edge.28" startsize 0.5 growthrate 1.2 sizelimit 15
attachfaces "fBase"  fixed
/ repeat for all buildings
...
/ create boundary layer over the domain base
blayer create "baseBL" first 0.05 growth 1.2 total 1.2979341056 rows
10 transition 1 trows 0 continuous
blayer attach "baseBL" volume "vDomain" face "fBase" add
/ mesh the base
face mesh "fBase" triangle
/ mesh the domain box
volume mesh "vDomain" tetrahedral
/ create the domain continuum
physics create "fetch" ctype "FLUID" volume "vDomain"
/ create and name boundaries
physics create "base" btype "WALL" face "fBase"
physics create "top" btype "SYMMETRY" face "fTop"
physics create "s1" btype "SYMMETRY" face "fSymmS"
physics create "outlet" btype "PRESSURE_OUTLET" face "fOutlet"
physics create "s2" btype "SYMMETRY" face "fSymmN"
physics create "inlet" btype "MASS_FLOW_INLET" face "fInlet"
/ export to .msh file
export fluent5 "110m4f06.msh"
```

Figure 4-17: Journal file 110m4f06.jou generated by CityZoom UP (part 2).

As the mesh quality increased, so did the mesh size and computational requirements. To speed up the simulations, parallel runs were performed in the School of Engineering Linux cluster, a machine with 23 dual-core 32-bit processors with 1 GB of RAM each, named Kolmogorov. During the course of the research the Kolmogorov cluster crashed and was integrated into the Prandtl cluster, adding 11 quad-core 64-bit processors with 4 GB of RAM each, to a total of 90 CPUs and 68 GBytes of RAM. The cluster was later updated again, replacing the old 23 dual-core 32-bit processors with 8 eight-core 64-bit processors, and receiving the name Stokes.

RANS simulations were run on the resulting meshes to test their quality and verify mesh independence. Table 4-9 presents some numerical results of the simulations. The columns "*b y+ min*", "*b y+ max*" and "*b y+ ave*" represent the minimum, maximum and average *y+* at the building walls, while the columns "*base ymin*", "*base ymax*" and "*base yave*" represent the same information but on the domain base. "*dom u max*", "*z3 u max*" and "*z1.5 u max*" are the maximum wind speeds in the whole domain, measured at the domain height 3 m and at the domain height 1.5 m respectively.

journal	b y+ min	b y+ max	b y+ ave	base ymin	base ymax	base yave	dom u max	z3 u max	z1.5 u max
110m4f02	21,5	975	379	28	1222	419	6,19	4,25	4,34
110m4f03	13,9	490	176,5	13,9	545	204,4	6,19	4,19	4,09
110m4f04	6,6	528	193	9,7	656	215	6,2	4,28	4,3
110m4f05	3,5	215	73	4,6	241	80	6,2	4,25	4,32
110m4f06	error								
110m4f07	14,6	509	185,5	12,9	602	203	6,19	4,24	4,3
110m4f08	error								
110m4f09	4,3	196,9	65,5	4	187,5	72,8	6,21	4,1	3,96
110m4f10	15	481	173,6	12	518	203	6,19	4,15	4,06

Table 4-9: Resulting y+ and speed for the generated meshes.

Figure 4-18 shows a plot of the wind speed along the Z axis for x = 110 m and y = 0 m, a straight line positioned at the centre of the built area and going from the base to the top of the domain (indicated by the blue dot in Figure 4-19).

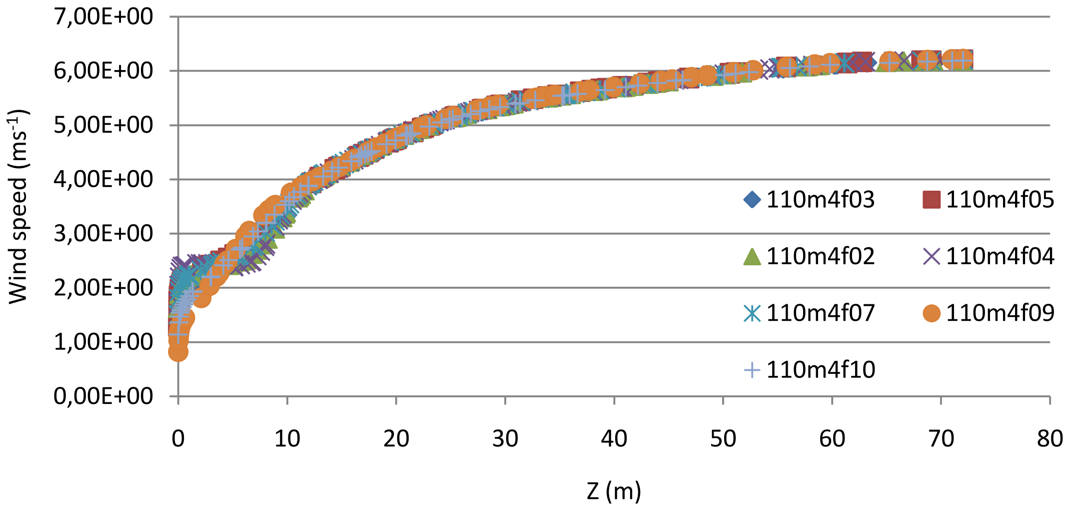

Figure 4-18: Velocity along Z axis at X = 110m, Y = 0m.

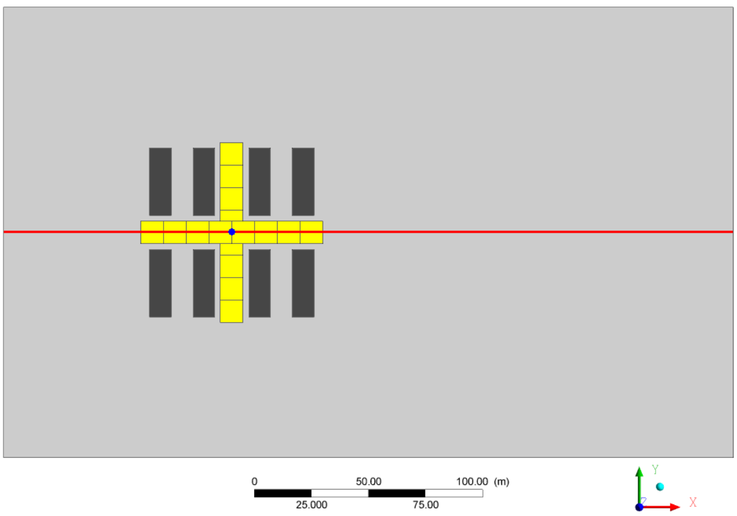

Figure 4-19: Sources along the street axes generated by CityZoom UP via Gambit.

This demonstrates CityZoom UP capability to quickly generate different meshes based on user-defined refinement parameters. This feature is of great use for mesh independence studies, reducing the time the user spends creating different meshes for his test scenario.

4.5. Multispecies Flow Simulation Tests

Once good mesh quality is achieved with the automated process, CFX can be used to perform CFD simulation of the transport of pollutants in the modelled urban scenario. CityZoom UP generates the sources of pollutants as part of the domain mesh. Using the discretization approach described in Chapter 3 to transform the line sources into point sources, the sources for CFD simulations are represented as a sequence of faces as shown in Figure 4-19. The yellow squares are sources, the dark gray blocks are the buildings, the light gray area is open space, the red line represents the sampling points along the X axis and the blue dot represents the vertical line for the sampling points along the Z axis.

The same scenario used for the mesh independence tests in the previous section (dimensions X = 312 m, Y = 195 m and Z = 72 m and with 8 buildings) was edited in CityZoom UP, and new journal files were generated to insert sources in the domain and to create a new set of meshes with different resolutions. The user-defined parameters used for the generated scenarios are listed in Table 4-10. These parameters are the size of the first boundary layer cell (BL 1st), the growth rate of the boundary layer (BL rate), the number of rows in the boundary layer (BL rows), the starting size of the cells generated by the size function (SF start), the growth rate of the size function (SF rate), and the maximum size of the cells generated by the size function (SF limit). The column *"journal"* indicates the name of the journal file generated for that test case, the column "*base faces*" represents the resulting number of faces in the base (ground) of the domain box, the column "*vol cells*" represents the resulting number of cells in the domain and the column "*timestep*" indicates the timestep used for simulating that particular mesh.

journal	BL 1st	BL rate	BL rows	SF start	SF rate	SF limit	base faces	vol cells	timestep
s06	0.05	1.1	7	0.5	1.2	10	15934	1318229	1
s08	0.02	1.1	10	1	1.2	12	7968	497447	1
s09	0.02	1.1	10	0.5	1.1	12	26285	2731742	1

Table 4-10: Refinement parameters used during automated meshing of scenarios with sources.

Two materials were added to the list of materials in CFX: *CO*, set as a pure gas with a molar mass of 28.01 kg/kmol, a density of 1.185 kg/m3, a specific heat capacity of 1003.7 J/kg.K and reference temperature 15° C at 1 atm; and *PollutedAir*, set as a variable composition ideal mixture of CO and air at 25° C. The default fluid in the domain was set to *PollutedAir*, the air inlet was set to have logarithmic profile for the speed and a mass fraction of CO equal to 0 (100% of air at 25° C and 0% of CO) and the sources along the streets were set to have a mass flow rate of 0.2 gs^{-1} and a mass fraction of CO equal to 1 (0% of air at 25° C and 100% of CO). Figure 4-20 shows a pseudocolor plot of the log profiled wind speed at the inlet and of the mass flow rate at the sources. Figure 4-21 shows a section of the domain with the air speed and mass flow vectors in each boundary.

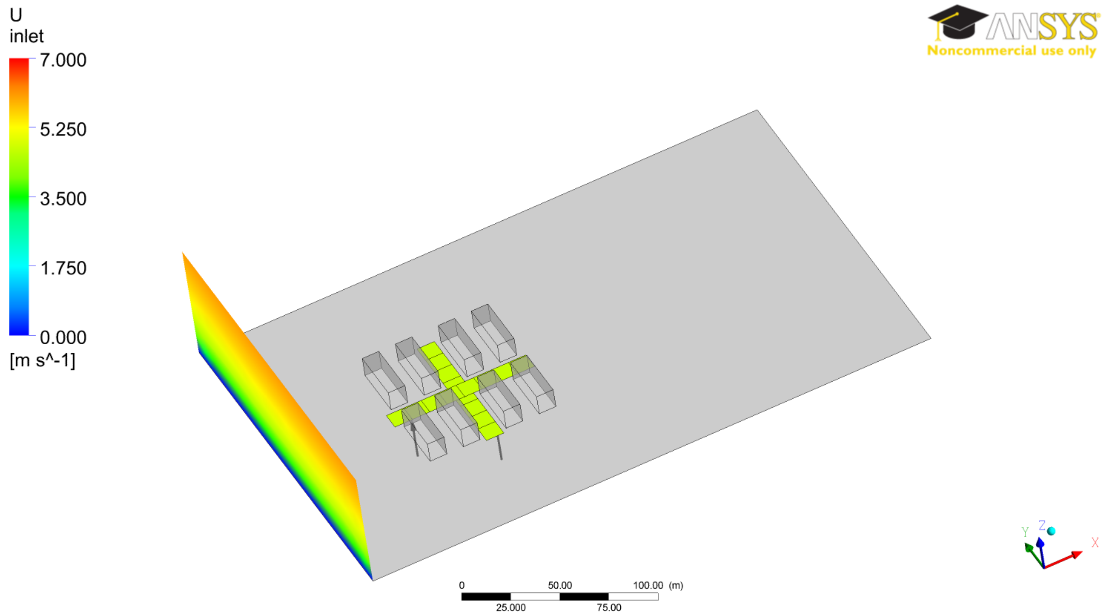

Figure 4-20: Domain air inlet and sources.

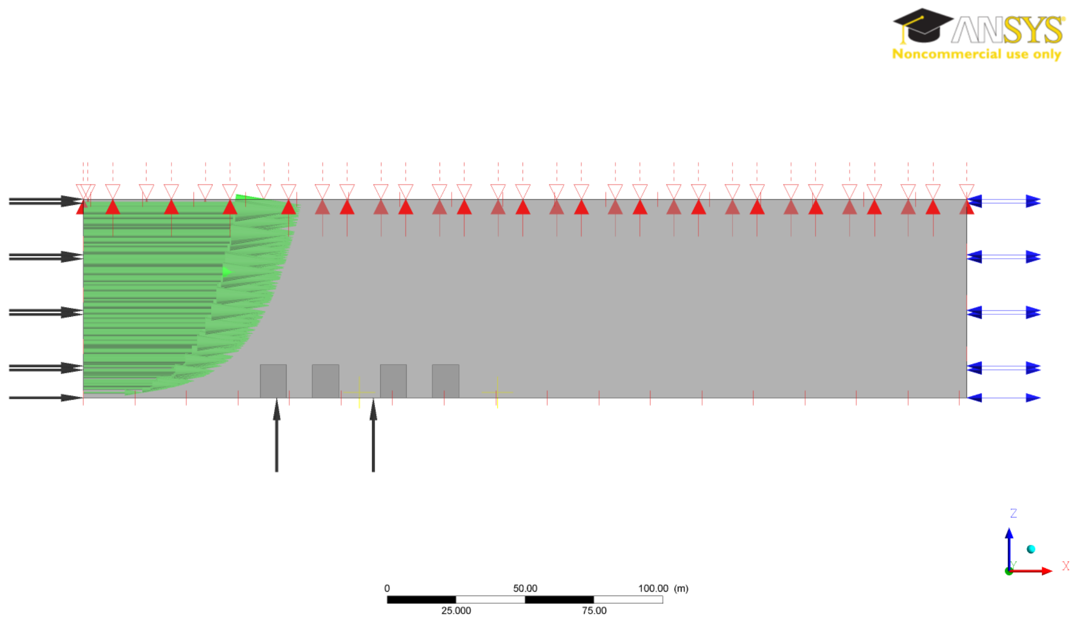

Figure 4-21: Logarithmic profile at the inlet.

Monitor points were added to the generated meshes and new simulations were set in CFX using different analyses types (both steady-state and transient) and time steps. Simulation parameters are set for isothermal simulation, using the k-ε turbulence model. Results for these simulations are presented next.

Figure 4-22 shows the resulting average concentrations for the transient simulation (average from the 4th to 5th minute of simulation) of the listed scenarios along the Z axis represented by the blue dot (X = 110, Y = 0) in Figure 4-19. Up to the height of 20 meters, concentrations from the 3 simulated scenarios are in agreement. Above the height of 20 meters, the concentrations are so small that the differences between the meshes are insignificant.

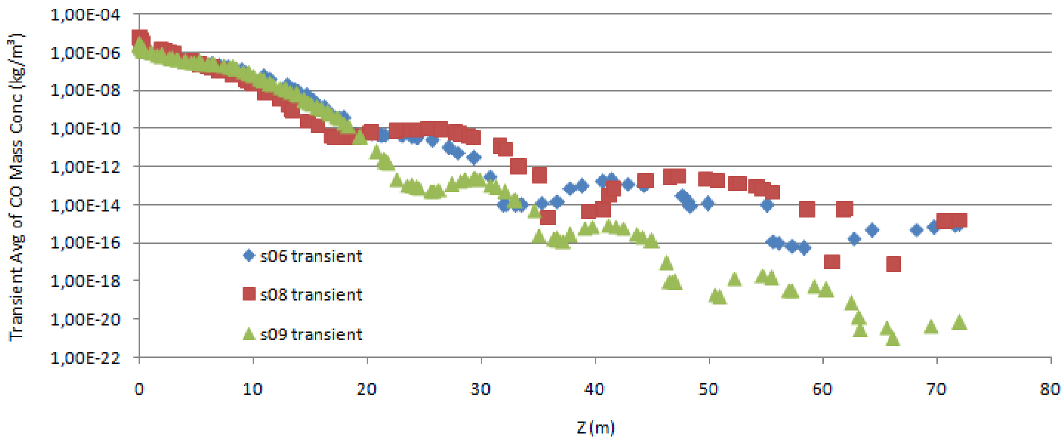

Figure 4-22: Transient average of CO mass concentration along Z axis on X = 110m, Y = 0m.

Figures 4-23 and 4-24 show the resulting average concentration (average from the 4th to 5th minute of simulation) and instantaneous concentration (at the end of the 5th minute) for the transient simulation of the modelled scenarios along the X axis represented by the red line (Y = 0, Z = 2) in Figure 4-19. The center of the built area is on X = 110, Y = 0, and the sources go from X = 70 to X = 150. Small differences are seen upwind from the sources, but again the concentrations are so small that the differences between the meshes are insignificant. Downwind concentrations show similar average results for scenarios s06 and s09, with a small underestimation on scenario s08.

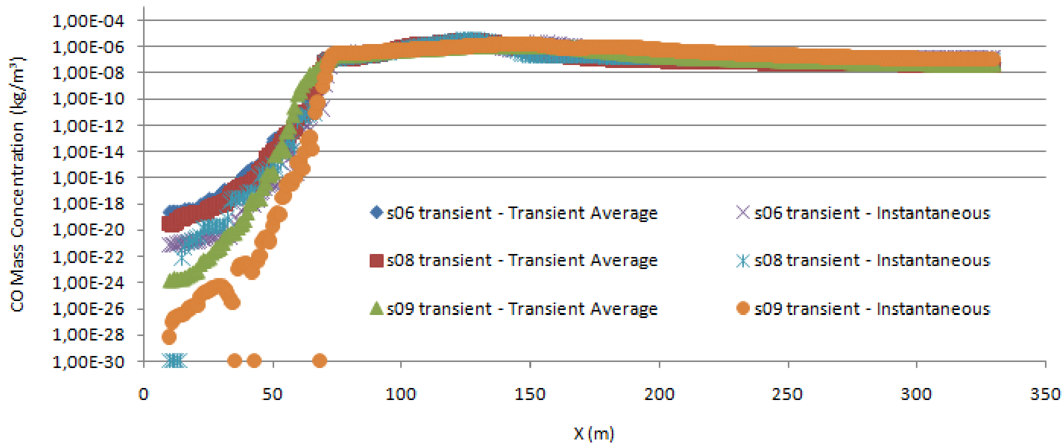

Figure 4-23: Instantaneous and transient average CO mass concentrations along X axis at Y = 0m, Z = 2m.

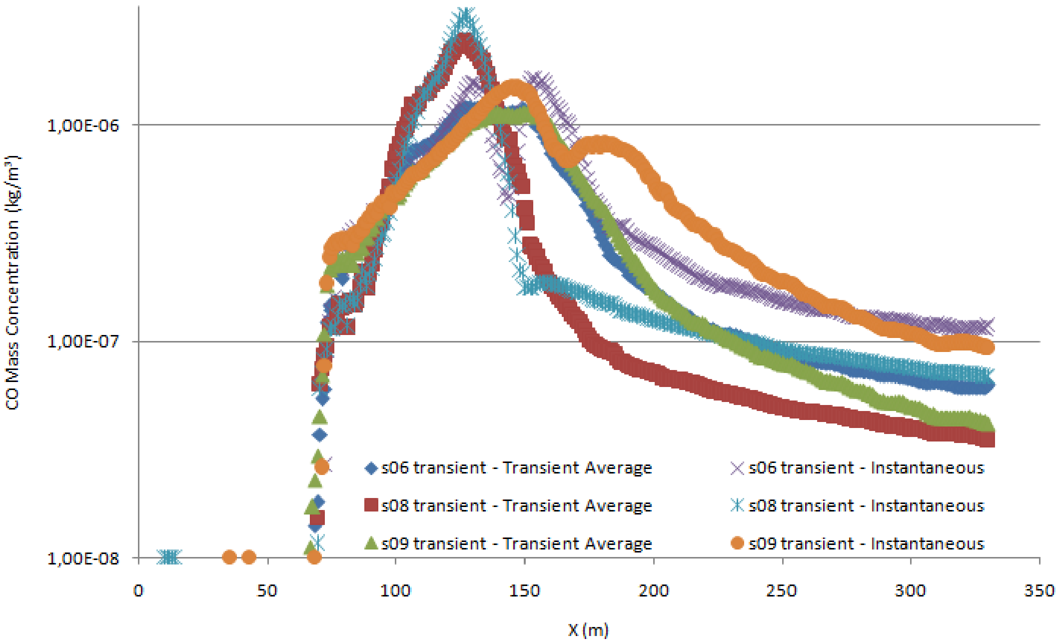

Figure 4-24: Zoom in on the downwind part of the instantaneous and transient average CO mass concentrations along X axis at Y = 0m, Z = 2m.

A contour plot of the transient average molar concentration of CO (average from the 4th to 5th minute of simulation) for the s06 transient case is shown in Figure 4-25.

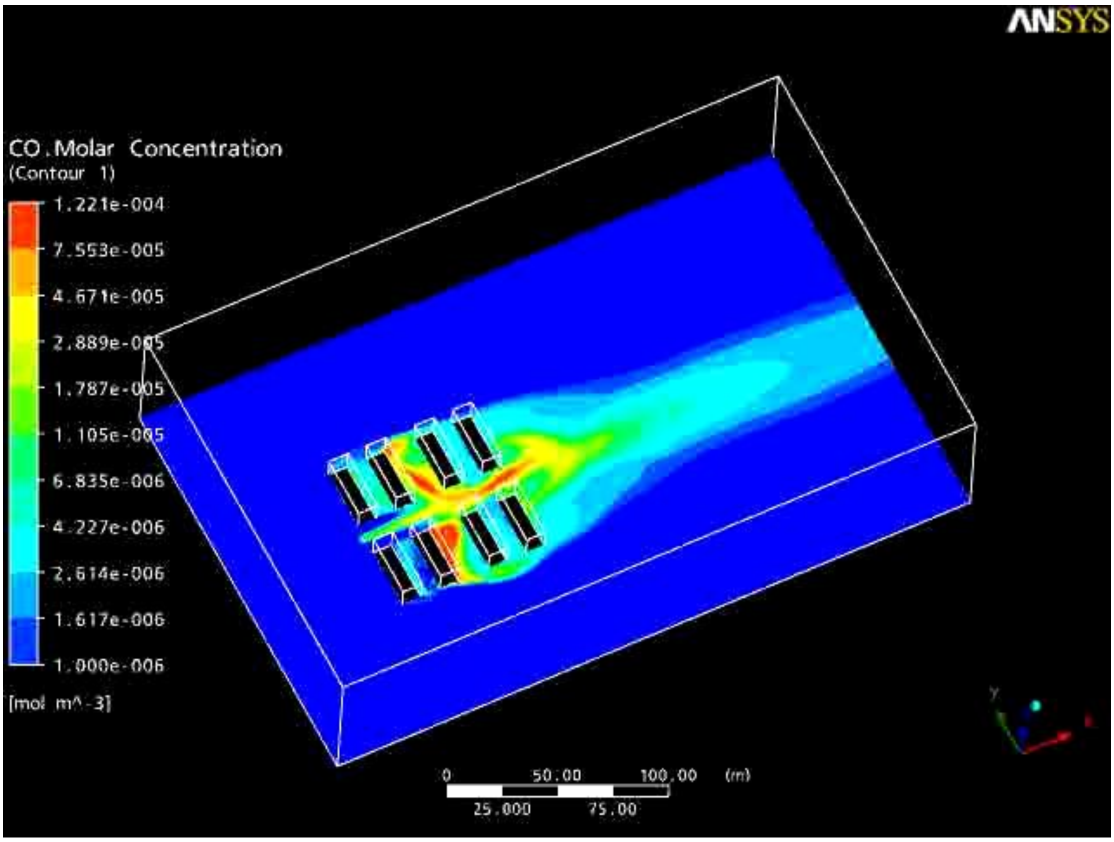

Figure 4-25: Contour plot of transient average of CO molar concentration on plane Z = 2m.

To make the use of CFD easier for CityZoom users, an empty case file was created with all necessary parameters pre-set: materials, equations for logarithmic profile, domain, boundaries, inlets, initial conditions and solver settings. Mesh files generated by CityZoom via Gambit come with all boundaries set using intuitive names, so that the user only needs to add the mesh into the empty case and associate the boundaries from the mesh file to the ones in the case file and then start the simulation. A brief tutorial on how to setup a CFX for simulation of an urban environment using a multispecies flow is presented in Appendix II.

4.6. Conclusions

Several tests of CityZoom UP as a tool to assist in the modelling and setup of urban scenarios for dispersion and CFD simulation have been presented in this chapter.

For the dispersion part of the research, sensitivity and validation tests of AERMOD for the simulation of the dispersion of pollutants in urban environments were performed. For the first time in the available literature AERMOD was used to perform dispersion simulation using tracer emission data from mobile vehicular sources in a complex urban scenario, considering building wake effects. For the CFD part, mesh generation and refinement tests, mesh independence tests, and semi-automated setup of multispecies flow simulation tests were performed.

Sensitivity of AERDMO was verified in neutral conditions regarding variations in the building heights, building distribution, surface wind speed, wind direction, surface roughness and emission profiles. Further tests are needed in order to completely validate the results under different meteorological conditions. A tool to automatically generate meteorological profiles based on user-defined stability classes could be of great value for such tests and future application of the developed framework.

Validation tests compared AERMOD outputs to measurement data available from the DAPPLE project. Results showed that AERMOD simulations of the dispersion in urban scenarios have some flaws, but do present trend agreement to wind tunnel and real world tracer experiments. Buildings are not represented in the AERMOD model as solid objects, as it can be noticed by the non-zero concentrations inside the building boundaries. Instead, the PRIME algorithms are used for estimating the building induced effects for sources within the building wakes, and how they restrict the rise that the plume would have in the absence of the building.

Nevertheless, these results are considered good for the amount of time needed to generate them. A typical AERMOD simulation can be set in minutes and run in a standard desktop in seconds, while CFD simulations are known to take hours or even days to be modelled and performed. The trend agreement in the results enables the user to identify potential problems (namely exceedingly high concentrations of pollutants) at specific areas in different scenarios.

The use of CityZoom UP with AERMOD has the potential to provide valuable data for strategic urban planning purposes, since fast results can be obtained for different urban scenarios and using large sets of emission profiles and meteorological conditions. It is important to keep in mind that AERMOD was not originally built for detailed urban simulations. While the simulations result can provide valuable strategic data, CFD approaches are recommended when accurate results are demanded.

It has also been shown how CityZoom UP can easily automate the generation of different meshes for a scenario, based on boundary layer and size function refinement parameters. This functionality is of great value when testing mesh independence for a CFD scenario, and can save a lot of time and frustration to the end user. Hours of work spent setting boundary layer refinement parameters around each building in the domain and trying to avoid inverted elements in the resulting mesh become minutes as CityZoom UP allows the user to change 1 or 2 parameters and watch as a new mesh is generated. All the boundaries in the generated mesh are identified using names related to their physics properties to be used in the simulation: domain base, top, inlet, outlet, buildings, and symmetries.

Meshes generated by CityZoom UP representing urban scenarios with buildings and sources were tested as input data for multispecies flow simulations. A brief tutorial was generated on how to setup CFX using a CityZoom UP generated mesh to perform multispecies flow simulation of an urban environment.

While the capability to automate the mesh generation based on user-defined refinement parameters and to automatically set the domain boundaries does not affect the computational time needed to run the CFD simulations, it does greatly reduces the time necessary for the setup of the CFD cases.

To further test and validate the use of CityZoom UP with CDF tools, existing scenarios must be modelled and simulated using different turbulence models, comparing the results to measured airflow and pollution data. Validation tests of the use of CityZoom UP with CFD tools for the simulation of urban environments could not be completed during the development of the present research. Nonetheless, the use of CFD tools for urban air quality and dispersion of pollutants simulation in simple and complex scenarios has already been tested and validated by many researches, such as Xie and Castro (2006 and 2009), Aristodemou et al. (2009), ApSimon and Pavlidis (2010) and Solazzo et al. (2008, 2009 and 2011),

5. Show Case

This chapter demonstrates the capabilities of CityZoom UP applied to a real world scenario. CityZoom UP is used to model the existing scenario and a possible future scenario, and to feed data to dispersion (AERMOD) and CFD (CFX) simulations. Although brief comparison of the results generated by each approach is presented, the real purpose of this chapter is not to discuss the quality of the results for these scenarios, but to show how CityZoom UP can assist in the modelling and setup of the simulation of urban scenarios. The city of Porto Alegre, Brazil, where the author resides since 1996, was chosen for this demonstration.

5.1. The Scenario

The Azenha neighbourhood is a traditional commercial and residential area of Porto Alegre, Brazil. The neighbourhood is famous for being the home of the football club *Grêmio Foot-Ball Porto Alegrense*, ranked 1st in Brazil by the Brazilian Football Confederation (CBF 2010). Grêmio's stadium, the *Estádio Olímpico Monumental*, with a maximum capacity of 45,000 people, was built in this neighbourhood in 1954. The stadium is located between avenues Dr. Carlos Barbosa, Cel. Gastão Haslocher Mazeron and Cascatinha, near the Azenha Avenue (Figure 5-1).

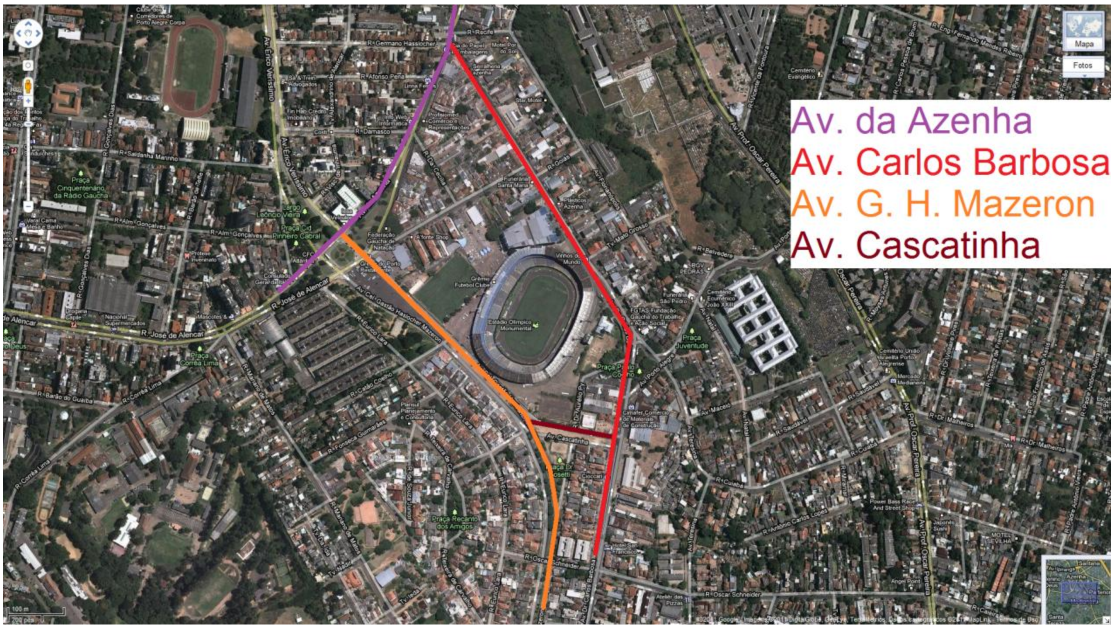

Figure 5-1: Area around the *Estádio Olímpico Monumental* (source: google maps 2010).

In an agreement between the football club and building contractor OAS in March of 2010, *Grêmio* traded the area where the *Olímpico* stadium is located (Figure 5-2) for a new stadium in the outskirts of the city, near the airport. After this new stadium is completed, OAS has a project to replace the *Olímpico* stadium with a major complex of residential and commercial buildings, as well as a mall (Figure 5-3). This region was selected for this demonstration of how the developed tools can be used to assist in the evaluation of the impact of radical changes in the built environment.

Figure 5-2: ***Estádio Olímpico*** **and surrounding area (picture taken by the author, 2010).**

Figure 5-3: OAS project for the ***Olímpico*** **stadium area (source: OAS 2010).**

5.2. Modelling of the Scenarios using CityZoom UP

Two scenarios were modelled for the same location in the Azenha neighbourhood: one representing the present situation with the *Olímpico* stadium and one representing the future situation after the stadium is removed and the project from OAS is completed. CityZoom UP was used to model the existing scenario, drawing the polygons for each building based on a satellite image from the region (from google maps 2010) and setting the heights of these buildings based a survey of the area (Figure 5-4). Due to the extensive size of the region and known hardware limitations for the mesh generation, the author decided to extend the model to include only 1 block to each direction around the *Olímpico* stadium. The origin of the domain (x = 0 m; y = 0 m) was set to be centre spot of the football pitch of the *Olímpico* stadium and the final dimensions of the built region are 773.9 m x 511.1 m x 30 m.

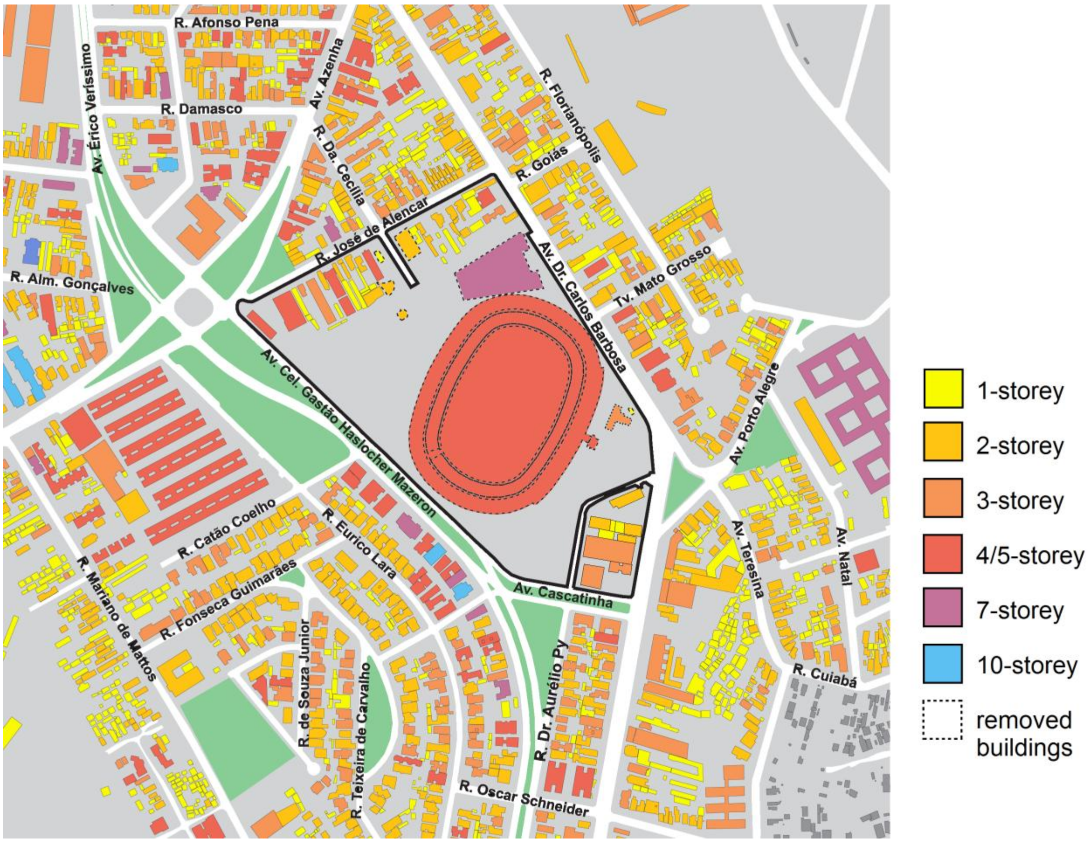

Figure 5-4: Survey of building heights near the *Olímpico* stadium.

To model the future scenario the author obtained the floor plan of OAS' project (Figure 5-5) and made it match the orientation and position of the existing area, then used CityZoom UP to remove the *Olímpico* stadium and a few other selected buildings from the model and include the proposed new buildings. Although some of the buildings in OAS' project are designed to have over 20 pavements, the author decided to model them all with a maximum of 10 pavements, so that the height of the built region would remain unchanged and consequently the extensions of the domain box for the CFD simulations would be the same for both present and future scenarios.

Figure 5-5: Floor plan of OAS project for the *Olímpico* stadium area (source: OAS).

A floor plan view of the modelled existing (a) and future (b) scenarios in CityZoom UP is shown in Figure 5-6. Figure 5-7 shows a 3D representation of the same present (a) and future (b) scenarios.

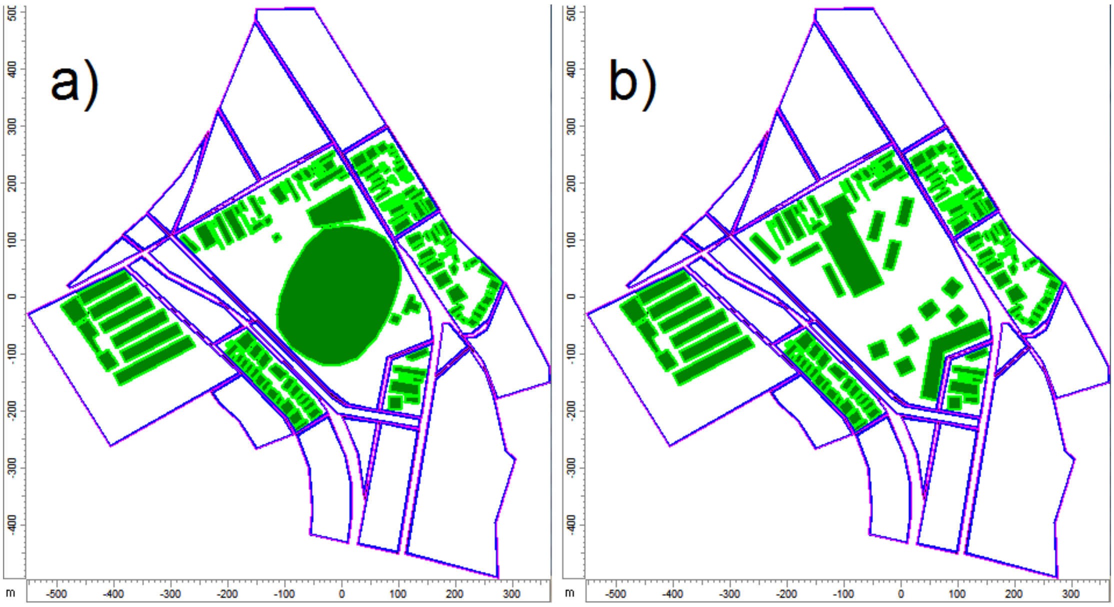

Figure 5-6: Floor plan view of the modelled scenarios in CityZoom UP: a) present and b) future.

5.3. Modelling of the Sources

The initial idea was to model the 2 main avenues closest to the stadium: Av. Carlos Barbosa and Av. G. H. Mazeron (indicated in Figure 5-8a). Even though the Azenha Avenue is considered to be one of the most important avenues in the neighbourhood, it's inclusion in the model was discarded as it would result in too much of an increase in the size of the domain.

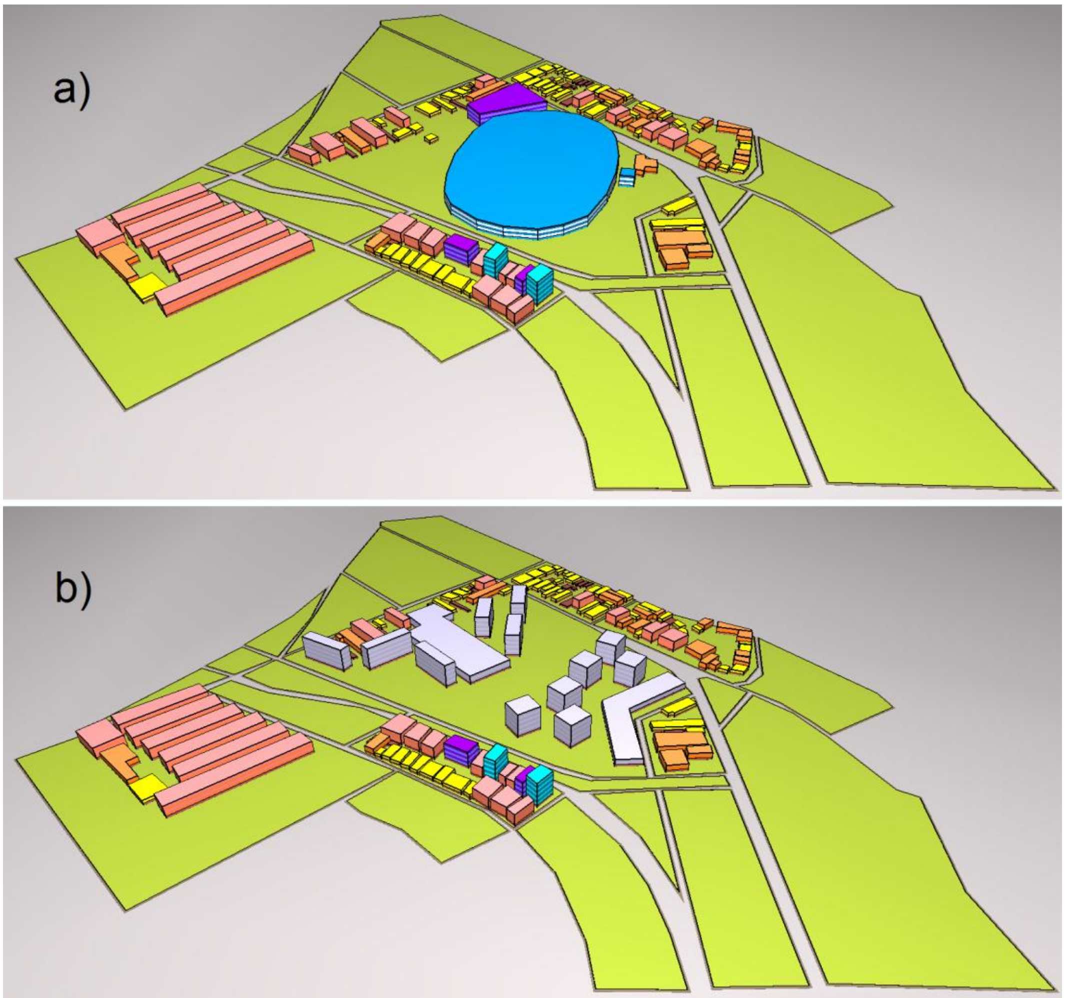

Figure 5-7: 3D representation of the modelled scenarios in CityZoom UP: a) present and b) future.

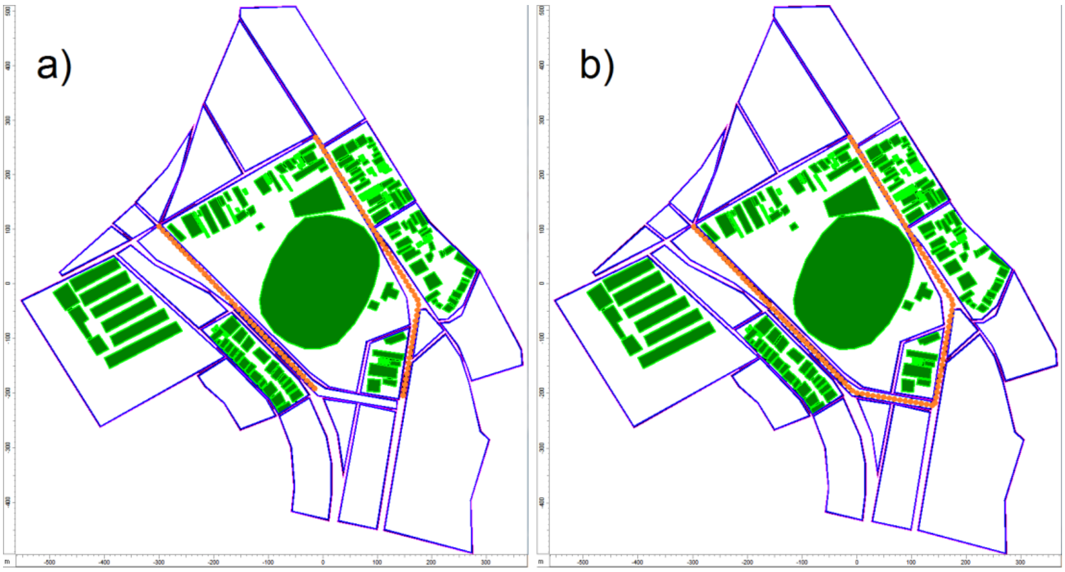

Figure 5-8: Avenues and resulting sources modelled in CityZoom UP: a) initial plan and b) final setup.

There are no real world measurements available for the traffic emissions around the *Olímpico* stadium, so the author had to resort to estimations. In order to create estimated profiles that could approximate the reality the author met with Prof. Helena Cybis, from LASTRAN - UFRGS, who had already helped him develop the parametric profiles used in Chapter 4 of the present work. Prof. Helena suggested the inclusion of Av. Cascatinha in the model, in order to create an "U" around the stadium. Although Av. Carlos Barbosa and Av. G. H. Mazeron are two-way avenues, it was decided that a one-way model would be more appropriate, resulting in a traffic pattern that moved counter-clockwise along the "U" generated by linking the 3 avenues. These avenues were modelled using CityZoom UP and sources were generated along the street axes, distributed 10 m from each other, resulting in 113 sources (Figure 5-8b).

To model the emission profiles, Av. Carlos Barbosa was considered to have heavy traffic, while Avenues G. H. Mazeron and Cascatinha were considered to have a normal level of traffic. Two zebra crossings (one on each side of the stadium, allowing pedestrians to cross the main avenues) and three traffic lights (at the beginning of Av. Carlos Barbosa, at the junction of Avenues Carlos Barbosa and Cascatinha, and at the ending of Av. G. H. Mazeron) were included in the model. The resulting emission profile for the whole system is represented in Figure 5-9 (VTK file generated by CityZoom UP for visualization using ParaView) and plotted in Figure 5-10.

Figure 5-9: Spatial distribution of sources and emission rates in gs^{-1}.

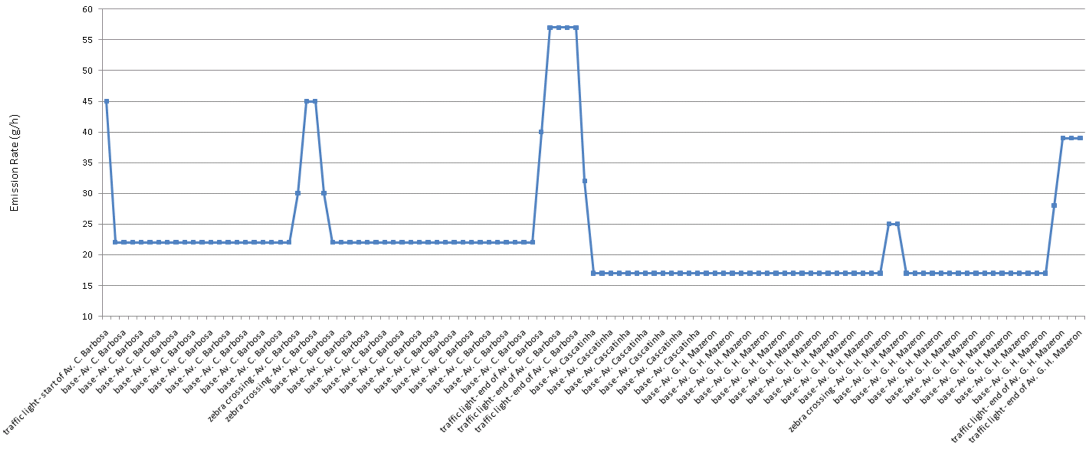

Figure 5-10: Plot of emission rates by source in g/h. Traffic flow is counter-clockwise along the modelled street axes.

The same profile is used for both the present and future scenarios. It is a known fact that the new buildings should cause major changes in the traffic patterns and emission profiles, however the goal of this show case is to demonstrate how changes to the built environment alone can cause variations in the way pollutants are dispersed in the area.

5.4. Dispersion Simulations Using AERMOD

Using CityZoom UP and performing the processes detailed in Chapter 3, the modelled present and future scenarios were converted into AERMOD setup files to run simulations for each scenario. On the first step the BPIP input files were automatically generated for each scenario, then BPIP was used to assess the downwash information for each source and finally this information was imported back into CityZoom UP.

On the second step the grid of receptors was created, using the following parameters: initial x position = -500 m; number of receptors along the x axis = 151; distance between receptors in the x axis = 10 m; initial y position = -500 m; number of receptors along the y axis = 101; distance between receptors in the y axis = 10 m. A total of 15251 receptors were created, covering an area of 1.5 km^2.

The third step was to create the surface meteorological data file and the profile meteorological data file to be used in the AERMOD simulation. In order to allow future comparison with CFD results, these files were created with parameters that tried to replicate the conditions normally used in CFD simulations, i.e., a neutral atmosphere. An overcast sky condition with a wind friction velocity of 0.5 ms^{-1} from West was assumed. Meteorological data was generated for the 24 hours of one single day.

Using the sources emission rates and downwash information, receptors positions and meteorological data filenames, CityZoom UP could generate the input files for AERMOD. Simulations were run for the defined day and the AERMOD text results were imported back to the receptor network in CityZoom UP. Simulation of each scenario, containing a total of 113 sources, 15251 receptors, and 24 hours worth of meteorological data, was executed in ≈4 minutes.

Finally, CityZoom UP was used to generate the VTK files for the visualization of the resulting concentrations of CO at each receptor for the present and future scenarios. Figures 5-11 and 5-12 show pseudocolor plots of the estimated concentration at 9AM for the present (Figure 5-11) and future (Figure 5-12) scenarios.

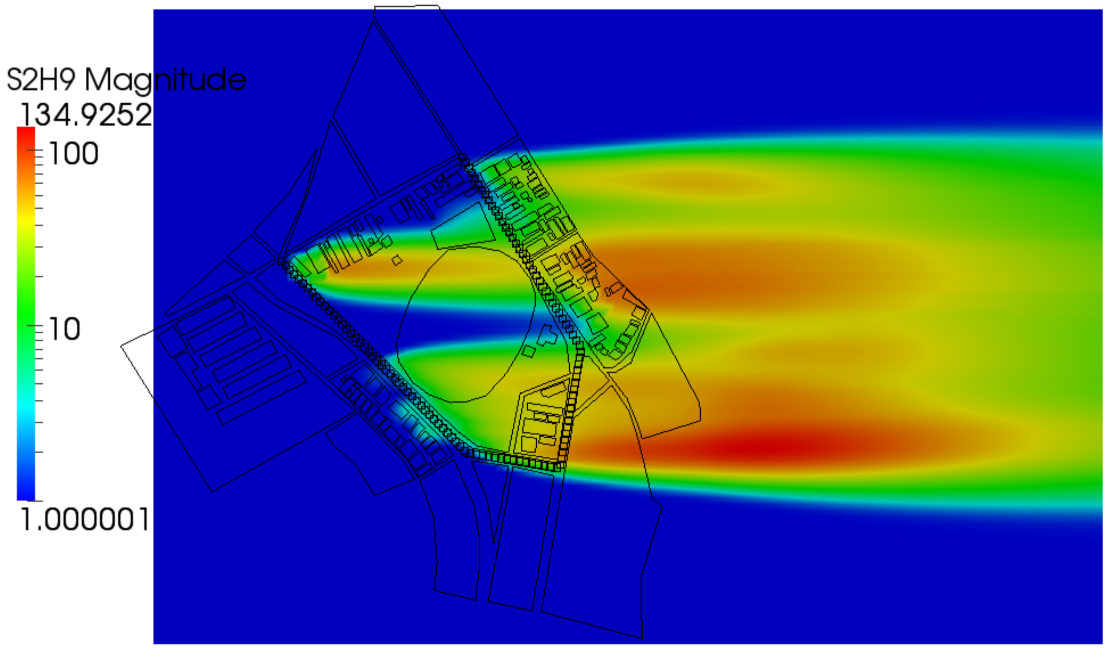

Figure 5-11: VTK pseudocolor plot of resulting AERMOD concentration of CO (micrograms/m^3) at 9AM, present scenario.

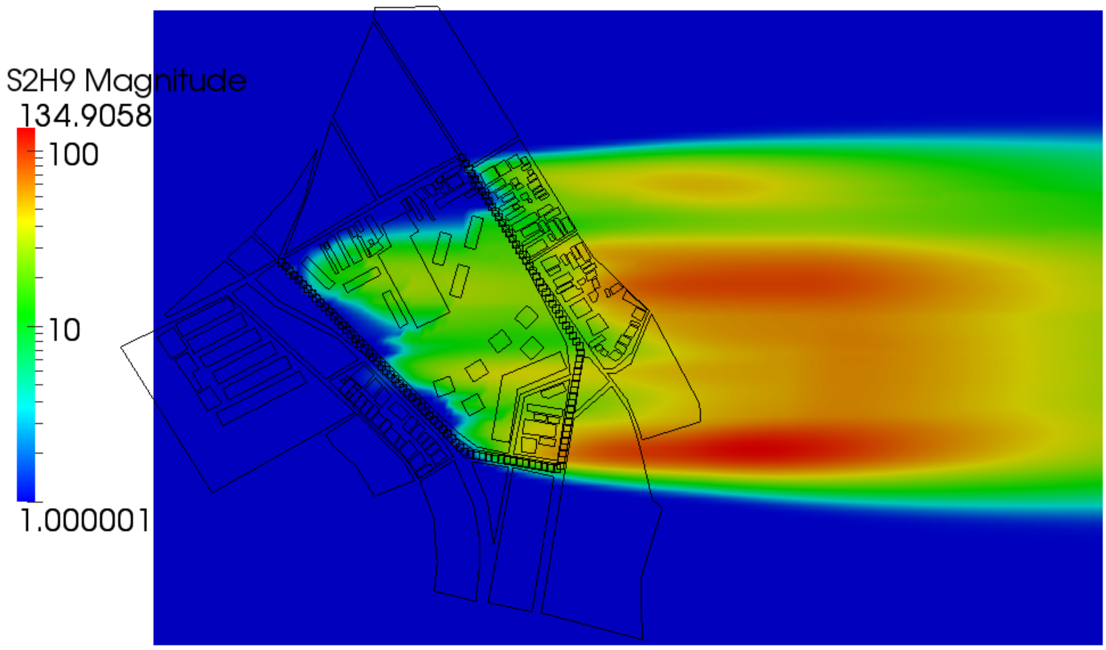

Figure 5-12: VTK pseudocolor plot of resulting AERMOD concentration of CO (micrograms/m^3) at 9AM, future scenario.

It is important to remember the buildings do not exist as solid objects in AERMOD, so receptors located in positions where buildings are located can have non-zero concentration. The concentrations along the centreline of the domain (y = 0 m) are plotted for each scenario in Figure 5-13.

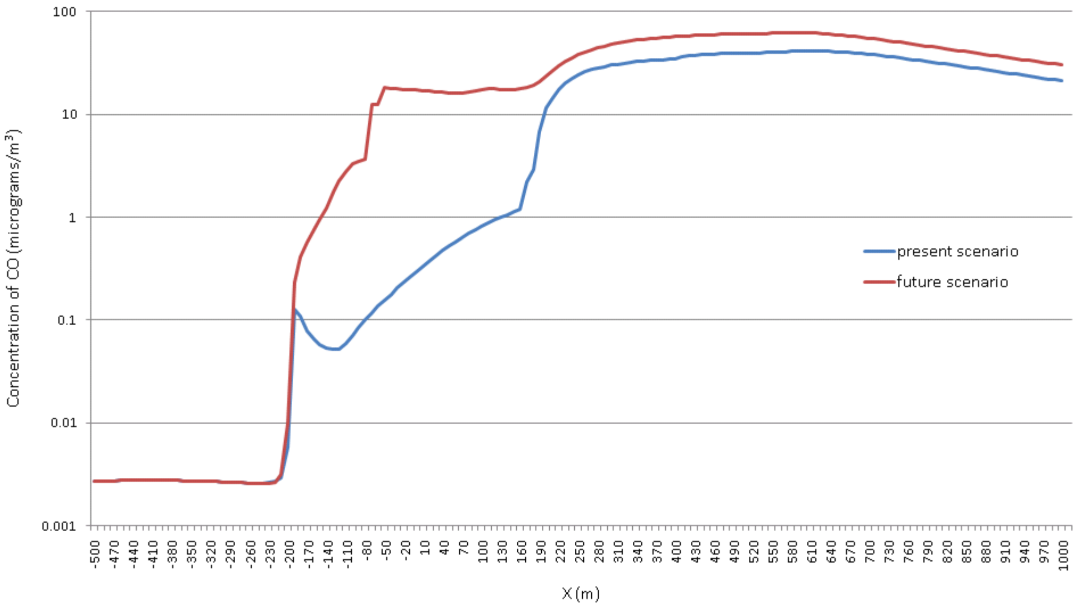

Figure 5-13: Concentration of CO (micrograms/m^3) at Y = 0 m for the simulated scenarios.

Although the buildings do not really exist as solid objects in AERMOD, their effect can be clearly noticed in Figure 5-11 to 5-13, with a great reduction in the resulting concentrations near the stadium for the present scenario. Meanwhile, the concentrations on the SE corner of the domain, where no building downwind from the sources was changed, remain unchanged. These are good indicators that AERMOD can indeed be used for the estimation of alterations in the dispersion patterns caused by changes in the surrounding built environment.

5.5. CFD Simulation Using CFX

As in the previous section, CityZoom UP was used and the processes detailed in Chapter 4 and Appendix II were executed to convert the modelled present and future scenarios into mesh files and to setup and run CFX multispecies flow simulations for each scenario.

The first step was to generate the meshes for the massive 111 ha domain. The built region of dimensions 773.9 m x 511.1 m x 30 m plus the distances recommended by Franke (2007) resulted in a domain of dimensions 1373.9 m x 811.1 m with a total height of 180 m. GAMBIT journal files with a range of values for the boundary layers and size functions parameters were created using CityZoom UP, to verify what was the most detailed mesh that could be generated using the available computational resources: a personal computer with an Intel Core 2 6320, 1.86 GHz processor and 2 GB of RAM.

Table 5-1 lists the parameters used and meshing results: Filename is the name of the journal file generated by CityZoom UP, H_m is the height of the tallest building in the domain, BF is the size of the first row of the boundary layers, BG is the boundary layers growth factor, BR is the number of boundary layer rows, SS is the starting size of the size functions, SG is the size functions growth rate, SL is the size functions size limit, Base is the number of faces in the base of the domain, Volume is the number of cells in the domain, Result indicates whether the meshing was successful or if there were problems during the meshing, "*hse*" indicates the number of highly skewed elements and "*ie*"indicates the number of inverted elements.

Filename	H_m	BF	BG	BR	SS	SG	SL	Base	Volume	Result
olimp.jou	18	0.02	1.1	10	0.5	1.2	10	100k+		Fail: too many faces
olimp2.jou	18	0.05	1.2	10	1	1.2	10	95834		Fail: out of memory
olimp3.jou	21	0.2	1.2	10	5	1.2	20			Fail: BLs overlapping
olimp4.jou	21	0.2	1.2	5	2	1.2	25	44454	1718975	Success: 3 hse, 1 ie
olimp5.jou	21	0.2	1.1	10	2	1.1	25			Fail: BLs overlapping
olimp6.jou	21	0.2	1.1	10	2	1.1	25			Fail: BLs overlapping
olimp7.jou	21	0.2	1.1	5	2	1.1	25	60272		Fail: out of memory
olimp8.jou	21	0.2	1.2	5	2	1.2	25	43008	1719593	Success: 249 hse
olimp9.jou	21	0.2	1.2	5	2	1.2	25	43120	1722212	Success
olimpico10	30	0.2	1.2	5	2	1.2	25	43658	1791859	Success: 5 hse
olimpico11	30	0.2	1.2	5	2	1.2	25	43414	1791373	Success
olimpOAS1	30	0.2	1.2	5	2	1.2	25	49648	2004035	Success
olimpOAS2	30	0.2	1.2	5	1	1.2	20	100k+		Fail: too many faces
olimpOAS3	30	0.2	1.2	5	2	1.2	20	50790	2084843	Success
olimpico13	30	0.2	1.2	5	2	1.2	20	44534	1871041	Success

Table 5-1: Meshing parameters and results.

The first four cases were used as an initial guess for the meshing capacity of the used PC, the maximum building height was lower than the real scenario and no sources were included. Cases 5 to 9 included the initial setup of sources distributed along the 2 main avenues as detailed above. Case 10 had the same source setup but increased the maximum building heights to match the existing building heights. After case 11, both scenarios were completely modelled including the final source positions. The files "*olimpico11*" and "*olimpico13*" were used to generate the meshes for the present scenario while "*olimpOAS1*" and "*olimpOAS3*" were used to generate the meshes for the future scenario.

The second step was to import the mesh into CFX Pre and setup the CFD run. The short tutorial in Appendix II lists the actions performed to complete this step. Simulation parameters are set for isothermal simulation, using the k-ε turbulence model. The domain is set as a stationary, non buoyant, fluid domain. The fluid in the domain is an ideal mixture of air and CO as a gas with molar mass = 28.01 kg $kmol^{-1}$, density = 1.185 kg m^{-3}, specific heat capacity = 1003.7 J kg^{-1} K^{-1}, specific heat type = constant pressure, reference temperature = 15 C, reference pressure = 1 atm, dynamic viscosity = 1.662e-05 Pa s, and thermal conductivity = 0.023 W m^{-1} K^{-1}.

Building, source and domain box geometry information are automatically generated by CityZoom UP, so they are already defined in the mesh file. To match the AERMOD case, the inlet was set to have a logarithmic profile boundary layer, with a friction velocity of 0.5 ms^{-1}. Source emission rates were set manually to match the profile in Figure 5-10. Definition files were created for each scenario for both steady state and transient simulations. The steady state runs were set to a maximum of 600 iterations or convergence criteria RMS = 10^{-4} and the transient runs were set to run for 600 seconds, using a time step of 1 second and outputting results every 10 seconds of simulation.

Oh the third step, these definition files were copied to the Linux cluster Stokes for parallel simulation. Stokes is comprised of 11 quad-core and 8 eight-core 64-bit processors, and is shared by many researchers from the University of Nottingham CFD group. Using the CFX standard MeTis multilevel k-way algorithm, each case was partitioned for parallel simulation in 4 cores. Total simulation times for steady state cases "*olimpico13s*" and "*olimpOAS3s*", and transient cases "*olimpico13t*" and "*olimpOAS3t*" are listed in Table 5-2.

Filename	Simulation Type	Elements	Partitions	Time (hh:mm)
olimpico13s	Steady State	1871041	4	01:25
olimpico13t	Transient	1871041	4	13:52
olimpOAS3s	Steady State	2084843	4	06:00
olimpOAS3t	Transient	2084843	4	20:36

Table 5-2: Total wall clock time for CFD simulations.

Finally, the simulation output files were copied back to the PC, where CFX Post was used for the visualization of the results. Steady state and transient average of mass concentration of CO along the centreline of the domain are plotted for each case in Figure 5-14.

The upwind concentrations are much lower for the transient cases, but the downwind ones are very similar. This reasserts the premise that steady state simulations could be a good and reliable alternative, while not being as time-consuming as transient simulations.

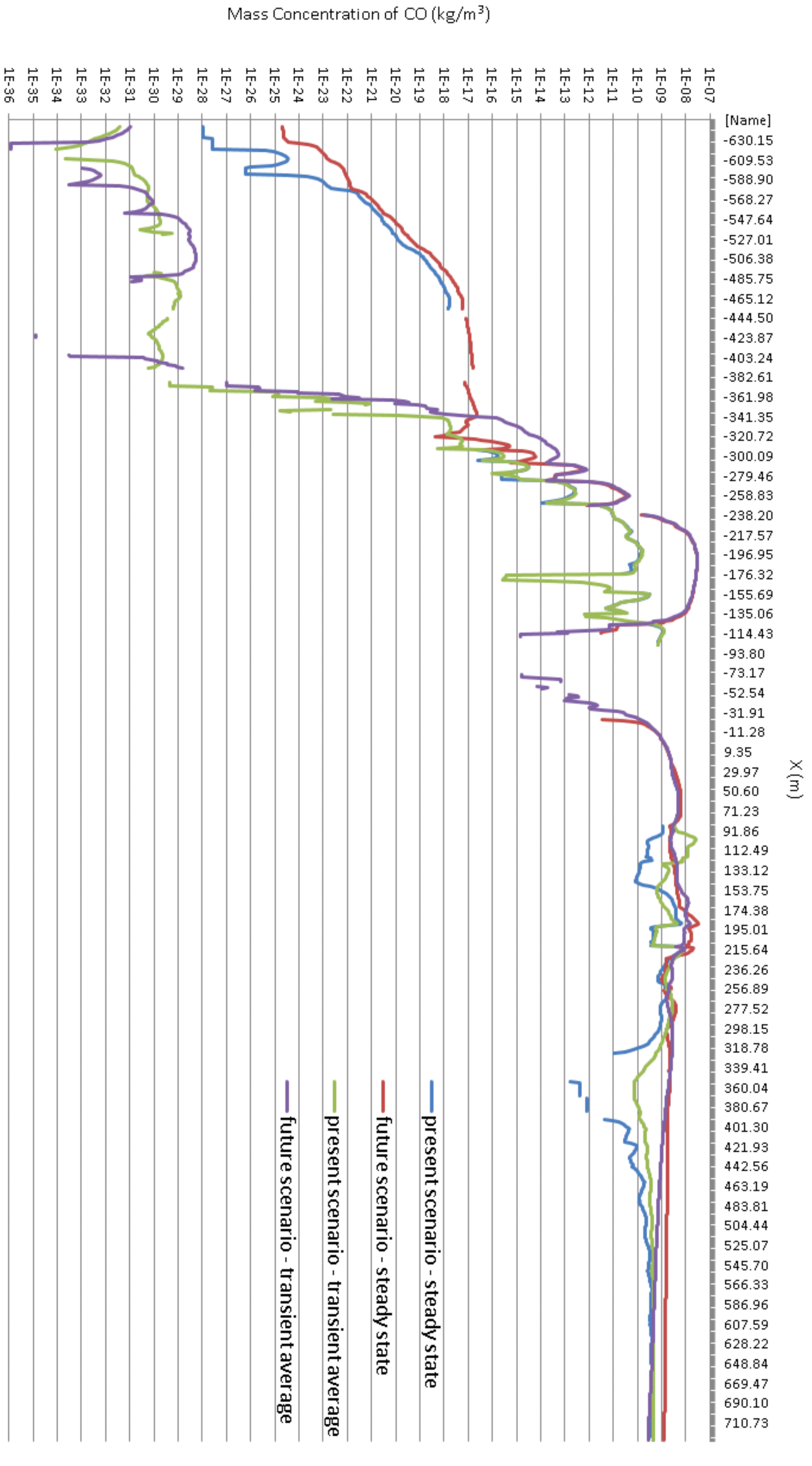

Figure 5-14: Mass concentration of CO along the X axis, y = 0 m, z = 1.5 m.

Contour plots of the steady state and transient average of mass concentration of CO for each case are shown in Figures 5-15 to 5-18. Data was extracted at plane XY with z = 1.5 m. Figure 5-15 shows a contour plot of the resulting mass concentration of CO after 600 seconds of steady state simulation of the present scenario. Figure 5-16 shows the contour plot of the transient average concentration of CO over the 600 seconds of transient simulation of the present scenario.

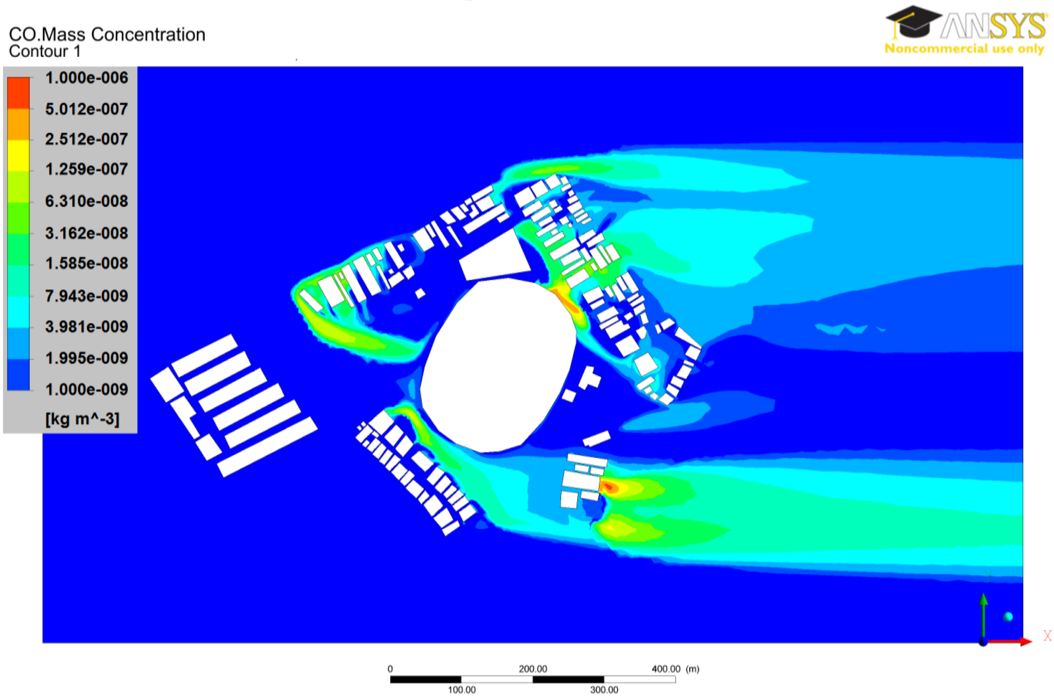

Figure 5-15: Contour plot of the steady state mass concentration of CO in the present scenario.

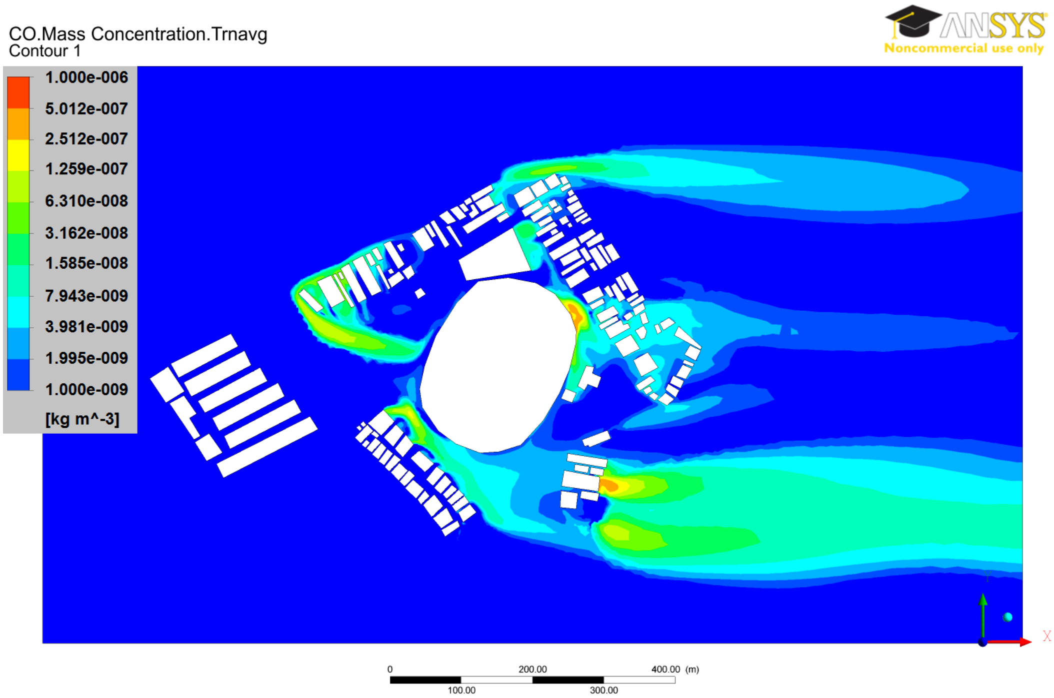

Figure 5-16: Contour plot of the transient average of mass concentration of CO in the present scenario.

Figures 5-17 and 5-18 show the same plots as Figures 5-15 and 5-16 respectively, but for the future scenario.

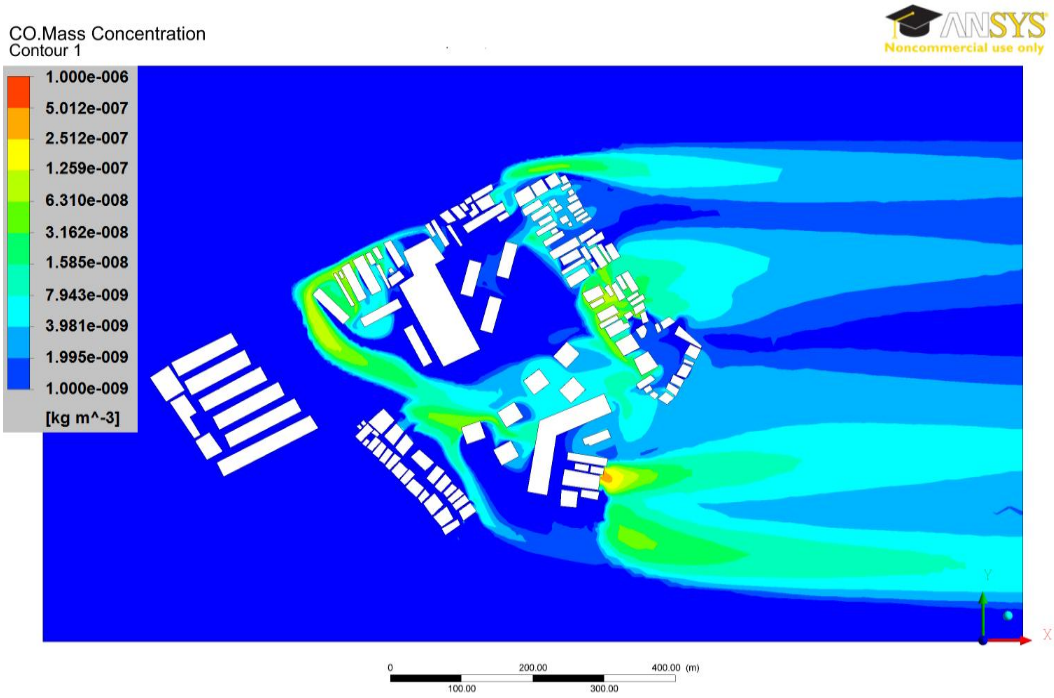

Figure 5-17: Contour plot of the steady state mass concentration of CO in the future scenario.

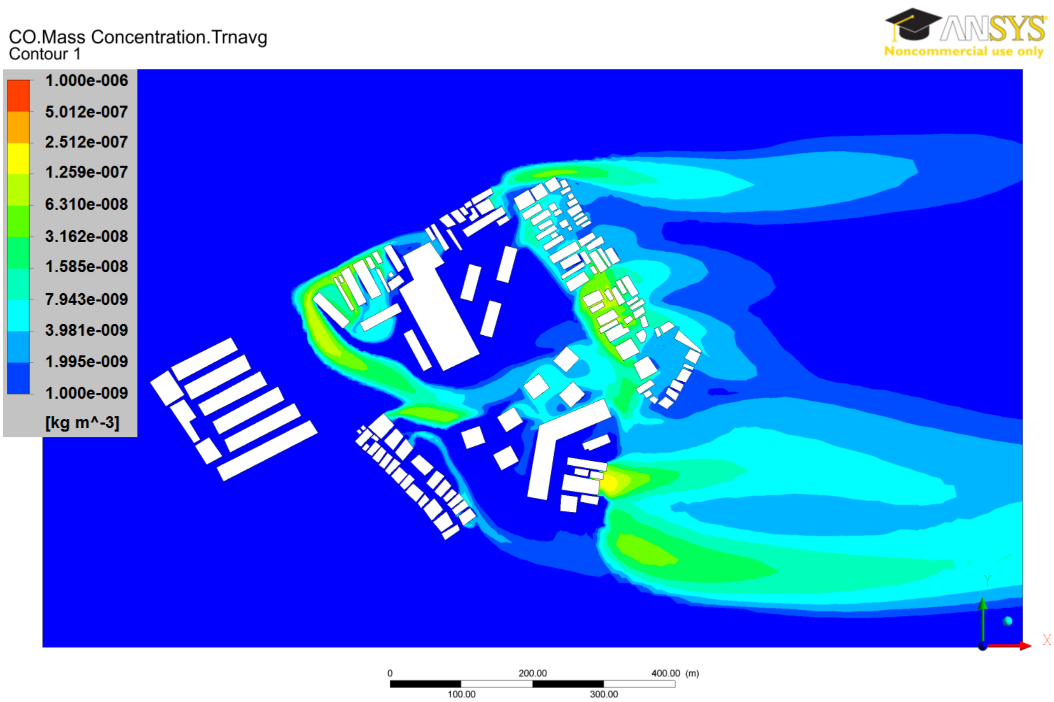

Figure 5-18: Contour plot of the transient average of mass concentration of CO in the future scenario.

These results can be used as indicators of areas where the concentration of pollutants could present risk to pedestrians and to the neighbourhood. Other outputs can be generated by CFX Post to assist in the understanding of the results, such as animations of the plume of pollutants, contour and vector plots of concentration and wind speed at different heights or at cross sections of the domain.

Due to computational resources limitations, mesh independence tests could not be performed for these scenarios. Given the size of the domains, even the best meshes obtained are rather coarse. Regardless, this was a good exercise to demonstrate how the developed tool can be used to quickly generate a wide variety of meshes for different modelled scenarios.

5.6. Comparison of Results and Discussion

Figure 5-19 shows the resulting mass concentration of CO at y = 0 along the X axis for both the AERMOD and CFX simulations detailed above. AERMOD output units, micrograms/m^3, were converted to kg/m^3, the default unit used by CFX.

Results for both approaches show the same trends: low concentration upwind for all cases and a higher concentration downwind in the future scenario when compared with the present scenario. This is consistent with the removal of the massive stadium, which is replaced by tall buildings with wide open spaces between them. The shape of the concentration curves is similar, but AERMOD lines are continuous since the buildings are not represented as solids (as explained in Chapter 3), while the CFX lines have several gaps where the concentration drops to zero because the points are located inside of buildings.

There is a difference of nearly 2 orders of magnitude in the absolute values, which could be a result of overestimations in the AERMOD simulation caused by the small value used for the urban surface roughness (z_0 = 0.5 m), or most likely because of underestimations in the CFD model caused by the rather coarse mesh used. The most detailed mesh that could be generated with the available computational resources contained triangular faces with sides of up to 25 m, since the CFD domain was over 1 km long. Higher capability hardware is needed, especially for the mesh generation, in order to perform further tests and to explain these differences.

The trend similarity between the approaches implies that good indications of local maximum and minimum concentrations could be obtained from the use of AERMOD for urban simulations, while having simulation times much smaller than the CFD simulations (≈4 minutes using AERMOD vs. 1h25m to 20h using CFD). Simulation times for AERMOD could be reduced even further if the concentration was calculated only on a small set of interest points, which can be done without damage to the results because the concentration in each position depends only on the sources' positions and their emission rates, not on the quantity of pollutants being transported through the surrounding cells.

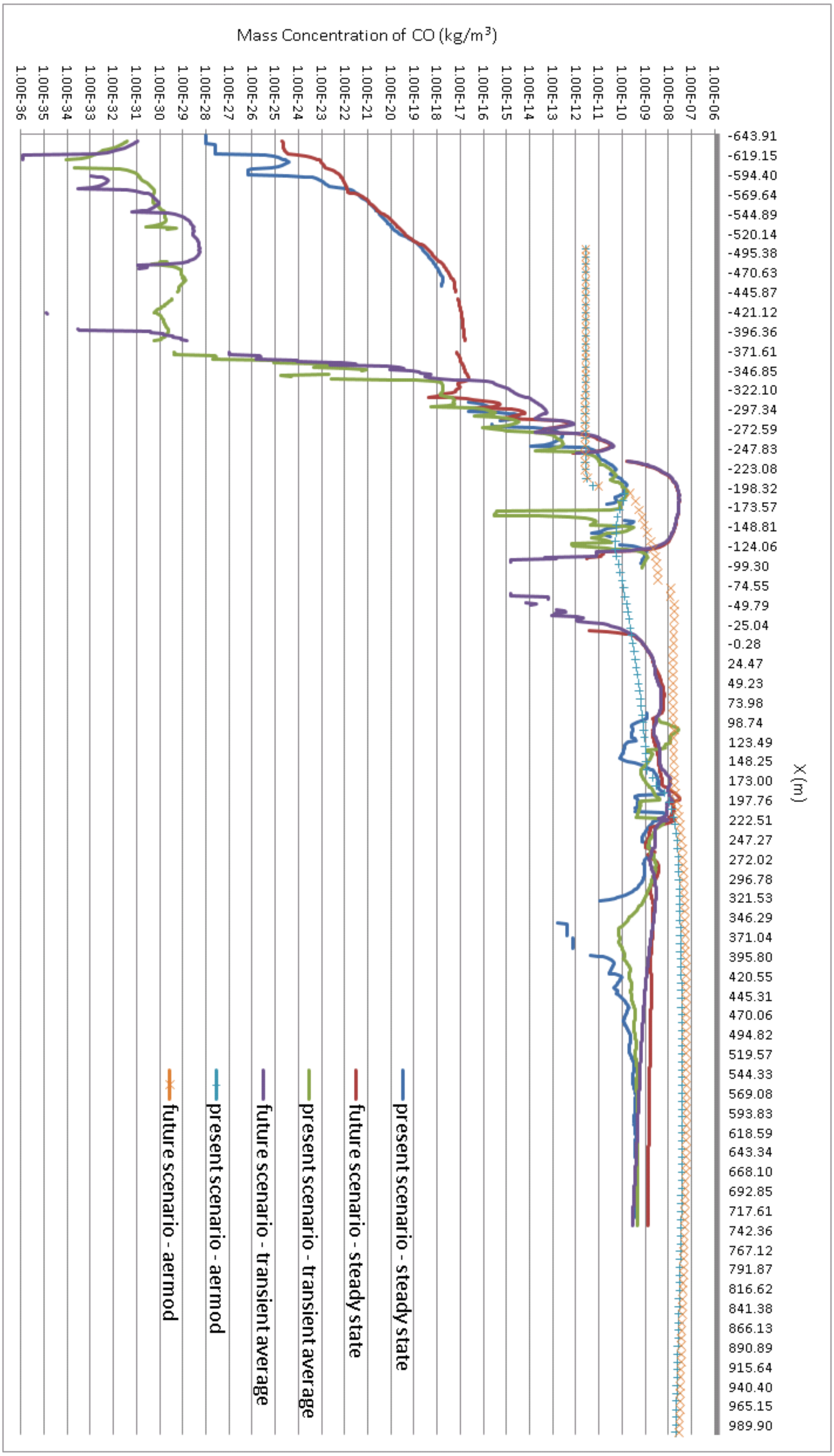

Figure 5-19: Centreline mass concentration of CO for AERMOD and CFX simulations.

It is important to emphasise once again that the purpose of this chapter was not to produce accurate results, but to demonstrate how CityZoom UP can be used to model different urban scenarios and to generate detailed input files for dispersion and CFD tools. Alternative scenarios for a given location, e.g. present situation and future scenario including a new tall building, can easily be generated by CityZoom UP. This includes the geometry of each scenario, input files for AERMOD, or journal files to create different meshes based on user-defined refinement parameters and to automatically set the domain boundaries to be used in CFD simulations. While these features do not affect the computational time needed to run the CFD simulations, they do greatly reduce the time necessary for the setup of CFD cases.

6. Conclusions

CityZoom UP represents the first attempt to extend existing urban planning software in order to directly provide data to air dispersion modelling tools, namely Gaussian dispersion and CFD models. Based on the previous capabilities and graphic user interfaces of CityZoom to model and validate urban scenarios based on Master Plan regulations, new graphic user interfaces, automatic mesh generation and data conversion algorithms have been created to seamlessly generate both geometry and simulation setup parameters in file formats usable by the widely used and accepted dispersion model AERMOD and CFD packages CFX and OpenFOAM.

Many tools exist that can aid the user in different stages of urban planning. Computer-aided design (CAD) tools and specialized parametric tools are often used to model urban scenarios, while simulation tools that can be used to assess the effects of proposed changes in the built environment. However, each of these tools is regularly used in a self-contained manner: one CAD model is created to represent land use (mapping commercial, residential or industrial buildings), a different tool is used to create a model of the streets for traffic simulations, a third set tool is used to simulate the dispersion of pollutants, and so on. To cross reference these models and to understand how they affect each other is a hard task that is seldom performed. An integrated computational tool capable of considering different urban aspects, such as the city's geometry, Master Plan regulations, insolation and meteorological data, as well as emission and dispersion of pollution parameters, could improve the quality of the decisions taken during the urban planning process, thus improving the quality of life of the population living in the cities.

A key feature of CityZoom UP is the introduction of vehicular pollution source parameters in dispersion and CFD models, allowing the urban designer to assess the local impact of adding or modifying a building or group of buildings on the street air quality. Traffic emissions are modelled as sequence of point sources, an approach that was well accepted by traffic specialists and later suggested in the reports from the DAPPLE project. CityZoom UP can handle pollution-related parameters (such as source and receptors locations, emission and concentration data, and meteorological data) in the same environment as the other urban parameters (city geometry, planning regulations, urban growth indexes, and others), even though the dispersion and CFD simulations are actually performed by third-party tools.

Fast dispersion models are used to assess the dispersion of pollutants in large scale urban environments. CityZoom UP can be used with atmospheric dispersion modelling tool AERMOD for strategic planning, quickly providing results for several different alternatives of built environment, meteorological and traffic profiles. CityZoom UP can be used to model or to generate urban scenarios and to set emission profiles, then AERMOD can simulate the dispersion of pollutants in no more than a few minutes.

Sensitivity of AERMOD was tested and verified in neutral conditions regarding variations in the building heights, building distribution, surface wind speed, wind direction, surface roughness and emission profiles. Further tests are needed in order to completely validate the results under different meteorological conditions.

For the validation tests, AERMOD simulation results were compared to wind tunnel and real world tracer experiments from the DAPPLE campaign. For the first time in the available literature AERMOD was used to perform dispersion simulation using tracer emission data from mobile vehicular sources in a complex urban scenario, considering building wake effects. Test results showed trend agreement to the DAPPLE data. Buildings are not represented in the model as solid objects, as it could be noticed by the non-zero concentrations inside the building boundaries. Instead, the PRIME algorithms are used for estimating the building induced effects for sources within the building wakes, and how they restrict the rise that the plume would have in the absence of the building.

Despite some flaws, the results generated by AERMOD for urban environment simulations are considered good for the amount of time needed to generate them. CityZoom UP and AERMOD have the potential to provide valuable data for strategic urban planning purposes, since fast results can be obtained for different urban scenarios and using large sets of emission profiles and meteorological conditions.

While the fast approach using dispersion models has great strategic value, AERMOD was not originally built for detailed urban simulations, and CFD techniques should be used when more precise results are demanded locally. For this reason CityZoom UP was designed to also provide automated 3D meshing, including mesh refinement, identification of physical boundaries in the mesh, and automatic setup of CFD simulations.

The developed tool can assist in the fast setup of various urban scenarios for CFD simulation. Tests showed how alternative scenarios for a given location, e.g. present situation and future scenario including a new tall building, can easily be generated by CityZoom UP.

It has also been shown how CityZoom UP can easily automate the generation of different meshes for the same scenario, based on boundary layer and size function refinement parameters. This functionality can greatly reduces the time necessary for the setup of CFD cases and for testing mesh independence of urban scenarios.

Tests to validate the results obtained by simulation of scenarios generated by CityZoom UP were planned, but could be performed during the development of the present research. Nevertheless, the use of CFD tools for urban air quality and dispersion of pollutants simulation in simple to complex scenarios has already been tested and validated by many researches.

The present and possible future situations of a real world scenario were modelled as a show case for the developed tool. Emphasis was given to demonstrate the potential to quickly generate alternative scenarios and setup AERMOD and CFD simulations based on those scenarios. The results for both approaches showed the same trends, but noticeably different absolute values, which could have been caused by several reasons. Regardless, the trend similarity between the approaches implies that good indications of local maximum and minimum concentrations could be obtained from the use of AERMOD for urban simulations, while having simulation times much smaller than the CFD simulations.

Further tests are needed, but the potential of the developed tools to facilitate and accelerate the setup of dispersion and CFD simulations is unquestionable. CityZoom UP – a new version of CityZoom – is novel in its capability to correlate different urban aspects (city geometry, urban growth indicators, Master Plan regulations, meteorological data and pollution parameters) in an integrated computational environment, which can improve the urban design by assisting architects, engineers, urban planners and even laymen in quickly generating and assessing a variety of "what if" scenarios. What if we allowed a massive mall to be built in this neighbourhood? What if we allowed 20-story buildings along this avenue? What if we changed the traffic direction on this road?

It is expected that the use of CityZoom UP with AERMOD and CFD tools can improve the understanding of how changes to the built environment induce alterations on the airflow and the dispersion of pollutants, resulting in better designs and ultimately in better informed decisions regarding the planning of urban areas.

6.1. Future Work

For the use of AERMOD with CityZoom UP, a tool to automatically associate the different stability classes with user-defined meteorological parameters (e.g., wind speed, wind direction, temperature) and generate the meteorology files, used by AERMOD simulations, would be useful to the setup of simulations for such different conditions. This tool would be interesting for comparative tests against wind tunnel and CFD scenarios, where the atmosphere conditions are well defined. It could also be useful when the measured meteorological data for a location are not readily available.

The author has several ideas for the refinement of the CityZoom UP for use with CFD models. The first and already discussed idea is to improve the OpenFOAM automation process to generate the setup files for multispecies flow simulation. Another possibility is to provide even further refinement of the automated meshing process, allowing the user to set different parameters to the boundary layers around each building. The third possibility would be to fully automate the setup of CFX simulations via scripts, an idea that was not pursued for two reasons: the use of OpenFOAM was considered the most innovative and there was the consensus that OpenFOAM would be more likely to be used outside of academic environments since it is a free tool.

Finally, it would be very important to run further tests using scenarios generated by CityZoom UP with both the AERMOD and CFD models in order to compare the results from both approaches. With the CityZoom UP prototype being fully functional, as demonstrated in the show case, it is simple to model cases for comparison with measurements from real world, wind tunnel or idealized scenarios. Many future researches can start from this point, using CityZoom UP to assist in the modelling of the scenario or scenarios to be studied, or even to generate complete alternative scenarios of possible future urban occupation.

References

Abadie, P. and Schiestel, R. (1986). "Prevision numérique de la convection forcée turbulente dans une cavité bidimensionnelle entrainéeNumerical prediction of turbulent forced heat convection in a bidimensional driven cavity flow." International Journal of Heat and Mass Transfer **29**(3): 417-427.

Ahn, K., Rakha, H., Trani, A., et al. (2002). "Estimating Vehicle Fuel Consumption and Emissions based on Instantaneous Speed and Acceleration Levels." Journal of Transportation Engineering **128**(2): 182-190.

Allwine, K. J., Leach, M. J., Stockham, L. W., Shinn, J. S., Hosker, R. P., Bowers, J. F., Pace, J. C., (2004). "Overview of Joint Urban 2003 - an atmospheric dispersion study in Oklahoma City." Symposium on Planning, Nowcasting and Forecasting in the Urban Zone. American Meteorological Society, Seattle, WA. http://ams.confex.com/ams/84Annual/techprogram/paper_74349.htm

Allwine, J. and Leach, M. (2007). "Editorial." Journal of Applied Meteorology and Climatology **46**(12): 2017–2018.

ApSimon, H and Pavlidis, D. (2010). "Application of the ‘Fluidity’ LES-CFD model to atmospheric dispersion." *Final Report to the Home Office*, DAPPLE2009/06 v2, Imperial College, London, 2010.

Ariotti, P., Cybis, H. B. (2012). "Abordagem hibrida de modelagem de tráfego para estimativa de emissões." XVI Pan-American Conference of Traffic and Transportation Engineering and Logistics, 2010, Lisboa. Anais, 2010.

Ariotti, P., Obelheiro, M., Cybis, H. B. (2008) . "Análise da Influência da Inclinação ascendentes da via na estimativa de emissões veiculares em áreas urbanas." XXII Congresso de Pesquisa e Ensino em Transportes, 2008, Fortaleza. Pannorama Nacional da Pesquisa em Transportes 2008. Rio de Janeiro: ANPET, 2008. v. 1. p. 1-12.

Aristodemou, E, Bentham, T, Pain, C, Colvile, R, Robins, A and ApSimon, H, (2009). "A comparison of mesh-adaptive LES with wind tunnel data for flow past buildings: Mean flows and velocity fluctuations." Atmospheric Environment, **43**(39), 6238-6253.

Arnold, S. J., ApSimon, H., Barlow, J., et al. (2004). "Introduction to the DAPPLE Air Pollution Project." Science of The Total Environment **332**(1-3): 139-153.

AutoCAD (1982). Autodesk AutoCAD. Mill Valey, CA, USA. Autodesk, Inc: http://usa.autodesk.com/autocad/

Baik, J.-J. and Kim, J.-J. (1999). "A Numerical Study of Flow and Pollutant Dispersion Characteristics in Urban Street Canyons." Journal of Applied Meteorology **38**(11): 1576-1589.

Baik, J.-J., Park, R.-S., Chun, H.-Y., et al. (2000). "A Laboratory Model of Urban Street-Canyon Flows." Journal of Applied Meteorology **39**(9): 1592-1600.

Baker, J., Walker, H. L. and Cai, X. (2004). "A study of the dispersion and transport of reactive pollutants in and above street canyons--a large eddy simulation." Atmospheric Environment **38**(39): 6883-6892.

Barlow, J, Belcher, S and Wood, C. (2010). "The flow above roof-level and its relation to canyon winds." *Final Report to the Home Office*, DAPPLE2009/05, University of Surrey, 2010.

Belcher, S. E. (2005). "Mixing and transport in urban areas." Philosophical Transactions of the Royal Society A: Mathematical, Physical and Engineering Sciences **363**(1837): 2947-2968.

Berkowicz, R. (2000a). "OSPM - A Parameterised Street Pollution Model." Environmental Monitoring and Assessment **65**(1): 323-331.

Berkowicz, R. (2000b). "A Simple Model for Urban Background Pollution." Environmental Monitoring and Assessment **65**: 259-267.

Berkowicz, R., Winther, M. and Ketzel, M. (2006). "Traffic pollution modelling and emission data." Environmental Modelling & Software **21**(4): 454-460.

Bigolin, M. and Kowarick, A. (2006). "O Ordenamento da Publicidade de Rua em Porto Alegre." Intercom Júnior - Trabalho Individual, XXIX Congresso Brasileiro de Ciências da Comunicação.

Biltoft, C.A. (2001). "Customer report for Mock Urban Setting Test." Report No. WDTC-FR-01-121, U.S. Army Dugway Proving Ground, Dugway, UT.

Blocken, B., Stathopoulos, T. and Carmeliet, J. (2007). "CFD simulation of the atmospheric boundary layer: wall function problems." Atmospheric Environment **41**(2): 238-252.

Caputo, M., Gimenez, M. and Schlamp, M. (2003). "Intercomparison of atmospheric dispersion models." Atmospheric Environment **37**(18): 2435–2449.

Carruthers, D. J., Holroyd, R. J., Hunt, J. C. R., et al. (1994). "UK-ADMS: A new approach to modelling dispersion in the earth's atmospheric boundary layer." Journal of Wind Engineering and Industrial Aerodynamics **52**: 139-153.

CBF (2010). Ranking da Confederação Brasileira de Futebol.

CFD-Online. (2008). "CFD Online." from http://www.cfd-online.com/

CFX (2008). ANSYS CFX. Canonsburg, USA, ANSYS, Inc**:** http://www.ansys.com/products/cfx.asp

Chan, A. T., Au, W. T. W. and So, E. S. P. (2003). "Strategic guidelines for street canyon geometry to achieve sustainable street air quality--part II: multiple canopies and canyons." Atmospheric Environment **37**(20): 2761-2772.

Chan, A. T., So, E. S. P. and Samad, S. C. (2001). "Strategic guidelines for street canyon geometry to achieve sustainable street air quality." Atmospheric Environment **35**(32): 5681-5691.

Chan, S. and Stevens, D. (2004). An Evaluation of Two Advanced Turbulence Models for Simulating the Flow and Dispersion Around Buildings. Air Pollution Modeling and Its Application XIV**:** 521-530.

Chan, T. L., Dong, G., Leung, C. W., et al. (2002). "Validation of a two-dimensional pollutant dispersion model in an isolated street canyon." Atmospheric Environment **36**(5): 861-872.

Chen, H. and Bell, M. (2002). "Instrumented city database analysts using multi-agents." Transportation Research Part C: Emerging Technologies **10**(5–6): 419-432.

Cimorelli, A. J., Perry, S. G., Venkatram, A., et al. (1998). AERMOD - Description of Model Formulation (Version 98314 (AERMOD and AERMET) and 98022 (AERMAP). USEPA, RTP, NC 27711**:** 113 pages.

Ciofalo, M. and Collins, M. W. (1989). "κ-ε Predictions of Heat Transfer in Turbulent Recirculating Flows Using an Improved Wall Treatment." Numerical Heat Transfer, Part B: Fundamentals **15**(1): 21 - 47.

CityCAD (2005). CityCAD. London, UK, Holistic City Limited: http://www.holisticcity.co.uk/

CityEngine (2008). Esri CityEngine. Redlands, CA, USA, Environmental Systems Research Institute: http://www.esri.com/software/cityengine/

CityZoom (2008). CityZoom. Porto Alegre, Brazil, SimmLab**:** http://www.cityzoom.net

Claro, A., Pereira, F. O. R. and Ledo, R. Z. (2005). APOLUX - An Innovative Computer Code for Daylight Design and Analysis in Architecture and Urbanism. IBPSA - International Building Performance Simulation Association. Montréal, Canada**:** 199-206.

Clawson, K. L., Carter, R. G., Lacroix, D. J., Biltoft, C. A., Hukari, N. F., Johnson, R. C., Rich, J. D., Beard, S. A. and Strong, T. (2005). "Joint Urban 2003 (JU03) SF6 Atmospheric Tracer Field Tests." NOAA Technical Memorandum OAR ARL-254, Air Resources Laboratory, Idaho Falls, Idaho, 237 pp. http://www.noaa.inel.gov/projects/ju03/docs/Final_JU03.pdf

Coelho, M. C., Farias, T. L. and Rouphail, N. M. (2005). "A methodology for modelling and measuring traffic and emission performance of speed control traffic signals." Atmospheric Environment **39**(13): 2367-2376.

Cooper, C. D. and Alley, F. C. (1990). Air Pollution Control: A Design Approach.

Cruz, M. A. S., Tucci, C. E. M. and Turkienicz, B. (2001). "Análise da influência dos instrumentos reguladores de ocupação no escoamento urbano." Avaliação e Controle da Drenagem Urbana. Porto Alegre: Editora Universidade – UFRGS, v. 2. p. 487-498.

CyberCity (2009). CyberCity 3D. El Segundo, CA, USA, CyberCity 3D Inc: http://www.cybercity3d.com/

DePaul, F. T. and Sheih, C. M. (1986). "Measurements of wind velocities in a street canyon." Atmospheric Environment (1967) **20**(3): 455-459.

Dobre, A, Arnold, SJ, Smalley, RJ, Boddy, JWD, Barlow, JF, Tomlin, AS and Belcher, SE. (2005). Flow field measurements in the proximity of an urban intersection in London, UK. *Atmospheric Environment*, **39,** 4647–4657.

Efthimiou, G. C., Bartzis, J. G. and Koutsourakis, N. (2011). "Modelling concentration fluctuations and individual exposure in complex urban environments." Journal of Wind Engineering and Industrial Aerodynamics(Article in Press).

Ely, V. H. M. B., Angelo, C., Ludvig, C., Bueno, A. and Trezub, D. (1999). "Sintaxe Espacial e o Sistema de Transporte Integrado na Ilha de Santa Catarina." Anais do Congreso de Sociedad Iberoamericana de Grafica Digital- SIGRAD, v. 01. p. 434-437.

EPA (1995). User's Guide for the Industrial Source Complex (ISC3) Dispersion Model (Revised). Volume II - Description of Model Algorithms. EPA-454/b-95-0036. U.S. Environmental Protection Agency, Research Triangle Park, NC**:** http://www.epa.gov/scram001/dispersion_alt.htm

EPA (2004). User's Guide for the AMS/EPA Regulatory Model - AERMOD. EPA-454/B-03-001. U.S. Environmental Protection Agency, Research Triangle Park, NC**:** http://www.epa.gov/scram001/dispersion_prefrec.htm

ESRI (2008). Environmental Systems Research Institute. Redlands, CA, USA**:** http://www.esri.com/

Fenger, J., Hertel, O. and Palmgren, F. (1998). Urban Air Pollution - European Aspects, Kluwer Academic Publishers.

Ferzigeer, J. H. and Peric, M. (1995). Computational Methods for Fluid Dynamics, Springer.

FLUENT (2008). ANSYS FLUENT. Canonsburg, USA, ANSYS, Inc**:** http://www.fluent.com/software/fluent/index.htm

Franke, J., Hellsten, A., Schlünzen, H., et al. (2007). Best Practice Guideline for the CFD simulation of flows in the urban environment. Brussels, COST Office**:** ISBN 3-00-018312-4.

Frey, H., Rouphail, N., Unal, A., et al. (2001). Emission reduction through better traffic management: an empirical evaluation based upon on-road measurements. N. C. D. o. Transportation. Report No. FHWA/NC/2002-001, USA, http://www.ncdot.org/planning/development/research/1999-08.html

GAMBIT (2007). GAMBIT. Canonsburg, USA, ANSYS, Inc.**:** http://www.fluent.com/software/gambit/index.htm

Gokhale, S. B., Rebours, A. and Pavageau, M. (2005). "The performance evaluation of WinOSPM model for urban street canyons of Nantes in France." Environmental Monitoring and Assessment **100**(1): 153-176.

Grazziotin, P., Morvan, H., Hargreaves, D., Cybis, H. B., Ariotti, P., Turkienicz, B. (2010). "Validation and sensitivity testing of CityZoom-AERMOD model." Fifth International Symposium on Computational Wind Engineering (CWE2010), 2010, Chapel Hill. Anais CWE2010, 2010.

Grazziotin, P. C., Pereira, F. O. R., Freitas, C. M. D. S., et al. (2002). Integration of Sunlight Access Control to Building Potential Simulator. SIGraDi - Simpósio Íbero-Americano de Gráfica Digital. Guimarães, Portugal.

Grazziotin, P. C. and Turkienicz, B. (1999). “Block.I.Magic - Ferramenta Computacional Para Simulação de Planos Diretores.” XI Salão de Iniciação Científica. Porto Alegre, Brazil.

Grazziotin, P. C., Turkienicz, B., Sclovsky, L., et al. (2004). Cityzoom - A tool for the visualization of the impact of urban regulations. SIGraDi - Simpósio Íbero-Americano de Gráfica Digital. São Leopoldo, Brazil**:** 216-220.

Gromke, C., Buccolieri, R., Di Sabatino, S., et al. (2008). "Dispersion study in a street canyon with tree planting by means of wind tunnel and numerical investigations - Evaluation of CFD data with experimental data." Atmospheric Environment **42**(37): 8640-8650.

Hanna, S. R. E., B. A. Purdum, J. Wagler, J. (2001). "Evaluation of the ADMS, AERMOD, and ISC3 dispersion models with the OPTEX, Duke Forest, Kincaid, Indianapolis and Lovett field datasets." INTERNATIONAL JOURNAL OF ENVIRONMENT AND POLLUTION **16**: 301-314.

Hanna, S. R., Paine, R., Heinold, D., Kintigh, E. and Baker, D. (2007). "Uncertainties in air toxics calculated by the dispersion models AERMOD and ISCST 3 in the Houston ship channel area." Journal of Applied Meteorology and Climatology **46**: 1372–1382.

Hargreaves, D. (1995). Analytical and Experimental Studies of Vehicle Emissions. Nottingham, UK, University of Nottingham.

Hargreaves, D. M. and Baker, C. J. (1997). "Gaussian puff model of an urban street canyon." Journal of Wind Engineering and Industrial Aerodynamics **69-71**: 927-939.

Hargreaves, D. M. and Wright, N. G. (2007). "On the use of the k-ε model in commercial CFD software to model the neutral atmospheric boundary layer." Journal of Wind Engineering and Industrial Aerodynamics **95**(5): 355-369.

Harsham, D. K. and Bennett, M. (2008). "A sensitivity study of the validation of three regulatory dispersion models." American Journal of Environmental Sciences **4**(1): 63–76.

Hickman, J., Hassel, D., Joumard, R., et al. (1999). Methodology for calculating transport emissions and energy consumption. - Deliverable 22 for the project MEET. Luxembourg, Office for Official Publications of the European Communities**:** pp. 362 http://www.inrets.fr/infos/cost319/index.html

IDRISI (2007). IDRISI Andes. Worcester, MA, USA, Clark Labs**:** http://www.clarklabs.org/

Jeong, S. J. and Andrews, M. J. (2002). "Application of the k-ε turbulence model to the high Reynolds number skimming flow field of an urban street canyon." Atmospheric Environment **36**(7): 1137-1145.

Jicha, M., Pospisil, J. and Katolicky, J. (2000). "Dispersion of Pollutants in Street Canyon under Traffic Induced Flow and Turbulence." Environmental Monitoring and Assessment **65**(1): 343-351.

Kaur, S., Nieuwenhuijsen, M. J. and Colvile, R. N. (2007). "Fine particulate matter and carbon monoxide exposure concentrations in urban street transport microenvironments." Atmospheric Environment **41**(23): 4781-4810.

Kim, J.-J. and Baik, J.-J. (2001). "Urban street-canyon flows with bottom heating." Atmospheric Environment **35**(20): 3395-3404.

Kim, J.-J. and Baik, J.-J. (2003). "Effects of inflow turbulence intensity on flow and pollutant dispersion in an urban street canyon." Journal of Wind Engineering and Industrial Aerodynamics **91**(3): 309-329.

Kim, J.-J. and Baik, J.-J. (2004). "A numerical study of the effects of ambient wind direction on flow and dispersion in urban street canyons using the RNG k-[var epsilon] turbulence model." Atmospheric Environment **38**(19): 3039-3048.

Kitware, I. (2008). ParaView, Kitware, Inc.**:** http://www.paraview.org/

Kovar-Panskus, A., Louka, P., Sini, J. F., et al. (2002). "Influence of Geometry on the Mean Flow within Urban Street Canyons – A Comparison of Wind Tunnel Experiments and Numerical Simulations." Water, Air, & Soil Pollution: Focus **2**(5): 365-380.

Lakes, E. S. (2008). ISC-AERMOD View - Interface for the AERMOD, ISCST3 and ISC-PRIME Models, Lakes Environmental Software**:** http://www.weblakes.com/ISCAERMOD/ISCAERFeatures.html

Lee, I. Y. and Park, H. M. (1994). "Parameterization of the pollutant transport and dispersion in urban street canyons." Atmospheric Environment **28**(14): 2343-2349.

Letzel, M. O., Krane, M. and Raasch, S. (2008). "High resolution urban large-eddy simulation studies from street canyon to neighbourhood scale." Atmospheric Environment **42**(38): 8770-8784.

Li, X.-X., Liu, C.-H. and Leung, D. Y. C. (2005). "Development of a k-[epsilon] model for the determination of air exchange rates for street canyons." Atmospheric Environment **39**(38): 7285-7296.

Li, X.-X., Liu, C.-H., Leung, D. Y. C., et al. (2006). "Recent progress in CFD modelling of wind field and pollutant transport in street canyons." Atmospheric Environment **40**(29): 5640-5658.

Liu, C.-H. and Barth, M. C. (2002). "Large-Eddy Simulation of Flow and Scalar Transport in a Modeled Street Canyon." Journal of Applied Meteorology **41**(6): 660-673.

Liu, C.-H., Barth, M. C. and Leung, D. Y. C. (2004). "Large-Eddy Simulation of Flow and Pollutant Transport in Street Canyons of Different Building-Height-to-Street-Width Ratios." Journal of Applied Meteorology **43**(10): 1410-1424.

Liu, C.-H., Leung, D. Y. C. and Barth, M. C. (2005). "On the prediction of air and pollutant exchange rates in street canyons of different aspect ratios using large-eddy simulation." Atmospheric Environment **39**(9): 1567-1574.

LLNL (2008). VisIt, Lawrence Livermore National Laboratory**:** https://wci.llnl.gov/codes/visit/.

Ludwig, G. R. and Sundaram, T. R. (1969). ON THE LABORATORY SIMULATION OF SMALL-SCALE ATMOSPHERIC TURBULENCE**:** Pages: 63.

MagicDraw (2008). MagicDraw UML. Kaunas, Lithuania, No Magic, Inc.**:** http://www.magicdraw.com/

Martin, K., Schroeder, W. and Lorensen, B. (2008). The Visualization Toolkit, Kitware, Inc.**:** http://www.vtk.org/

McGlashan, L. (2008). Installing OpenFOAM CYGWIN port for use on Windows. Cambridge, UK**:** pp. 4.

Melo, A. M. V., Santos, J. M., Mavroidis, I. and Junior, N. C. R. (2012). "Modelling of odour dispersion around a pig farm building complex using AERMOD and CALPUFF. Comparison with wind tunnel results." Building and Environment **56**: 8-20.

Met Office (2012). UK National Weather Service. Historic Station Data. Exeter, UK: http://www.metoffice.gov.uk/climate/uk/stationdata/

Modelur (2009). Modelur. Slovenia, UBRS d.o.o.: http://www.modelur.com/

Modena, M., Grazziotin, P. C. and Turkienicz, B. (1999). “Impacto de Normativas Urbanísticas.” XI Salão de Iniciação Científica. Porto Alegre, Brazil.

Morvan, H. P. (2005). "Automating CFD for non-experts." Journal of Hydroinformatics **7**: 17-29.

Morvan, H. P., Stangroom, P. and Wright, N. G. (2007). "Automated CFD analysis for multiple directions of wind flow over terrain." WIND AND STRUCTURES **10**: 99-120.

Murena, F., Garofalo, N. and Favale, G. (2008). "Monitoring CO concentration at leeward and windward sides in a deep street canyon." Atmospheric Environment **42**(35): 8204-8210.

Namdeo, A., Mitchell, G. and Dixon, R. (2002). "TEMMS: an integrated package for modelling and mapping urban traffic emissions and air quality." Environmental Modelling & Software **17**(2): 177-188.

Nejadkoorki, F., Nicholson, K., Lake, I., et al. (2008). "An approach for modelling CO2 emissions from road traffic in urban areas." Science of The Total Environment **406**(1-2): 269-278.

Nunez, M. and Oke, T. R. (1977). "The Energy Balance of an Urban Canyon." Journal of Applied Meteorology **16**(1): 11-19.

Oke, T. R. (1987). Boundary Layer Climates. London, UK, Routledge.

Oke, T. R. (1988). "Street design and urban canopy layer climate." Energy and Buildings **11**(1-3): 103-113.

Oliveira Panão, M. J. N., Gonçalves, H. J. P. and Ferrão, P. M. C. (2009). "Numerical analysis of the street canyon thermal conductance to improve urban design and climate." Building and Environment **44**(1): 177-187.

OpenCFD (2007). OpenFOAM - Open Field Operation and Manipulation CFD Toolbox. Reading, UK, OpenCFD Ltd - GNU General Public License**:** http://www.opencfd.co.uk/openfoam/

Orloff, K. G., Kaplan, B. and Kowalski, P. (2006). "Hydrogen cyanide in ambient air near a gold heap leach field: measured vs. modeled concentrations." Atmospheric Environment **40**(17): 3022–3029.

Paine, R. J., Lee, R. F., Brode, R., Wilson, R. B., Cimorelli, A. J., Perry, S. G., Weil, J. C., Venkatram, A., and Peters, W. (1998). "Model evaluation results for AERMOD". http://www.epa.gov/scram001/7thconf/aermod/evalrep.pdf

Pasquill, F. (1961). "The estimation of the dispersion of windborne material." The Meteorological Magazine **90**(1063): 33-49.

Pereira, F. O. R., Silva, C. A. N. and Turkienikz, B. (2001). "A methodology for sunlight urban planning: a computer-based solar and sky vault obstruction analysis." Solar Energy **70**(3): 217-226.

Perry, S. G., Cimorelli, A. J., Paine, R. J., Brode, R. W., Weil, J. C., Venkatram, A., Wilson, R. B., Lee, R. F. and Peters, W. D. (2004). "AERMOD: a dispersion model for industrial source applications. Part II: Model performance against 17 field study databases." Journal of Applied Meteorology **44**(5): 694–708.

PixelActive (2008). PixelActive World Editor. Carlsbad, CA, USA, PixelActive Inc.: http://pixelactive3d.com/

Pullen, J., Boris, J. P., Young, T., et al. (2005). "A comparison of contaminant plume statistics from a Gaussian puff and urban CFD model for two large cities." Atmospheric Environment **39**(6): 1049-1068.

Rakha, H. and Ahn, K. (2004). "Integration Modeling Framework for Estimating Mobile Source Emissions." Journal of Transportation Engineering **130**(2): 183-193.

Red Hat, I. (2008). Cygwin, Red Hat, Inc.**:** http://www.cygwin.com/

Richards, P. J. and Hoxey, R. P. (1993). "Appropriate boundary conditions for computational wind engineering models using the k-[epsilon] turbulence model." Journal of Wind Engineering and Industrial Aerodynamics **46-47**: 145-153.

Robins, A. G. (2011). "Executive summary – the HO-DAPPLE and SIRANE projects." Final Report to Home Office, DAPPLE 2009/13, University of Surrey, 2011.

Santiago, J. L. and Martín, F. (2005). "Modelling the air flow in symmetric and asymmetric street canyons." International Journal of Environment and Pollution **25**(1/2/3/4): 145-154.

Scheidegger, C., Castro, B., Grazziotin, P. C., Turkienicz, B. and Sclovsky, L. (2002) "Cityzoom - Ambiente Integrado de Suporte a Decisão em Planejamento Urbano." X Feira de Iniciação Científica. Porto Alegre, Brazil.Scheidegger, C. E., Silva, B. C. and Turkienicz, B. (2001). Mosaic - Uma ferramenta de análise espacial para o ambient CityZoom. SIC - Salão de Iniciação Científica. Porto Alegre, Brazil.

Schulman, L. L., Strimaitis, D. G. and Scire, J. S. (2000). "Development and Evaluation of the PRIME Plume Rise and Building Downwash Model." Journal of the Air & Waste Management Association **50**(3): 13.

SCRAM (2008). Support Center for Regulatory Atmospheric Modeling, EPA's Air Quality Modeling Group**:** http://www.epa.gov/scram001/

Seangkiatiyuth, K., Surapipith, V., Tantrakarnapa, K. and Lothongkum, A. W. (2011). "Application of the AERMOD modeling system for environmental impact assessment of NO2 emissions from a cement complex." Journal of Environmental Sciences **23**(6): 931-940.Shallcross, DE, Martin, D, Price, CS, Nickless, G, White, IR, Petersson, F, Britter, RE, Neophytou, MK, Tate, JE, Tomlin, AS, Belcher, SE, Barlow, JF and Robins, A, (2009). "Short-range urban dispersion experiments using fixed and moving sources." Atmos. Sci. Let. 10: 59 – 65.

Shallcross, DE, Petersson, KF, White, IR, Martin, D and Robins, AG, (2010). "The 2007 tracer dispersion experiments at the DAPPLE field site." Final Report to Home Office, DAPPLE 2009/02, University of Surrey, 2010.

Silverman, K. C., Tell, J. G., Sargent, E. V. and Qiu, Z. (2007). "Comparison of the industrial source complex and AERMOD dispersion models: case study for human health risk assessment." Journal of the Air & Waste Management Association **57**(12): 1439–1446.

SimmLab (2012). Laboratório para Simulação e Modelagem em Arquitetura e Urbanismo - Universidade Federal do Rio Grande do Sul. Porto Alegre, Brazil: http://www.simmlab.ufrgs.br/

Sini, J.-F., Anquetin, S. and Mestayer, P. G. (1996). "Pollutant dispersion and thermal effects in urban street canyons." Atmospheric Environment **30**(15): 2659-2677.

Smagorinsky, J. (1963). "General Circulation Experiments with the Primitive Equations. I. The Basic Experiment." Mon. Weather Rev. **91**: 99–164.

So, E. S. P., Chan, A. T. Y. and Wong, A. Y. T. (2005). "Large-eddy simulations of wind flow and pollutant dispersion in a street canyon." Atmospheric Environment **39**(20): 3573-3582.

Solazzo, E., Cai, X. and Vardoulakis, S. (2008). "Modelling wind flow and vehicle-induced turbulence in urban streets." Atmospheric Environment **42**(20): 4918-4931.

Solazzo, E., Cai, X. and Vardoulakis, S. (2009). "Improved parameterisation for the numerical modelling of air pollution within an urban street canyon." Environmental Modelling & Software **24**: 381-388.

Solazzo, E., Vardoulakis, S. and Cai, X. (2007). "Evaluation of traffic-producing turbulence schemes within Operational Street Pollution Models using roadside measurements." Atmospheric Environment **41**(26): 5357-5370.

Solazzo, E., Vardoulakis, S. and Cai, X. (2011). "A novel methodology for interpreting air quality measurements from urban streets using CFD modelling." Atmospheric Environment **45**(29): 5230-5239.

Soulhac, L., Méjean, P. and Perkins, R. J. (2001). "Modelling the transport and dispersion of pollutants in street canyons." International Journal of Environment and Pollution **16**(1-6): 404 - 413.

Soulhac, L., Puel, C., Duclaux, O., et al. (2003). "Simulations of atmospheric pollution in Greater Lyon an example of the use of nested models." Atmospheric Environment **37**(37): 5147-5156.

Stein, A. F., Isakov, V., Godowitch, J. and Draxler, R. R. (2007). "A hybrid modeling approach to resolve pollutant concentrations in an urban area." Atmospheric Environment **41**(40): 9410–9426.

Taseiko, O. V. (2009). "Air pollution dispersion within urban street canyons." Atmospheric Environment **In Press, Accepted Manuscript**.

Tate, J. E. (2005). "A novel research tool - presenting the highly instrumented car." *Traffic Engineering and Control*, **46**, 7, 262-265.

Tate, J. (2010). "The 2008 line-source tracer release experiments in central London". Dispersion Experiments in London, *Final Report to the Home Office*, DAPPLE 2009/03, University of Surrey, 2010.

Tennekes, H. and Lumley, J. L. (1972). A First Course in Turbulence. Cambridge, MA, MIT Press.

Trinity, C. I. (2008). BREEZE AERMOD GIS Pro 6 - BREEZE AERMOD Air Quality Model Version 6, Trinity Consultants, Inc.**:** http://www.breeze-software.com/prod/AERMOD-ISC/Feature/index.html

Tsai, M. Y. and Chen, K. S. (2004). "Measurements and three-dimensional modeling of air pollutant dispersion in an Urban Street Canyon." Atmospheric Environment **38**(35): 5911-5924.

Turkienicz, B. (1994). Indicações Estratégicas para o Adensamento Urbano de Porto Alegre. Porto Alegre, Brazil.

Turkienicz, B., Gonçalves, B. B. and Grazziotin, P. C. (2007). CityZoom. eCAADe - Education and Research in Computer Aided Architectural Design in Europe. Frankfurt, Germany**:** 375-382.

Turkienicz, B., Gonçalves, B. B. and Grazziotin, P. C. (2008). "CityZoom: A Visualization Tool for the Assessment of Planning Regulations." International Journal of Architectural Computing **6**(1): 79-95.

Turkienicz, B., Grazziotin, P. C., Sclovsky, L. (1998). "CityZoom." I Conferência Latino-americana de Informática no Ensino de Arquitetura e IV Seminário Nacional de Informática no Ensino de Arquitetura. Florianópolis, Brazil.

Turkienicz, B., Sclovsky, L., Mittmann, M., et al. (1999). Simulation of building regulations in a computational environment. CUPUM - Computers in Urban Planning and Urban Management. Venice, Italy.

Turner, D. B. (1970). Workbook of Atmopsheric Dispersion Estimates (revised edition). Washington, D. C., U. S. Govt. Printing Office.

UrbanPAD (2009). Ürban PAD. Lyon, France, Gamr7: http://www.gamr7.com/

USEPA (1986). Guideline on air quality models (Revised). Research Triangle Park, N.C., U.S. Environmental Protection Agency, Office of Air and Radiation, Office of Air Quality Planning and Standards.

Vardoulakis, S., Fisher, B. E. A., Pericleous, K., et al. (2003). "Modelling air quality in street canyons: a review." Atmospheric Environment **37**(2): 155-182.

Vardoulakis, S., Valiantis, M., Milner, J., et al. (2007). "Operational air pollution modelling in the UK--Street canyon applications and challenges." Atmospheric Environment **41**(22): 4622-4637.

Venkatram, A. (1980). "Estimating the Monin-Obukhov length in the stable boundary layer for dispersion calculations." Boundary-Layer Meteorology **19**(4): 481-485.

Venkatram, A., Isakov, V., Yuan, J. and Pankratz, D. (2004). "Modeling dispersion at distances of meters from urban sources." Atmospheric Environment **38**(28): 4633–4641.

Versteeg, H. K. and Malalasekera, W. (1995). An Introduction to Computational Fluid Dynamics - The Finite Volume Method. New York, US, Pearson Education Limited.

WeatherOnline (2012). "Archive of weather observations." WeatherOnline Ltd. - Meteorological Services: http://www.weatheronline.co.uk/

Wood, CR, Arnold, SJ, Balogun, AA, Barlow, JF, Belcher, SE, Britter, RE, Cheng, H, Dobre, A, Lingard, JJN, Martin, D, Neophytou, MK, Petersson, FK, Robins, AG, Shallcross, DE, Smalley, RJ, Tate, JE, Tomlin, AS and White, IR, (2009). "Dispersion Experiments in Central London: The 2007 DAPPLE project." Bull. Amer. Meteor. Soc., 90, 955-969.

Xia, J. Y., Leung, D. Y. C. and Hussaini, M. Y. (2006). "Numerical simulations of flow-field interactions between moving and stationary objects in idealized street canyon settings." Journal of Fluids and Structures **22**(3): 315-326.

Xie, X., Huang, Z., Wang, J., et al. (2005). "Thermal effects on vehicle emission dispersion in an urban street canyon." Transportation Research Part D: Transport and Environment **10**(3): 197-212.

Xie, X., Liu, C.-H. and Leung, D. Y. C. (2007). "Impact of building facades and ground heating on wind flow and pollutant transport in street canyons." Atmospheric Environment **41**(39): 9030-9049.

Xie Z.-T. and Castro I.P. (2006). "LES and RANS for turbulent flow over arrays of wall-mounted cubes." Flow, Turbulence and Combustion, **76** (3), 291-312.

Xie, Z.-T. and Castro, I.P. (2009). "Large-eddy simulations for flow and dispersion in urban streets." Atmospheric Environment **43**(13), 2174-2185.

Yakhot, V., Orszag, S. A., Thangam, S., et al. (1992). "Development of turbulence models for shear flows by a double expansion technique." Physics of Fluids A: Fluid Dynamics **4**(7): 1510-1520.

Yang, Y., Gu, M., Chen, S., et al. (2009). "New inflow boundary conditions for modelling the neutral equilibrium atmospheric boundary layer in computational wind engineering." Journal of Wind Engineering and Industrial Aerodynamics **97**(2): 88-95

Zhang, Q. Y., Wei, Y. M., Tian, W. L. and Yang, K. M. (2008). "GIS-based emission inventories of urban scale: a case study of Hangzhou, China." Atmospheric Environment **42**(20): 5150-5165.

Zou, B., Zhan, F. B., Wilson, J. G. and Zeng, Y. (2010). "Performance of AERMOD at different time scales." Simulation Modelling Practice and Theory **18**(5): 612–623.

Appendix I – Moving source simulation data

I.1 Co-ordinate systems

Standard co-ordinate system (East, North, ϕ), where ϕ indicates the direction wind is blowing from relative to north, positive clockwise. Site co-ordinate or street-aligned system (x, y, θ), with the x axis along Marylebone Road and the y axis along Gloucester Place, θ indicates the direction wind is blowing to relative to Marylebone Road, positive anticlockwise (Tate 2010).

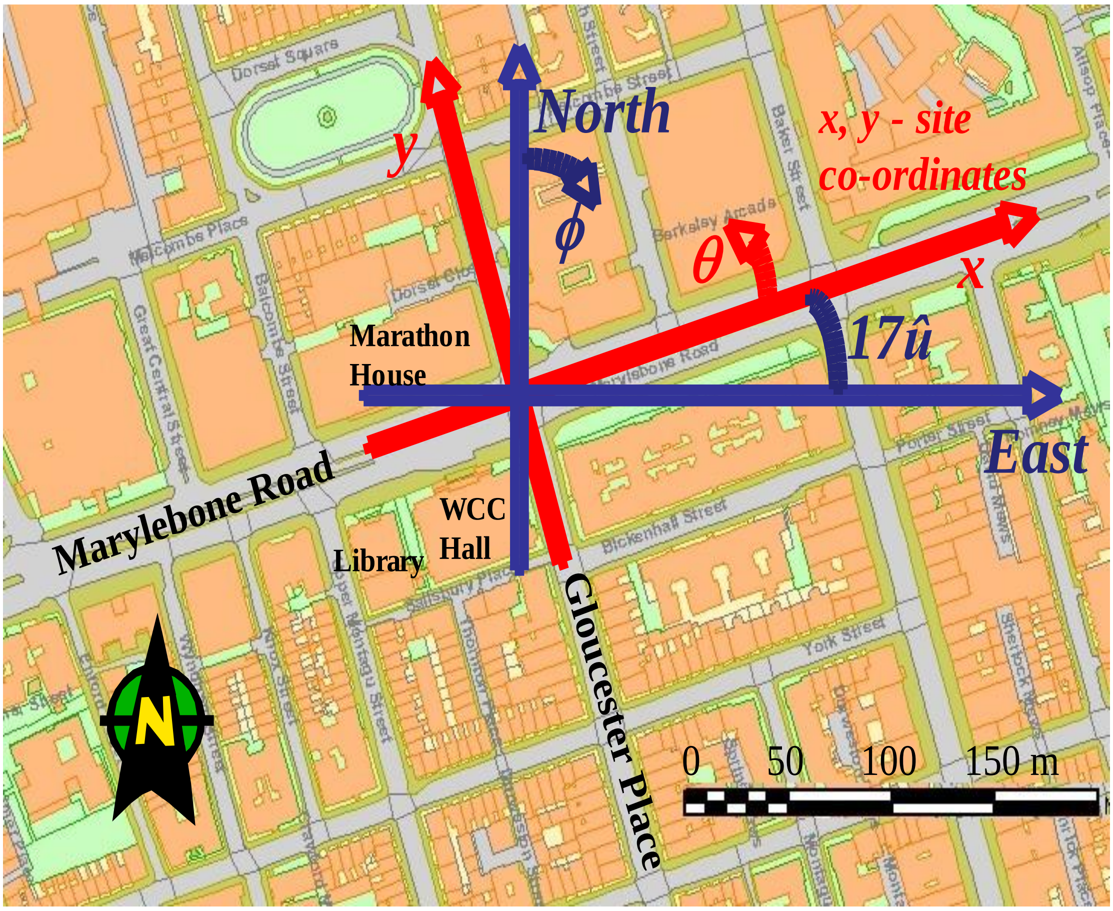

Figure A-1: Definition of the standard co-ordinate system (East, North, ϕ) and the street-aligned system (x, y, θ). (source: Tate 2010)

I.2 Meteorological conditions

Experiment	1	2	3	4	5	6	7	8
Wind Direction θ (degrees)	24	19	23	26	28	32	55	69
Wind Speed (ms^{-1})	2.3	2.7	2.5	2.3	2.3	2.3	2.0	1.7

Table A-1: Roof top wind conditions during the 30 minute experimental periods (Tate 2010).

For whole period:

- sensible heat flux, Q_H = 40 Wm^{-2};
- Monin-Obhukov length scale estimate, L = -380 m;
- boundary layer depth, Z = 580 m;
- relative humidity, RH = 80%; and
- surface temperature, T_0 = 6° C.

I.3 Emissions rates

Experiment	1	2	3	4	5	6	7	8
Release Rate ($10^{-9}kgs^{-1}$)	227	218	213	209	207	205	211	208
Amount Released ($10^{-6}kg$)	25.7	23.3	22.4	33.0	30.2	40.1	25.6	35.3

Table A-2: Emission rate and amount of tracer released for each experiment (Tate 2010).

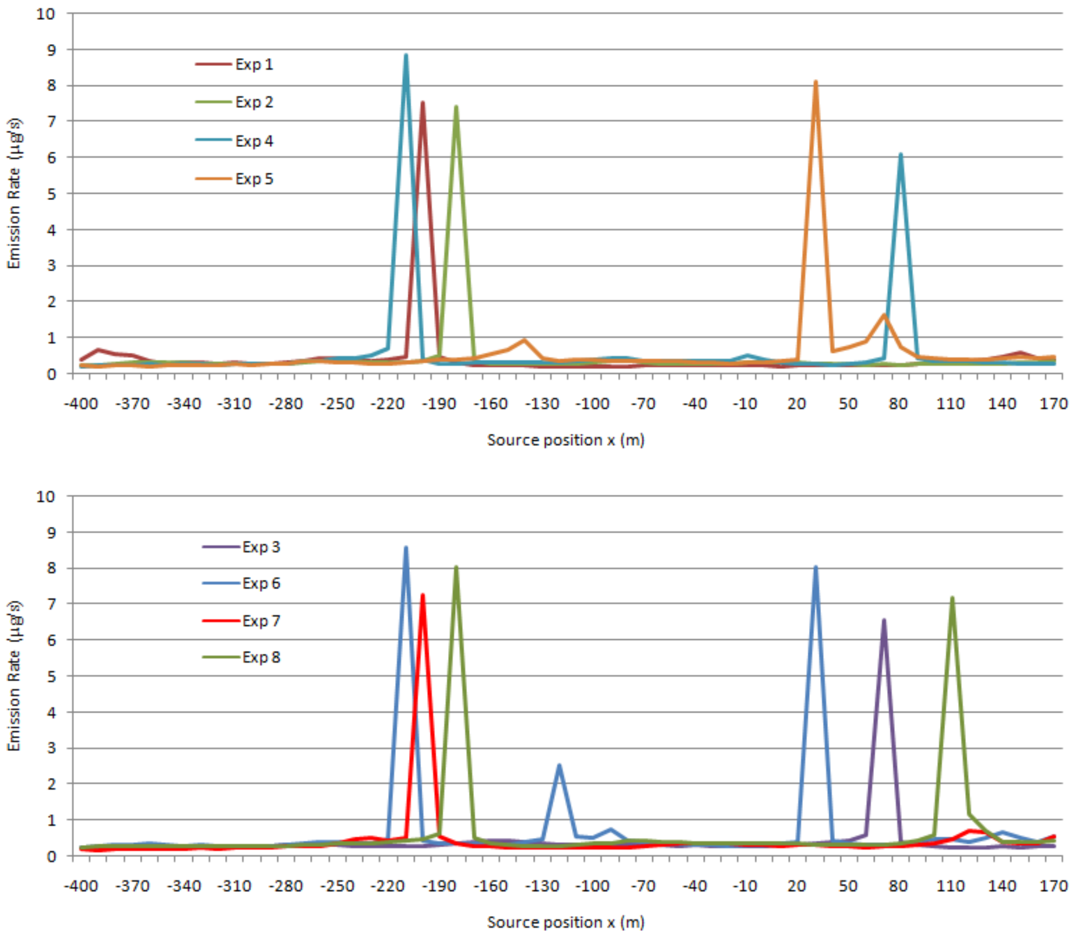

Figure A-2: Emission rates by source position x for experiments 1 to 8. The runs are presented in two separate plots for clarity.

Segment start	Emission Rate per 10 m segment (μgs^{-1})							
(m)	Exp 1	Exp 2	Exp 3	Exp 4	Exp 5	Exp 6	Exp 7	Exp 8
0	0.409	0.349	0.234	0.272	0.455	0.574	0.549	0.416
10	0.454	0.283	0.234	0.272	0.414	0.390	0.380	0.374
20	0.590	0.283	0.213	0.272	0.476	0.513	0.359	0.395
30	0.477	0.262	0.234	0.293	0.414	0.677	0.401	0.395
40	0.386	0.262	0.213	0.314	0.373	0.533	0.654	0.707
50	0.341	0.262	0.213	0.355	0.393	0.410	0.717	1.165
60	0.295	0.240	0.213	0.355	0.393	0.492	0.464	7.197
70	0.318	0.240	0.234	0.334	0.414	0.472	0.359	0.562
80	0.272	0.240	0.277	0.439	0.455	0.410	0.338	0.437
90	0.250	0.218	0.383	6.082	0.725	0.328	0.274	0.333
100	0.250	0.240	6.560	0.418	1.620	0.328	0.274	0.312
110	0.250	0.218	0.554	0.314	0.890	0.308	0.232	0.312
120	0.227	0.240	0.426	0.251	0.745	0.349	0.274	0.291
130	0.227	0.262	0.383	0.230	0.600	0.451	0.295	0.291
140	0.227	0.262	0.341	0.251	8.114	8.057	0.338	0.291
150	0.227	0.283	0.277	0.251	0.373	0.410	0.317	0.333
160	0.204	0.283	0.277	0.293	0.331	0.349	0.295	0.333
170	0.227	0.283	0.256	0.376	0.311	0.308	0.317	0.354
180	0.227	0.283	0.256	0.481	0.290	0.308	0.338	0.333
190	0.227	0.262	0.256	0.355	0.269	0.287	0.380	0.333
200	0.227	0.262	0.256	0.355	0.311	0.308	0.380	0.354
210	0.250	0.262	0.277	0.355	0.311	0.308	0.380	0.354
220	0.227	0.262	0.256	0.355	0.331	0.349	0.359	0.374
230	0.227	0.262	0.277	0.355	0.331	0.369	0.317	0.374
240	0.227	0.305	0.298	0.355	0.352	0.390	0.295	0.416
250	0.204	0.371	0.298	0.439	0.352	0.451	0.253	0.416
260	0.204	0.349	0.277	0.418	0.352	0.759	0.253	0.333
270	0.204	0.283	0.298	0.376	0.373	0.513	0.232	0.333
280	0.204	0.240	0.277	0.334	0.373	0.554	0.253	0.291
290	0.204	0.240	0.298	0.314	0.352	2.522	0.232	0.250
300	0.204	0.240	0.320	0.293	0.414	0.492	0.232	0.250
310	0.227	0.240	0.383	0.314	0.932	0.390	0.253	0.270
320	0.227	0.262	0.426	0.314	0.642	0.308	0.253	0.291
330	0.227	0.262	0.426	0.293	0.518	0.308	0.295	0.333
340	0.250	0.349	0.362	0.293	0.435	0.349	0.295	0.499
350	0.318	7.412	0.320	0.272	0.373	0.369	0.359	8.050
360	0.477	0.501	0.277	0.272	0.373	0.349	0.549	0.624
370	7.514	0.349	0.256	0.376	0.331	0.431	7.258	0.478
380	0.477	0.305	0.234	8.841	0.311	8.590	0.506	0.437
390	0.386	0.305	0.234	0.711	0.269	0.472	0.443	0.395
400	0.363	0.283	0.256	0.502	0.248	0.369	0.506	0.354
410	0.409	0.327	0.256	0.439	0.290	0.349	0.464	0.333
420	0.454	0.371	0.277	0.418	0.290	0.390	0.359	0.333
430	0.454	0.349	0.277	0.334	0.331	0.390	0.295	0.312
440	0.363	0.305	0.277	0.334	0.331	0.349	0.295	0.291
450	0.318	0.262	0.277	0.272	0.269	0.328	0.274	0.270
460	0.295	0.262	0.234	0.272	0.248	0.287	0.253	0.270
470	0.295	0.262	0.256	0.251	0.228	0.267	0.232	0.250
480	0.318	0.262	0.234	0.251	0.248	0.287	0.253	0.270
490	0.295	0.262	0.213	0.230	0.228	0.287	0.211	0.250
500	0.318	0.262	0.213	0.251	0.228	0.308	0.232	0.270
510	0.318	0.305	0.234	0.272	0.207	0.287	0.211	0.270
520	0.295	0.305	0.213	0.230	0.207	0.328	0.211	0.250
530	0.341	0.305	0.213	0.251	0.186	0.369	0.211	0.270
540	0.522	0.283	0.234	0.209	0.207	0.308	0.190	0.250
550	0.568	0.262	0.213	0.209	0.207	0.308	0.190	0.250
560	0.658	0.218	0.213	0.230	0.186	0.287	0.169	0.250
570	0.409	0.218	0.213	0.188	0.207	0.246	0.190	0.229

Table A-3: Emission rate per 10 m segment from the experiment starting position (Tate 2010).

I.4 Dosages and Concentrations

Site		Exp 1		Exp 2		Exp 3		Exp 4	
		DAPPLE	AERMOD	DAPPLE	AERMOD	DAPPLE	AERMOD	DAPPLE	AERMOD
2	Result	-0.16	1.82	-0.24	2.16	-0.14	1.94	-0.10	2.12
	Trend	small	small	small	small	small	small	small	small
	Distance	medium		medium		medium		medium	
	Position	upwind/crosswind		upwind/crosswind		upwind/crosswind		upwind/crosswind	
3	Result	-0.05	1.24	0.00	0.90	-0.21	3.15	-0.01	2.32
	Trend	small	small	small	small	small	small	small	small
	Distance	medium		medium		medium		medium	
	Position	upwind/crosswind		upwind/crosswind		upwind/crosswind		upwind/crosswind	
5	Result	-0.14	8.66	-0.20	7.39	-0.20	30.20	-0.02	21.30
	Trend	small	small	small	small	small	medium	small	medium
	Distance	near		near		near		near	
	Position	upwind/crosswind		upwind/crosswind		upwind/crosswind		upwind/crosswind	
6	Result	9.34	20.43	18.40	47.28	126.00	15.77	14.80	11.79
	Trend	medium	medium	high	high	high	medium	high	medium
	Distance	very near		very near		very near		very near	
	Position	downwind		downwind		downwind		downwind	
9	Result	2.29	31.45	18.50	32.97	8.00	31.21	8.83	27.85
	Trend	small	medium	high	medium	medium	medium	medium	medium
	Distance	very near		very near		very near		very near	
	Position	downwind		downwind		downwind		downwind	
10	Result	0.19	5.87	13.10	8.90	34.70	17.39	15.60	10.38
	Trend	small	small	high	small	high	medium	high	medium
	Distance	average		average		average		average	
	Position	downwind		downwind		downwind		downwind	
11	Result	5.89	47.03	10.80	56.04	5.34	32.52	13.90	44.57
	Trend	medium	high	medium	high	medium	medium	high	high
	Distance	medium		medium		medium		medium	
	Position	downwind		downwind		downwind		downwind	

Table A-4: Normalised mean experimental dosages, *D/M*, normalised simulated concentrations, C/Q_t, ($10^{-6}sm^{-3}$), trend, average distance between receptor site and sources, and position of receptor site for mobile source experiments 1 to 4 at receptor sites 2 to 11. (f = failed sample).

Site		Exp 1		Exp 2		Exp 3		Exp 4	
		DAPPLE	AERMOD	DAPPLE	AERMOD	DAPPLE	AERMOD	DAPPLE	AERMOD
12	Result	9.24	55.83	6.65	58.73	6.81	26.73	5.46	46.54
	Trend	medium	high	medium	high	medium	medium	medium	high
	Distance	medium		medium		medium		medium	
	Position	downwind		downwind		downwind		downwind	
13	Result	2.45	33.39	6.63	49.42	2.56	61.90	4.15	49.21
	Trend	small	medium	medium	high	small	high	medium	high
	Distance	medium		medium		medium		medium	
	Position	downwind		downwind		downwind		downwind	
14	Result	f	15.77	2.61	3.98	2.00	6.46	2.99	17.01
	Trend	f	medium	small	small	small	small	small	medium
	Distance	far		far		far		far	
	Position	straight downwind		downwind		downwind		straight downwind	
15	Result	3.52	0.00	1.72	-0.51	1.23	-0.16	2.25	0.04
	Trend	medium	small	small	small	small	small	small	small
	Distance	far		far		far		far	
	Position	downwind		downwind		downwind		downwind	
17	Result	87.90	171.32	64.00	136.07	223.00	165.43	741.00	148.43
	Trend	high	high	high	high	high	high	high	high
	Distance	very near		very near		very near		very near	
	Position	upwind/crosswind		upwind/crosswind		upwind/crosswind		upwind/crosswind	
20	Result	f	4.04	0.67	2.62	0.58	1.76	3.11	2.77
	Trend	f	small	small	small	small	small	small	small
	Distance	medium		medium		medium		medium	
	Position	upwind/crosswind		upwind/crosswind		upwind/crosswind		upwind/crosswind	
21	Result	1.74	-0.15	1.90	-0.12	2.13	-0.13	1.35	-0.18
	Trend	small	small	small	small	small	small	small	small
	Distance	far		far		far		far	
	Position	downwind		downwind		downwind		downwind	

Table A-5: Normalised mean experimental dosages, *D/M*, normalised simulated concentrations, C/Q_t, ($10^{-6}sm^{-3}$), trend, average distance between receptor site and sources, and position of receptor site for mobile source experiments 1 to 4 at receptor sites 12 to 21. (f = failed sample).

Site		Exp 5		Exp 6		Exp 7		Exp 8	
		DAPPLE	AERMOD	DAPPLE	AERMOD	DAPPLE	AERMOD	DAPPLE	AERMOD
2	Result	-0.09	1.89	-0.15	2.01	-0.11	1.21	-0.17	1.50
	Trend	small	small	small	small	small	small	small	small
	Distance	medium		medium		medium		medium	
	Position	upwind/crosswind		upwind/crosswind		upwind		upwind	
3	Result	-0.02	2.74	-0.07	1.57	f	0.51	0.06	2.54
	Trend	small	small	small	small	f	small	small	small
	Distance	medium		medium		medium		medium	
	Position	upwind/crosswind		upwind/crosswind		upwind		upwind	
5	Result	-0.14	19.75	-0.15	10.97	-0.18	11.38	-0.11	23.69
	Trend	small	medium	small	medium	small	medium	small	medium
	Distance	near		near		near		near	
	Position	upwind/crosswind		upwind/crosswind		upwind		upwind	
6	Result	9.96	12.53	21.00	11.08	31.20	98.79	6.79	68.93
	Trend	medium	medium	high	medium	high	high	medium	high
	Distance	very near		very near		very near		very near	
	Position	downwind		downwind		downwind		downwind	
9	Result	4.81	67.69	5.88	48.02	3.45	45.06	4.37	179.32
	Trend	medium	high	medium	high	medium	high	medium	high
	Distance	very near		very near		very near		very near	
	Position	downwind		downwind		downwind		downwind	
10	Result	16.40	9.75	f	3.44	7.16	-0.45	23.80	-0.38
	Trend	high	medium	f	small	medium	small	high	small
	Distance	average		average		average		average	
	Position	downwind		downwind		crosswind		crosswind	
11	Result	5.12	36.85	7.89	48.19	4.60	15.27	2.92	10.14
	Trend	medium	medium	medium	high	medium	medium	small	medium
	Distance	medium		medium		medium		medium	
	Position	downwind		downwind		downwind		downwind	

Table A-6: Normalised mean experimental dosages, *D/M*, normalised simulated concentrations, C/Q_t, ($10^{-6}sm^{-3}$), trend, average distance between receptor site and sources, and position of receptor site for mobile source experiments 5 to 8 at receptor sites 2 to 11. (f = failed sample).

Site		Exp 5		Exp 6		Exp 7		Exp 8	
		DAPPLE	AERMOD	DAPPLE	AERMOD	DAPPLE	AERMOD	DAPPLE	AERMOD
12		5.55	25.46	7.21	40.16	7.62	28.35	3.83	25.89
	Trend	medium	medium	medium	high	medium	medium	medium	medium
	Distance	medium		medium		medium		medium	
	Position	downwind		downwind		downwind		downwind	
13		4.47	71.55	6.28	44.06	3.25	23.15	3.27	6.53
	Trend	medium	high	medium	high	medium	medium	medium	small
	Distance	medium		medium		medium		medium	
	Position	downwind		downwind		downwind		downwind	
14	Result	2.63	7.30	5.35	17.94	3.00	14.51	1.52	9.16
	Trend	small	small	medium	medium	small	medium	small	small
	Distance	far		far		far		far	
	Position	downwind		straight downwind		straight downwind		straight downwind	
15	Result	1.50	-0.23	3.67	4.05	4.71	20.90	2.37	9.39
	Trend	small	small	medium	small	medium	medium	small	medium
	Distance	far		far		far		far	
	Position	downwind		downwind		straight downwind		straight downwind	
17	Result	172.00	170.64	297.00	131.93	201.00	383.65	f	1025.62
	Trend	high	high	high	high	high	high	f	high
	Distance	very near		very near		very near		very near	
	Position	upwind/crosswind		upwind/crosswind		upwind		upwind	
20	Result	0.88	1.10	2.70	2.30	2.32	3.44	6.81	4.73
	Trend	small	small	small	small	small	small	medium	small
	Distance	medium		medium		medium		medium	
	Position	upwind/crosswind		upwind/crosswind		cross/downwind		cross/downwind	
21	Result	0.67	-0.39	1.88	-0.21	7.11	18.81	6.70	22.74
	Trend	small	small	small	small	medium	medium	medium	medium
	Distance	far		far		far		far	
	Position	downwind		downwind		straight downwind		straight downwind	

Table A-7: Normalised mean experimental dosages, *D/M*, normalised simulated concentrations, C/Q_t, ($10^{-6}sm^{-3}$), trend, average distance between receptor site and sources, and position of receptor site for mobile source experiments 5 to 8 at receptor sites 12 to 21. (f = failed sample).

I.5 Pseudocolor Plots

I.5.1 Experiment 1

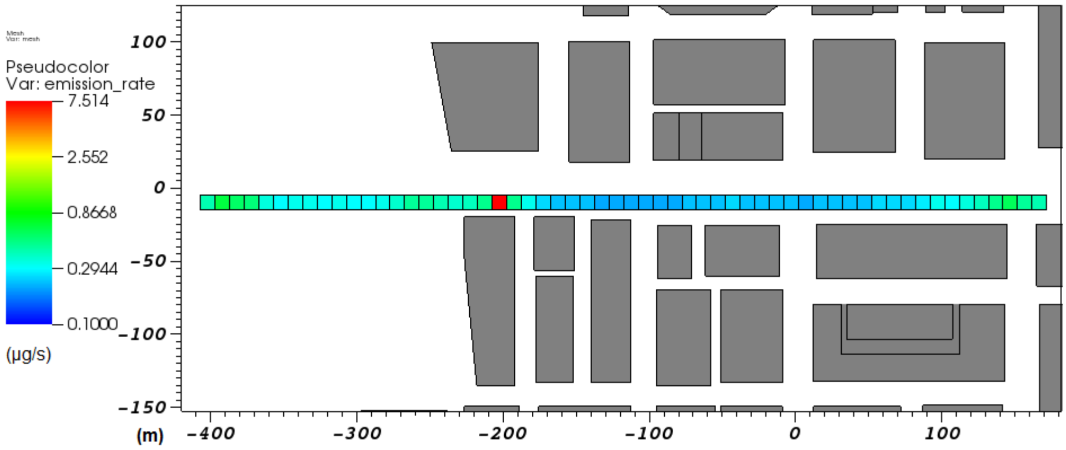

Figure A-3: Pseudocolor plot of emission rates by source position for experiment 1.

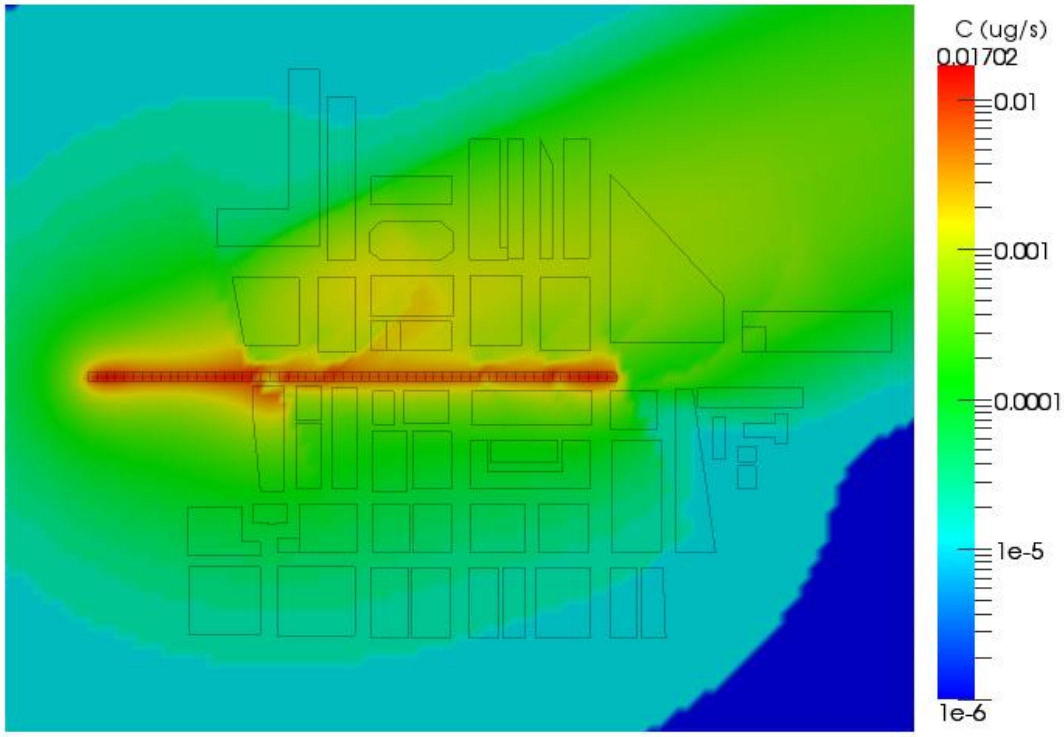

Figure A-4: Pseudocolor plot of the entire domain for experiment 1.

I.5.2 Experiment 2

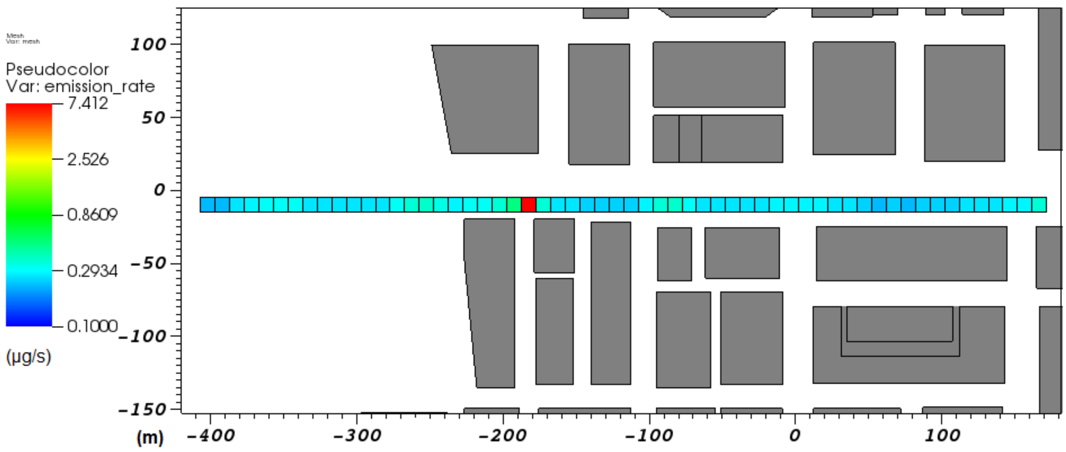

Figure A-5: Pseudocolor plot of emission rates by source position for experiment 2.

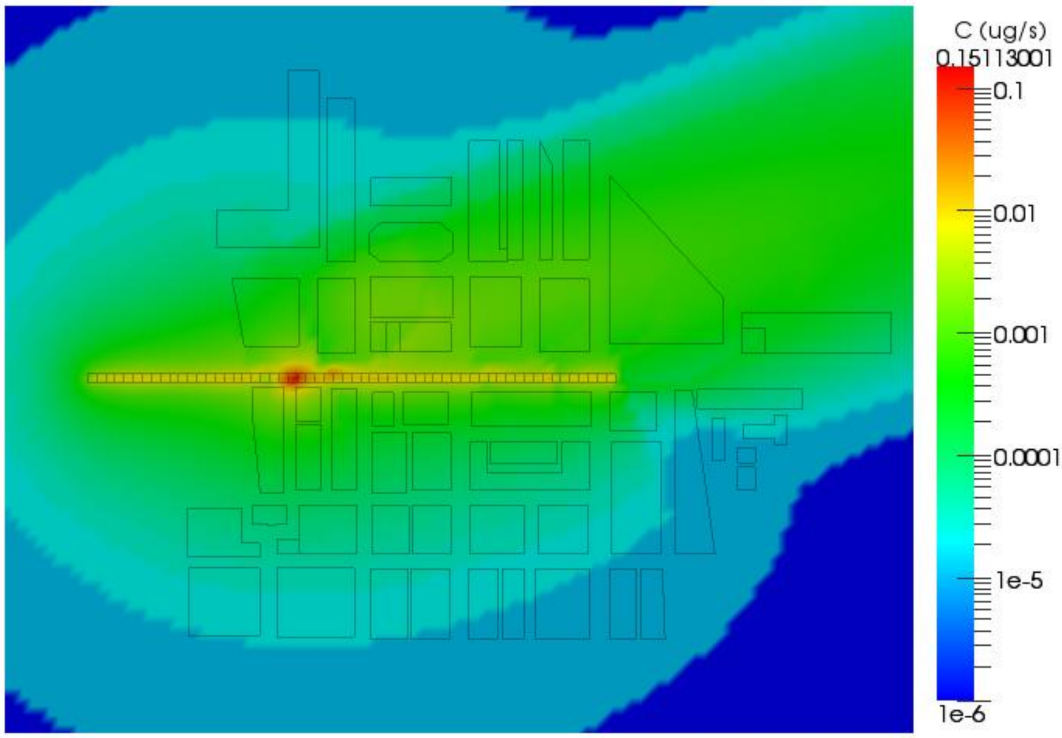

Figure A-6: Pseudocolor plot of the entire domain for experiment 2.

I.5.3 Experiment 3

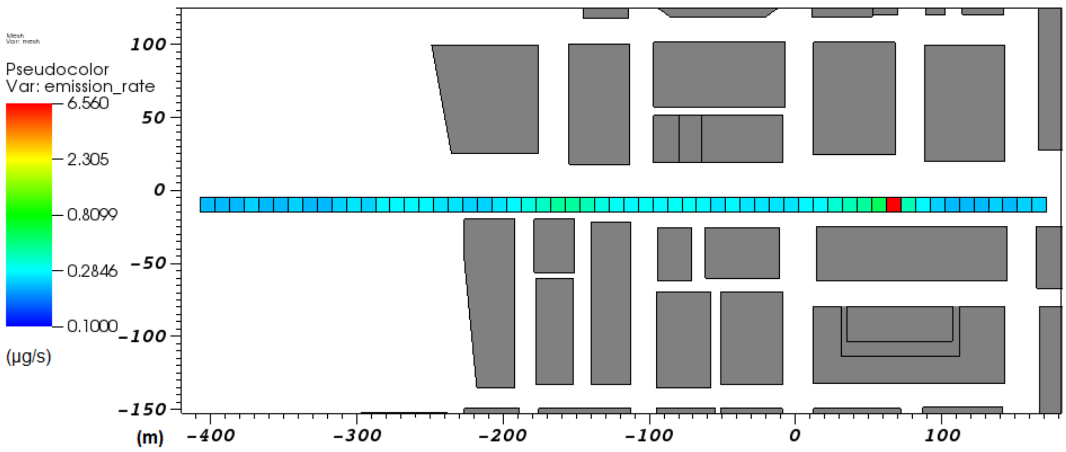

Figure A-7: Pseudocolor plot of emission rates by source position for experiment 3.

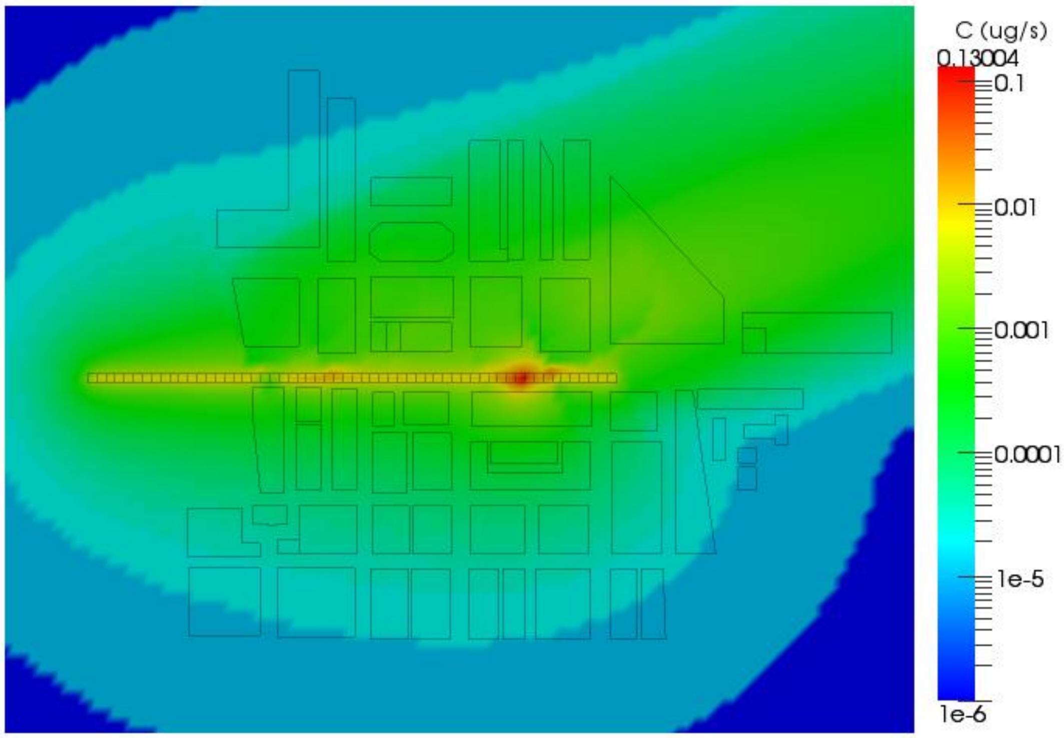

Figure A-8: Pseudocolor plot of the entire domain for experiment 3.

I.5.4 Experiment 4

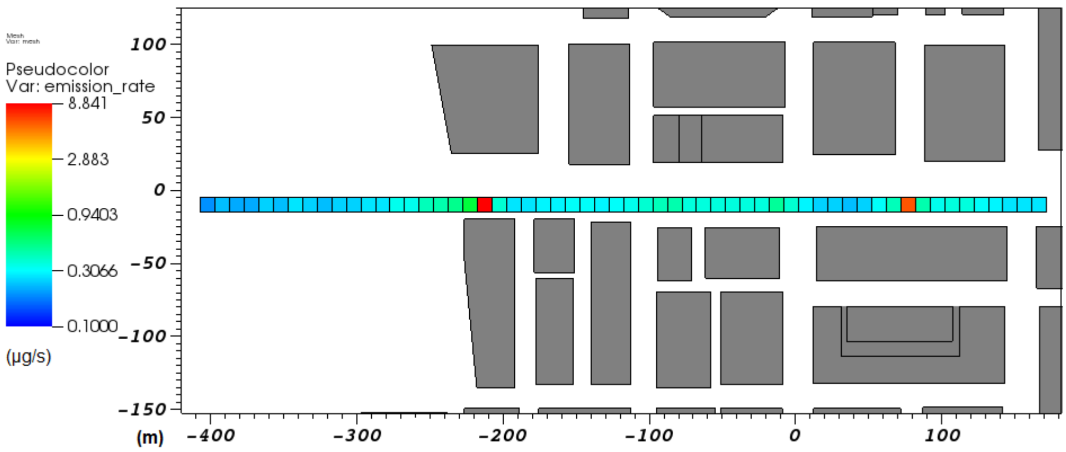

Figure A-9: Pseudocolor plot of emission rates by source position for experiment 4.

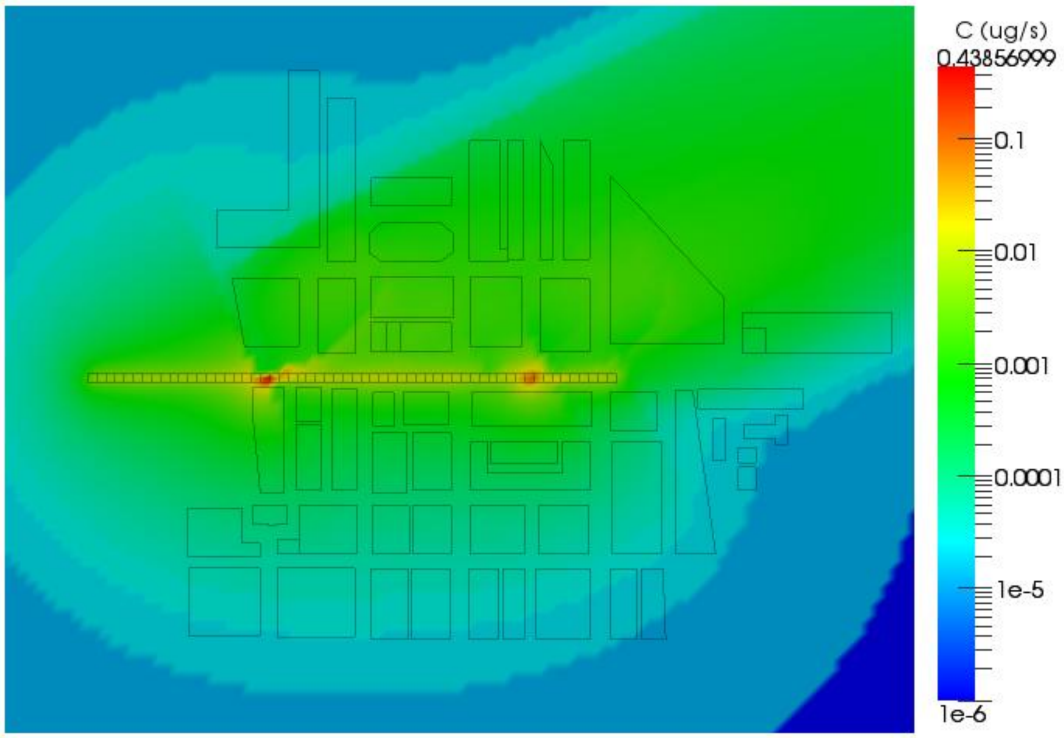

Figure A-10: Pseudocolor plot of the entire domain for experiment 4.

I.5.5 Experiment 5

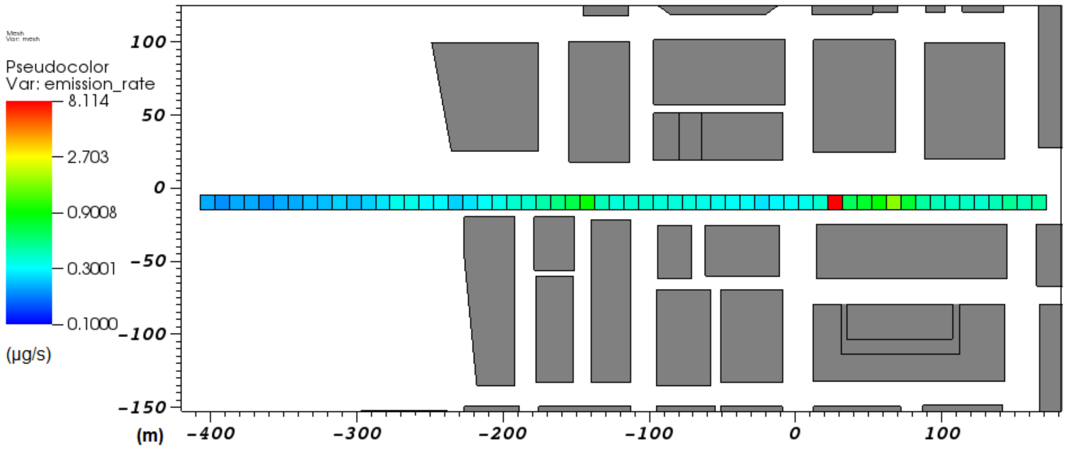

Figure A-11: Pseudocolor plot of emission rates by source position for experiment 5.

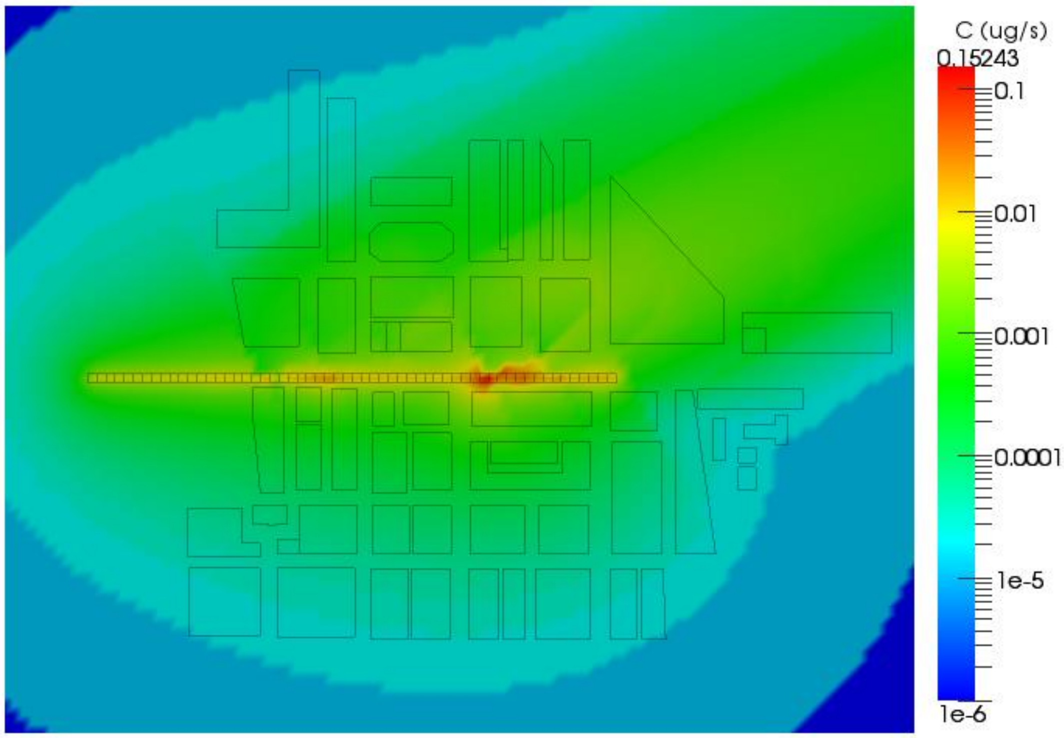

Figure A-12: Pseudocolor plot of the entire domain for experiment 5.

I.5.6 Experiment 6

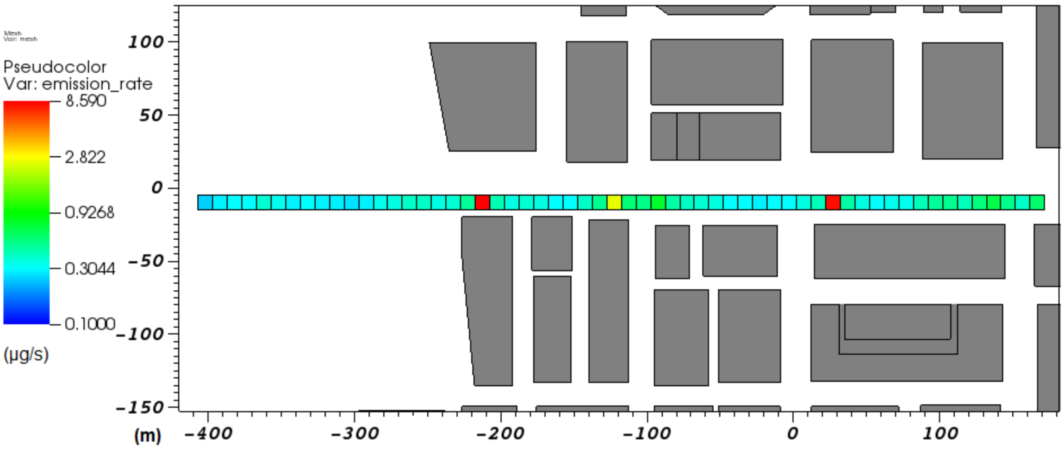

Figure A-13: Pseudocolor plot of emission rates by source position for experiment 6.

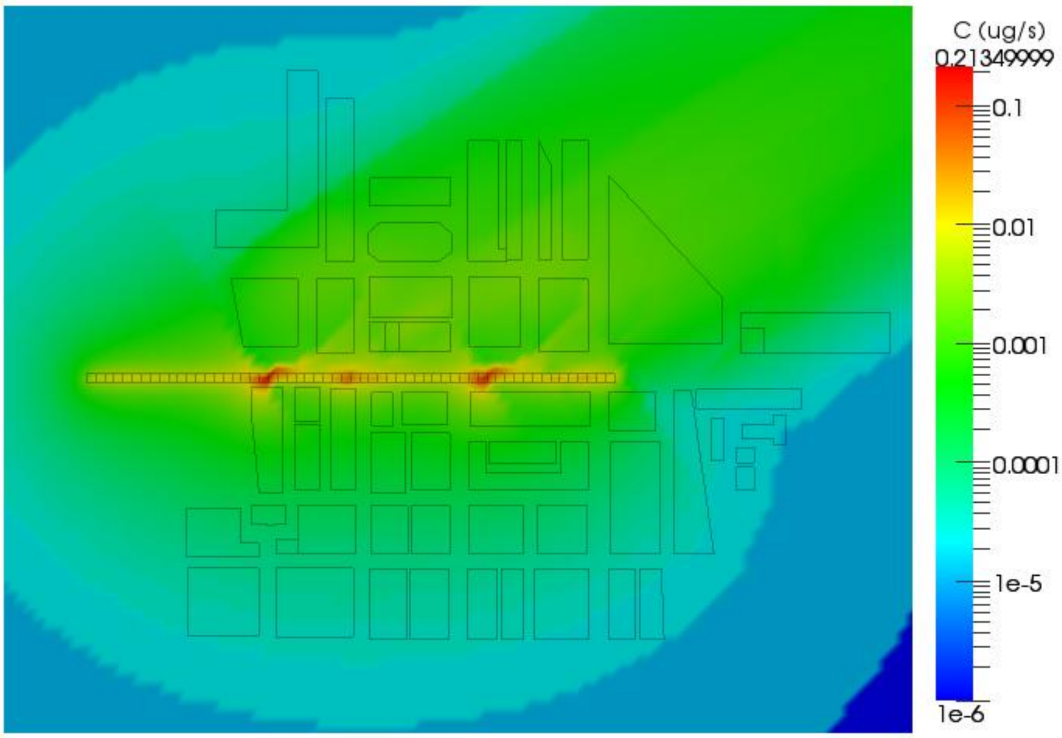

Figure A-14: Pseudocolor plot of the entire domain for experiment 6.

I.5.7 Experiment 7

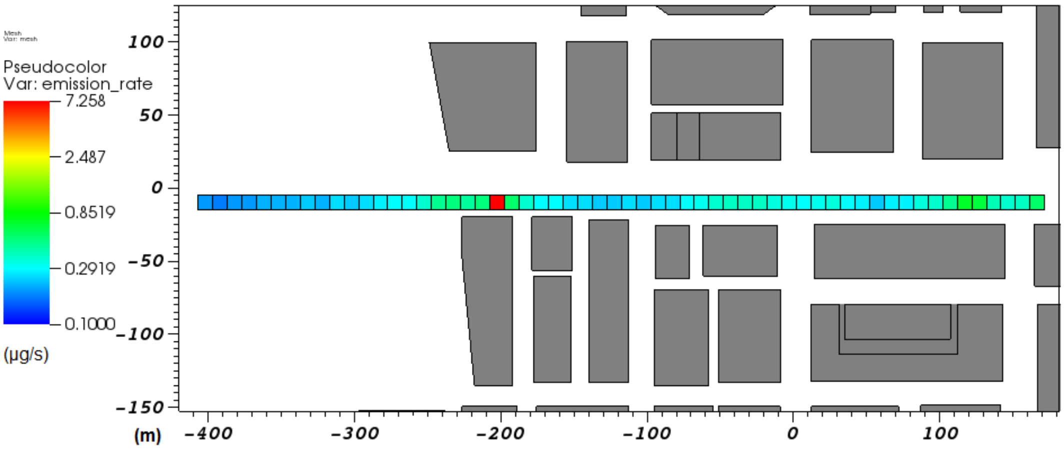

Figure A-15: Pseudocolor plot of emission rates by source position for experiment 7.

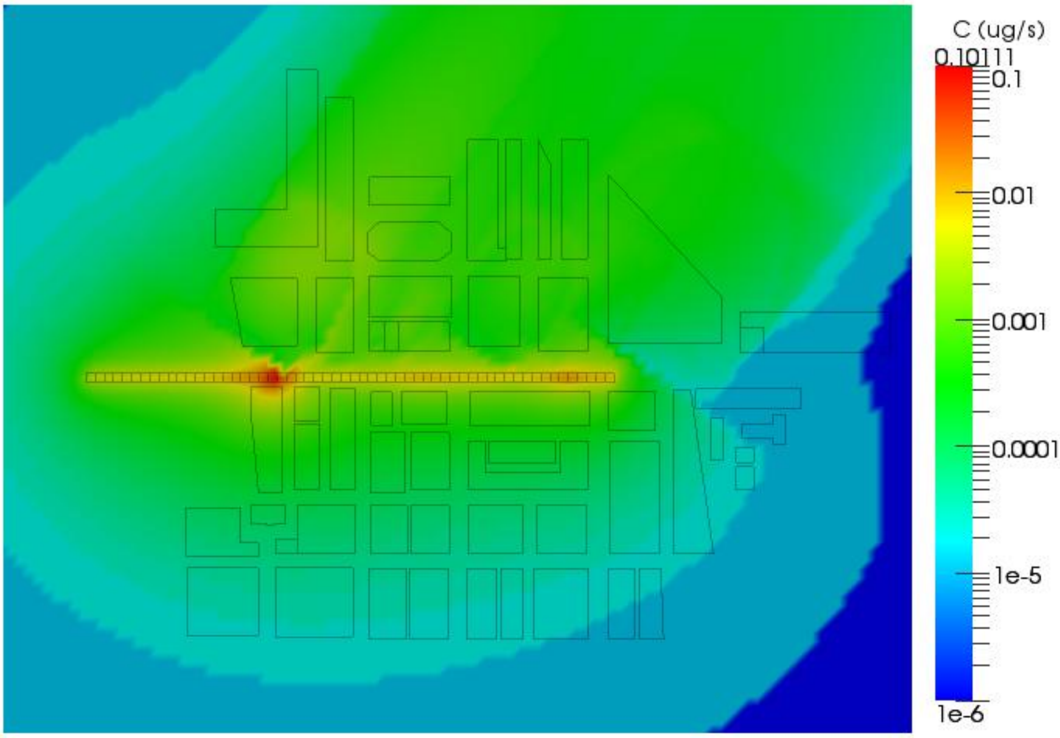

Figure A-16: Pseudocolor plot of the entire domain for experiment 7.

I.5.8 Experiment 8

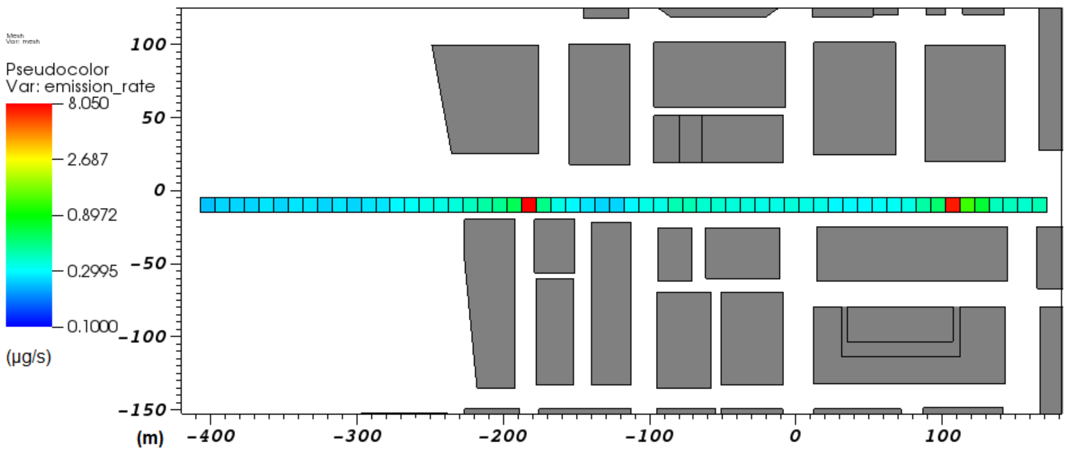

Figure A-17: Pseudocolor plot of emission rates by source position for experiment 8.

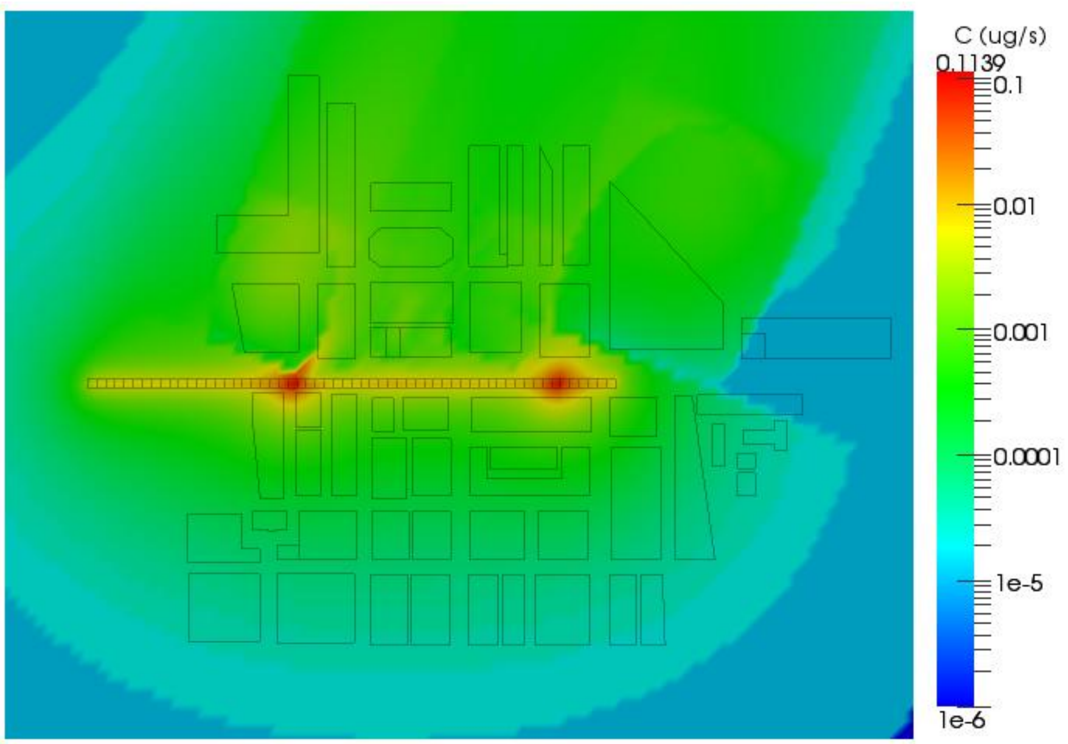

Figure A-18: Pseudocolor plot of the entire domain for experiment 8.

Appendix II – Step by Step Short Tutorial of CFX Setup for Multispecies Flow in Urban Environments

1. Start a new case.

2. Create the material to be transported, e.g. CO:

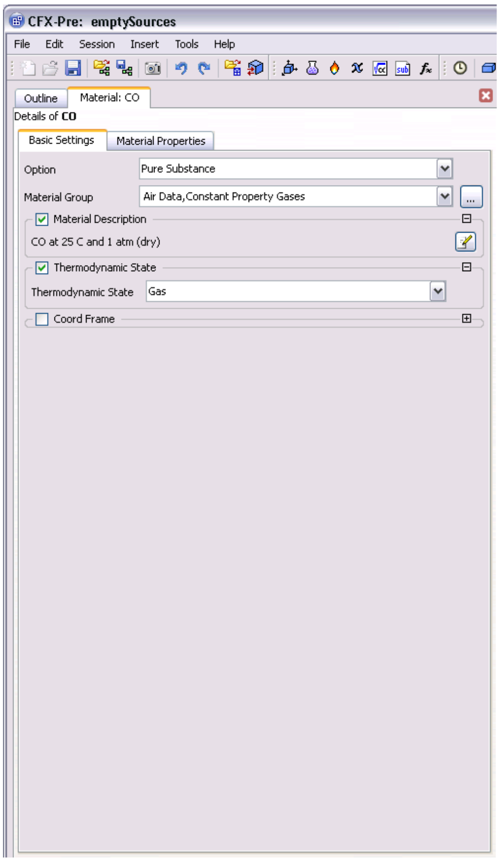

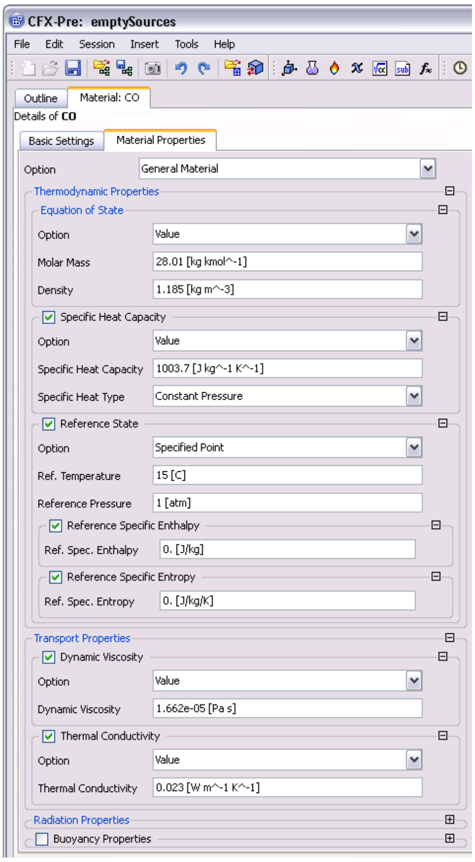

3. Create the mixture material, Polluted Air:

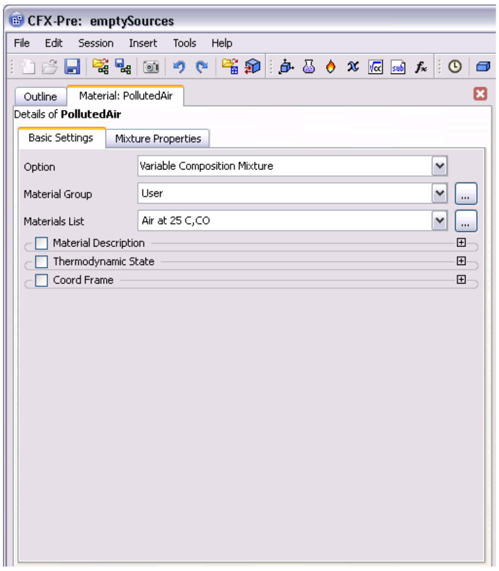

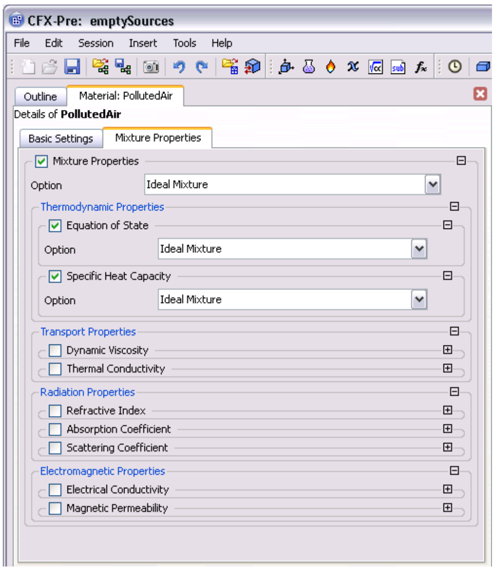

4. Import the mesh generated by CityZoom via Gambit journals. This mesh has intuitive names for every boundary.

5. Create and set the domain:

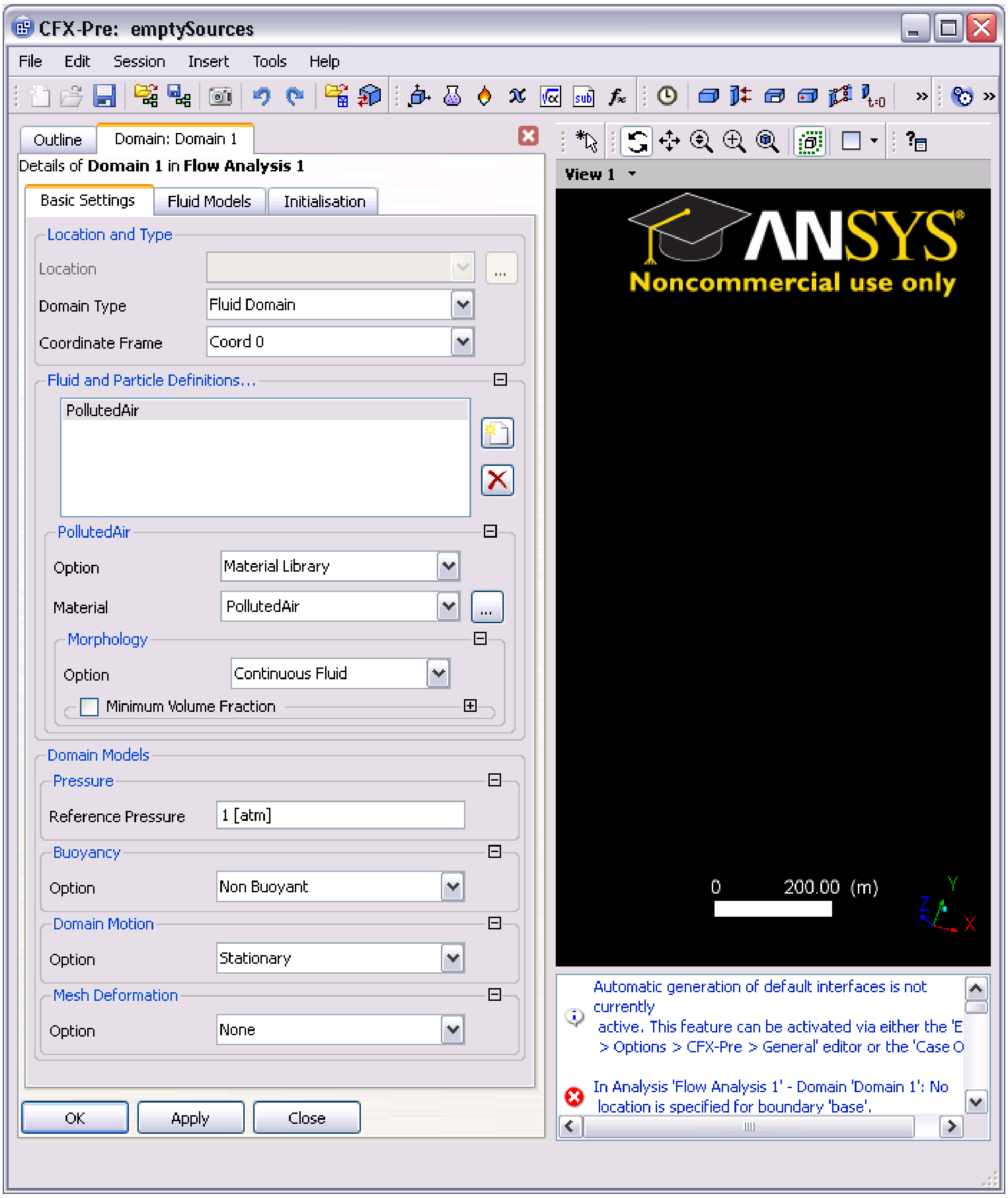

6. Create the domain boundaries and associate them to the mesh boundaries:

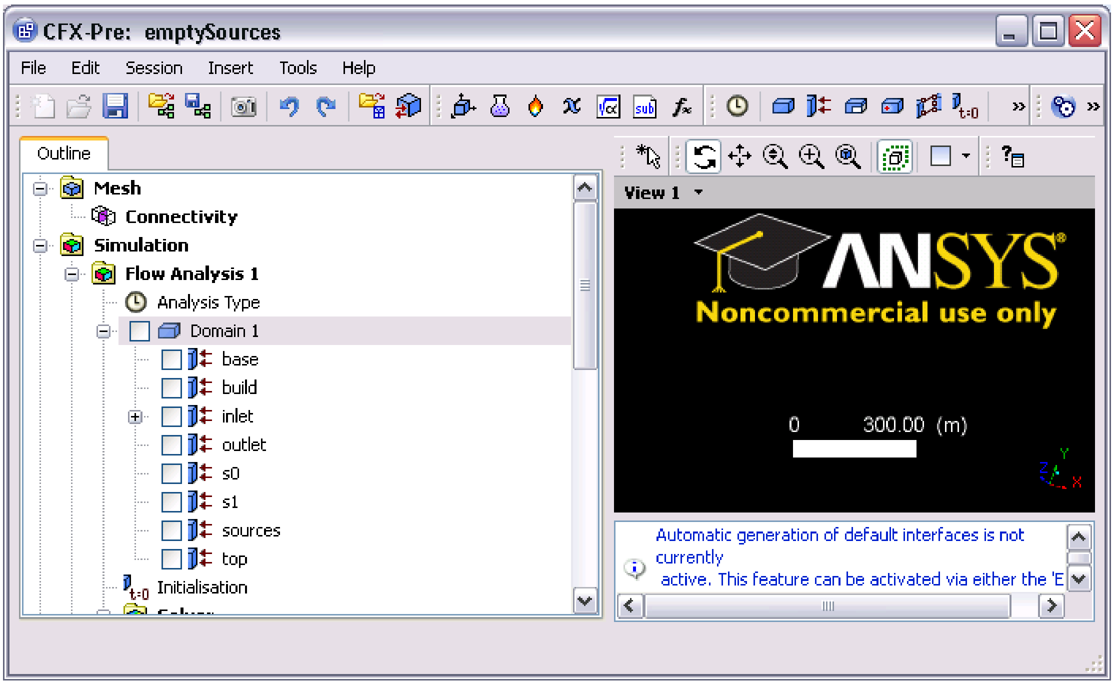

7. Create the expressions for the inlet boundary layer using the CCL editor:

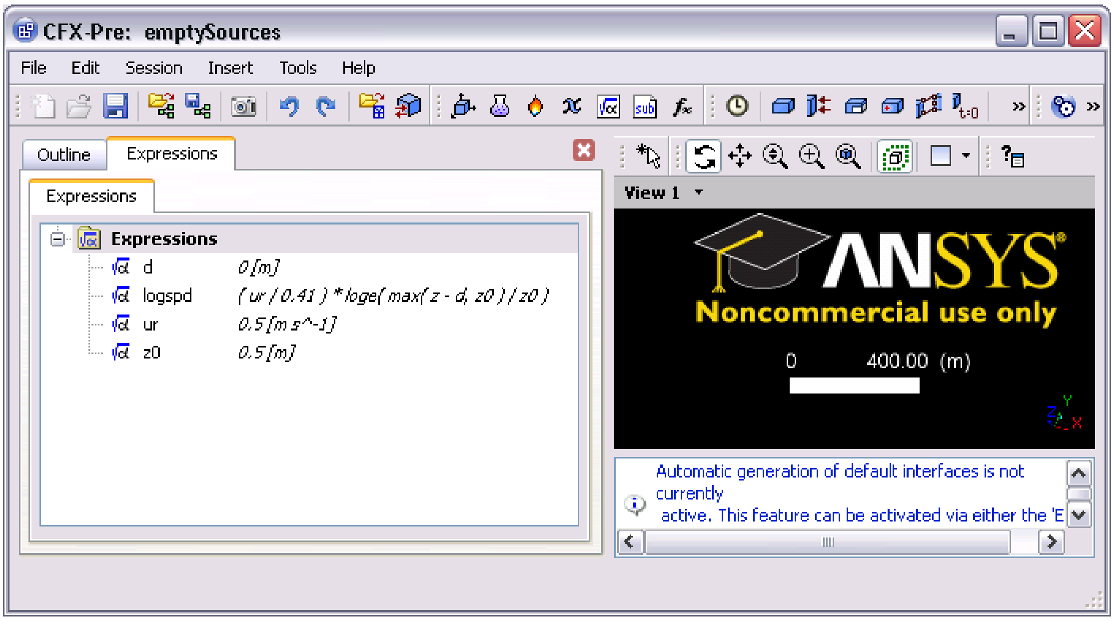

8. Set the inlet velocity using the expressions and set zero value for the mass fraction:

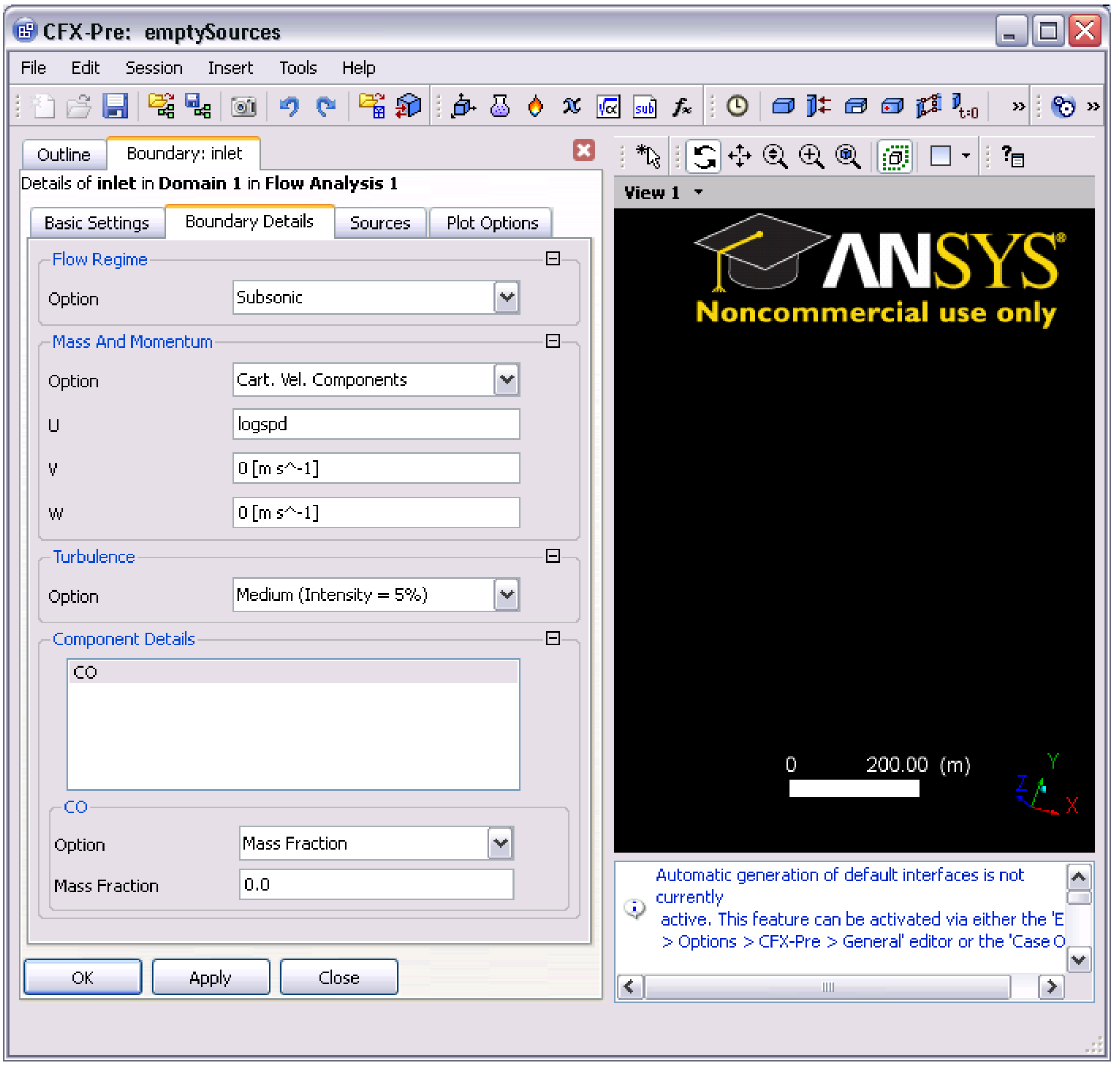

9. Set the sources mass flow rate and mass fraction. In this example all sources have the same values, but different boundary conditions could be created and associated to each source:

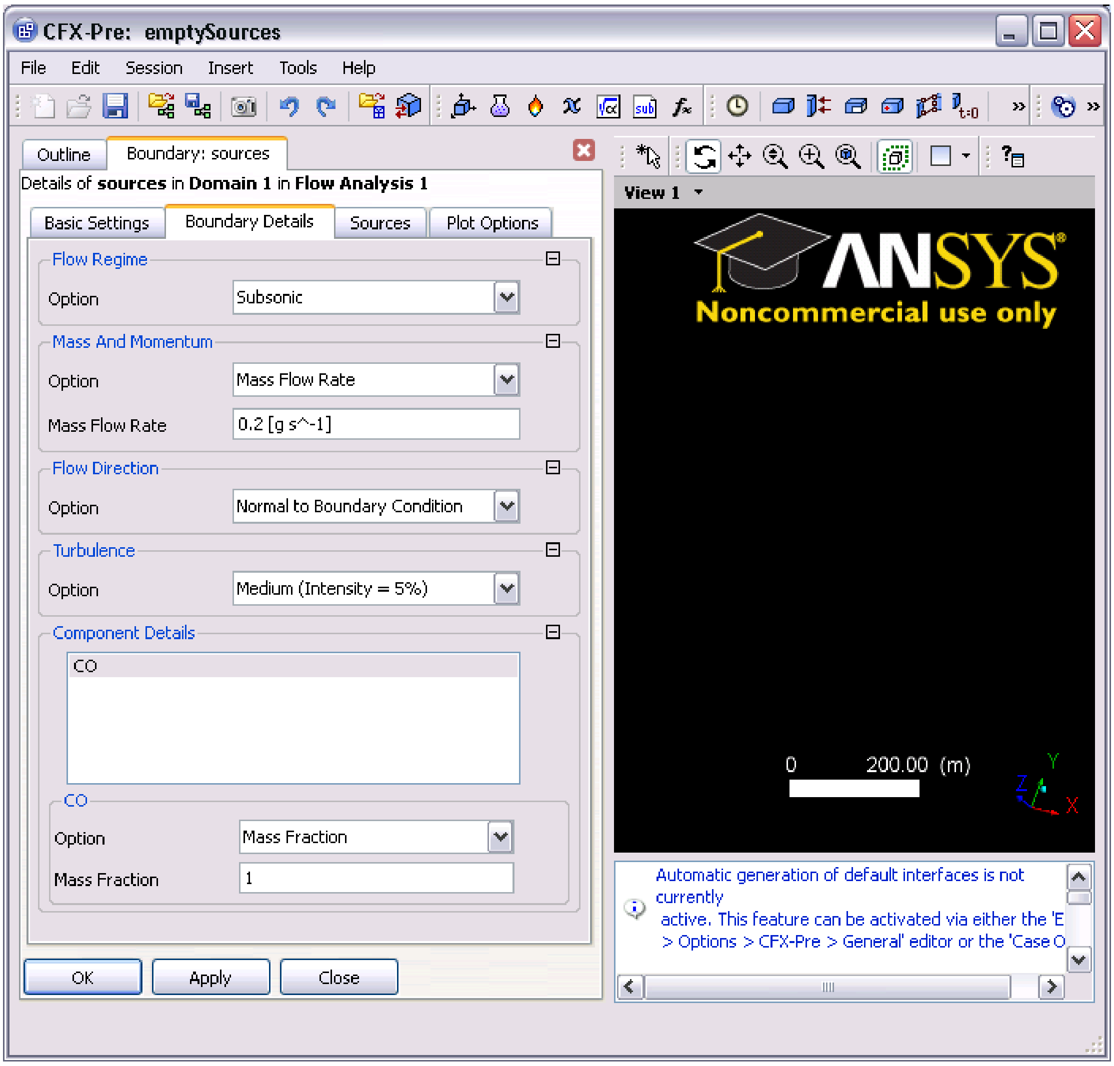

10. Set the Global Initialization:

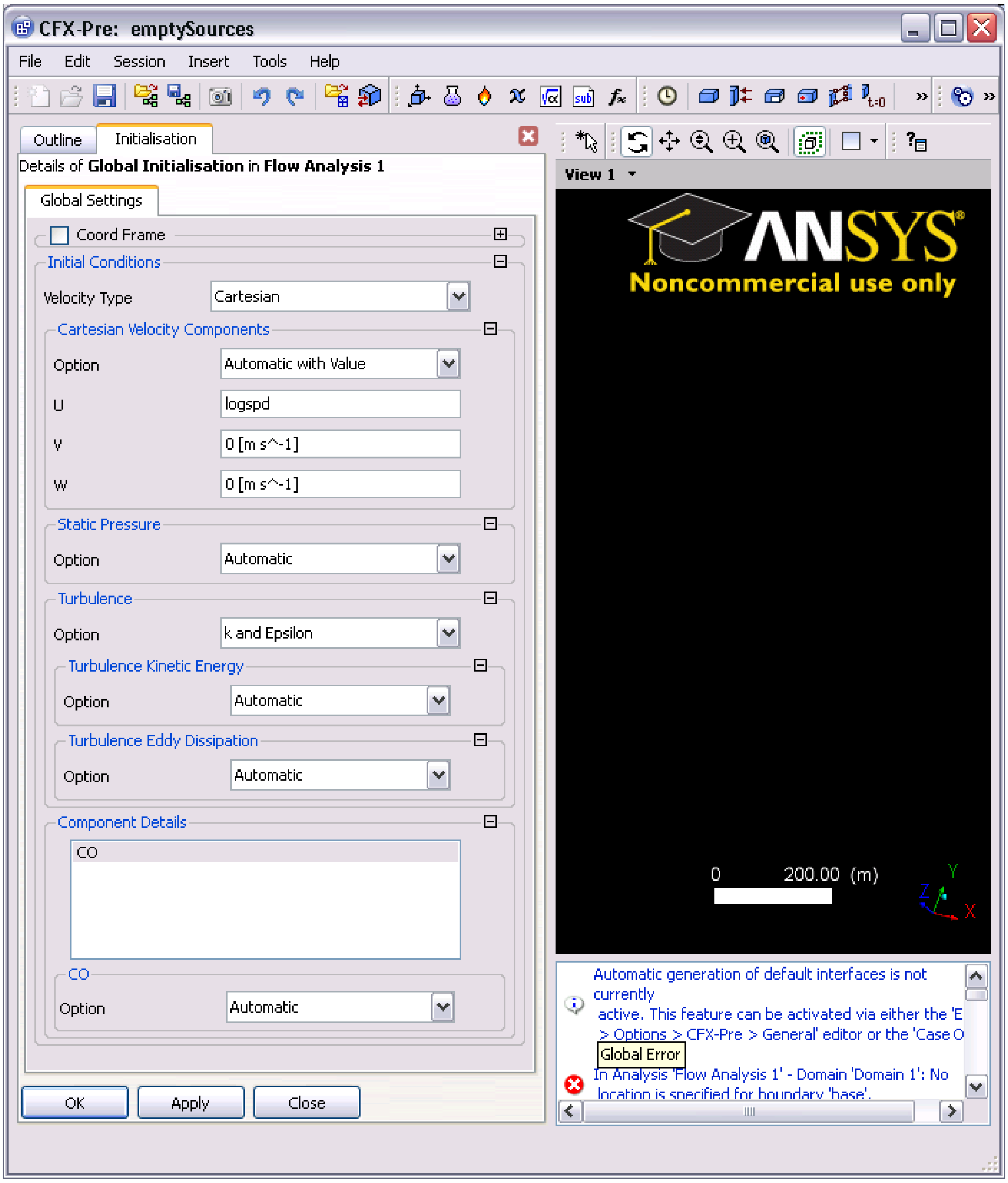

11. Set the analysis type (optional).

12. Set the output control and monitor points (optional).

13. Set the solver control.

14. Write the definitions file and launch CFX Solver.